Detailed analysis of modulating effects of Clusterin in insulin and IGF-1 signal transduction

A thesis submitted for the degree of

doctor rerum naturalium (Dr. rer. nat.)

at the

Faculty of Chemistry, Pharmaceutical Sciences and Geosciences,

Johannes Gutenberg-University Mainz

by

Benjamin Johannes Renner

born in Kemnath

Mainz 2017

Dean:

Primary reviewer:

Secondary reviewer:

Date of oral Exam: 08. December 2017

D77

Detailed analysis of modulating effects of Clusterin in insulin and IGF-1 signal transduction

by Benjamin Renner, M.Sc.

Institute of Pharmacy and Biochemistry,

Johannes-Gutenberg University Mainz

Abstract

In recent years, several studies addressed the involvement of Clusterin, an extracellular chaperone, in the modulation of signal transduction pathways. Despite intense research, only little is known concerning its interaction with signalling receptors or the underlying mechanisms. In this work, one group of growth factor receptors, the so-called receptor tyrosine kinases, are screened for potential interaction partners of Clusterin. This initial experiment revealed the insulin receptor as a positive candidate for Clusterin-mediated signal transduction. The insulin receptor as well as its close relative, the IGF-1 receptor, are known to play a crucial role in the development of Alzheimer's disease. Based on this fact, the role of Clusterin in neuronal protection was assessed via the neuroblastoma cell line N2A. Subsequent analyses addressed the modulating effects of Clusterin on Akt phosphorylation levels and its impact on the cellular viability in the presence of either insulin or IGF-1. While the results for insulin were distorted by the levels of glucose in the culturing media, the co-stimulation of Clusterin with IGF-1 revealed its enhancing effects on IGF-1 stimulation. With the help of biochemical methods and the examination of structural mutants of Clusterin, the interaction of IGF-1 with Clusterin was further elucidated. These methods demonstrated a distinct binding of both molecules and highlighted the necessity of structural domains of Clusterin. In conclusion, this thesis sheds light on the ability of Clusterin to modulate signal transduction pathways and evaluates its physiological role in the onset of Alzheimer's disease.

Contents

1 Introduction 1

1.1 The extracellular chaperone Clusterin 1

1.1.1 Expression cycle – from gene to secreted glycoprotein 2

1.1.1.1 Genetic regulation of the human Clu expression 2

1.1.1.2 Transcription variants stem from one pre-mRNA 3

1.1.1.3 Translation and processing of secretory Clusterin 4

1.1.1.4 Secretion of mature Clusterin and occurring mislocations 5

1.1.2 In-depth description of structural key features of secretory Clusterin 6

1.2 Signal transduction pathways – cellular hub in expression and action of Clusterin 9

1.2.1 Extracellular stimuli in form of hormones 9

1.2.1.1 The metabolism-regulating peptide hormone insulin 10

1.2.1.2 IGF-1 – an Insulin homologue with anabolic effects 12

1.2.2 Receptors form recipients for extracellular signals 13

1.2.2.1 IGF-1-Receptor, Insulin-Receptor and their interplay in signal recognition 14

1.2.2.2 Members of the LDL-receptor family are Clusterin interacting partners 15

1.2.3 Variations of intracellular signalling cascades 17

1.2.3.1 Transcription- and translation regulation with MAPK/ERK pathway 18

1.2.3.2 Cell cycle regulation with PI3K/Akt pathway 18

1.3 Clusterin, a good or bad key player in a physiological context 19

1.3.1 Alzheimer's disease & neuronal illnesses 21

1.3.2 Clusterin-Receptor interaction and modulation of signal transduction pathways 23

1.4 Aims and objectives 25

2 Materials 26

2.1 Equipment 26

2.2 Consumables 27

2.3 Software & web applications 28

2.4 Chemicals 28

2.5 Buffers & solutions 30

2.6 Cell culture media 33

2.7 Kits & reagents 33

2.8 Enzymes & inhibitors 34

2.9 Marker & Standards 34

2.10 Primer 34

2.11 Plasmids 35

2.12 Antibodies 35

2.13 Cell lines 36

3 Methods 37

3.1 Eukaryotic cell culture 37

3.1.1 Propagation of adherent cell lines 37

3.1.2 Preparing cell-based experiments 38

3.1.3 Long-term storage of cell lines 38

3.1.4 Stimulation and harvesting of cell lines 39

3.2 In-vitro Mutagenesis 39

3.3 RNA preparation 41

3.4 Reverse transcription 41

3.5 PCR/RT-PCR 41

3.6 Agarose gel electrophoresis 43

3.7 Transformation & selection of positive clones 43

3.8 Plasmid preparation 44

3.9 Transfection 44

3.10 Stable clone generation 44
3.11 Production of recombinant protein 45
3.11.1 Expression of RAP in a prokaryotic host 46
3.11.2 Expression of Clusterin in an eukaryotic host 46
3.11.2.1 Gathering Clusterin-enriched cell culture supernatant 46
3.11.2.2 First purification and buffer exchange steps 47
3.11.3 Purification of His-tagged proteins with FPLC 47
3.11.4 Sample concentration and buffer exchange 48
3.12 Bradford assay 48
3.13 TCA precipitation 49
3.14 SDS-PAGE 49
3.15 Immunoprecipitation 50
3.16 2D-gel electrophoresis 51
3.17 Western blot 51
3.18 Coomassie staining 53
3.19 RTK Signalling Array Kit 53
3.20 MTS Assay 53
3.21 HPLC 54
3.21.1 Detection of Clusterin chain disintegration 55
3.21.2 Alterations of IGF-1 and Insulin polarity after denaturation 55
3.22 CD-spectroscopy 56
3.23 ELISA 56
3.24 Clusterin deglycosylation 57
3.25 Chaperone assay 58
4 Results 59
4.1 Unravelling Clusterin-interacting receptors involved in signal transduction mechanisms 59
4.2 Elaborating the Clusterin effects on signal transduction during insulin stimulation 62
4.2.1 The Ins-R downstream target Akt is inconsistently modified by Clusterin 63
4.2.2 Screening of multiple cell cultivation variables reveals glucose as disturbance factor for Clusterin signalling modulation 63
4.2.2.1 Clusterin alters the effect of insulin in an ambivalent manner 64
4.2.2.2 Cultivating N2A on low glucose medium stabilises Clusterin effects 66
4.2.3 Low glucose-cultured N2A display a stressed cell character 68
4.2.3.1 Low glucose leads to general protein-dependent Akt activation 69
4.2.3.2 Phenotypical changes are observed in N2A cultured in low glucose medium 71
4.3 Characterisation of the IGF-1-Clusterin-interplay in the modulation of signal transduction pathways 73
4.3.1 IGF-1 qualifies as a novel Clusterin ligand with a glucose-independent Akt stimulation 73
4.3.2 The LRP2 receptor is not involved in observed Clusterin effects 75
4.3.3 Human Clusterin exerts similar effects as murine Clusterin on IGF-1 stimulation 77
4.3.3.1 Comparison of structural features between human and murine Clusterin 77
4.3.3.2 Human Clusterin enhances IGF-1-induced Akt phosphorylation in both human and murine cell lines 79
4.3.4 Functional properties of Clusterin are concentration dependent and administration form independent 80
4.4 Investigation of additional signalling pathways for an influential effect of Clusterin 82
4.4.1 Clusterin exhibits no effect on EGF stimulation 82
4.4.2 Investigation of Clusterin effects on HGF in Hep G2 is obstructed by high cellular stress levels 83
4.4.3 Re-examination of previous experiments towards ERK modulation reveals small side effects 85
4.5 Consequences of the IGF-1/Clusterin Interplay and its potential function in a physiological context 86
4.5.1 Akt phosphorylation enhancement by Clusterin and IGF-1 is reflected in MTS studies 86
4.5.1.1 Clusterin treatment leads to increased cell viability 87
4.5.1.2 High stress levels in Hep G2 and low glucose-cultured N2A are confirmed by MTS analysis 89
4.5.2 Clusterin is not able to sustain IGF-1 effects in the presence of IGFBP3 90
4.5.3 Enhancing abilities of Clusterin seem to be based on active interactions with IGF-1 91
4.5.3.1 Clusterin is able to bind IGF-1 and to a lesser extent other growth hormones 91

4.5.3.2 Physicochemical alterations of IGF-1 influence the binding affinity of both Clusterin and IGFBP3 93
4.5.3.3 Combined heat and DTT treatment of IGF-1 leads to structural alterations and decreased activity 93
4.6 The necessity of structural key features in the Clusterin molecule 95
4.6.1 Introduction of mutations in structural key features of Clusterin alter its physicochemical behaviour 95
4.6.1.1 Mutations cause changes in the distribution of secondary structure elements 97
4.6.1.2 Deletion of the Cys 2-9 disulphide bond destabilises the Clusterin molecule 98
4.6.2 The Clusterin chaperone activity is dependent on its disulphide bonds in both a reducing and non-reducing environment 100
4.6.3 Both hsClu-Cys and hsClu-Pro display severe impairments in the binding of IGF-1 102
5 Discussion 105
5.1 Modulation of insulin stimulation by Clusterin yields inconclusive results 105
5.1.1 Revelation of insulin receptor as potential Clusterin target 106
5.1.2 Akt acts as a downstream target of Clusterin treatment during insulin stimulation 108
5.1.3 Low glucose medium in insulin-mediated experiments stabilises Clusterin effects but triggers cellular stress responses 108
5.2 Clusterin promotes positive effects of IGF-1 stimulation 111
5.2.1 The activation of Akt is the major link in the Clusterin-associated signalling pathway 112
5.2.2 Akt phosphorylation depends on the concentration of secreted Clu 112
5.2.3 Clusterin effects on IGF-1 stimulation are conserved among mouse and human 114
5.2.4 Involvement of the LDL-receptor family 114
5.2.5 Physiological relevance of observed Clusterin effects on Akt phosphorylation during IGF-1 stimulation 117
5.3 Other growth factors specify the spectrum efficacy of Clusterin 121
5.3.1 Combined application of EGF and Clusterin displays no effects 121
5.3.2 HGF-induced Akt phosphorylation is elevated by Clusterin in a cell model experiencing increased stress levels 122
5.4 Uncovering the Clusterin-IGF-1-interplay 123
5.4.1 Structural alterations of IGF-1 impair binding by Clusterin 124
5.4.2 Site-directed mutations influence the folding state of Clusterin 125
5.4.3 Characterisation of the domains in the Clusterin molecule that are essential for its chaperone activity and IGF-1 binding 127
6 Summary 130
7 References VIII
8 Supplemental Data XXIV
9 Abbreviations XXXI
10 Truthful attestation XXXIII
11 Acknowledgement XXXIV
12 Curriculum vitae XXXV

1 Introduction

1.1 The extracellular chaperone Clusterin

During the long-lasting process of discovery, characterisation and classification, Clusterin (Clu) was bestowed with a variety of different names and exceptional roles in physiological conditions. Just like the names, most of those roles, such as intracellular induction of apoptosis (Hochgrebe, et al., 1999) or regulation of complement activation (Leskov, et al., 2003), however, were short-lived. Many observations turned out to be a dead-end or were amended by subsequent research results. Despite the many setbacks in Clusterin research, some of the glamour and fascination for this glycoprotein still prevails since its first discovery in 1982 (Blaschuk, et al., 1982). During said year, Clusterin, found in ram rete testis fluid, was isolated and characterised for the first time. In this early stage of research, it was already apparent that Clusterin is a highly glycosylated dimeric protein of approximately 80 kDa with an indistinct glycosylation pattern (Blaschuk, et al., 1983). Furthermore, it received its characteristic name due to its clustering effect on Sertoli-, TM4 testicular cells and erythrocytes *in-vitro* (Fritz, et al., 1983). Other research groups discovered identical proteins in a variety of species and types of tissue independent from the findings of Blaschuk *et al.* which led to a variety of names for the same protein. Some findings like the proteins SGP-2 (Collard & Griswold, 1987), gp80 (Urban, et al., 1987), SP-40,40 (Murphy, et al., 1988) and ApoJ (de Silva, et al., 1990), which turned out to be Clusterin (Cheng, et al., 1988; Kirszbaum, et al., 1989; Hartmann, et al., 1991), not only expanded the portfolio of various names but also added new structural and functional insights to the nature of Clusterin. To bring together all collected data about Clusterin, a workshop with representatives from each research field was held in 1993. During this workshop, not only knowledge was exchanged but also the protein's name for future references was finally defined to be Clusterin (Fritz & Murphy, 1993).

Due to the cross-talk between different fields of expertise, the publication rate picked up significantly in the following years. One breakthrough followed another but, as already mentioned, not all of them could be confirmed. This led to discrepancies as to the actual role of Clusterin which decelerated its upswing in research. Controversial subjects were the cytoprotective or cytotoxic effect of Clusterin in brain lesions and atherosclerosis (Sivamurthy, et al., 2001; Gelissen, et al., 1998), the effects of intracellular Clusterin (iClu) versus secreted Clusterin (sClu) (Reddy, et al., 1996; Prochnow, et al., 2013) as well as its bivalent role in tumor suppression/activation (Rizzi & Bettuzzi, 2009), all of which are still not fully elucidated to this date. However, there were also bright spots in Clusterin research such as the recently discovered protective and restorative function during disruption of the ocular surface (Bauskar, et al., 2015). Yet, the most striking discovery associated with Clusterin was the observation

of its chaperone and scavenging activity (Lakins, et al., 2002; Bartl, et al., 2001). Due to this ability, Clusterin is one member of a very small group of molecules that act as extracellular chaperones.

1.1.1 Expression cycle – from gene to secreted glycoprotein

Secretory Clusterin (sClu) is found in almost every bodily fluids and is nearly ubiquitously expressed in all types of tissue. Human Clusterin is mainly found in blood serum, cerebrospinal fluid and seminal fluids where it was first discovered. The average concentrations vary from 35 - 105 µg/mL in blood serum (Murphy, et al., 1988), 3,8 - 4,6 µg/mL in CSF (Schweiger, et al., 2007; Kaya-Dagistanli & Ozturk, 2013) up to 2 - 15 mg/mL in seminal plasma (O'Bryan, et al., 1990). However, before a completely mature Clusterin is secreted, several complex splicing events and posttranslational modifications are executed prior to secretion.

1.1.1.1 Genetic regulation of the human Clu expression

Starting from the *CLU* gene which is located at chromosome 8p21 (Dietzsch, et al., 1992; Fink, et al., 1993; Purrello, et al., 1991) as a single copy gene (Purrello, et al., 1991) with approximately 17 kbp in size, a mRNA containing nine exons and eight introns is transcribed (Wong, et al., 1994). Besides the constitutive activation of the *CLU* promotor in a host of cells, there are several stimuli that lead to an increase in the transcription rate. For instance, it was shown that mRNA levels of Clusterin are elevated in some forms of Alzheimer's disease (Duguid, et al., 1989; May & Finch, 1992) or in retinitis pigmentosa (Jones, et al., 1992). Furthermore, it was also observed that aged rats possess increased amounts of renal Clusterin mRNA. This phenomenon was even further amplified in obese diabetic animal models (Laping, et al., 1998). The activation of Clusterin gene transcription is highly regulated due to the fact that the gene sequence possesses several regulatory elements. Besides the typical TATAA box promotor sequence at position -26, some examples are AP-1, SP-1 and NF-E2 motifs located upstream at -87 to -73 (Wong, et al., 1994). Interestingly, a highly conserved region named CLE (Clusterin element) was found within the stretch of regulatory elements. With the exception of one base, this motif is similar to the heat shock element (HSE) found in genes for heat shock proteins (HSP) (Michel, et al., 1997). Additionally, an activation of Clu mRNA transcription could be observed when cells were subjected to heat or oxidative stress proving the activation of the *CLU* gene through binding of heat shock factors (HSF) to the CLE motif (Michel, et al., 1997; Viard, et al., 1999). These findings supported the observation of the Clusterin chaperone activity. Another crucial regulatory element

found upstream of the *CLU* gene is the E-box-like motif (Kim, et al., 2011; Oh, et al., 2015). This element is the target sequence for the prosurvival factor c-myc. C-myc is an essential regulator of cell growth, proliferation and differentiation and is known to regulate a plethora of different genes via the E-Box motif (Zeller, et al., 2006), including the apolipoprotein ApoE (Salero, et al., 2003).

While binding of specific transcription factors is one way of transcriptional regulation, the *CLU* gene sequence with its CpG-rich region suggests a regulation on an epigenetical level (Wong, et al., 1994). DNA methylation as well as histone acetylation were both shown to modulate transcriptional activity of the *CLU* promotor (Nuutinen, et al., 2005; Suuronen, et al., 2007). Most of these regulatory mechanisms are highly conserved among mammalian species, especially between well-studied organisms such as rats and humans (Wong, et al., 1993; Rosemblit & Chen, 1994; Rosemblit, et al., 1996). Studies with quails, however, revealed that homology doesn't cross the border to all vertebrates. Quails not only lack a classical TATA box promotor, but also show alterations in their AP-1 response element localisation. Strikingly, the Clusterin-specific heat shock response element CLE is still highly conserved and quails possess a PUR site which is avian-specific (Herault, et al., 1992; Herault, et al., 1993).

1.1.1.2 Transcription variants stem from one pre-mRNA

Despite the high homology of Clusterin gene regulation within mammalians, the human Clusterin differs greatly when it comes to the actual transcript. While other species, such as mice, produce one distinct mRNA variant, humans have the potential to generate three, based on the existence of three independent exons 1, named 1a, 1b and 1c (Fig. 1B). This fact was already suggested in the beginnings of Clusterin research (Wong, et al., 1994) and was later proven by combining *in silico* analyses of sequence data bases via genetical cell screening (Andersen, et al., 2007). Furthermore, a fourth splice variant lacking exon 2 was discovered which was proposed to play a role in irradiated cells (Yang, et al., 2000; Leskov, et al., 2003). The major transcript of those four is variant 1 with exon 1a (Fig. 1B). Hence, variant 2 starting with exon 1b and variant 3 with exon 1c are only barely present in cellular transcriptomes (Prochnow, et al., 2013). Derived from variant 1 is variant 1 delExon2 which lacks exon 2 containing a coded endoplasmic reticulum (ER) signal peptide (SSCR) and the canonical start codon for secreted Clusterin (sClu). An expression, however, is still possible through a downstream start codon located on exon 3 which is present in all four variants. *Prochnow et al.* could show that upon proteotoxic stress, all variants are upregulated but with variant 1 still being the dominant form with four to five orders of magnitude higher amounts compared to the others. Although variant 2 and 3

both hold the canonical start codon on exon 2, their transcription levels were barely detectable. This is due to on independent upstream open reading frames (ORF) spanning the start codon and thereby inhibiting translation initiation. These ORFs specifically form when either exon 1b or 1c is present in the transcribed mRNA (Prochnow, et al., 2013). Two additional key features are a third start codon in variant 3 which is encoded on exon 1c and the fact that the stop codon in all variants is at the beginning of exon 9, which excludes most of its sequence from being translated.

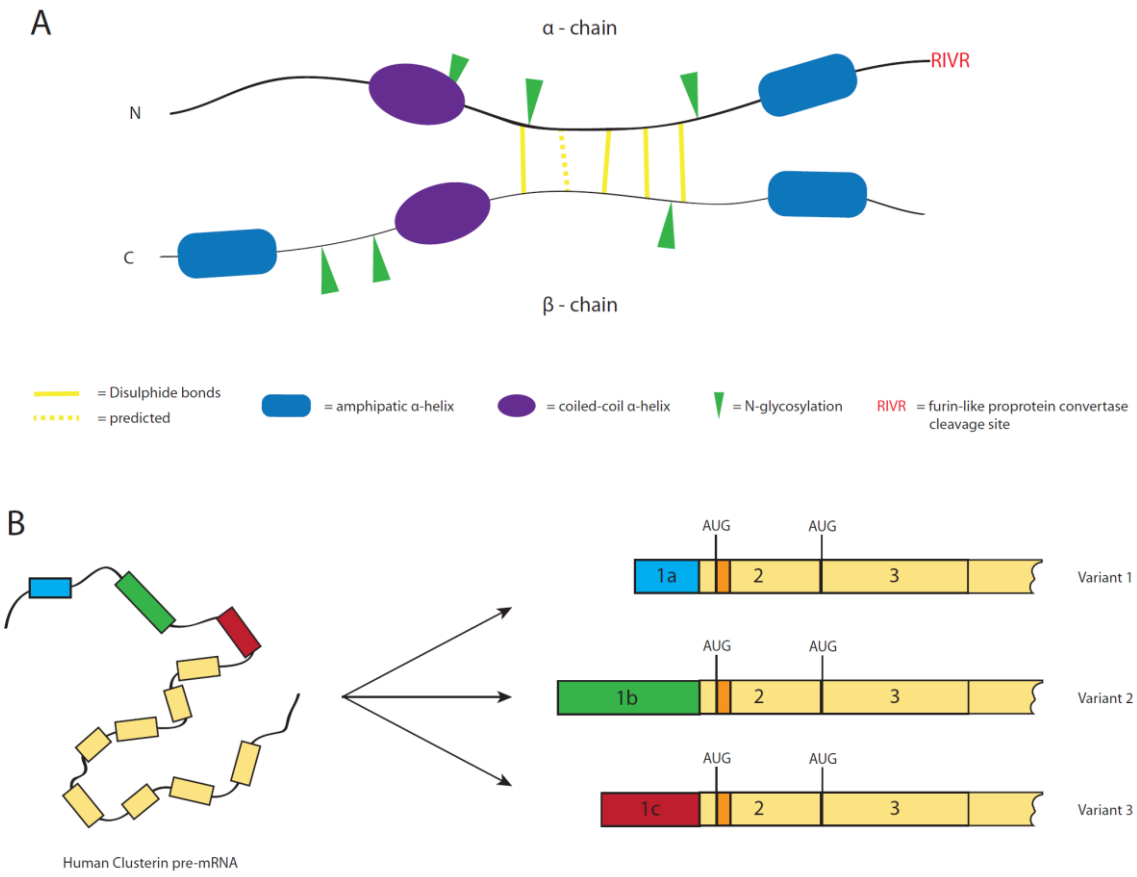

***Fig. 1*: Characteristics of Clusterin structure and its transcription.** *(A) Graphical depiction of structural elements in the mature Clusterin after posttranslational modifications. (B) Splice events during the transcription of Clusterin mRNA. Pre-mRNA contains three different exon 1 (blue, green and red box) resulting in three different Clusterin mRNA variants. The orange highlight in exon 2 marks the coded ER signal peptide. For information about references see respective paragraphs.*

1.1.1.3 Translation and processing of secretory Clusterin

The canonical start codon on exon 2 of variant 1 is the starting point for the translation of fully mature secreted Clusterin. Translation of Clusterin mRNA takes place at the surface of the rough ER, where the growing amino acid chain is co-translationally located to the ER lumen. In a first step, the ER signal

peptide is proteolytically removed. Furthermore, intracellular disulphide bonds are formed between five cysteine residues located towards the N-terminus and five close to the C-terminus (Murphy, et al., 1988; Kirszbaum, et al., 1989; Jenne & Tschopp, 1989) (Fig. 1A). The Clusterin precursor protein also contains six asparagine residues which form potential N-glycosylation sites (Kirszbaum, et al., 1989; Jenne & Tschopp, 1989). It could be shown that all six sites are in fact glycosylated in the mature sClu (Kirszbaum, et al., 1992). After its processing in the ER it is modified up to a glycoprotein-typical high-mannose form which is not its final glycosylation state (Burkey, et al., 1991). For further processing, the pre-mature Clusterin is translocated to the Golgi network. During its passage through the cis-, medial- and trans-Golgi-compartments the high-mannose glycosylation pattern is transformed to a cell-specific type of complex N-glycans (Burkey, et al., 1991; Kapron, et al., 1997; Sabatte, et al., 2011) via specific enzymes, such as mannosidases and glycosyltransferases. In the trans-Golgi network Clusterin receives its final modification by cleavage of the singular precursor protein into two heterodimeric disulphide-bonded chains called α- and β-chain (Burkey, et al., 1991) (Fig. 1A). This is the final step of several post-translational modifications of Clusterin before its actual secretion into the extracellular space.

1.1.1.4 Secretion of mature Clusterin and occurring mislocations

Mature Clusterin is packed into exocytotic vesicles and transported along the ER-Golgi-PM pathway under control of exocytic mechanisms. In MDCK cells it was shown that vectorial secretion of Clusterin towards the apical side takes place (Urban, et al., 1987). In contrast, other studies also revealed a basolateral secretion in hepatocytes (Jenne & Tschopp, 1992) via regulated secretion or a secretion via chromaffin granules in neuroendocrine cell lines (Fischer-Colbrie, et al., 1984). However, these diverse findings are not completely unexpected since all described secretion mechanisms are specific pathways in the respective cell and tissue type.

Although Clusterin is initially characterised as a secreted protein, intracellular Clu variants have been described (Reddy, et al., 1996; Leskov, et al., 2001). Several mechanisms were hypothesised to explain the appearance of these intracellular Clu variants but none could be fully elucidated by experimental setups. One obvious idea was an alternative translation initiation at the upstream start codon on exon 3. Initiation at this point would generate a protein lacking the ER signal peptide. Together with the detection of a nuclear localisation site located upstream of the start codon, it was postulated that intracellular Clu translated from the exon 3 start codon could be translocated to the nucleus (Reddy, et al., 1996). This new Clu variant, termed nuclear Clusterin (nClu) (Leskov, et al., 2001), was the subject

for various following studies addressing its potential physiological role (Caccamo, et al., 2006; Leskov, et al., 2011; Kim, et al., 2012b; Kim, et al., 2012a; Fuzio, et al., 2013). Besides the postulated Clu variant lacking exon 2 resulting in the start codon on exon 3 being the first initiation site (see Fig 1B, (Burkey, et al., 1991)), other possible mechanisms for the occurrence of nClu could be reinitiation and context-dependent leaky scanning (Kozak, 2002) as well as usage of an internal ribosome entry site (IRES) (Macejak & Sarnow, 1991). With the exception of *Leskov et al.* showing exon 2 deletion, none of the published articles suggesting alternative translation initiation ever clarified any possible mechanism for the emergence of intracellular Clu variants. Further mechanisms that could actually be observed in experiments are the retrotranslocation from the ER/Golgi-network (Nizard, et al., 2007) and the cotranslational rerouting to the cytosol (Choi, et al., 2013). In the case of retrotranslocation, the trigger was shown to be increased ER stress which causes accumulation of Clusterin in the secretory system and subsequent translocation into the cytosol. Usually proteins are then degraded in a mechanism called ER-associated degradation (ERAD). The high protein load, however, also causes proteasomal stress leading to accumulation of retrotranslocated Clusterin in the cytosol. Whether Clusterin retrotranslocates from the ER or the cis-Golgi network is not fully elucidated (Nizard, et al., 2007), but it could be shown that the ER-chaperone GRP78 plays a crucial role in this process (Li, et al., 2013). In case of membrane proteins, the mechanism for retrotranslocation was extensively studied by Baldridge and Rapoport (Baldridge & Rapoport, 2016), however, little is known about the mechanics in retrotranslocation of secretory proteins (Pilon, et al., 1997). The mechanism of cotranslational rerouting is based on the fact that the efficiency of the signal sequence of Clu is negatively influenced during ER stress (Choi, et al., 2013). A similar feature was already observed in previous studies of prion proteins (Hay, et al., 1987; Fons, et al., 2003). In contrast to prion proteins which are degraded after rerouting, Clusterin seems to accumulate in the cytosol (Choi, et al., 2013).

The physiological relevance of intracellular Clusterin variants resulting from above described mechanisms was assessed by *Prochnow et al.* with quantitative methods. As already mentioned in 1.1.2, the amount of intracellular Clusterin in both normal and stressed cells had no effect on the cellular integrity. Further experiments addressing the postulated apoptotic effect of Clusterin (Leskov, et al., 2011; Kim, et al., 2012a) or its nuclear localisation (Reddy, et al., 1996) were also disproven (Prochnow, et al., 2013).

1.1.2 In-depth description of structural key features of secretory Clusterin

During its maturation process, Clusterin undergoes a series of essential structural modifications. These changes are crucial for its behaviour and role in a physiological context. However, to what extent these

alterations influence the function of Clusterin is still not fully elucidated. In the following paragraph four major structural characteristics will be addressed.

Intracellular disulphide bonding. The linkage between the five cysteine residues present on both chains is in an antiparallel manner. Early studies showed that all cysteine residues are linked to form disulphide bridges since no free thiol group could be detected (Kirszbaum, et al., 1992). Furthermore, enzymatic proteolysis of Clusterin followed by fragment analysis revealed antiparallel cysteine bonds which are, counted from the N-terminus, 1-10, 3-8, 4-7 and 5-6. In case of cysteine residue 2 and 9, a connection was only assumed since an isolation of a fragment containing only this bridge was not possible (Choi-Miura, et al., 1992b). All cysteine residues are located in a condensed cluster in the core of each chain. This domain is one of few which displays high homology across all clusterin-expressing species. Despite this fact, current research lacks further insight in the role and function of this ordered antiparallel disulphide bonding cluster. Only a handful of publications addressed its influence on Clusterin maturation and secretion (Losch & Koch-Brandt, 1995; Lee, et al., 2012) as well as its possible role in pathogenesis of Alzheimer's disease (Bettens, et al., 2015).

Secondary structure elements. The cysteine core on both chains is surrounded by distinct α-helical elements. One amphipathic α-helix is located towards the cleavage site on each chain whereas one coiled-coil α-helix per chain can be found in the other direction. An additional amphipathic α-helix motive is located close to the C-terminus of the β-chain (de Silva, et al., 1990; Tsuruta, et al., 1990; Andersen, et al., 2007; Leskov, et al., 2003). The description of these distinct patterns is solely based on *in silico* predictions since all attempts to perform x-ray crystallography, NMR- or MS-analysis with Clusterin failed (Jones & Jomary, 2002; Asea & Brown, 2008). Recent CD-spectroscopy analyses revealed an overall secondary structure distribution of approximately 62% α-helices, 8% β-sheets, 12% turns and 18% unordered regions for Clusterin (Rohne, et al., 2014; Wilson & Zoubeidi, 2017). Under physiological conditions Clusterin forms dimers, tetramers and higher molecular complexes (Blaschuk, et al., 1983) probably via the hydrophobic character of the α-helical coiled-coil domains (Leskov, et al., 2003). These domains are also involved in ligand interaction, such as binding of intracellular Clu to Ku70 (Yang, et al., 1999) or Bcl-XL (Kim, et al., 2012a). However, this binding was only observed in stressed cells potentially undergoing apoptosis which disrupts cellular membranes and permits Clusterin to access denatured intracellular proteins. Furthermore, Clusterin was shown to have additional domains for ligand- as well as for receptor binding. The area surrounding the cleavage site is a potential domain for binding of soluble Aβ and human IgG, whereas the highly conserved disulphide-cluster potentially binds to LRP2 and other members

of the LDL-receptor family (Lakins, et al., 2002; Kounnas, et al., 1995; Bartl, et al., 2001; Bajari, et al., 2003; Leeb, et al., 2014). Clusterin has the exceptional ability to bind a plethora of stressed proteins undergoing unfolding processes similar to sHsps (Humphreys, et al., 1999; Poon, et al., 2002). Hydrophobic helices at the α-chain N-terminus and β-chain C-terminus contribute to the formation of a molten globule-like tertiary structure which is capable of binding various unfolded or hydrophobic molecules (Dunker, et al., 2001; Bailey, et al., 2001). Simultaneous binding of ligand and receptor (Lakins, et al., 2002) enables scavenging of unfolded proteins and debris from body fluids and directing them into cells for lysosomal degradation (Bartl, et al., 2001; Hammad, et al., 1997) or functional recovery through refolding chaperones, as tested *in vitro* with Hsc70 (Poon, et al., 2000).

Influence of Glycosylation. Clusterin contains six sites for N-glycosylation, three on each of the two chains, which are fully glycosylated in the mature secreted Clusterin (Kirszbaum, et al., 1992; Burkey, et al., 1991). About 30% of the sClu's total molecular weight are contributed by the attached glycans (de Silva and H, et al., 1990). Besides the mannose-rich core glycosylation Clusterin can display a host of different variations in terminal glycosylation based on the expressing tissue origin (Kapron, et al., 1997; Sabatte, et al., 2011; Tousi, et al., 2012; Liang, et al., 2015). These distal glycosylation patterns are assumed to provide the prerequisite for specific functions (Sabatte, et al., 2011; Merlotti, et al., 2015), however, core glycosylation alone is sufficient for the chaperone activity of Clu (Rohne, et al., 2014). In contrast, Clusterin lacking any posttranslational modifications, which would be the case in mistranslocated Clu, shows a significant drop in chaperone activity and change in overall secondary structure distribution (Rohne, et al., 2014). Furthermore, abolished glycosylation in MDCK cells altered the polarised secretion of Clusterin which suggests that glycosylation is essential for its proper sorting inside the cell (Urban, et al., 1987).

Cleavage of the proprotein. During its maturation in the Golgi network, Clusterin is cleaved between position Arg-205 and Ser-206 (de Silva, et al., 1990) by a furin-like proprotein convertase (Nakayama, 1997; Duckert, et al., 2004; Nizard, et al., 2007) which recognises the RXXR (RIVR in human Clusterin) motif. Studies showed no significance of proteolytic maturation for the proper secretion and chaperone activity of Clusterin (Urban, et al., 1987; Rohne, et al., 2014). However, in combination with a reducing environment, the chaperone activity of uncleaved Clusterin is drastically impaired (Rohne, et al., 2014).

1.2 Signal transduction pathways – cellular hub in expression and action of Clusterin

The evolution of human language was an essential milestone in the formation of tribes, cultures and eventually the society as we know it today. A comparable tool for the development of multicellular organisms was the establishment of cellular communication networks. While early protozoa only had to react to different environmental challenges, higher evolved pro- and eukaryotes already started to interact with one another to form sustainable colonies. For the next step in the evolutionary ladder towards multicellular organisms, however, these early interactions had to improve dramatically. The network had to be capable of transmitting a broad range of different signals in a short period of time, since every cell in the organism was essential for its future continuance. As a consequence of the advancing evolution towards more complex organisms, the communication networks also expanded into a dynamic and multifaceted system which until today we are only able to understand in its basics (Fig. 2). Although the first discovery assuming such networks dates back to the 1850s (Cornell, et al., 2014), the term of “signal transduction” known today was initially shaped in 1972 (Rensing, 1972). Signal transduction encompasses the whole mechanism of cellular information processing, starting with the detection of an extracellular stimulus via different types of receptors spanning the cellular membrane. These receptors are usually linked to adaptor molecules inside the cell which forward signals, mostly by transfer of phosphorylation, to a cascade that eventually causes changes of the cellular condition. It is of note, that signalling pathways are not solely restricted to the previously described model. Every aspect of it underlies variations depending on the examined pathway. In case of glucocorticoids for example, the receptor is located in the cytosol as a soluble protein, which translocates to the nucleus after ligand binding, thereafter acting directly as a transcription factor. Furthermore, stimuli can also origin from within the cell as is the case in DNA damage responses, intrinsical apoptosis or the activation of autophagy.

1.2.1 Extracellular stimuli in form of hormones

At the beginning of every signal transduction cascade exists a stimulus that is recognised by the cell. The forms a stimulus can adopt, are highly variable. Besides a vast amount of molecular substances that can trigger signalling pathways, a cell also harbours sensors for changes in physical parameters, such as temperature, light or mechanical forces. The types of molecular substances that can act as a signalling trigger comprise every biological substance class, but can also be of anorganic nature such as the second messenger nitric oxide. Members in the lipid class of signalling molecules range from

simple fatty acids to complex structures like steroids. Similar complexity can be found in the protein branch which expands from amino acids and small peptides like glycine and oxytocin to high molecular weight complexes as formed by Clusterin and its ligands. The last group are nucleic acids which play a crucial role in pathogen detection and immune system activation. All signalling molecules can be classified into four different groups depending on their localisation and function. However, the boundaries are blurry as some molecules can have multiple tasks. The four groups consist of neurotransmitters, growth factors, cytokines and hormones, whereby the terms growth factors and cytokines are often harmonised in scientific publications.

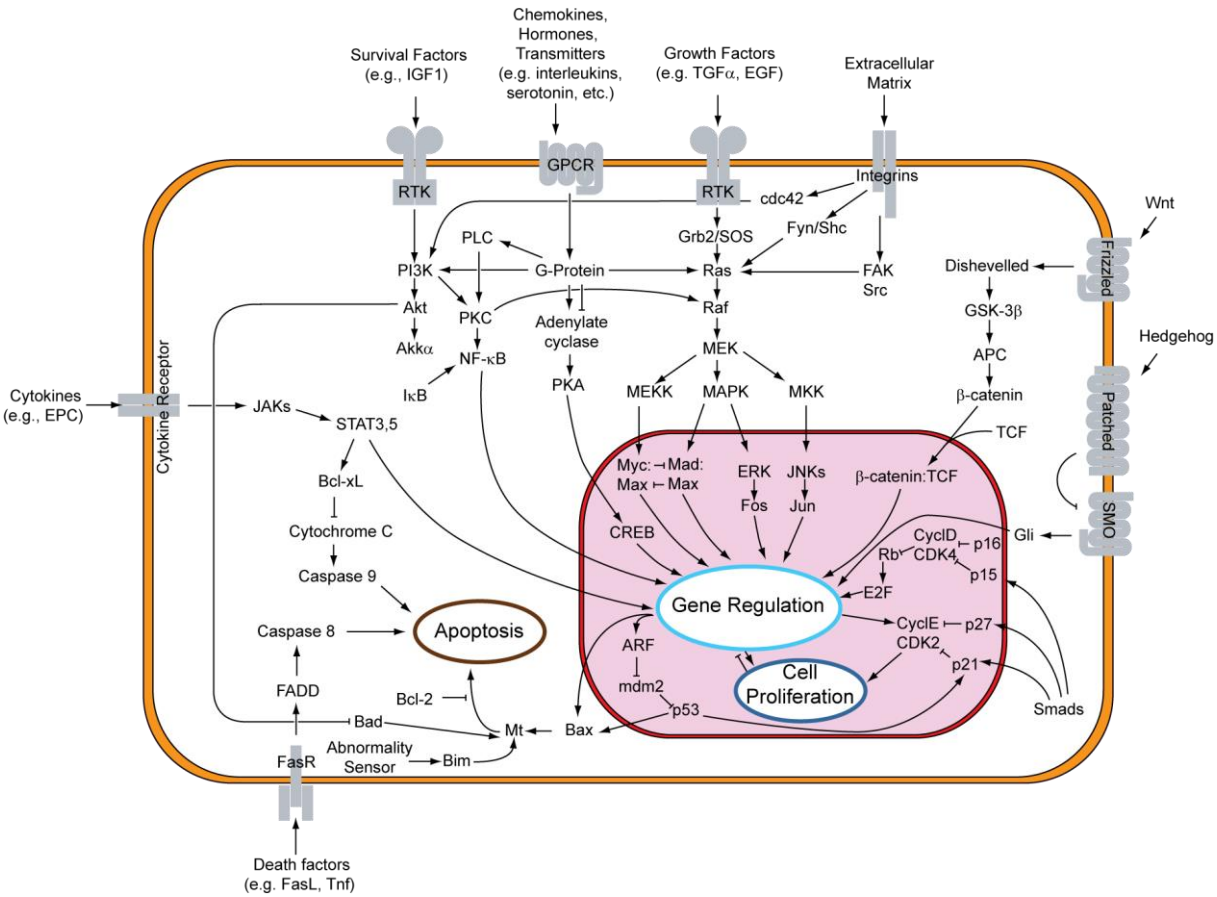

Fig. 2*: *Overview of various cellular signal transduction pathways. *Pathways are simplified and reduced to key molecules which eventually trigger a generic cellular response. Reprinted with permission from (Lodish, 2008).*

1.2.1.1 The metabolism-regulating peptide hormone insulin

The peptide hormone insulin, which is produced in β-cells of the pancreatic islets, was the first peptide to be fully sequenced (Sanger & Tuppy, 1951a; Sanger & Tuppy, 1951b; Sanger & Thompson, 1953a; Sanger & Thompson, 1953b). Mature insulin consists of two independent chains linked by two

disulphide bonds. It is generated from a preproprotein containing a signal peptide for ER sorting and a so-called c-peptide which are both cleaved off during the passage through the ER and Golgi network. In the trans Golgi network, mature insulin is packed into secretory vesicles where it is stored until a releasing stimulus reaches the cell. The major stimulus for insulin secretion is an increased level of glucose in the blood serum upon which insulin is released from the secretory vesicles into the blood stream. From there it is transported to effector organs such as liver and skeletal muscles. Insulin exhibits many different effects, which are however all linked to metabolic alterations. Its main task is to stimulate the uptake of glucose from the blood to reduce the glucose level and the synthesis of glycogen for glucose storage. Additionally, it enhances lipid metabolism and induces amino acid uptake which in turn activates protein synthesis. In the course of this, lipolysis and proteolysis events are decreased and survival mechanisms such as autophagy are inhibited (Neely, et al., 1974). These effects are triggered by binding of insulin to its corresponding receptor called insulin receptor. Upon binding, signalling cascades are activated including PI3K/Akt and MAPK/ERK. Besides the before mentioned effects, these cascades also influence cell proliferation and differentiation. Based on the extensive influence of insulin on the whole metabolism, it is of no surprise that malfunctions of this system cause severe illnesses. One of the most common diseases in relation to insulin is Diabetes which had an estimated global incidence of 422 million adults in 2014 (WHO & others, 2016). It is important to distinguish between two main types of Diabetes, called type 1 and type 2 Diabetes. Type 1 is characterised by a loss of β-cells in the pancreatic islets due to autoimmune attacks which ultimately leads to a complete loss of insulin in the blood serum. Usually the disease already occurs in childhood or adolescence, whereas Type 2 has its onset typically at an advanced age. The background for type 2 Diabetes occurrence is still not fully elucidated but so far it is known that it correlates with a decreased response of insulin receptor to its ligand (Truglia, et al., 1985) and altered expression rates of insulin in the β-cells (Lillioja, et al., 1993). A potential trigger for Diabetes type 2 development is a deficiency in Clusterin which was shown to induce insulin resistance during a high-fat diet (Kwon, et al., 2014). Additionally, three SNPs in the Clu gene were detected to be associated with type 2 Diabetes (Daimon, et al., 2011). Earlier studies also revealed a role of Clusterin in the embryonic development of pancreas tissue (Min, et al., 1998) by stimulating differentiation to insulin-secreting cells (Kim, et al., 2006). In adults, Clusterin is overexpressed during tissue injury in the pancreas where it plays a critical role in β-cell regeneration and tissue remodelling (Kim, et al., 2001; Lee, et al., 2011).

Type 2 Diabetes was shown to be a potential risk factor for AD (Hölscher, 2011) and recent studies revealed that insulin and the two growth hormones IGF-1 and IGF-2 are also expressed in some areas of the brain (Steen, et al., 2005; de la Monte and Suzanne & Wands, 2005) which further intensifies the link to AD development.

1.2.1.2 IGF-1 – an Insulin homologue with anabolic effects

Structurally seen, the peptide IGF-1 shares high homology with proinsulin. The amino acid sequence exhibits highly conserved domains and the three cross-linking disulphide bonds lead to a somewhat similar tertiary structure, although IGF-1 is not proteolytically cleaved (Rinderknecht & Humbel, 1978). In case of expressing tissue and physiological function, both molecules differ from each other. The main source of IGF-1 is the liver, but cells stimulated by IGF-1 also start to express it in an auto- and paracrine manner (Hernandez, et al., 1992; Schofield, 1992). Secreted IGF-1 is, like insulin, transported through the blood stream. However, for transport IGF-1 is bound to so-called IGF binding proteins. So far seven IGFBPs are known (Oh, et al., 1996), of which IGFBP3 accounts for about 80% of IGF-1 binding (Jones & Clemmons, 1995). IGFBP-4 has increased affinity to IGF-1 compared to its receptor causing an indirect inactivation of IGF-1 by withdrawal from the system (Mohan, et al., 1989; Culouscou & Shoyab, 1991). When IGF-1 reaches a target cell, it binds to its corresponding receptors, the IGF-1 receptor and to some extent to the insulin receptor (Treadway, et al., 1992). This interaction triggers several pathways with the PI3K/Akt cascade being the most prominent. Although, slight metabolic changes similar in modulation but not in intensity to insulin are detectable (Guler, et al., 1987), the major effect of IGF-1 is its cell growth stimulation. This function can be phenotypically seen in malfunctions such as Dwarfism and Acromegaly in which IGF-1 levels are decreased or elevated respectively (Laron, 2001; Chanson & Salenave, 2008). Furthermore, IGF-1 plays a crucial role in progression of some types of cancer and is therefore a potent target in tumour therapy (Sachdev, 2008; Pollak, 2008; Yang & Yee, 2012). In connection with Clusterin, IGF-1 acts as a stimulator increasing expression levels of secretory Clusterin which acts as a pro-survival factor (Criswell, et al., 2005; Goetz, et al., 2011; Luo, et al., 2014). Together, both molecules enabled an IGF-1-stimulated activation of the PI3K/Akt pathway in human non-small cell lung cancer cells, whereas Clu knock-down inhibited this activation (Ma & Bai, 2012). A single study in 2008 drew another picture of the Clusterin involvement in IGF-1 signalling. During serum deprivation in which IGF-1 exerts anti-apoptotic effects, Clusterin blocks the activation of the PI3K/Akt signalling pathway (Jo, et al., 2008). This is in contrast to many other observations as previously described. Again, these results demonstrate the controversial character of Clusterin and extend it on to the area of signal transduction.

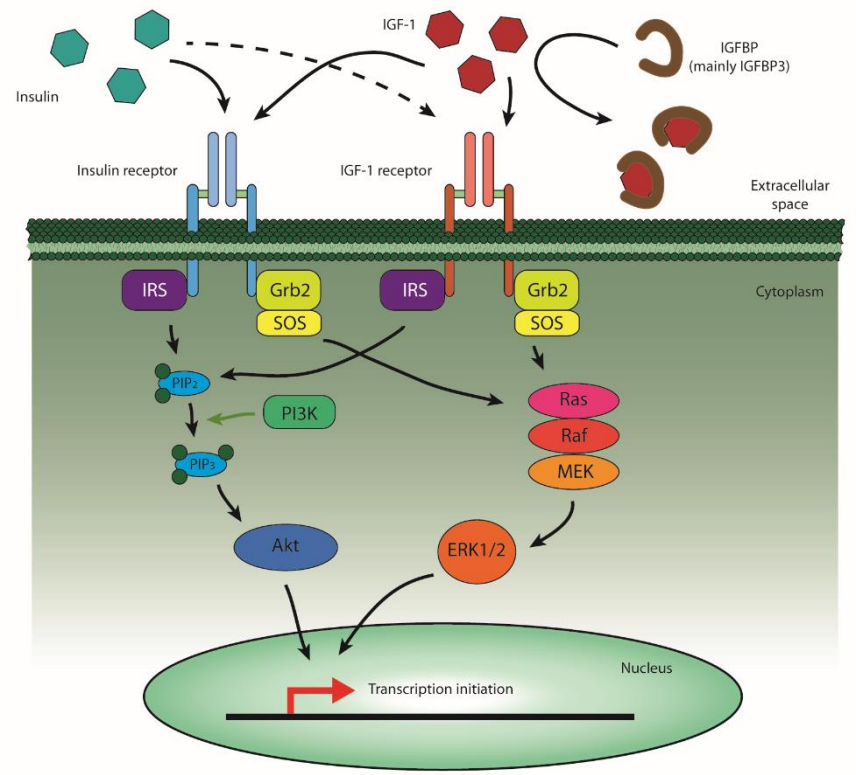

Fig. 3*: *Schematic diagram of the Insulin & IGF1 signalling pathways. *The two major pathways are the PI3K/Akt- and the MAPK/ERK-pathway which can both be activated by either Insulin or IGF-1 receptor. Two crucial adaptor molecules are IRS and Grb2 which trigger their distinct signalling pathway. The activation of either one of those adaptors will eventually lead to an alteration of transcriptional regulation of corresponding gene targets. All shown signalling pathways are simplified in both localisation and pathway mechanisms. For information as to references, see respective paragraphs.*

1.2.2 Receptors form recipients for extracellular signals

Every stimulus that reaches a cell has to be recognised to launch a cellular response. This task is accomplished by receptors, proteins with a highly complex structure. Each receptor has one or a set of ligands which can be specifically bound to trigger subsequent actions. Receptors can be divided into two groups depending on their localisation. The first group called intracellular receptors are located in the cytosol. Ligands for these receptors enter the cells and interact with their corresponding receptors in the cytoplasm, which causes a translocation of the complex to the nucleus where it acts as a transcription factor. The second group are transmembrane receptors, which consist of three distinct domains, the extracellular, the transmembrane and the cytoplasmic domain. The extracellular domain is essential for ligand recognition, whereas the cytoplasmic domain displays binding sites for adaptor molecules or contains an enzymatic domain that is triggered after receptor stimulation. The basic roles of the transmembrane domain are of structural nature. It acts as an anchor point for the entire receptor construct and is able to form pores in the membrane or to interact with other transmembrane domains leading to di- or oligomerisation of monomeric receptor subunits. Based on these structural

differences, transmembrane receptors can be further subdivided. One group are ionotropic receptors that form ion channels in the membrane which are activated after ligand binding. G protein-coupled receptors, the second group of transmembrane receptors, constitute an exception in their ligand binding mechanics. They consist of seven transmembrane domains that form a cavity in the membrane for ligand interaction. Small molecules enter the cavity and bind directly to the transmembrane domains. Only more space-filling ligands use the classical way by binding to the extracellular N-terminal domain (Takahashi, et al., 1993). A special group of transmembrane receptors are for example the Notch receptor which is proteolytically cleaved after ligand binding. The last group is formed by enzyme-linked receptors which, as the name already suggests, are receptors that are either linked to or contain an enzymatic domain in their cytoplasmic tail. Binding of a ligand triggers the activation of this enzymatic function and subsequently causes an alteration of target molecules in the cytoplasm.

1.2.2.1 IGF-1-Receptor, Insulin-Receptor and their interplay in signal recognition

Typical members of the enzyme-linked receptors are the IGF-1 and insulin receptor (IR), which can be further characterised as receptor tyrosine kinases. Both receptors are expressed as a single protein precursor and are subsequently cleaved into an α- and β-subunit during the maturation process. The α-chain forms the extracellular ligand binding domain, while the β-chain spans the plasma membrane with a cytoplasmic and transmembrane part and anchors the α-subunit to the membrane by an intermolecular disulphide bond. For ligand binding, two monomers have to interact with their α-subunit to form a fully active receptor (Massague, et al., 1980; Ullrich, et al., 1985). Dimerisation also brings both cytoplasmic domains in close proximity. These domains contain a tyrosine kinase active site which is activated by conformational changes in the α-chain after ligand binding. The consequence of kinase activation is a trans-autophosphorylation of tyrosine residues within the cytoplasmic tails. Phosphorylated tyrosine residues can subsequently be recognised and bound by adaptor molecules, such as insulin response substrate 1, which are starter molecules for intracellular signalling cascades (Fig. 3). The insulin receptor can form homo- and heterodimers since IR mRNA codes for two isoforms, IR-A and IR-B, differing in the presence of an exon 11 close to the cleavage site (Seino, et al., 1989) (Fig. 4). IR-A, the isoform without exon 11, shows binding to IGF-2 (Frasca, et al., 1999) and increased affinity towards insulin (Mosthaf, et al., 1990), whereas IR-B seems to have elevated tyrosine kinase activity (Kosaki, et al., 1995). The binding affinity to IGF-1 between both isoforms differs as well (Yamaguchi, et al., 1993). Furthermore, the insulin receptor is capable of forming heterodimers with the IGF-1 receptor (Soos & Siddle, 1989), expanding the possible binding partners for IGF-1 (Soos, et al., 1990; Soos, et al., 1993) (Fig. 4). Those heterodimers exhibit high affinity to IGF-1 but decreased

binding capabilities to insulin (Soos, et al., 1993). Since both IR-A or IR-B can dimerise with IGF-1 receptor monomers, attempts to characterise the benefits of this behaviour were even more aggravated (Pandini, et al., 2002; Slaaby, et al., 2006).

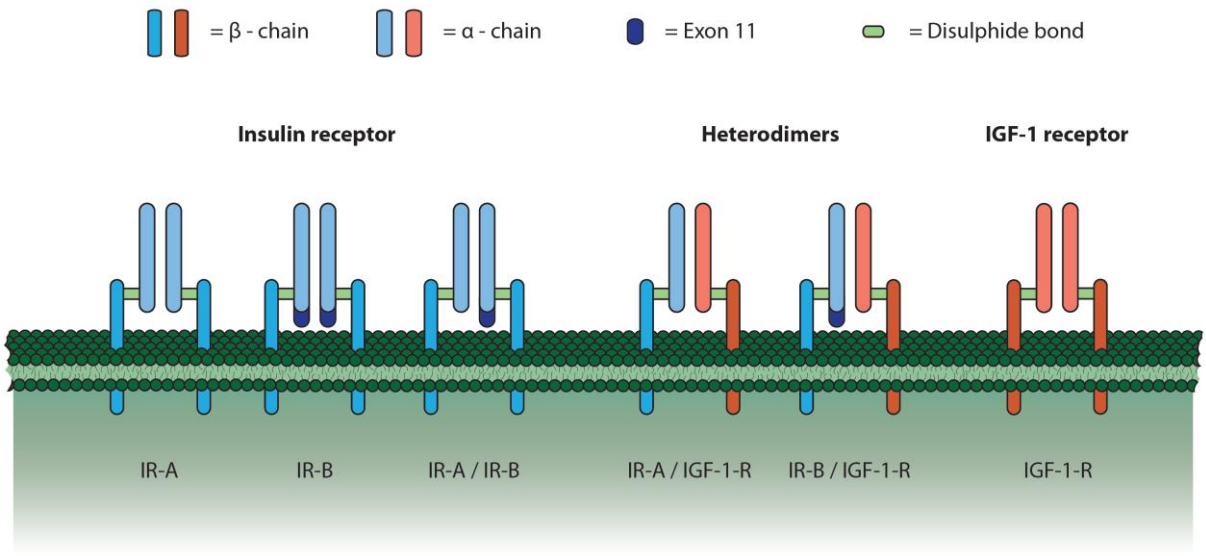

Fig. 4*: *Dimer combinations of insulin and IGF-1 receptor monomers on the cellular surface. *The illustration shows all known dimeric isoforms of the insulin receptor (IR) and IGF-1 receptor (IGF-1-R). All monomers consist of a transmembrane-spanning β-chain and an extracellular α-chain which are connected via disulphide bonds. The difference between IR-A and IR-B lies in the exon 11 which is spliced in the IR-A isoform. For information as to references, see respective paragraphs.*

1.2.2.2 Members of the LDL-receptor family are Clusterin interacting partners

The family of LDL-receptors consists of seven core members and three distantly related members. The seven core members are LDLR, VLDLR, ApoER2, LRP4/MEGF7, LRP1, LRP1b and LRP2/megalin (Fig. 5A). They all share three common structural conserved domains, some of which can also be found in the three distantly related receptors called LRP5, LRP6 and SorlA (Kim, et al., 1998; Brown, et al., 1998; Jacobsen, et al., 1996) (Fig. 5B). EGF-precursor homology domains (EPD) as well as ligand binding-type repeat domains (LBD) can be found within the extracellular domain of each member. LBDs are located at the N-terminus of the extracellular domain but can also be found to link two EPDs in some members such as LRP2. The EPDs are a conglomerate of EGF receptor-like repeats and YWTD β-propeller repeats (Springer, 1998) which participate as a unit in the pH-dependent ligand release after endocytosis (Beglova & Blacklow, 2005). The third crucial conserved domain is found in the cytoplasmic tail and only consists of a NPxY motif acting as an adaptor domain in signal transduction and endocytosis (Trommsdorff, et al., 1998; Chen, et al., 1990). During the expression and maturation of LDL receptors, the LBDs, essential for ligand binding (Russell, et al., 1989), are blocked by a coexpressed chaperone

called receptor-associated protein (RAP) or LRPAP1 to prevent premature ligand binding and receptor degradation (Herz, et al., 1991; Bu, et al., 1995; Willnow, et al., 1996b). RAP exhibits the highest affinity towards LDL receptor binding sites to ensure unlimited protection until receptors are fully mature (Bu, et al., 1995). Besides developmental regulations in embryogenesis (Willnow, et al., 1996a; Diaz-Mendoza, et al., 2014), this receptor family encloses a plethora of different functions which are further expanded due to their interaction with a variety of co-receptors, such as cubilin (Moestrup & Verroust, 2001) or uPA receptor (Nykjaer, et al., 1992). The main task of LDL receptors is the uptake of lipids by endocytic events (Moestrup & Verroust, 2001; Willnow, et al., 1994). Other molecules endocytosed by some members include vitamin-carrier complexes (Moestrup & Verroust, 2001), immune globulins (Nagai, et al., 2011), HSPs and toxins (Herz & Strickland, 2001).

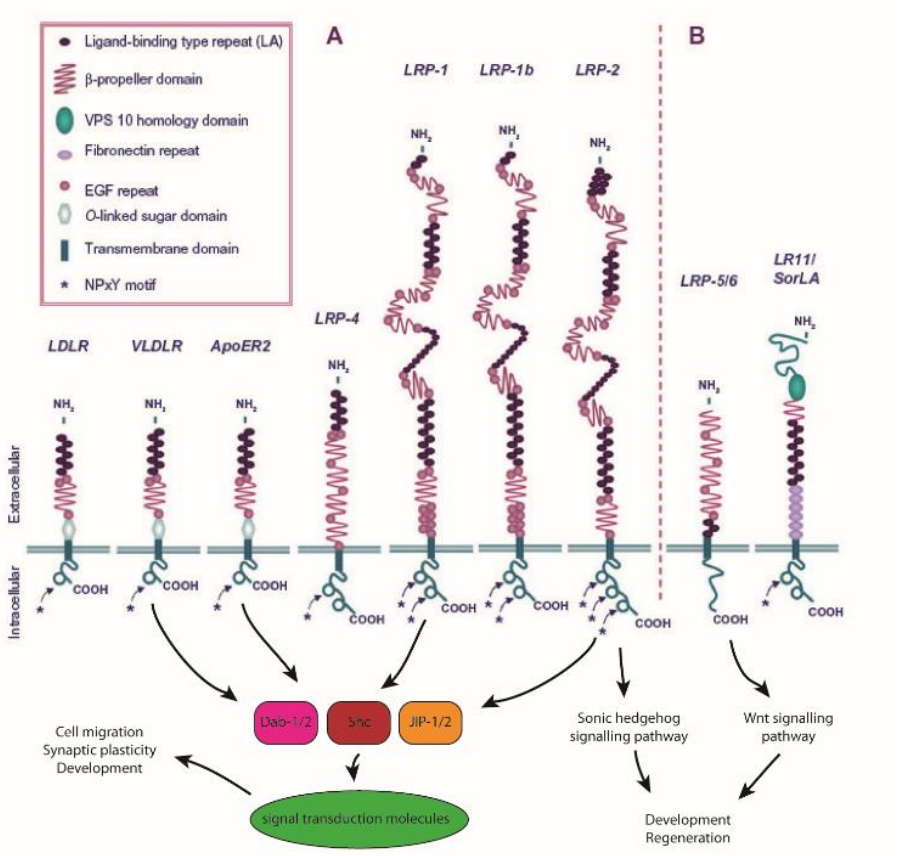

***Fig. 5*: Detailed structural description of LDL-receptor family members, related receptors and their signalling pathways.** *The LDL receptor family contains structural domains conserved across all members. From these receptors ApoER2 and VLDLR are known to be involved in Reelin signalling. LRP-1 and LRP-2 are co-receptors and also signal via the three depicted adaptor molecules. Every signalling event is transferred to signalling molecules such as Akt or ERK. LRP2 and LRP5/6 are also involved in developmental processes and tissue regeneration which is mediated by the sonic hedgehog- or Wnt signalling pathway respectively. (A) Depiction of all seven members of the LDL-receptor family with in-depth characterisation of structural features. (B) Comparison of three closely related receptors with distinct alterations in their anchor region and N-terminal domain. Depicted signalling pathways are simplified. Reprinted and modified from (Emonard & Marbaix, 2015). For information as to references, see respective paragraphs.*

Furthermore, they can trigger signalling cascades via the NPxY motif which is a target for adaptor and scaffolding proteins (Fig. 5) such as Dab-1 (Gotthardt, et al., 2000), Shc (Barnes, et al., 2001) or JIP-1/2 (Gotthardt, et al., 2000). These lead to alterations in cell migration (Trommsdorff, et al., 1999), synaptic plasticity (Gotthardt, et al., 2000) or activity in proteolytical processing (Nykjaer, et al., 1992). Furthermore, LRP2 and LRP5/6 are known to be involved in developmental processes (Fig. 5). While LRP2 is involved in sonic hedgehog signalling (Christ, et al., 2016), LRP5/6 act as co-receptors for Wnt signalling (Li & Bu, 2005). As previously described some LDL receptors also interact with Clusterin, namely LRP1, LRP2, VLDLR and ApoER2. The best described interacting partner of Clusterin is LRP2, which act together as a recycling machinery for misfolded proteins or cellular debris (Zlokovic, et al., 1996) as well as a recovery system in renal filtration (Morales, et al., 1996). Similar actions can be seen in the interaction with LRP1 (Bartl, et al., 2001; Wyatt, et al., 2011). In case of ApoER2 and VLDLR, Clusterin facilitates signalling effects comparable to Reelin (Leeb, et al., 2014).

1.2.3 Variations of intracellular signalling cascades

The final step in stimulus transmission is the activation of intracellular signalling pathways. They can range from short mechanisms to complex networks which can be further intertwined with each other. One well-described cascade is the Notch signalling pathway that triggers a proteolytical cleavage of its cytoplasmic tail after ligand binding. This domain directly translocates to the nucleus where it alters gene expression (Artavanis-Tsakonas, et al., 1999). Mechanistically different pathways are TGFβ- or Jak/STAT-cytokine-receptor signalling pathways. They are designed as multistep cascades that act via a chain of phosphorylation events, a wide-spread mechanism in signal transduction. Further types of signal transmission include activation of enzymes for second messenger production like adenylate cyclase, conformational changes to allow binding of effector molecules as seen in GTPases or redox-based alterations of various proteins. In diverse signalling cascades, a combination of the mentioned transmission types is essential for a tight regulation. One cellular response that combines mechanisms of protease activity with phosphorylation events is the hedgehog signalling pathway which is indispensable for accurate embryonic development (Nüsslein-Volhard & Wieschaus, 1980; Mohler, 1988) and activation of stem cells (Bhardwaj, et al., 2001). Many essential signalling cascades controlling global cellular responses involve the two molecules Akt and ERK which will be further described in the following paragraphs. Due to their complex nature, however, the description will be reduced to its essentials.

1.2.3.1 Transcription- and translation regulation with MAPK/ERK pathway

Major stimuli for the activation of the MAPK/ERK signalling pathway are growth factors, such as EGF or PDGF and hormones like insulin (Fig. 2). Upon binding to their corresponding receptors, they induce autophosphoryation of the tyrosine residues on the cytoplasmic tail of the receptor, enabling the interaction with SH2 domain-containing adaptor molecules. The crucial adaptor for subsequent ERK activation is GRB2. In case of insulin- and the IGF-1 receptor, the first molecule bound to the receptor is IRS-1 followed by GRB2. Receptor-bound GRB2 presents its SH3 domains which are recognised by a second adaptor called SOS. Thus, SOS is activated and as a consequence removes GDP from the small GTPase Ras which in turn can bind GTP. The bound GTP leads to a reconfiguration of Ras, followed by recruitment of the protein kinase RAF (Avruch, et al., 2001). This kinase is the first in a signalling cascade regulated by directional phosphorylation. RAF phosphorylates MEK followed by ERK. At this point, several pathways branch off to different target molecules which regulate various cell responses. Phosphorylation of ribosomal S6 kinase stimulates protein translation (Pende, et al., 2004), whereas CREB and c-myc are targets that activate genes for cell proliferation and cell cycle control, respectively (Daniel, et al., 2014; Hanson, et al., 1994). This pathway can often be observed to be constitutively activated in tumorigenic cells (Barry, et al., 2001; Jiang, et al., 2014). Studies have shown that the Clusterin gene is also regulated by the MAPK/ERK pathway (Criswell, et al., 2005) and that Clusterin itself signals via ERK in astrocytes to stimulate differentiation (Shim, et al., 2009).

1.2.3.2 Cell cycle regulation with PI3K/Akt pathway

A central signalling pathway in the regulation of various cellular responses is the PI3K/Akt pathway. Triggered by a variety of receptors, Akt and its downstream targets regulate a plethora of different cell responses such as cell differentiation (Mogi, et al., 2008), survival (Jun, et al., 2011), metabolism (Cerniglia, et al., 2015) or structural reorganisation (Qian, et al., 2004). Similar to the MAPK/ERK pathway, it all begins with the binding of an adaptor molecule to the autophosphorylated tyrosine residues of the receptor. In this case the adaptor is called p85 which interacts with p110 after binding. Both molecules together form the active PI3K. Substrate for the kinase activity is a membrane-bound phosphatidylinositol that is phosphorylated to PIP_3. At this point, the signalling pathways already starts to branch as several proteins contain the necessary pleckstrin homology or FYVE domain for binding to PIP_3. Two of those proteins are Akt and PDK1 which are brought in close proximity by binding to PIP_3. Upon interaction with PIP_3, Akt undergoes a conformational change exposing a threonine and serine residue to PDK1. While PDK1 only phosphorylates the Thr residue causing a partial activation of

Akt, other kinases such as PDK2 phosphorylate the Ser residue to grant Akt its full activation. In this state, Akt is capable of regulating major components such as mTOR, GSK3, FOXO, BAD and NF-κB. The PI3K/Akt pathway is an essential mechanism in insulin and IGF-1 signal transduction as well as other pro-survival cell responses rendering it a potential cause for a variety of diseases (Hers, et al., 2011). Similar to ERK, Akt activation also stimulates Clusterin expression (Ma & Bai, 2012). Conversely, Clusterin modulates cell responses via the PI3K/Akt pathway. These responses include pro-survival effects (Jun, et al., 2011; Yu, et al., 2016), meiosis in germ cells (Riaz, et al., 2017) and cell migration (Kang, et al., 2014) but they can also be exploited by cancer cells to promote metastasis (Lamoureux, et al., 2014).

1.3 Clusterin, a good or bad key player in a physiological context

Clusterin was observed in many different physiological setups within a short period of time (Fig. 6). It all started with its discovery in ram rete testis fluid and following experiments showing its clustering effect on different cell types. Following studies addressing the role of Clusterin in the male reproductive tract and spermatogenesis showed an influence of Clusterin on the success rate of *in-vitro*-fertilisation and an association of Clu molecules to spermatozoa (O'Bryan, et al., 1990). The majority of molecules were observed in relation to abnormal spermatozoa, whereas only approximately 10% of normal spermatozoa showed a positive staining for Clusterin. However, in-depth experiments revealed a second Clusterin variant in the acrosome cap in all spermatozoa (O'Bryan, et al., 1994; Atlas-White, et al., 2000; Han, et al., 2012). These differences were assumed to stem from distinct glycosylation patterns which in turn are a prerequisite for the binding of Clusterin to the pattern recognition receptor DC-SIGN on dendritic cells in the female reproductive tract. Evidence for this assertion is the fact that, in contrast to semen Clusterin, serum Clusterin does not bind to DC-SIGN (Sabatte, et al., 2011). Since one of these Clusterin variants was mainly found on abnormal spermatozoa, it was assumed that they are the key for targeted endocytosis by dendritic cells (DC). These cells then present antigens derived from the abnormal spermatozoa causing a desensibilisation of the female immune system towards male antigens (Merlotti, et al., 2015). Additionally, the binding of Clusterin to DC-SIGN blocks the immune system from recognising HIV-1 (Sabatte, et al., 2011). In this case the blockage seems unfavourable, however, HIV-1 exploits the binding to DC-SIGN to reach secondary lymphoid organs, where it infects stationed T cells (Geijtenbeek, et al., 2000). These and other observations (Jenne & Tschopp, 1989) create a link to early publications which showed a regulatory influence of Clusterin on the complement system by inhibiting the proper formation of the C5b-9 membrane attack complex (Kirszbaum, et al., 1989; Murphy, et al., 1988; Ibrahim, et al., 1999).

Further aspects of Clusterin function stem from its ability to bind lipids and its association with HDL (de Silva and H, et al., 1990; Stuart, et al., 1992). The combined ability to inhibit complement activation and to bind to lipids and HDL, makes Clusterin a preferred target in atherosclerosis research, due to its potential protective behaviour (Schwarz, et al., 2008; Gelissen, et al., 1998; Navab, et al., 2005). However, the bivalent character of Clusterin also strikes in this subject, since several other studies showed cytotoxic and promoting effects of Clusterin on the development of atherosclerosis (Miyata, et al., 2001; Millis, et al., 2001; Hamada, et al., 2011). Another intensively debated topic until today is the role of Clusterin in apoptosis. Although early studies postulated a cytoprotective function of Clusterin, the predominant opinion for more than one decade was to the contrary. This opinion arose from the observations which were in relation to the discovery of intracellular Clusterin forms and nClu in particular. As already described in 1.1.2, intracellular Clu forms were shown to bind to Ku70, inhibiting DNA repair mechanisms.

In recent years, Clusterin also became a preferred target as a biomarker in urinary system injuries (Yerramilli, et al., 2016; Won, et al., 2016), for fertility (Novak, et al., 2010; Fukuda, et al., 2016) and several other pathologies (Zhang, et al., 2016; Sol, et al., 2016; Dukic, et al., 2016). Furthermore, the therapeutic value of Clusterin was pushed by observations which were made in relation to cancer treatment. During the progression of prostate cancer, the expression of Clusterin is elevated to act as an anti-apoptotic factor. Antisense oligonucleotide knock-down of the Clusterin gene in prostate cancer-derived cells increased their vulnerability towards typical chemotherapeutical substances (Miyake, et al., 2000). Based on these findings, a novel therapeutic antisense oligonucleotide, called custirsen or OGX-011, was developed as a synergistical additive in established anticancer therapies against prostate cancer (Chi, et al., 2008; Laskin, et al., 2012). Interestingly, this strategy turned out to be also applicable in therapies targeting various types of cancer, such as breast (Biroccio, et al., 2005), lung (Cao, et al., 2005), renal (Nishikawa, et al., 2017) and hepatocellular cancer (Wang, et al., 2015) as well as osteosarcoma (Lamoureux, et al., 2014). In some cases, preclinical trials were completed successfully with promising results, others are still pending. This enabled further data acquisition in following clinical phases, which are currently ongoing up to clinical phase III for prostate and non-small cell lung cancer therapy (Xiu, et al., 2015). An additional therapeutical field of application besides cancer treatment disclosed with the ability of Clusterin to act as a protective component in dry eye disease. The expression of Clusterin at the ocular surface barrier is essential for the prevention of desiccation and structural damage (Bauskar, et al., 2015).

1.3.1 Alzheimer's disease & neuronal illnesses

The most extensively studied pathological occurrence related to Clusterin is its influence on the development and progression of Alzheimer's disease (AD). Distinct features of this neurodegenerative disease are the formation of insoluble plaques which have cytotoxic effects on neuronal networks leading to extensive cortical atrophy. These plaques are formed by insoluble Aβ1-42 peptides, a released fragment stemming from the APP transmembrane protein (Glenner & Wong, 1984; Hardy & Allsop, 1991; Beyreuther & Masters, 1991; Selkoe, 1991), which is cleaved by specific β- and γ-secretases (Busciglio, et al., 1993; Shoji, et al., 1992). A second candidate causing plaque formations are intracellular hyperphosphorylated Tau proteins, delivering their cytotoxic effect directly to the harbouring neuronal cell (Goedert, et al., 1991). Causes for the formation and cytotoxicity of both Aβ and Tau plaques, however, are still not fully elucidated. The most common factor for dominantly inherited early-onset AD are mutations in the genes encoding APP and presenilin 1 & 2 (Goate, et al., 1991; Hendriks, et al., 1992; Wisniewski, et al., 1991; Scheuner, et al., 1996). In contrast, forms of sporadic or nondominantly inherited AD can have a plethora of different triggers. Genetic linkage studies revealed Clusterin as a potential mediator in the formation of late-onset AD (Sillén, et al., 2011) which was further backed by subsequent publications (Lambert, et al., 2013). So far, the best studied candidate, however, is the *APOE* gene in form of the ε4 allele (Strittmatter, et al., 1993). The expressed protein, which is a crucial cholesterol carrier, shows decreased efficiency in removal of Aβ plaques from the cerebrospinal fluid (CSF) compared to other alleles causing accumulation and subsequent aggregation of Aβ (Polvikoski, et al., 1995; Lane-Donovan & Herz, 2017). In general, it is assumed that a disturbed transport and clearance of Aβ from the CSF is a potential trigger for late-onset AD development (Mawuenyega, et al., 2010). Recent studies revealed a possible role of the newly discovered glymphatic system in Aβ clearance malfunction (Iliff, et al., 2012). Further mentioned risk factors in the literature are for example Diabetes/insulin resistance (Hölscher, 2011), elevated cholesterol levels (Kivipelto & Solomon, 2006) and brain injuries (Fleminger, et al., 2003).

Shortly after Clusterin was discovered and characterised, first evidences arose that linked Clusterin to Alzheimer's disease. One observation was the increased level of expressed Clusterin in isolated rat brain with developed AD compared to healthy individuals (May, et al., 1990). This fact was later on confirmed and further examined which led to the conclusion that elevated Clusterin levels correlate with the amount of ApoE ε4 allele variant (Bertrand, et al., 1995; Gupta, et al., 2016), a potent risk factor for late-onset AD. Secondly, early studies also revealed a binding of Clusterin to Aβ (Choi-Miura, et al., 1992a; Ghiso, et al., 1993). Following studies further specified this interaction, showing that Clusterin binds to both Aβ monomers and aggregates (Matsubara, et al., 1995) and actively blocks

plaque formation (Matsubara, et al., 1996). As elucidated with other ligands earlier, Clusterin engaged in its typical chaperone duties by first binding and then delivering its ligand to a corresponding recipient. In this case bound Aβ was either shuttled to glial cells for degradation (Cole & Ard, 2000; Nuutinen, et al., 2007) or to the Blood Brain Barrier for efflux (Zlokovic, 1996; Bell, et al., 2007). Both pathways were shown to be mediated by LRP2 and other members of the LDL receptor family (Zlokovic, et al., 1996; Shibata, et al., 2000). In the early stages of AD, Clusterin exerts a protective function due to its role as a molecular chaperone. However, when it comes to further progression of AD, the role of Clusterin changes to a more bivalent one, as already seen in several other studied subjects. Detailed examination of Aβ plaque formation and Clusterin influence described a ratio-dependent correlation between positive and negative effects of Clusterin. Whilst in an early stage, the expression of Clusterin exceeds the amounts of soluble Aβ during AD development. At this point Clusterin is able to clear upcoming Aβ accumulations via the previously described mechanisms. However, when the ratio of Clusterin to Aβ reaches approximately 1:10, the aggregation and plaque formation is even promoted due to binding but inefficient clearing of Aβ by Clusterin (Yerbury, et al., 2007). Besides that, other studies also assume a promoting cytotoxic effect of Clusterin independent of any ratios (Oda, et al., 1995; Lambert, et al., 1998; DeMattos, et al., 2002).

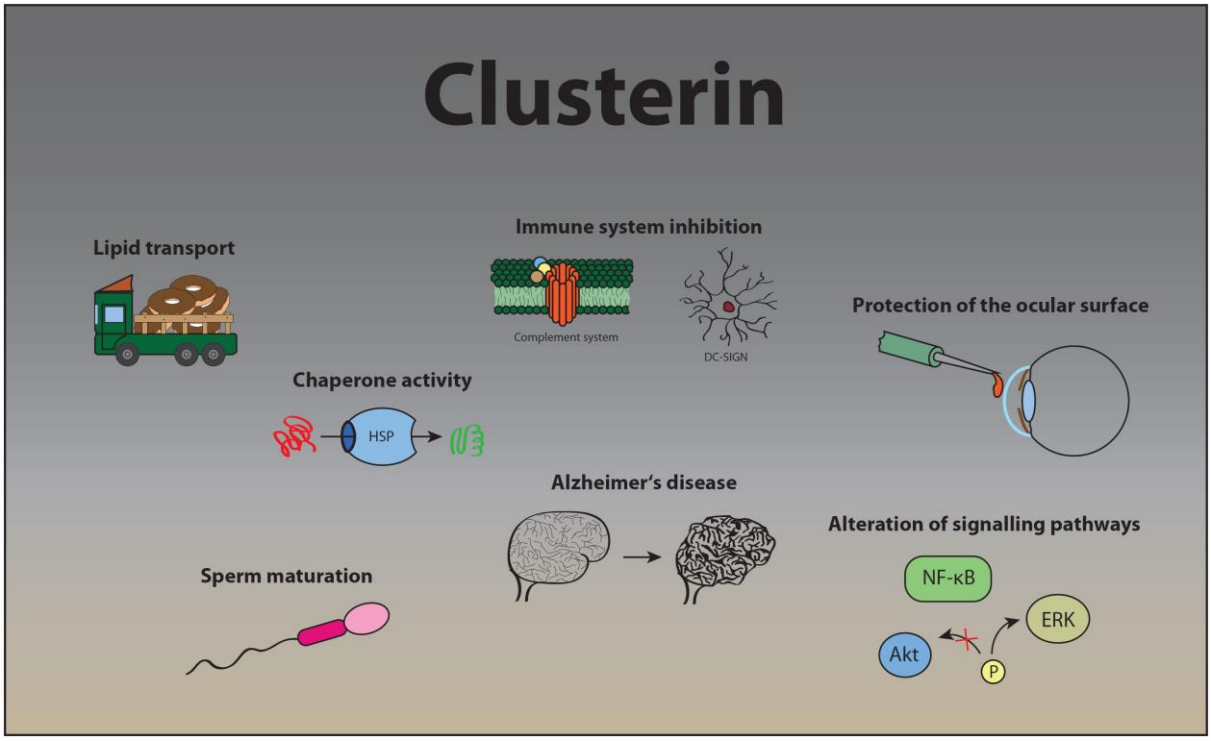

Fig. 6*: *Composition of several different subjects with postulated and proven involvement of Clusterin. *Besides the often-described chaperone activity, Clusterin exhibits distinct roles in sperm maturation, immune system modulation and lipid transport. Furthermore, Clusterin is known to be a crucial component in the clearance of Aβ associated with AD. Recent studies revealed a positive effect of Clusterin in the pathology of dry eye disease. In several studies Clusterin influenced different signalling pathways which will also be addressed in this work. For information about references see respective paragraphs.*

Taken together, Clusterin is involved in mechanisms which cover several aspects of potential risk factors in the development of AD, such as interference in Aβ plaque formation or elimination of Aβ from the CSF with a linkage to ApoE ε4 allele. Additionally, the ability of Clusterin to bind lipids (de Silva and H, et al., 1990) and interfere with the complement system (Kirszbaum, et al., 1989; Murphy, et al., 1988) increases its involvement in AD, since proper cholesterol distribution is essential for neuronal integrity and inflammation caused by brain injuries is a risk factor with growing importance (Salminen, et al., 2009; Ferretti, et al., 2012). All these facts turn Clusterin into a prominent studying target for potential AD-related SNPs (Woody & Zhao, 2016).

1.3.2 Clusterin-Receptor interaction and modulation of signal transduction pathways

As described earlier, Clusterin is involved in binding and transport of various ligands. The major target for this transport is a receptor of the LDL receptor family called LRP2 or megalin. This receptor is also the best described and studied target receptor for Clusterin. In adult organisms, it can be found in many different organs, such as the brain, kidney and hypothalamus (Christensen & Birn, 2002). While in the first two mentioned organs, LRP2 solely acts as an endocytic receptor for degradation or recovery of ligands delivered by Clusterin and other proteins (Zlokovic, et al., 1996; Morales, et al., 1996), the endocytosis of Clusterin in the hypothalamus also enhances leptin signalling cascades (Gil, et al., 2013; Byun, et al., 2014). LRP, another member of the LDL-receptor family, as well as so-called scavenger receptors were also shown to be a target for debris clearance mediated by Clusterin in non-phagocytic cells (Bartl, et al., 2001; Wyatt, et al., 2011). Furthermore, LRP and megalin are not the only LDL receptors which interact with Clusterin. Both the ApoER2 and the VLDL receptor bind Clusterin to trigger a Reelin-like signalling cascade together with the adaptor molecule Dab1 in Reelin-deprived tissue (Leeb, et al., 2014). Recently it was also shown that Clusterin modulates meiosis in germ cells via those two receptors (Riaz, et al., 2017). An already earlier mentioned target receptor of Clusterin is the pattern recognition receptor DC-SIGN. Binding of Clusterin seems to mask male proteins from the female immune system and it also acts as a source for antigen presentation (Sabatte, et al., 2011; Merlotti, et al., 2015). Another link to Alzheimer was also recently discovered by the observation that Clusterin strongly binds to the plexin A4 receptor, a widely distributed receptor in the adult brain. This receptor was shown to be significantly reduced in human AD brains. Knock-out mouse models confirmed these results by demonstrating behavioural impairments (Kang, et al., 2016).

Besides the receptors Clusterin is able to interact with, it can also influence signal transduction pathways for which the corresponding receptor is still not known. One of these pathways is the NF-κB signalling pathway which is involved in apoptotic regulation. Due to the lack of information on how Clusterin excerts its influence on this pathway, it is not surprising that various studies about this subject are highly divergent. The results revealed contradictory data from positive (Xu, et al., 2015; Wang, et al., 2012; Zoubeidi, et al., 2010) and negative (Santilli, et al., 2003; Takase, et al., 2008) regulation of the NF-κB signalling pathway as well as no regulation at all (Prochnow, et al., 2013). Analogous antagonising observations were gathered for the PI3K/Akt signalling pathway, a major cascade in proapoptotic mechanisms. The majority of publications accredit Clusterin a positive stimulus on the Akt signal transduction pathway (Ammar & Closset, 2008; Jun, et al., 2011), however, the opposite was also shown (Jo, et al., 2008). Especially in relation to the stimulating hormone IGF-1, researchers came to no satisfying consensus (Jo, et al., 2008; Ma & Bai, 2012). Nevertheless, studies exist that indistputably describe signalling events mediated by Clusterin. Some of these events involve members of the LDL receptor family. The binding of Clusterin to ApoER2 and VLDLR is shown to stimulate male germ cell meiosis (Riaz, et al., 2017) and to induce a Reelin-like signalling pathway (Leeb, et al., 2014). Whereas in case of LRP2, Clusterin administration potentiates the Leptin signalling in the hypothalamus (Byun, et al., 2014). In addition, seminal Clusterin was observed to play a crucial role in immunogenic responses mediated by the binding to DC-SIGN (Merlotti, et al., 2015).

1.4 Aims and objectives

Previous studies revealed an involvement of Clusterin in various signal transduction pathways. Despite the observations made, it was unclear how Clusterin modulates intracellular signalling molecules. Known receptors that interact with Clusterin are DC-SIGN and members of the LDL receptor family, however, only ApoER2 and VLDLR were shown to transmit a signalling stimulus triggered by Clusterin. The initial goal of this work is aimed at the revelation of additional Clusterin-interacting receptors that could close the gap in the Clusterin-mediated activation of intracellular signalling molecules such as Akt. In the process of examining various candidates of the receptor tyrosine kinase family, two crucial ligands, namely insulin and IGF-1, emerge as potential interacting partners of Clusterin. Both ligands are involved in the development and progression of Alzheimer's disease. The subsequent analysis of mediating effects of Clusterin on insulin and IGF-1 stimulation is based on the assumption of a potential role in AD. Main investigation target in the modulation of signal transduction is Akt, which plays a central role in both insulin and IGF-1 signalling. Since LRP2 is a major interacting partner of Clusterin and essential for its role of Aβ clearance as well as a known co-receptor of the insulin receptor, its role in Clusterin-mediated signal modulation is assessed. For an overall evaluation of the role of Clusterin in cell survival and growth, its effect on the cellular proliferation and metabolism in the face of IGF-1 stimulation is further studied.

These studies should involve cell viability experiments, the execution of binding assays and examination of structural requirements which mainly focus on the elucidation of the interaction of Clusterin and IGF-1. To assess the ability of Clusterin to actively bind IGF-1, several binding studies are executed. During these studies IGF-1 should be subjected to various denaturing conditions to elucidate the necessity of a native IGF-1 conformation for the binding by Clusterin. By introducing mutations in structurally crucial domains of the Clusterin molecule, the binding site(s) to IGF-1 were assessed. Furthermore, the mutants were biochemically analysed to determine variations in structure, stability and biological activity. The biological activity of the different Clusterin variants should be measured by chaperone assays and by examining the influence of the introduced mutations on IGF-1 binding.

These analyses should facilitate new approaches for the elucidation of Clusterin-mediated cell signalling and the necessity of various structural elements for the biological activity of Clusterin. In the long run, these insights should broaden the understanding of the physiological role of Clusterin, especially in respect to the development of AD.

2 Materials

2.1 Equipment

The following list contains all equipment used in the process of this thesis. Routine equipment like freezers, refrigerators, shaker, scales, etc. are not listed separately.

Type	Name	Company
Agarose gel chamber	custom-made, 13 x 10 cm, 10 x 5 cm	-
Analytical balance	Excellence XA204 DeltaRange	Mettler Toledo
Aspirator	SUC-O-MAT	WISA
Blotting device	Mini Trans-Blot Module	Bio-Rad
Bottle-top filter unit	Polysulfone reusable bottle-top filter, 45 mm, 500 mL	Thermo Scientific
CD-spectrophotometer	J-815	Jasco
	MPTC-490S	Jasco
CO_2-incubator	01-22021	Binder
Cuvette	Suprasil Quarz Küvette	Hellma Analytics
Documentation microscope	Motic AE-21	Motic
	Moticam 1000	Motic
Electronic dispenser	Multipette® stream	Eppendorf
Filtration unit	Minimate™ TFF Capsule with Omega™ membrane (30 kDa)	Pall
FPLC	Äktabasic 10	Amersham Pharmacia Biotech
	XK16/20 column	GE Healthcare
	C10/10 column	GE Healthcare
Gel imaging system	AlphaImager	Alpha Innotech
	Motorized zoom lens	Computar
Graduated pipette (glass)	5 mL, 10 mL, 20 mL	Brand
Hemocytometer	Zählkammer Neubauer improved	Roth
HPLC	Varian Prostar	Varian
	Vydac 208TP™ C8 column	Grace
	Vydac 218TP™ C18 column	Grace
Incubation shaker	Ecotron	Infors HAT
Incubator	BM600	Memmert
Isoelectric focusing system	IPGphor	Amersham Pharmacia Biotech
Microplate spectrophotometer	PowerWave XS	BioTek
Microscope	Wilovert S	Hund
PCR thermocycler	peqSTAR 2X Gradient	Peqlab
	Tpersonal	Biometra
Peristaltic pump	MP-GE	Ismatec
pH-meter	pH-Meter 765 Calimatic	Knick
Pipette	10 µL, 100 µL, 200 µL, 1000 µL	Eppendorf, Gilson
	Transferpette® 5 mL, 10 mL	Brand
Pipette controller	accu-jet®	Brand
Power supply	Power Pack P25 T	Biometra

	E734	Consort
Refrigerated centrifuge	Multifuge 1S-R, Sorvall Heraeus 75002000 & 75003348 rotor	Thermo Scientific
	Sigma 3K15	Sigma Laborzentrifugen
Safety cabinet	Safe 2020 1.2	Thermo Scientific
Scanner	CanoScan LiDE 210	Canon
SDS-PAGE device	Mini-PROTEAN Tetra Cell	Bio-Rad
Spectrophotometer	BioPhotometer plus	Eppendorf
Tabletop centrifuge	Spectrafuge™ Mini	Labnet
	Spectrafuge™ 24D	Labnet
Ultrasonic cell disruptor	HTU SONI130	Heinemann
Western Blot imaging system	Stella 3200	Raytest

2.2 Consumables

The following list contains all consumables used in the process of this thesis.

Type	Name	Company
2D-GE strips	IPG *Blue*Strip 4-7 / 7 cm	SERVA
Blotting paper	BF4	Sartorius
Cell culture flasks	CELLSTAR® filter cap 25 cm2, 75 cm2, 175 cm2	Greiner Bio-One
Cell culture microplates	Advanced TC™ 96-well	Greiner Bio-One
Cell culture multiwell plates	CELLSTAR® 6 well, 12 well, 24 well, 48 well	Greiner Bio-One
Centrifugal filter unit	Amicon® Ultra-15 Centrifugal Filter Unit 50,000 NMWL	Merck Millipore
Cryogenic tubes	Cryo.s™ 2 mL	Greiner Bio-One
Cuvettes	Uvette® 220 nm – 1600 nm	Eppendorf
Injection needles	FINE-JECT®	Henke-Sass Wolf
Membrane filter	Cellulose acetate membrane filter, 0.2 µm pore size	Sartorius
Microplates	96-well; MICROLON® 96-well ELISA	Greiner Bio-One
Nitrocellulose membrane	Amersham Protran Supported 0.45 NC	GE Healthcare
Pasteur pipettes	LLG-Pasteur pipettes, Soda-lime glass	Buddeberg
Petri dish	94/16 mm	Greiner Bio-One
Pipette filter tips	peqGOLD SafeGuard™ 10 µL, 100 µL, 1000 µL	Peqlab
Pipette tips	200 µL, 1000 µL	Greiner Bio-One
	10/20 µL Xl RPT	STARLAB
	5 mL, 10 mL	Brand
Reaction tubes	2 mL, 1.5 mL, 0.5 mL	Greiner Bio-One
	Sapphire PCR tube 0.2 mL	Greiner Bio-One
Scalpel	Cutfix® single-use	B. Braun
Serological pipettes	5 mL, 10 mL, 25 mL	Sarstedt
Syringes	1 mL NORM-JECT® Luer	Henke-Sass Wolf
Tubes	15 mL, 50 mL	Greiner Bio-One

2.3 Software & web applications

Any software used for the analysis or visualisation of gathered results is listed in the following table. Software that is specifically designed for equipment and necessary for its operation is not listed separately.

Type	Name (+ URL)	Company
CD-spectrum analysis	DichroWeb (http://dichroweb.cryst.bbk.ac.uk/html/home.shtml)	Dr. L. Whitmore (Whitmore & Wallace, 2004)
Data visualisation and statistical analysis	Prism 6	GraphPad Software
Graphical visualisation	Adobe Illustrator CS5	Adobe Systems
Molecular biology software	Serial Cloner 2.6.1	Serial Basics
Nucleotide/Protein sequence alignment	Web BLAST (https://blast.ncbi.nlm.nih.gov/Blast.cgi)	NCBI
Primer design	NetPrimer (http://www.premierbiosoft.com/netprimer/)	PREMIER Biosoft
Protein sequence alignment	EMBOSS Needle (http://www.ebi.ac.uk/Tools/psa/emboss_needle/)	EMBL-EBI
Western Blot quantification	Image Studio™ Lite	LI-COR Biotechnology

2.4 Chemicals

The following list contains all basic chemicals and reagents used in the process of this thesis.

Name	Serial ID	Company
10x PBS	L182-10	Biochrom
10x Trypsin	T4174	Sigma Aldrich
Acetic acid	3738.5	Roth
Acetone	CP40.1	Roth
Acetonitrile	10407440	Fisher Scientific
Agarose	28649	FMC
Albumin fraction V (BSA)	T844.2	Roth
Ampicillin	K029.2	Roth
APS	9592.3	Roth
Blasticidin S hydrochloride	CP14.2	Roth
Bromophenol blue	1610404	Bio-Rad
Carbon dioxide	A71001501	Westfalen
Catalase	C9322	Sigma Aldrich
CHAPS	1479.2	Roth
Chloramphenicol	3886.2	Roth
DEPC	K028.3	Roth
Diethanolamine	0332.1	Roth
Disodium phosphate dihydrate	4984.3	Roth
DMEM	D5671	Sigma Aldrich

DMEM low glucose	D5546	Sigma Aldrich
DMSO	A994.1	Roth
DNA Gel Loading Dye (6X)	R0611	Thermo Scientific
dNTP	R0192	Thermo Scientific
DTT	6908.1	Roth
EDTA	8043.2	Roth
EGF	E9644-.2MG	Sigma Aldrich
Ethanol p.a.	32205-1L	Sigma Aldrich
Ethidium bromide solution, 0.025%	HP47.1	Roth
FBS	F0804	Sigma Aldrich
Glycerin	3783.1	Roth
Glycine	3908.3	Roth
GST	recombinantly expressed	by Steven Wolf & Philipp Rohne
IGF-1	100-11	Peprotech
IGFBP3	10430H07H100	Sino Biological
Imidazole	A1073.0500	AppliChem
Insulin	I6634-50MG	Sigma Aldrich
IPTG	37-2020	Peqlab
Isopropanol	CP41.3	Roth
LB-agar	X969.2	Roth
LB-medium	X964.2	Roth
L-glutamine	G7513	Sigma Aldrich
Lysozyme	8259.2	Roth
Magnesium chloride hexahydrate	2189.1	Roth
Methanol	CP43.3	Roth
Mineral oil	17-1335-01	GE Healthcare
Monosodium phosphate dihydrate	T879.2	Roth
Nitric acid, 65%	124660010	Acros
Non-essential amino acids	M7145	Sigma Aldrich
Opti-MEM	31985047	Invitrogen
Panexin	P04-95800	Pan Biotech
Penicillin/Streptomycin	P0781	Sigma Aldrich
PMSF	6367.1	Roth
pNPP	4165.1	Roth
Poly-dT 12-18 primer	HP27.1	Roth
Powdered milk	T145.2	Roth
Protein A sepharose	17-0780-01	GE Healthcare
Protino Ni-IDA resin	745210.30	Macherey-Nagel
rhHGF	11343413	ImmunoTools
Roti®-Blue, 5x	A152.1	Roth
Roti®-Quant, 5x	K015.1	Roth
Rotiphorese® Gel 30 (37,5:1)	3029.2	Roth
SDS	4360.2	Roth
Sodium acide	19038-1000	Acros
Sodium bicarbonate	6329	Merck
Sodium carbonate monohydrate	S-4132	Sigma Aldrich

Sodium chloride	3957.2	Roth
Sodium dichloroisocyanurate	204115000	Acros
Sodium hydroxide	6467	Merck
Sodium pyruvate	S8636	Sigma Aldrich
TCA	8789.2	Roth
TEMED	2367.3	Roth
TFA	P088.1	Roth
Tris	4855.5	Roth
Tris hydrochloride	9090.3	Roth
Triton X-100	A1388.1000	AppliChem
Tween20	9127.1	Roth
Urea	3941.2	Roth

2.5 Buffers & solutions

All buffers and solutions prepared for the execution of experiments are listed with their respective composition. If not stated differently in the table, all buffers were prepared with mpH_2O. Buffers marked with an asterisk (see 3.11.) in the subsequent paragraphs were sterile filtered and degasified before usage. For buffers with distinct concentration indication in the name, the recipe is not listed separately.

Name	Component	Amount
0,1 M Sodium bicarbonate		
0,1 M Sodium carbonate monohydrate		
0.1% DEPC-H_2O		
0.1 M Nitric acid		
0.1 M Sodium hydroxide		
0.5 M Sodium hydroxide/0.04 M Sodium dichloroisocyanurate		
1M Tris, pH 6.8		
2 M Sodium hydroxide		
3M Tris, pH 8.8		
Ampicillin, 1000x	Ampicillin	100 mg/mL
APS, 10%		
Blasticidin S, 1000x	Blasticidin S hydrochloride	50 mg/mL
Cell lysis buffer, pH 8	Tris	50 mM
	Sodium chloride	25 mM
	Triton X-100	0.1% (v/v)
	Glycerin	7% (v/v)
add for prokaryotic cell lysis buffer:	PMSF	0.1 mM
	Lysozyme	1 mg/mL
add for eukaryotic cell lysis buffer:	cOmplete™ ULTRA Tablets	1 tablet/10 mL
	Phosphatase Inhibitor Cocktail Set V, 50X	2% (v/v)

Chloramphenicol, 1000x	Chloramphenicol Ethanol	34 mg ad. 1 mL
Coating buffer, pH 9.5	0,1 M Sodium bicarbonate 0,1 M Sodium carbonate monohydrate	70% (v/v) 30% (v/v)
Coomassie staining solution	mpH_2O Methanol Roti®-Blue, 5x	60% (v/v) 20% (v/v) 20% (v/v)
Destaining solution	mpH_2O Methanol	75% (v/v) 25% (v/v)
ELISA substrate solution	pNPP Diethanolamine Magnesium chloride hexahydrate	1 mg/mL 10 mM 0,5 mM
Elution buffer, pH 8	Monosodium phosphate dihydrate Sodium chloride Imidazole	50 mM 300 mM 250 mM
Equilibration buffer, pH 8.8	Urea Tris Glycerin SDS Bromophenol blue DTT	6 M 50 mM 30% (v/v) 2% (w/v) 1 µM 80 mM
Ethanol, 20%		
Lew, pH 8	Monosodium phosphate dihydrate Disodium phosphate dihydrate Sodium chloride	5.8 mM 44.2 mM 300 mM
Lew/7% glycerin		
PBS, 1x		
PBST	PBS, 1x Tween 20	2 L 2 mL
PBST/5% powdered milk (w/v)		
Phosphate buffer, pH 7	Monosodium phosphate dihydrate Disodium phosphate dihydrate	0.95 mM 9.05 mM
Precipitation buffer, 10x	Monosodium phosphate dihydrate Disodium phosphate dihydrate Sodium chloride	0.5 M 0.5 M 1.5 M
Rehydration buffer	Urea CHAPS Bromophenol blue SERVA HPE™ IPG strip buffer DTT	8 M 2% (w/v) 1 µM 0.02% (v/v) 80 mM
Rotiquant, 20%		
SDS, 10%		
SDS-loading buffer, 1x		

SDS-loading buffer, 5x	Tris hydrochloride	0.225 M
	Glycerin	50% (v/v)
	SDS	5% (w/v)
	Bromophenol blue	0.05% (w/v)
for reducing SDS-PAGE:	DTT	80 mM
SDS-PAGE resolving gel, 9%	mpH_2O	5.6 mL
(for 2 gels)	Rotiphorese® Gel 30 (37,5:1)	3 mL
	3M Tris, pH 8.8	1.25 mL
	SDS, 10%	100 µL
	APS, 10%	75 µL
	TEMED	15 µL
SDS-PAGE stacking gel	mpH_2O	3.45 mL
(for 2 gels)	Rotiphorese® Gel 30 (37,5:1)	850 µL
	1M Tris, pH 6.8	630 µL
	SDS, 10%	50 µL
	APS, 10%	37.5 µL
	TEMED	7.5 µL
SDS-Running buffer, 5X, pH 8.8	Tris	0.5 M
	Glycine	1.92 M
	SDS	0.5% (w/v)
Solvent A	TFA	1 mL
	mpH_2O	ad. 1 L
Solvent B	Acetonitrile	900 mL
	TFA	1 mL
	mpH_2O	ad. 1 L
TAE-buffer, 50x	Tris	2 M
	Acetic acid	1 M
	EDTA	50 mM
Tank blot buffer, pH 8.3	Tris	25 mM
	Glycine	150 mM
	Methanol	20% (v/v)
TBS, 25x, pH 7.5	Tris	1.25 M
	Sodium chloride	3.75 M
TBST	TBS, 1x	1 L
	Tween 20	1 mL
TBST/2% Albumin fraction V (BSA) (w/v)		
Trypsin, 1x		

2.6 Cell culture media

The following list contains all media used for cultivation, selection and storage of eukaryotic and prokaryotic cells.

Starvation Medium		**N2A / Hep G2**	**SK-N-MC / HEK-293**
	DMEM	480 mL	485 mL
	Sodium pyruvate	5 mL	5 mL
	L-glutamine	5 mL	5 mL
	Non-essential amino acids	5 mL	-
	Penicillin/Streptomycin	5 mL	5 mL

Name	Component	Amount
Freezing medium (eukaryotes)	FBS DMSO	90% (v/v) 10% (v/v)
Growth medium	Starvation medium FBS	450 mL 50 mL
Selection medium	Growth medium with 1:1000 Blasticidin S, 1000x	
Freezing medium (prokaryotes)	LB-medium Glycerin	75% (v/v) 25% (v/v)
LB-medium + antibiotics	antibiotics are added 1:1000 to prepared LB-medium	
LB-agar + antibiotics	antibiotics are added 1:1000 to prepared LB-agar	

2.7 Kits & reagents

The following list contains all commercially available kits and ready-to-use reagents used in the process of this thesis.

Name	Type & Serial ID	Company
CellTiter 96® Aqueous One Solution Cell Proliferation Assay	Cell viability measurement, G3580	Promega
GeneJET Plasmid Miniprep Kit	Plasmid preparation, K0503	Thermo Scientific
innuPREP Gel Extraction Kit	Agarosegel extraction, 845-KS-5030250	Analytik Jena
innuPREP RNA Mini Kit	RNA preparation, 845-KS-2040250	Analytik Jena
Lipofectamine™ 3000	Transfection reagent, L3000008	Thermo Scientific
Maxima Hot Start Green PCR Master Mix (2X)	PCR premix, K1062	Thermo Scientific
NucleoBond® Xtra Midi EF	Plasmid preparation, 740420.10	Mackerey-Nagel
PathScan® RTK Signaling Antibody Array Kit	Multiplex RTK screening, 7982S	NEB
Western Lightning Plus-ECL	Chemiluminescent detection solution, NEL104001EA	Perkin Elmer

2.8 Enzymes & inhibitors

The following list contains all commercially available enzymes and inhibitors used in the process of this thesis.

Name	Type & Serial ID	Company
***BamHI* (+ 10x Unique buffer)**	Restriction enzyme, ER0051	Thermo Scientific
cOmplete™ ULTRA Tablets	Protease inhibitor cocktail, 05892791001	Roche
HindIII	Restriction enzyme, ER0501	Thermo Scientific
KAPAHiFi PCR Kit	PCR Polymerase with proof-reading ability, 07-KK2100-01	Peqlab
LY294002	PI3K inhibitor, L9908	Sigma Aldrich
Phosphatase Inhibitor Cocktail Set V, 50X	Phosphatase inhibitor cocktail, 524629-1ML	Merck
RevertAid Reverse Transcriptase	Reverse transcription enzyme, EP0441	Thermo Scientific
SERVA HPE™ IPG strip buffer	2D-gel electrophoresis buffer, 43368.01	Serva
T4 DNA Ligase	DNA ligation enzyme, EL0014	Thermo Scientific

2.9 Marker & Standards

The following list contains all commercially available standards for agarose gel and SDS-PAGE analysis used in the process of this thesis.

Name	Type & Serial ID	Company
GeneRuler 100 bp Plus DNA Ladder	Agarose gel DNA standard, SM0322	Thermo Scientific
MassRuler Express Forward DNA Ladder Mix	Agarose gel DNA quantification standard, SM1283	Thermo Scientific
PageRuler™ Prestained Protein Ladder, 10 to 180 kDa	SDS-PAGE protein standard, 26616	Thermo Scientific

2.10 Primer

The list contains all primers used in the process of this thesis. For each target, the forward and reverse primer is given followed by its specific melting temperature (T_m).

Name	Forward primer (5' -> 3')	T_m	Reverse primer (5' -> 3')	T_m	Usage
ApoER2 human	GGAGAACTGCTCAGATTGG	52	CAGGGTAGTCCATCATCTTC	51	RT-PCR
ApoER2 mouse	GTCACCGCTGCTGTCATTGG	60	GAGGGTTCTTCGGGAGTTGG	61	RT-PCR
c-Met/HGF-R	CTTGAACAGAATCACTGACATA	50	TTCATCCAGCATACAGTTTC	50	RT-PCR
hsClu-Cys mutation C113A	CAGGCAGGGCTTAGCCTCTTCCCAG	72	CTGGGAAGAGGCTAAGCCCTGCCTG	72	in vitro-mutagenesis
hsClu-Cys mutation C305A	ACAAGATCTCCCGAGCCTTGTCACACTG	72	CAGTGTGACAAGGCTCGGGAGATCTTGT	72	in vitro-mutagenesis
hsClu-Pro mutation	GAACGGGTCTGGCATGACATCTGGC	72	GCCAGATGTCATGCCAGACCCGTTC	72	in vitro-mutagenesis
LRP1 mouse/human	TGATGCCTGAGTGCCAGT	56	GTTGGTAGGCTTGTCAGG	56	RT-PCR
LRP2/Megalin human	CAGGAACAACCGCAGTA	49	CTTCACTCATTGCCATTG	49	RT-PCR
LRP2/Megalin mouse	CGAGAGGCATCCCTCCAGGGACGACA	71	GGATCTATGGACCTTCCATAGTTCTG	63	RT-PCR
pcDNA6	TAATACGACTCACTATAGGG	53	CTGGCAACTAGAAGGCACAG	59	*in vitro*-mutagenesis, colony PCR, sequencing

2.11 Plasmids

The following list contains all plasmids used for cloning and transformation/transfection of cells.

Name	Description	Company
pcDNA6/V5-His B	Basic plasmid (see Fig. 7)	Life technologies
pcDNA6-msClu	Plasmid containing the msClu gene	generated by Koch-Brandt workgroup
$pT_7H_6FX\alpha_2MRAP$	Plasmid containing the human RAP gene	generous gift by Prof. Dr. T. Willnow

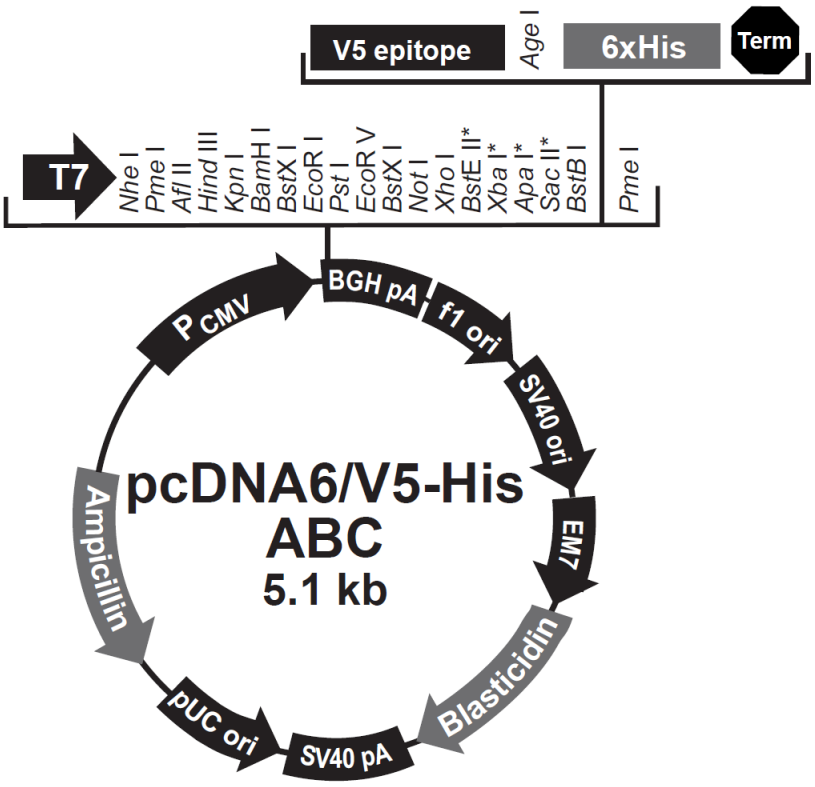

Fig. 7: Structural overview of the pcDNA6 vector used for the cloning and transfection of native Clusterin and variants. *For the experiments, the pcDNA6 variant B was used. Reprinted and modified from the electronical manual of the product by Thermo Scientific.*

2.12 Antibodies

The following list contains all antibodies used in the process of this thesis. For the working dilution the 35hosphor-antibodies and respective secondary antibodies were always diluted in TBST/2% BSA. All other antibodies were diluted in PBST/5% powdered milk. The given working dilution was used in all Western blot experiments. For working concentrations of other applications, such as ELISA, refer to the respective figure legends.

Name	Serial ID	Working dilution	Company
Primary antibodies			
6x-His Tag	MA1-21315	1:1000	Thermo Scientific
Akt	2920S	1:1000	NEB
Akt pThr308	4056S	1:1000	NEB
Clusterin β-chain	sc-6419	1:1000	Santa Cruz
IGF-1 receptor beta	9750S	1:1000	NEB
Insulin receptor beta	3020S	1:1000	NEB
Insulin receptor pTyr1146/IGF-1 receptor pTyr1131	3021S	1:1000	NEB
p44/42 MAPK (Erk1/2)	4695S	1:1000	NEB
p44/42 MAPK (Erk1/2) (pThr202/pTyr204)	4377S	1:1000	NEB
V5 tag	R960-25	1:5000	Thermo Scientific
α-Tubulin	T5168	1:5000	Sigma Aldrich
Secondary antibodies			
Anti-Goat IgG-HRP	A5420-1ML	1:10000	Sigma Aldrich
Anti-mouse IgG-AP	12-446		Upstate
Anti-mouse IgG-HRP	7076S	1:10000	NEB
Anti-rabbit IgG-HRP	7074S	1:10000	NEB

2.13 Cell lines

The list contains all cell lines used in the process of this thesis.

Name	Description
HEK-293	Human embryonic kidney cells
Hep G2	human hepatocellular carcinoma cells
N2A	Mouse neuroblastoma cells
SK-N-MC	Human neuroblastoma cells
HEK-293-hsClu-RIVQ	HEK-293 stably transfected with pcDNA6-hsClu-RIVQ plasmid
BL21	*E.coli* expression strain, chloramphenicol resistance
DH5α	*E.coli* cloning strain

3 Methods

In this section, standard procedures which were used during experimental projects are described. Besides a quick glimpse on the basic principles, the practical course of action for each method is explained step-by-step. Variations in experimental conditions, such as incubation times, working concentrations for reagents or general alterations will be indicated directly in the caption of respective figures.

3.1 Eukaryotic cell culture

All work related to cellular-based experiments was executed under sterile conditions on a sterile workbench. This includes the direct work with cell lines described in upcoming sections as well as preparation of reagents and solutions used in experiments done with cells. Cultivation of eukaryotic cells was always executed in a CO_2-incubator set to 37 °C with a humidified atmosphere containing 5% CO_2.

3.1.1 Propagation of adherent cell lines

A fresh cryo vial of eukaryotic cells suspended in freezing medium was retrieved from a stock stored at -80 °C and thawed at 37 °C in a water bath. The completely thawed cell suspension was added dropwise to a 15 mL tube filled with 5 mL of cell line specific growth medium to dilute the DMSO-containing freezing medium. After centrifuging the tube at 1000 xg for 5 min, the supernatant was aspirated and the residual cell pellet was resuspended in 10 mL growth medium. For propagation, the whole suspension was transferred to a T75 tissue culture flask and filled up to 15 mL (30 mL for T175 flasks) with growth medium.

Cells were then cultivated in an incubator set to 37 °C with a humidified 5% CO_2 atmosphere until they reached full confluency. For further steps, the cells had to be harvested by removing the growth medium and by rinsing the cell layer with 5 mL 1x PBS. To detach cells from the plastic surface, they were covered with 3 mL of 1x trypsin and kept in the incubator for 3 min (5 min for HepG2). With the addition of 7 mL growth medium the trypsin was inactivated and residual cells were washed of the plastic surface. The mixture of cells, inactivated trypsin and growth medium was transferred to a 15 mL tube and again centrifuged as mentioned above. The cell pellet was separated from the supernatant and dissolved in 10 mL growth medium.

At this point, cells could be either used for experimental approaches, setting up a new -80 °C cryo stock or continuous cultivation.

For the last mentioned option, the obtained cell suspension was diluted 1:2 – 1:10 with growth medium depending on the cell demand for upcoming experiments. As before, 15 mL of the now diluted cell solution were transferred back to one or more T75 culture flasks, if needed. All used cell lines were kept in culture for no more than six passages before a new cryo stock was used.

3.1.2 Preparing cell-based experiments

To guarantee similar conditions throughout every experimental setup, the amount of cells used in each approach had to be kept constant. Therefore, the cell content in the harvested 10 mL of suspension had to be determined. By loading a Neubauer haemocytometer with 10 µL of a 1:10 (1:20 for HepG2) diluted aliquot, the amount of cells was counted and extrapolated to obtain a final concentration of cells per mL.

For following general experimental procedures harvested cells were seeded in 6-well plates (except MTS-assays) with 250,000 cells per well (500,000 for HepG2) (except in experiments testing for optimal cell density) in a final volume of 2 mL growth medium. Seeded plates were kept in the incubator for 24 h (46 h for HepG2) before replacing the growth medium with starvation medium. To do so, the growth medium was aspirated and the cell layer in each well was rinsed with 1 mL 1x PBS, followed by addition of 1,5 mL starvation medium. After another 24 h (2 h for HepG2) in the incubator, the plates were ready for subsequent stimulation with different reagents.

3.1.3 Long-term storage of cell lines

Starting from the harvested cell suspension, the amount of cells in solution was calculated as described above. For each cryo tube 1,000,000 cells (3,000,000 cells for HepG2) were transferred to a new 15 mL tube and centrifuged at 1000 xg for 5 min. The supernatant was removed and the cell pellet was resuspended in 1 mL freezing medium per cryo tube. The explicitly labelled cryo tubes were filled with the prepared cell solution and quickly stored in an isolated container at -80 °C.

3.1.4 Stimulation and harvesting of cell lines

The prepared 6-well plates were stimulated with different reagents and under varying conditions. In general, to treat one well, the needed stimulants were added to a 1.5 mL tube and mixed with appropriate amounts of medium from the respective well to obtain a final reaction volume of 1 mL. The rest of the medium from the well was discarded. The conditioned medium was then returned to the well. The stimulated plate was brought back to the incubator and was incubated for the indicated times in the corresponding figures in the results section. In case of preincubation experiments, the procedure was the same for the pre-stimulants. To apply the second stimulants, they were again added to a 1.5 mL tube but then mixed with approximately 200 µL of reaction volume from the well. The solution was returned to the well and the plate was briefly swayed before placing it back into the incubator.

After the appropriate incubation time, the cells had to be harvested. To do so, the supernatant was aspirated and the cell layer was rinsed with 1 mL 1x PBS before 80 µL of eukaryotic cell lysis buffer was added. The plates were incubated at 4 °C to fully lyse cells. After this step, cells were scraped off of the well surface and the emulsion of cell debris and lysis buffer was transferred to a 1.5 mL tube. To remove cellular debris from soluble components, the samples were centrifuged at 20.000 xg for 30 min. The supernatant containing the soluble cell extract was collected and either directly used in assays or stored at -20 °C for future experiments.

3.2 *In-vitro* Mutagenesis

For the *in-vitro* mutagenesis of Clusterin a so-called fusion PCR was used (Fig. 8). In this method two independent amplificates were generated by using a primer flanking one end of the gene of interest and one spanning the site of mutagenesis. The primers at each end of the gene contained a sequence for restriction enzymes for the subsequent vector cloning while the two primers spanning the site of mutation contained the actual mutated nucleotide sequence (Fig. 8, purple asterisk) and are complementary to each other. Together with those primer pairs, the Clusterin gene template was amplificated in two independent PCRs (see 3.5; Fig. 8, Step 1). The amplificates were separated with an agarose gel and the Vol.s of interest were cut out from the gel under UV-light. The gel pieces were then solubilised to isolate the generated amplificates. This was done with the innuPREP Gel Extraction Kit according to instructions in the manual. The isolated amplificates were then mixed and used in a subsequent PCR as template (Fig. 8, Step 2). As primers, gene-flanking primers were used. Due to the complementary mutated sequence on one end of each amplificated, they are able to dimerise in this

region. In the PCR process the primer then attached to the dimerised hybrid and the polymerase filled in the missing nucleotides until it reached the end of the dimerised amplificate. The resulting hybrid amplificates then contained a restriction site on each end and the mutation at the desired site. The final amplificate was then again separated and purified from an agarose gel. For more details about the generation of the mutated Clusterin sequences, see the bachelor thesis by Christian Czysch.

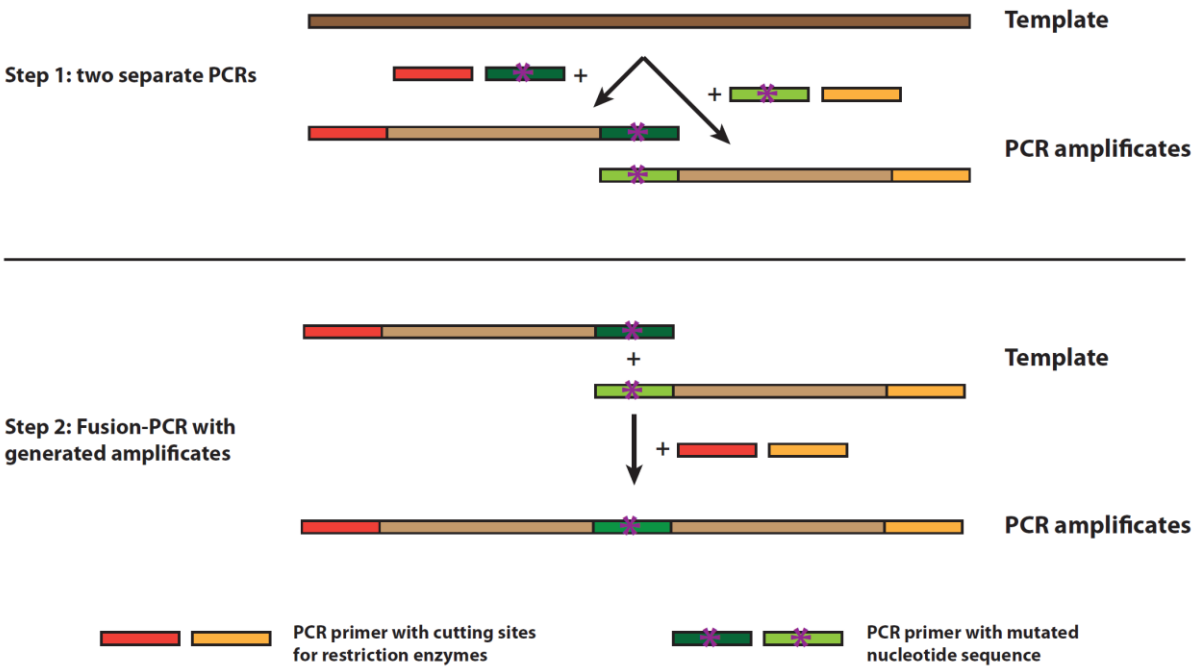

Fig. 8: Schematic depiction of the general procedure of the fusion-PCR for in vitro-mutagenesis. *In the first step two separate amplificates containing the desired mutation (purple asterisk) are generated. In the second step those amplificates serve as templates for the subsequent PCR. Due to the homologue sequence of both mutated ends (green primer) the two amplificates hybridise and the residual gap on each side is filled by the polymerase.*

For the following vector generation, the hybrid amplificate and the vector were separately digested with 1 µL of each *BamHI* and *HindIII* in 4 µL of 10x Unique-buffer filled up to 40 µL with mpH_2O. Digestion was executed at 37 °C for 90 min. To separate the digested nucleic acids from the solution, the samples were again loaded and isolated from an agarose gel. The isolated insert and vector were mixed in a molar ratio of 3:1 with 40 ng of vector as starting value. Vector and insert were subsequently ligated by addition of 1 µL T4-DNA ligase with 2 µL 10x T4-Ligase buffer filled up to 20 µL mpH_2O and incubation at rt overnight. The ligated vector was then used for bacteria transformation as described in 3.7. After transformation and plasmid preparation, the plasmid had to be sequenced to verify the insertion of the desired mutation and to check for unwanted mutations. This was done by the company

SEQLAB – Sequence Laboratories Göttingen GmbH with the help of a Sanger sequencing method. For the sequencing, the samples were prepared as stated in the company's instructions.

3.3 RNA preparation

For the preparation of RNA, stimulated cells were harvested from a 6-well plate by removal of the medium and addition of 100 µL 1x trypsin per well with a subsequent incubation at 37 °C in a CO_2-incubator for 3 min. The detached cells were gathered with 900 µL medium and transferred to a fresh tube. The cell suspension was centrifuged for 10 min at 1000 xg and the supernatant was discarded. The residual cell pellet was processed with the innuPREP RNA Mini Kit according to the manufacturer's manual. In the elution step, the bound RNA was removed from the filter matrix by addition of 30 µL DEPC-H_2O. The concentration of isolated RNA in the gathered solution was measured with a photometer similar to the described procedure in 3.8 with the exception that the dilution was prepared with DEPC-H_2O. As blank value DEPC-H_2O was used respectively. The RNA solution could be stored at -20 °C for short-term or used in following experiments.

3.4 Reverse transcription

The analysis of the cellular transcriptome was done by reverse transcription of isolated RNA into cDNA followed by PCR analysis. To generate cDNA, 5 µg of RNA was used from each sample and filled up with mpH_2O to a final volume of 12 µL. The RNA solution was mixed with 1 µL Oligo-dT primer and incubated at 65 °C on a heating block for 5 min. In a following step the sample was first incubated on ice for 2 min and subsequently mixed with 2 µL dNTPs and 4 µL 5x RT-buffer and incubated at 42 °C for 2 min. To finally start the reverse transcription 1 µL of reverse transcriptase was added to the tubes and the incubation at 42 °C was carried on for 1 h. At the end of the transcription, the enzyme was heat inactivated at 70 °C for 10 min. The sample was retrieved from the heating block and mixed with 180 µL mpH_2O to obtain a final cDNA concentration in the finished sample of 20 ng/µL.

3.5 PCR/RT-PCR

The PCR was used for the amplification of desired nucleotide sequences in the course of the analysis of the cellular transcriptome (RT-PCR) or for cloning methods (see 3.2). The essential components for a PCR are dNTPs, polymerase with corresponding buffer, template and specific primers enclosing the

sequence of interest. Depending on the subsequent needs for amplificates, the polymerase was chosen depending on its abilities to prove-read synthesised DNA strands. In case of cloning, the prove-reading ability was an essential prerequisite to avoid unwanted mutations in the cloned sequence whereas RT-PCR was solely dependent on the length of the amplificates. To start a PCR, the samples were mixed in a 0.2 mL tube according to the values displayed in Table 1 and subsequently placed in a PCR cycler. Depending on the sample, the program shown in Table 2 together with the primer information from 2.10 was uploaded and executed. The cycle count was individually adjusted depending on the executed application and resulting amplificate concentration. The usual cycle count was between 30 and 35 cycles. Finished samples were retrieved from the cycler and subsequently analysed in an agarose gel electrophoresis. Some samples had to be mixed with DNA Gel Loading Dye (6X) before applying on a gel.

Table 1: Pipetting scheme for various PCR experiments

	RT-PCR/Colony-PCR	***In vitro*-mutagenesis**
Polymerase	Maxima Hot Start PCR Mix 10 µL	KAPAHiFi polymerase 0,5 µL
dNTP (10 mM)		0,75 µL
Buffer		5x High fidelity buffer 5 µL
Primer forward (10 µM)	1 µL	0,75 µL
Primer reverse (10 µM)	1 µL	0,75 µL
Template	1 µL (cDNA 20 ng/µL) 5 µL (bacteria solution)	4 – 20 ng
H_2O	ad. 20 µL	ad. 25 µL

Table 2: General program used in PCR experiments.

Step	Temperature	Time
Initiation	95 °C	10 min
Cycle Denaturation	95 °C	30 s
Cycle Hybridisation	lowest T_m-1	30s
Cycle Elongation	72 °C	30s
Finalisation	72 °C	10 min

3.6 Agarose gel electrophoresis

Nucleic acid analysis was accomplished by size separation of samples in an agarose gel. The agarose gel was prepared by melting 1.2 g (for subsequent gel extraction 0.6 g) lyophilised agarose powder in 60 mL 1x TAE-buffer under constant heating until the liquid was completely homogenous. For the staining of nucleic acids two drops of EtBr solution were added to the molten solution and mixed by gentle swaying. The final agarose solution was poured into the prepared gel chambers for setting. A comb was inserted into the gel to form pockets for sample loading. The polymerised gel was then completely covered with 1x TAE-buffer and the comb was removed to allow sample loading. As a standard a specific marker was also loaded in one pocket to estimate the size of applied samples (GeneRuler, see 2.9). In case of concentration estimation of a loaded sample, the marker was used as standard for defined DNA concentrations (MassRuler, see 2.9). The loaded gel was then run at constant 80 V until the lower dye front nearly reached the edge of the gel. Then the gel was removed from the chamber and was ready to be analysed under UV-light which visualised the EtBr intercalated into the double strand of the amplificates. The highlighted gel was documented and later on analysed with the help of the mass standard.

3.7 Transformation & selection of positive clones

Newly constructed plasmids for protein expression or other applications can be multiplied and stored by integration into competent DH5α. For subsequent protein expression, the competent *E.coli* strain BL21 was used. This procedure, called transformation, was done by mixing a finished ligation preparation (20 µL) or 6 ng of already purified plasmid with 200 µL of competent bacterial cell solution in a 1.5 mL tube. The mixture was kept on ice for 30 min followed by a heat shock at 42 °C for 45 s which prompted the cells to internalise surrounding plasmids. After another 5 min on ice, the sample was filled up with 800 µL fresh LB-medium and incubated at 37 °C for 1 h. Cells were spun down at 4000 xg for 5 min and 900 µL of supernatant was discarded. The cell pellet was resuspended in the residual 100 µL of LB-medium and equally plated on two prewarmed LB-agar + antibiotics Petri dishes with a sterile Drigalski spatula. The dishes were then kept in an incubator at 37 °C overnight to allow proper colony growth. The following day several single clone colonies were isolated from the dish by scraping them off with a 10 µL pipet tip and resuspension in 20 µL mpH_2O. The isolated clones were checked for positive transformation in a Colony-PCR (see 3.5) by using 5 µL of the resuspended colony as template and 2 µL primer mix consisting of two primers targeting the flanking ends of the vector around the Clusterin gene. After detection of positive clones, the respective residual colony suspension

in mpH_2O was transferred to a 15 mL tube filled with 5 mL LB-medium + antibiotics to be propagated in an incubator shaker at 37 °C with 160 rpm overnight. The next day, the fully dense bacterial solution was then either used for plasmid preparation or stored by mixing 100 µL of cell suspension with 100 µL of freezing medium (prokaryotes) mixture in a 1.5 mL tube which could then be kept at -80 °C.

3.8 Plasmid preparation

For low amounts of plasmid 2 mL of liquid culture of bacteria containing the desired plasmid were processed with the GeneJET Plasmid Miniprep Kit, whereas for higher quantities of plasmid 100 mL cell suspension were used in the NucleoBond® Xtra Midi EF kit. Both preparations were performed according to the manufacturer's manual of the respective kit. For the final elution step (Midi prep: reconstitution step) 50 µL (Midi prep: 250 µL) mpH_2O were used. To determine plasmid concentration in the isolated sample, a dilution of 1:100 with mpH_2O was analysed in triplicates in a photometer and a quartz cuvette at 260 nm. As a blank value, the cuvette was filled with mpH_2O. With the Lambert-Beer-formula, the resulting extinction value was calculated into a final plasmid concentration.

3.9 Transfection

Integration of foreign plasmids into eukaryotic cells was done by using the commercially available Lipofectamine 3000 Reagent. The transfection reaction in this reagent is carried out by DNA-absorbing lipid-nanoparticles which are taken up by all types of eukaryotic cells. For the transfection of a single well on a 6-well plate with an approximately 60% cell density, 5 µL of Lipofectamine 3000 Reagent were used. All other components and steps were done according to manufacturer's manual. Under gentle agitation, the final transfection solution was added dropwise to the well. Cells were grown for 24 h before medium was changed to either 1.5 mL starvation medium in case of following experiments (see 3.1.4) or 2 mL growth medium for stable clone generation (see 3.10).

3.10 Stable clone generation

The generation of a stable cell line simplifies applications which need cells with specific attributes such as recombinant protein expression, in this case the expression and secretion of recombinant Clusterin variants. After successful transfection of HEK-293 (see 3.9) with a Clusterin-containing plasmid, the 6-well plate was incubated until full confluency was reached. Cells were harvested by aspirating

medium, rinsing with 1 mL 1x PBS and incubating on 200 µL 1x trypsin at 37 °C in an incubator for 3 min (analogous to section 3.1.1). Cells were detached with 800 µL growth medium and transferred to a 15 mL tube in which they were centrifuged at 1000 xg for 5 min. Before the cell pellet was resuspended in 10 mL selection medium the supernatant was removed. The homogeneous cell suspension was transferred to a T75 flask, filled up to 15 mL with selection medium and brought to an incubator at 37 °C for cultivation. The fully dense flask was splitted once 1:3 in a new T75 flask as described in 3.1.1 with the exception that cells were always kept on selection medium instead of growth medium. After cells reached full confluency again they were harvested and the cell count was determined (see 3.1.2). From the cell suspension, a volume containing 100 cells was transferred to a 15 mL tube with 10 mL fresh selection medium and mixed thoroughly. The 10 mL were then distributed across a 96-well plate with 100 µL per well with a gentle mixing of the solution in between every 12 wells to prevent sedimentation of cells. The goal of this procedure was to transfer a single cell in each well. Over the following days the wells were monitored with a microscope for cell growth and positive wells with only one initial cell were marked. When the marked wells reached full confluency they were harvested and transferred to the next higher well size, in this case a 48-well plate. This procedure was continued until 6-well plates were reached. The amounts of used 1x PBS, 1x trypsin and selection medium for harvesting were scaled down proportionally from the 6-well plate procedure as previously explained. The fully grown stable single clones were tested for their ability to express the introduced protein. Therefore one half of the harvested cells from the final 6-well were transferred to a new 6-well whereas the rest was further cultivated to generate cryo stocks (see 3.1.3) for future application. The 6-well plate for expression analysis was set on starvation medium for 24 h after cells were fully dense. The supernatant was collected and separated from residual cells and debris by centrifugation at 1000 xg for 15 min. The cell layer was lysed and harvested as described in 3.1.4. Gathered samples were then ready to be analysed by Western blot. In case of the supernatant 30 µL were used as sample size. Based on the results of the Western blot only the clone with the highest expression and secretion rate of recombinant protein was selected for further experiments.

3.11 Production of recombinant protein

To study the characteristics and effects of Clusterin and RAP, not only a large amount of these proteins was needed but also the demand for high purity was crucial. These requirements could be fulfilled by recombinantly expressing both proteins. In case of RAP, the expression was executed in *E.coli* whereas expression of Clusterin and its mutants had to be realised in HEK-293 since glycosylation is an essential posttranslational modification for their functionality.

3.11.1 Expression of RAP in a prokaryotic host

The effectively transformed and selected *E.coli* BL21 colony holding the plasmid for RAP expression was propagated in 10 mL of LB-medium + antibiotics in an incubation shaker at 37 °C o. n.. With 6 mL of this overnight culture a baffled flask with 150 mL LB-medium + antibiotics was inoculated and incubated at 30 °C under constant shaking until an OD_{600} of approximately 0,7 was reached. At this point, the expression of RAP was force-started by adding 0,5 mM of IPTG to the flask. The expression was kept running for 3 h at 30 °C on the shaker before the bacterial cells were harvested. The cells were separated from the LB-medium by transferring the solution to 50 mL tubes and subsequent centrifugation at 4000 xg for 30 min. The supernatant was decanted and the cell pellet was resuspended in 4 mL prokaryotic lysis buffer. After 10 min of incubation on ice, the suspension was equally divided into three 2 mL tubes and subsequently sonicated. The sonifier was set to 25% amplitude and the sample was sonicated for 1 s on and 1 s off for a total of 60 s. During this step the samples were kept on ice to avoid overheating and foam formation. The sonicated samples were pooled in a 50 mL tube and filled up to 50 mL final volume with Lew/7% glycerin*. The final sample was purified by FPLC as described in 3.11.3. A summary of the purification by FPLC can be seen in Fig. S6.

3.11.2 Expression of Clusterin in an eukaryotic host

The Clusterin variants were all purified from stably transfected HEK293 cell lines. In case of murine, human and RIVQ-mutant Clusterin, the stably transfected cells were already present as cryo stocks in our institute. Both proline and cysteine mutants, however, were generated as described in 3.10.

3.11.2.1 Gathering Clusterin-enriched cell culture supernatant

The procedure for Clusterin expression was started by taking the needed stable cell line into cultivation as described in 3.1.1. The cells were then propagated starting in one T75 flask. As soon as the cell layer reached full confluency, the cells were splitted 1:5 and transferred to two T75. From there on the next step was cultivation in two T175 flasks diluted 1:3 followed by the final growth period in ten T175 flasks. At this point the cells were grown to full confluency and kept at this stage for one more day before removing the growth medium, rinsing the cells with 10 mL 1x PBS and adding 20 mL starvation medium per flask. Starvation medium was used to reduce the protein load in the supernatant since Clusterin was afterwards purified from it. After 60 h on starvation medium the supernatant containing

the expressed mature Clusterin was collected in 50 mL tubes and centrifuged at 4600 xg for 30 min. The separated supernatant was decanted into a 250 mL glass bottle.

3.11.2.2 First purification and buffer exchange steps

Small proteins and peptides as well as different ions were removed from the harvested supernatant with a Minimate™ TFF Capsule with Omega™ membrane (30 kDa). A peristaltic pump piped the solution through tubes from the 250 mL glass bottle reservoir to the membrane where it got filtered and separated into filtrate and retentate. The filtrate was discarded and the retentate containing recombinant Clusterin was led back to the reservoir container. When the residual volume hit 100 mL, the reservoir bottle was sealed hermetically and a third tube leading from the reservoir to a storage bottle filled with LEW/7% glycerin* was attached. Due to the low pressure caused by continuous removal of filtrate, liquid was drawn from the storage bottle containing Lew/7% glycerin* mixture into the supernatant reservoir. This led to a permanent buffer exchange which was necessary for the upcoming purification step. After about 300 mL of Lew/7% glycerin* were used for the buffer replacement, the solution in the reservoir was ready for further processing.

Before and after each purification with buffer exchange, the filter unit had to be washed to remove residual molecules from the membrane which would otherwise clog it. Therefore 500 mL of mpH_2O were pumped across the membrane followed by 300 mL of 0,1 M nitric acid, 0,1 M sodium hydroxide and 0,5 M sodium hydroxide/0,04 M sodium dichloroisocyanurate in the given order. Finally, again 500 mL of mpH_2O were applied for rinsing. At this point the filter unit was either ready for use or was washed with 200 mL of 20% ethanol for storage at 4 °C.

3.11.3 Purification of His-tagged proteins with FPLC

Both RAP as well as all Clusterin variants were expressed with a six times His residue at the N-terminus. This allows for purification of the proteins via a column filled with Ni-IDA silica beads connected to an ÄKTA. IDA is a chelating compound with nickel ion as the central particle. In this complex two chelating sites are vacant for His-tagged proteins to bind to.

To start with the purification, the column as well as the ÄKTA system had to be prepared. The XK16/20 column was loaded by filling 2 g (1 g for C10/10 column) of Ni-IDA silica beads in a slurry with 25 mL mpH_2O into the column glass tube with the bottom seal attached. After the beads had settled, the top seal was inserted up to the border between beads and liquid avoiding to enclose any air bubbles.

Before the column was attached to the ÄKTA, the whole system including both pumps were washed with 100 mL 20% ethanol* and 100 mL mpH_2O* at a flow rate of 10 mL/min. For a clean protein elution, pump A was already primed with approximately 30 mL elution buffer* and pump B was again washed with 100 mL mpH_2O*. The flow rate was set to 2 mL/min and the gradient was kept at 100% pump B while the column was attached to the system. With 60 mL of mpH_2O* the column was washed first and then primed with 60 mL of Lew*. The column was now ready to be loaded with either the prepared RAP (C10/10 column) or the Clusterin (XK16/20 column) solution. During following steps the pressure was kept below 2 bar and every flow through was collected in a separate fraction. Once the protein solution was fully loaded onto the column it was washed with Lew* until baseline was reached (approximately 90 mL). Unspecifically bound proteins and molecules were removed by changing the gradient to 90% pump B adding 10% of elution buffer* to the Lew* solution. After hitting the baseline again (approximately 90 mL), the bound His-tagged protein was eluted by decreasing the gradient to 0% pump B and 100% pump A with elution buffer* until 30 mL were collected.

At the end of the run the column was washed with 100 mL mpH_2O* and 100 mL 20% ethanol*, was disconnected from the ÄKTA system and kept at 4 °C for storage. In a final step, the flow rate was set back to 10 mL/min and the whole system was washed with 100 mL 20% ethanol*.

3.11.4 Sample concentration and buffer exchange

The collected elution fraction was concentrated by applying it to an Amicon® Ultra-15 Centrifugal Filter Unit 50,000 NMWL and subsequently centrifuging it at 4600 xg until approximately 1 mL residue was left. To remove present Imidazole in the concentrated sample, which would sophisticate planned experiments, the residual volume was filled up to 15 mL with 1x PBS and again centrifuged until approximately 1 mL was left. This step was repeated twice. Afterwards, the sample was retrieved from the Amicon and the protein content was measured with a Bradford assay (see 3.12). To simplify subsequent application of purified proteins, the concentration was adjusted to a specific value (usually 1 µg/µL) with 1x PBS.

3.12 Bradford assay

Isolated cell lysate samples contain undefined amounts of proteins which makes their use in following experiments close to impossible. To generate coherent data from these lysates, the concentration of proteins needs to be measured. With the Coomassie Brilliant Blue dye, the content of protein in a

solution can be determined. This is based on the stabilising effect of proteins on the blue anionic form of the dye. The lysates were first diluted 1:20 with mpH_2O and triplicates with 10 µL of the dilution were pipetted on a 96-well microtiter plate. A set of duplicates of a BSA protein standard was also added to the plate with which the concentration of the lysates was calculated afterwards. All samples were mixed with 190 µL of 1x Rotiquant by adding it with an Eppendorf multistream pipet. The plate was analysed with an ELISA reader at 595 nm with automatic path length correction turned on. The corrected values were then used for calculation of protein concentrations. The standard curve function was calculated with the regression line of the BSA protein standard values.

3.13 TCA precipitation

To determine the amount of Clusterin in the conditioned medium collected from wild type HEK-293 and HEK-293 stably transfected with msClu, each sample was subjected to TCA precipitation. For the precipitation 500 µL of conditioned medium were mixed with 50% of ice-cold TCA in a ratio of 2:1 and incubated on ice for 30 min. The sample was centrifuged at 20,000 xg and 4 °C for 30 min. The supernatant was discarded and the residual pellet was washed with 1 mL of ice-cold acetone prior to an additional incubation on ice for 5 min. The sample was centrifuged a second time with the parameters described above and the supernatant was discarded. For full removal of residual acetone, the sample was dried (lid open) at rt for 1 h. The dried pellet was then ready for SDS-PAGE analysis by resuspending it in 30 µL of 1x SDS loading buffer and subsequent heating (see 3.14).

3.14 SDS-PAGE

By means of a SDS-polyacrylamide gel electrophoresis, protein samples, such as whole cell lysates, can be fractionated based on the molecular weight of particular proteins. To do so, both gel and samples had to be prepared beforehand. About 60 – 80 µg of isolated whole cell lysates (variations in used amounts are mentioned in the corresponding Figure Legends) were transferred to a new 1.5 mL tube and then mixed with an appropriate amount of 5x SDS-loading buffer resulting in a final sample with 1x SDS-loading buffer. The negatively charged SDS in the loading buffer denatures all proteins and interacts with them in a molar ratio to the size of each protein. Denaturing of proteins is further supported by the reducing agent DTT in the loading buffer and by subsequent heating of the whole sample which was done at 95 °C for 1 min followed by a quick-spin to collect the sample at the bottom of the tube. As a standard to determine Protein sizes later on, 3 µL per gel of PageRuler™ Prestained protein Ladder 10 to 180 kDa were also heated. For the gel preparation, the glass plates were wiped

with ethanol and set into the gel pouring device. First, the separating gel was mixed in a 15 mL tube as described in 2.5 and 4.4 mL were added in between the two glass plates with a 5 mL pipet. The gel solution was covered with isopropanol to guarantee a straight edge. After the gel polymerised, the stacking gel was set up in a 15 mL tube as stated in 2.5 and the isopropanol on the separating gel was removed. Now the stacking gel was poured from the tube in between the glass plates up to the top and either a 10- or 15-pocket comb was inserted. The gel was ready to be set into the electrophoresis running chamber when the stacking gel was fully polymerised. The comb was removed from the glass plates and the running chamber was filled with SDS-running buffer up to the top and set into the tank which was also filled with an appropriate volume of SDS-running buffer. The gel was then ready to be loaded with the prepared samples and the protein standard. After all samples were loaded in their respective pocket, the chamber was closed and connected to a power supply. First, constant 25 V were applied for 2 h followed by 60 V until the bromophenol blue front from the SDS-loading buffer reached the lower edge of the glass plates. At this point the electrophoresis was stopped and the gel was retrieved from the device. Subsequently, the gel with the separated protein samples was ready to be either stained with Coomassie Brilliant Blue (see 3.18) or used in Western blotting (see 3.17).

3.15 Immunoprecipitation

A desired protein can be isolated from whole cell lysates by using specific antibodies targeted against an epitope on the respective protein of interest. In this process 250 µg whole cell lysate were incubated with 5 µg of capture antibody at 4 °C on an overhead rotor overnight. The next day the Protein A sepharose slurry was prepared by mixing 200 µL lyophilised sepharose beads with 1 mL mpH_2O and letting it swell for 20 min. The swollen matrix was quickly spun down and the supernatant was removed. For storage, 600 µL 20% ethanol were added to the residual slurry. From this prepared stock 20 µL per sample were transferred to a new tube and washed with lysis buffer three times by continuous quick centrifugation and removal of supernatant. In the last washing step, the slurry was filled up to its original volume with lysis buffer and 20 µL were pipetted - under constant stirring to avoid sedimentation of the swollen beads - to the lysate-antibody mix. The samples were again incubated at 4 °C on an overhead rotor for 1 h to allow for binding of the antibody to the sepharose beads. After incubation, the beads were again washed three times with lysis buffer as described above. At the final washing step, the residual slurry was mixed with 30 µL 1x SDS-loading buffer and incubated for 10 min. The sample was treated similar to normal SDS-PAGE samples starting with a heating step at 95 °C. After the brief centrifugation, the supernatant was ready to be loaded on a SDS-PAGE (see 3.14) and subsequently analysed by Western blot (see 3.17).

3.16 2D-gel electrophoresis

Separation of proteins by molecular weight as conducted with SDS-PAGE can be insufficient in some cases. To evaluate alterations of for example two isoforms or the phosphorylation status of a protein, the proteins have to be separated differently. A crucial value that changes with modification of the protein is its isoelectric point. With the usage of a 2D-gel electrophoresis, the protein samples and also whole cell lysates, can initially be separated by their isoelectric point followed by separation by molecular weight in a subsequent SDS-PAGE. At first, the samples were prepared for the isoelectric focusing by filling up 100 µg of whole cell lysate with a rehydration buffer to a final volume of 130 µL. The mixed sample was transferred to the ceramic chambers used for focussing. The immobilised pH gradient acrylamide gel strip (IPG BlueStrip 4-7 / 7 cm) was carefully placed on the sample fluid film avoiding any bubble enclosements. After 10 min of incubation at rt, the strip was covered with mineral oil to protect the strip from desiccation and subsequently the ceramic chamber was set into the focussing device. The isoelectric focussing was run overnight with the following program:

Rehydration			**min. 6 h**
Focussing	Step and Hold	300 V	30 min
	Gradient	1000 V	30 min
	Gradient	5000 V	90 min
	Step and Hold	5000 V	40 min

The next day, when the program was finished, the gel strip was retrieved from the ceramic chamber and carefully released from residual mineral oil using a paper towel. For the preparation of the second separation by SDS-PAGE, the strip was incubated in equilibration buffer on a rocking table for 30 min. After incubation, the strip was recovered and placed in between the glass plates of a polyacrylamide gel that was casted without a comb and a small gap in between the glass border and the stacking gel front. The strip was covered with a 0.5% agarose solution to keep it in place. The next steps were executed analogously to a normal SDS-PAGE followed by Western blot analysis.

3.17 Western blot

The separation of proteins in cell extracts with SDS-PAGE is the first step allowing to analyse changes in a single protein. However, to gain access to the proteins, they must be fully retrieved from the gel without disturbing the separation pattern. This step is essential for the following analysis with antibodies which target a specific epitope at their respective protein. As a supporting material to

accommodate the proteins, a nitrocellulose membrane is used. This material absorbs any protein equally effective due to its hydrophobic as well as charged nature forming an openly accessible layer of bound proteins. The transfer itself can be conducted with two different methods the so-called Tank-blot or semi-dry blot. Since the semi-dry blot method has deficits in transferring high molecular weight proteins at approximately >100 kDa the Tank-blot was the method of choice. For the actual transfer, three Whatman papers were cut to the size of the blotting cassette and one piece of nitrocellulose was cut to the size of the gel. All components were soaked in desalinated H_2O and together with the gel placed in the cassette. The cassette was closed and set into the blotting device. Together with a cool pack and a stirring bar, the blotting device was installed into the tank which was then filled with the appropriate volume of Tank blot buffer. The entire tank was set on a magnetic stirrer, the lid was closed and it was connected to the power supply. The stirrer was turned on to ensure even distribution of cooled buffer since the high current during blotting causes excess heating which could be harmful for proteins. The blotting process was conducted at constant 400 mA for 1 h. The loaded nitrocellulose membrane was removed from the blotting device and instantly transferred to a washing tray to block potential unspecific binding sites for antibodies. This was done with 6 mL of either TBST/2% BSA for the following treatment with phospho-antibodies or PBST/5% powdered milk for all other antibodies on a rocking table for 1 h. During this time, the needed amount of primary antibody solutions for protein target detection were prepared as described in 2.12. All following washing and incubation steps were always performed on a rocking table. After the blocking of unspecific binding sites was completed, the membrane was covered with the primary antibody solution and incubated at 4 °C overnight. For detection of multiple targets, the membrane was cut accordingly and incubated with the respective antibody solutions separately. The next day, the antibody solution was discarded and the membrane was washed three times for 5 min with 5 mL of TBST or PBST respectively. Depending on the host of the used primary antibody, the secondary antibody solution was prepared according to 2.12 which was then incubated at room temperature for 1 h. The membrane was again rinsed three times for 5 min with 5 mL TBST or PBST before it was ready for chemiluminescent detection. Signal detection was done with a Stella and the corresponding software. Therefore, the membrane was laid on a piece of transparency and covered with a previously prepared Western Lightning Plus-ECL solution according to the manufacturer. After 30 s incubation with the detection solution, the membrane was carefully covered with a second transparency without pushing out the residual solution. The membrane was arranged in the dark chamber of the Stella device and pictures were taken at 30 s and 90 s exposure time. With the white light in the chamber turned on, the marker Vol.s were quickly documented for later evaluation of the chemiluminescent signals. For further analysis of other protein targets or total- and loading controls, the membrane was rinsed twice for 5 min with 5 mL PBST. Now

the membrane was ready for further incubation with another primary antibody solution as described above. Stripping of membranes was avoided since loss of protein was an issue.

3.18 Coomassie staining

In contrast to Western blotting, the staining with Coomassie Brilliant Blue can only target and detect all proteins at once but needs no further steps to access the separated proteins on the gel. After application, the dye interacts with basic side chains of amino acids. The gel from the finished SDS-PAGE was therefore transferred to a plastic tray containing 18 mL of Coomassie staining solution. The gel was then incubated at room temperature on a rocking table overnight. Since the Coomassie dye also stains the polyacrylamide matrix, it was necessary to destain the gel with 20 mL of destaining solution to visualise the protein Vol.s. This was done for at least 6 h but could be extended to overnight incubation. The destained gel was then documented with a scanner by placing it in between two transparencies.

3.19 RTK Signalling Array Kit

With the PathScan® RTK Signaling Antibody Array Kit it was possible to screen for a variety of targets and their phosphorylation pattern with merely one sample. The kit consists of a microscope slide with applied carrier membranes which are spotted with various immobilised capture antibodies for different targets. After addition of cell lysates, the targets are bound to their corresponding antibody. The now immobilised antigens can be checked for phosphorylation by applying a detection antibody cocktail followed by a secondary antibody coupled to horseradish peroxidase. The visualisation of bound targets is done by chemiluminescent reaction similar to Western blot (see 3.17). For this approach, cells were previously stimulated as indicated in corresponding figure legends and harvested as usual (see 3.1.4). For binding, 650 µg of cell lysate per sample were loaded into the chamber and incubated overnight. Subsequent steps were performed in accordance with the manufacturer's guide.

3.20 MTS Assay

The influence of different stimuli on eukaryotic cell metabolism can be measured by using a so-called MTS assay. In this assay the chemical MTS is reduced by NADH/NADPH produced in vital cells leading to formazan formation which can be photometrically measured at 490 nm. The rate of formazan

generation is directly proportional to the metabolising rate of cells within a reaction chamber. When similar cell numbers are seeded into each well, differences in colour formation after various stimulations are indications for either increased metabolism or proliferation. For this study 1,500 (4,000 for HepG2) cells per well in 50 µL growth medium were seeded into a 96-well plate. Every sample stimulation was done in triplicate with a fourth cell-free well as blank control. Outer wells were not seeded and empty wells were filled with 100 µL growth medium to minimise evaporation effects. On a second 96-well plate, a single triplicate with a fourth blank well was prepared as a reference point for the beginning of a stimulation phase. Both plates were cultivated for 48 h (70 h for HepG2) before replacing the growth medium by starvation medium for another 24 h (2 h for HepG2). All steps of medium replacement were done without the aspirator and a washing step with 1x PBS in between to reduce loss of cells. The actual stimulation on one plate was done by replacing the starvation medium from the wells with 50 µL of previously prepared stimulants in fresh starvation medium. The blank well was always stimulated first to prevent cross contamination with cells. The plate was then incubated for 6 h. At the same time, the four wells of the second plate are filled with 10 µL of the MTS solution followed by incubation for 2 h with a measurement every hour. This revealed the basal metabolism rate of the cells before stimulation and incubation. For the measurement, the plate was set into an ELISA reader to determine the absorption at 490 nm and 630 nm. At 490 nm the formazan has its absorption maximum whereas the 630 nm value needs to be measured to subtract the background caused by the phenol red in the medium. After 6 h incubation, the stimulated plate was also treated with 10 µL MTS per well and measured as described above.

3.21 HPLC

In this work a reversed-phase HPLC method was performed by using solvent A as polar and solvent B as nonpolar phase. All solvents were connected to their corresponding suction tube of pump A or B. The previously processed samples (see section 3.21.1 & 3.21.2) were injected into a 100 µL loop with a syringe. The respective detection method was started and after 10 min the loaded sample was manually fed onto a C8 vydac precolumn to retain any particles or contaminations. The actual fractionation of sample components was done with a C18 column. The analytes adsorb to the surface of the loaded silica in the column and elute at a specific concentration of solvent A & B depending on their polarity. The detection of the analytes was executed at 214 nm, the absorption maximum of peptide bonds. Changes in retention times can be seen due to the varying treatment of the samples resulting in altered polarity. Before each test day, the pump system including the columns were

washed with the “Wash method” seen in Table 3. At the end of an experimental series, a final washing step was performed with 30 min 100% solvent A followed by another 30 min 100% solvent B.

Table 3: Overview of the used methods for the execution of HPLC analyses.

Wash method		**Clusterin method**		**Insulin method**	
Point of time [min]	Gradient Solvent A	Point of time [min]	Gradient Solvent A	Point of time [min]	Gradient Solvent A
0	0	0	100	0	100
40	100	10	100	10	100
70	0	Sample injection		Sample injection	
90	0	15	65	15	75
		45	45	35	55
		55	45	45	55

3.21.1 Detection of Clusterin chain disintegration

One key factor of Clusterin are the four to five disulphide bonds between the two separated chains. These bonds were reduced by mixing 17.5 µg Clusterin with 40 mM DTT (20 mM for Clusterin Cys mutant) in a maximum volume of 140 µL filled up with mpH_2O and incubation for 1 h at 4 °C. A respective sample without DTT was also incubated as a control. Both solutions were then analysed by HPLC as described in 3.21 with the “Clusterin method” from Table 3.

3.21.2 Alterations of IGF-1 and Insulin polarity after denaturation

The susceptibility of IGF-1 and Insulin upon treatment with heat and/or DTT was estimated by HPLC analysis. Therefore 8 µg of either IGF-1 or Insulin in a final volume of 160 µL filled up with mpH_2O were treated using different approaches. Control samples and those treated with 20 mM DTT only were incubated for 6 h (3 h for Insulin) at 4 °C. The heat-treated samples with or without 20 mM DTT were kept on 50 °C for the respective time. To analyse the effects of all treatments on the IGF-1 and Insulin conformation, all samples were analysed by using the “Insulin method” from Table 3 in an HPLC approach as described in 3.21.

3.22 CD-spectroscopy

The distribution of secondary structures in a pure protein solution can be determined by measuring the circular dichroism (CD) in a far UV spectrum. When circularly polarised light travels through an optically active medium, left- and right-handed polarised waves are absorbed unequally causing a circular dichroism. In case of protein solutions, the different forms of secondary structures exhibit a variable absorption of either left or right-handed polarised waves at a specific wavelength. The method of CD-spectroscopy measures the difference in absorption rates between both polarised waves. For the measurement, a 0.1 µg/µL protein solution was prepared in phosphate buffer. The solution was loaded in a quartz cell with a thickness of 1 mm and analysed in a Jasco J815s. Under constant conditions of 20 °C and a fully saturated nitrogen atmosphere, the measurement was carried out in a step-scan mode from 190 nm to 260 nm with 1 nm step resolution and 5 nm Vol.width. From each sample five accumulations were gathered, corrected by subtracting the blank value (phosphate buffer only or phosphate buffer + DTT where necessary) and subsequently smoothened with a Savitzky-Golai convolution. Detailed information as to experimental conditions can be found in Fig. S13.

The resulting data was further analysed with the web application Dichroweb (Whitmore & Wallace, 2004; Whitmore & Wallace, 2008) to determine the secondary structure distribution based on the CD-spectroscopy results. The algorithm embedded in the chosen analysis program (CDSSTR, (Compton & Johnson, 1986; Manavalan & Johnson, 1987; Sreerama & Woody, 2000)) to calculate the secondary structure distribution requires the molecular weight and length of the analysed protein (hsClu variants: 478 aa, 70 kDa; msClu: 477 aa, 67.5 kDa; IGF-1: 70 aa, 7.65 kDa) to determine the mean residue ellipticity (MRE). Together with the measuring conditions and a data reference set (Set 7 (Sreerama & Woody, 2000; Sreerama, et al., 2000)) the program calculated the mean percental distribution of secondary structure elements in the analysed protein.

3.23 ELISA

A quick and easy way to detect and quantify a unique protein in a sample is accomplished with the help of an ELISA. In this assay, the target protein is labelled with specific antibodies which can be measured by an enzyme-based chromogenic detection later on. The principle of an ELISA can be applied to a broad spectrum of experimental setups with various aims. Based on the source material it is possible to either coat it directly onto the ELISA microtiter plate or use antibodies to capture the wanted protein for further treatment. In this work, the goal was to determine the potential of protein-protein interactions between several different protein classes. Method of choice was the direct coating

of one interaction partner to the surface of an ELISA microtiter plate. This was done by mixing coating buffer with the amount of protein indicated in respective figures to a final volume of 100 µL per well. Uncoated control samples were only filled with 100 µL coating buffer. As stated in the figure legends, all samples were measured in duplicates or triplicates. The filled plate was incubated in a humidified chamber at room temperature overnight. Before addition of 150 µL PBST/5% powdered milk to each well for blocking, they were rinsed three times with 300 µL PBST to remove residual uncoated protein. After 1 h of blocking buffer incubation on a rocking table, the wells were filled with 100 µL solution of PBST/5% powdered milk containing the appropriate amounts of the second interaction partner as indicated in the figure legends. The incubation was again executed on a rocking table for 1 h. All wells were again rinsed with PBST as described above. Detection of the bound second interaction partner was done by targeting the 6x His tag of the protein with a corresponding antibody. For each well 100 ng of 6x His primary antibody was mixed with PBST/5% powdered milk to obtain a final volume of 100 µL and incubated, as usual, on a rocking table for 1 h. Well rinsing and incubation was repeated with the alkaline phosphatase-linked secondary antibody in the same manner, however, the amount of antibody was increased to 200 ng per well. During the 1 h incubation of the secondary antibody the ELISA substrate solution was prepared. To remove unbound secondary antibody, all wells were again rinsed with PBST as above. For the detection 100 µL of ELISA substrate solution was added to each well. The containing pNPP is a substrate for the alkaline phosphatase coupled to the secondary antibody which enzymatically hydrolyses pNPP into the chromogenic product p-nitrophenol. This reaction was stopped via addition of 50 µL 2 M sodium hydroxide as soon as the colour development reached satisfactory levels. With an ELISA reader set to 405 nm and path length correction turned on, the colour intensity was measured. Subsequently, the corrected values were used in the statistical evaluation of the results.

3.24 Clusterin deglycosylation

For the generation of deglycosylated Clusterin, 100 µL of a 1 µg/µL Clusterin solution were mixed with 2 µL PNGase F and incubated for 12 h at 37 °C in a shaker. No additional buffer was used to avoid disturbance of subsequent experiments. After incubation, the PNGase F was inactivated at 70 °C for 10 min. As a control, non-treated Clusterin was also incubated for 12 h at 37 °C and heated to 70 °C for 10 min. This control sample was used as normal Clusterin sample in experiments containing the deglycosylated Clusterin sample.

3.25 Chaperone assay

By executing a chaperone assay, it is possible to determine the capabilities of selected proteins to keep a non-chaperone target protein in solution during denaturing conditions. The level of denaturation is measured by viewing the turbidity of the solution which can be monitored at 360 nm with an ELISA reader. Since structural elements in chaperones are crucial for their functionality, it was of great interest to see whether preincubation with the reducing agent DTT has an influence on the chaperone effectivity. For the preparation of a chaperone assay 22.5 µL of each potential chaperone with a concentration of 1 µg/µL were incubated with 2.5 µL of either mpH_2O or 200 mM DTT solution at 37 °C on a shaker for 12 h. To start the chaperone assay, all necessary components were mixed on a microtiter plate with the following volumes:

	Blank	**Control samples**	**BSA**	**Clusterin**
10x Precipitation buffer	10 µL	10 µL	10 µL	10 µL
Catalase (12,5 mg/mL)	/	/	8 µL	8 µL
Protein	/	7,5 µg	7,5 µg	7,5 µg
H_2O	90 µL	82,5 µL	74,5 µL	74,5 µL

All samples were measured in triplicate. The prepared microtiter plate was set into the 50 °C preheated ELISA reader and the experiment was started. Every 150 s for a maximum of 150 min the turbidity at 360 nm was measured and the values were saved. The gathered data was analysed by subtracting the control values from their corresponding sample values and subsequently normalising the corrected values on the first measured value to determine the alteration in turbidity along the measured time points.

4 Results

In the past years of Clusterin research, many research groups tried to evaluate the role of Clusterin in the course of signal transduction. Although several promising observations have been made, only few managed to overcome the perpetual critical discourse and controversial studying results. An issue that was often taken up was the influence of Clusterin on Akt phosphorylation. The opinions and observations on the ability of Clusterin to alter the levels of Akt stimulation couldn't be more divergent. While some studies observed direct effects of Clusterin on Akt, others postulated cooperations with molecules involved in signal transduction. However, most studies lacked deeper insights into possible mechanisms entangled in the modulation of signalling pathways. Furthermore, most published data on Clusterin involvement in Akt phosphorylation was not further pursued by the respective research groups causing distrust about the scientific relevance of otherwise promising results. Therefore, my work will pick up on this topic to elucidate the role of Clusterin in the modulation of signal transduction pathways involving Akt phosphorylation.

This work will demonstrate evidences for potential pathways modulated by Clusterin. Besides the effects of Clusterin on signalling molecules and overall cellular responses, the involvement of structural features of Clusterin will be intensively studied. By analysing the binding abilities of Clusterin to signalling pathway stimulants, its physiological role, especially in the development of AD, will be further assessed.

4.1 Unravelling Clusterin-interacting receptors involved in signal transduction mechanisms

Many studies described modulations of signalling pathways by Clusterin without investigating or suggesting a target receptor. This included the postulated influence of Clusterin on growth factor stimulation. Although some target receptors for Clusterin are known, like members of the LDL-receptor family or DC-SIGN, none of them are directly linked to the detection of growth factors. The facts, that Akt is often observed as a target for Clusterin effects and that it is a highly essential signal molecule, inevitably led to the necessity of concentrating the research focus. A group of receptors that combine both detection of growth factors and stimulation of Akt phosphorylation are the cell surface receptor tyrosine kinases (RTK). Therefore, a starting point for the revelation of potential receptor interaction partners of Clusterin was the characterisation of its effect on the activation of RTKs.

Despite the fact that the family of RTKs consists of >50 members, there was the possibility to easily cover several targets by with a single experimental approach. By using the PathScan® Signaling Array Kit for RTK (Cell Signaling Technologies) one sample could be screened for 28 different RTKs in addition to several common downstream signalling molecules including Akt.

One question that research groups were pondering about for many years was whether Clusterin itself is able to modulate signal transduction pathways. To address this issue, HEK-293 cells were treated with 40 µg/mL Clusterin for 10 min and compared to control cells. The results for both samples displayed no significant changes in the phosphorylation pattern of any screened target present in the assay (Fig. 9A). Since other studies described cooperative effects of Clusterin when other signalling molecules were present, the experiment was repeated by adding 2% Panexin, an artificial serum supplement containing insulin. Panexin was used to simultaneously deliver a broad spectrum of potential activators for RTKs. It was preferred to FBS as every charge has globally standardised contents with constant concentrations. The addition of Panexin led to increased activation of various targets including Ins-R (Fig. 9B). Strikingly, the sample treated with Clusterin had significantly decreased Ins-R and HGF-R phosphorylation levels (Fig. 9B, blue boxes) compared to the non-treated sample. An interesting side observation was the constitutively active HGF-R phosphorylation in untreated HEK-293 (Fig. 9A). This led to the decision that in a first attempt the Ins-R modulation and subsequent activation of linked signal transduction pathways should be studied more intensively.

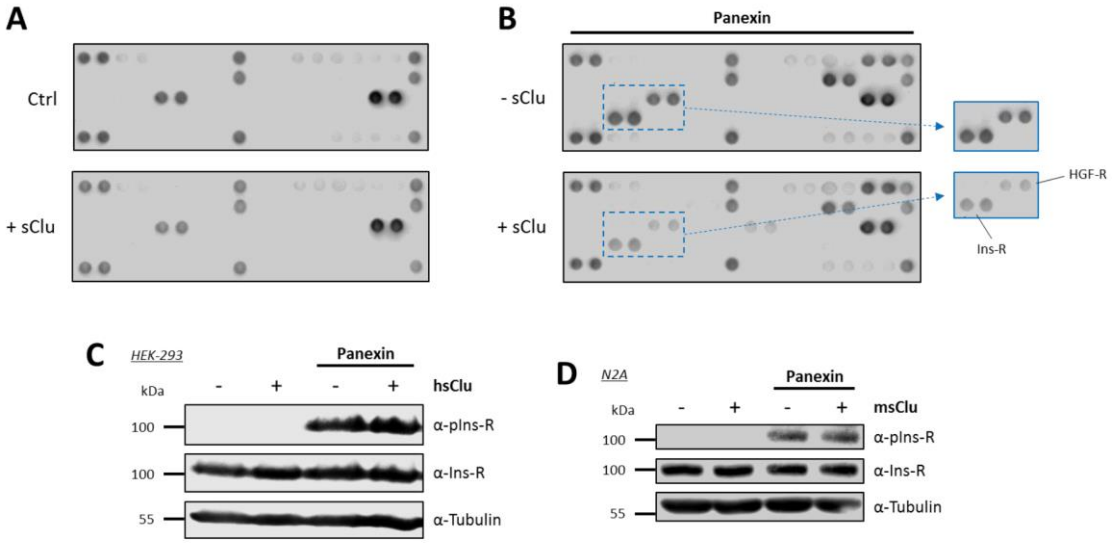

Fig. 9: Influence of Clusterin on phosphorylation levels of various RTK after extracellular stimuli. *After 24 h of serum starvation cells were treated with 2% Panexin in the presence or absence of 40 µg/mL Clusterin. (A, B) HEK-293 stimulated with hsClu and Panexin for 10 min were harvested and 650 µg of each cell lysate were used with the PathScan® RTK Signaling Antibody Array Kit according to the manufacturer's manual. Each target is captured in duplicate and significant changes between samples are highlighted (blue markings). For more details about each target on the test strip refer to Fig. S12 (C) Lysates of HEK-293 cells treated with hsClu and Panexin were used in Western blot analysis to determine Ins-R phosphorylation. (D) Experimental setup from C was repeated with the murine neuroblastoma cell line N2A and msClu.*

Initially, the observed effect of Clusterin on the Ins-R phosphorylation was further examined. This was achieved by directly staining for Ins-R phosphorylation with specific antibodies in a Western blot using whole cell lysate of HEK-293 treated with Panexin and Clusterin. Although the experimental conditions were kept constant, the observed results from the RTK Array could not be confirmed (Fig. 9C). Since Clusterin is thought to be involved in Alzheimer's disease, an *in vitro* model with the murine neuroblastoma cell line N2A and murine recombinant Clusterin (msClu) had been established. With Diabetes type 2 being a risk factor for AD, the results with Clusterin decreasing the phosphorylation levels of Ins-R became even more eminent. As a consequence, the previous experiment in HEK-293 from Fig. 1C was repeated with the N2A cell model. Change of the model organism, however, did not alter the result (Fig. 9D) but rather confirmed the observations already made in HEK-293 (Fig. 9C). In both Western blot attempts with either HEK-293 or N2A, the decrease in Ins-R phosphorylation seen in the RTK Array kit samples stimulated with Panexin and Clusterin could not be reproduced. A reason for the lack of modulation could have been a way of how Ins-R phosphorylation is detected in the RTK Array kit. While the Western blots in Fig. 9C and D were stained with a particular p-Ins-R antibody recognising a specific epitope, the RTK Array kit uses an antibody detecting the overall tyrosine phosphorylation in a captured molecule. The differences in Ins-R phosphorylation levels seen in the RTK kit could be the result of phosphorylated tyrosine residues not detected by the specific p-Ins-R antibody. Subsequent studies addressing this problem were established. First attempts to stain the Western blots with p-Tyr antibody failed since whole cell lysates contain a vast amount of phosphorylated tyrosine residues making it impossible to detect any changes (data not shown). A preceding Ins-R immunoprecipitation step followed by p-Tyr staining yielded no results possibly due to insufficient input or loss of target protein during the process (data not shown). Further studies to separate and determine the involved phosphorylation sites, by addressing the change in isoelectric mobility under increased phosphorylation levels, were executed with a 2D-gel electrophoresis. The isoelectrically focused and separated samples were stained with Ins-R antibody. A separation of the different InsR entities was achieved but the comparison of Clusterin-treated and -untreated samples showed no significant differences (Fig. S1). One cannot rule out the possibility, that changes were masked by the dominant spots or the levels of distinct pIns-R entities were insufficient for staining since the Ins-R contains 57 predicted phosphorylation sites.

4.2 Elaborating the Clusterin effects on signal transduction during insulin stimulation

Since the effects in the RTK Array kit could not be ignored in the subsequent experimental process, this subject was further pursued by adjusting the experimental setup. Information as to the composition of Panexin given by the manufacturer revealed that it contains insulin but no other growth factors. To exclude side effects from other components, Panexin was substituted with porcine insulin. Furthermore, the amount of Clusterin used was reduced to 5 µg/mL since other research groups worked with less amounts of Clusterin and still observed effects. Also, a dosis of 40 µg/mL for every stimulation wouldn't have been sustainable in the long run. Establishing a reliable cell model to investigate the effect of Clusterin on the Ins-R was an essential prerequisite for the subsequent examination of possible effects on the associated intracellular signalling cascades.

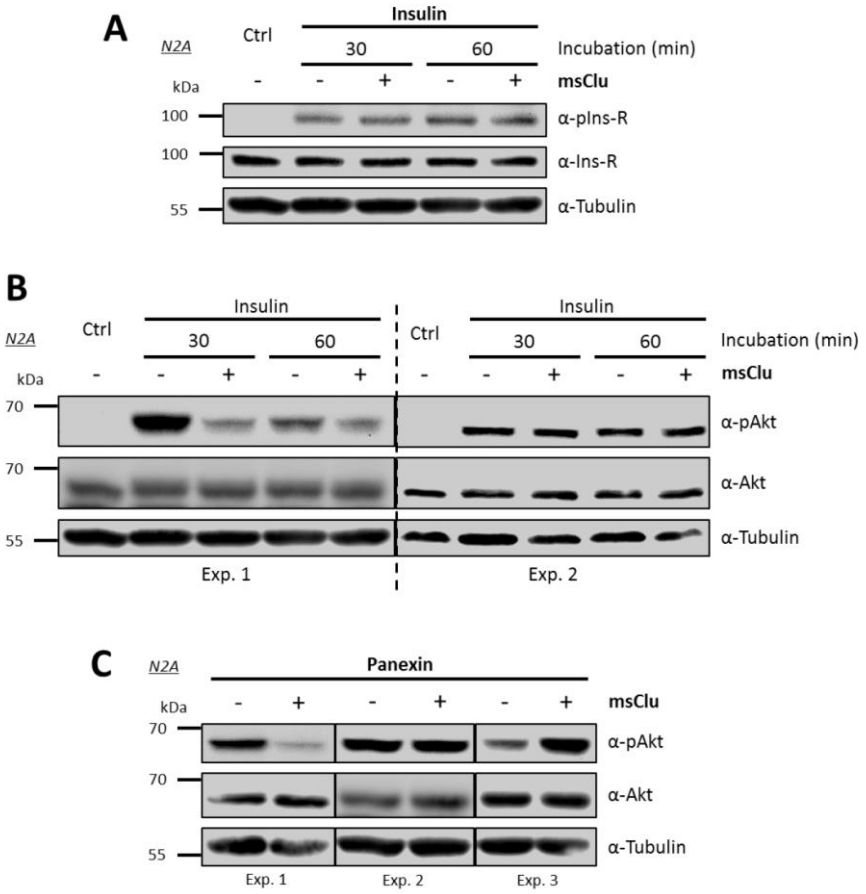

Fig. 10: Analysis of modulating effects of Clusterin on members of the insulin signalling pathway and its ambivalent behaviour. *(A, B) Serum-depleted N2A were stimulated with 0.5 µg/mL insulin and 5 µg/mL msClu for the indicated time. Whole cell lysates were analysed by Western blot. (C) Treatment of N2A with 5 µg/mL msClu was performed in combination by adding of 2% Panexin for the indicated time to check Akt phosphorylation in Western blot analysis. Illustrations in B and C show a selection of several independent experiments (Exp.), depicting the ambivalent results gathered throughout the project.*

4.2.1 The Ins-R downstream target Akt is inconsistently modified by Clusterin

To test the new adaptions made in the experimental conditions, the experiment shown in Fig. 9D was repeated using the described conditions. Despite the changes, a reduction of Ins-R phosphorylation could not be measured (data not shown). In a next step, the incubation times were increased to exclude a possible time dependency of the phosphorylation signal (Fig. 10A). However, these adaptions did not yield any promising results either. To eventually eliminate the suggested theories for the inconsistent findings in Western blot and RTK Array kit, the phosphorylation levels of the Ins-R downstream target Akt were analysed. Again, N2A cells were treated with insulin and Clusterin over an extended period of time to determine the Akt phosphorylation level and, strikingly, the Western blot analysis revealed a prominent decrease in Akt phosphorylation in the Clusterin-treated sample (Fig. 10B, Exp. 1). After both 30 and 60 min, the phosphorylation levels of Akt were significantly reduced. These observations strengthened the assumption that Clusterin might influence phosphorylation sites at the Ins-R not detected by the specific p-Ins-R antibody. Additional consecutive experiments, however, revealed a highly inconsistent effect of Clusterin on Akt phosphorylation (Fig. 10B, Exp. 2). Similar results were obtained using HEK-293 cells as experimental cell model (data not shown) which excluded the chosen cell model as a potential influential factor for the observed inconsistency. To test whether the composition of Panexin might have a stabilising effect on the overall initial cell condition, the Panexin experiments from Fig. 9D were repeated and subsequently stained with p-Akt antibodies (Fig. 10C). The substitution of insulin by Panexin did not influence the inconsistency of Akt modulation seen in the Clusterin-treated samples.

Despite their ambivalence, the alterations in the Akt phosphorylation by Clusterin in the presence of either Panexin or insulin were not reflected in the pIns-R levels. Thus, the assumption of other phosphorylation sites being targeted by Clusterin was more than justified since it would have been in accordance with the RTK Array kit observations.

4.2.2 Screening of multiple cell cultivation variables reveals glucose as disturbance factor for Clusterin signalling modulation

The established N2A cell model yielded decent results for the Akt phosphorylation screening. The chosen concentrations and time periods seemed to yield the expected observations. Nonetheless, the modulation of Akt by Clusterin was far from being reliable as the Clusterin effects covered the whole spectrum of possible outcomes with no distinct tendency. To further improve the used cell model and

to eliminate potential disturbing factors, several other variables had to be modified and tested. A crucial factor that could have caused the ambivalent results seen in Akt phosphorylation was the initial cellular status prior to stimulation. This status is influenced by the cultivation conditions selected for the execution of the experiments. These conditions include cell density in the cultivation receptacle, serum deprivation time as well as cultivation medium composition. For all parameters, the optimal setup had to be determined.

4.2.2.1 Clusterin alters the effect of insulin in an ambivalent manner

The standard cultivation conditions for N2A were an initial cell count of 500,000 cells per well on a 6-well plate. In combination with a 24 h growth period and 24 h of starvation this resulted in a well containing approximately 90% confluent cells prior to stimulation. A possible reason for the variations in Akt signals could be that cells cultivated at these conditions were on the verge of sliding into a stressed condition. With this assumption, a reasonable modification in culture conditions was to reduce either the cell density or the starvation time, two potential cell stress factors. As new experimental parameters, the starting cell number was reduced to 250,000 cells per well and starvation time to 12 h. To distinguish between effects resulting from either cell density or starvation, one parameter was kept at a standard condition while the other was changed to the new condition. The samples for each parameter were analysed by Western blot and subsequently quantified and normalised to the respective insulin-only samples to compare the results with each other (Fig. 11A). The discrepancy between single experimental outcomes declined over time in the samples cultivated at standard conditions and under 12 h starvation. Balancing of the signals was more prominent in the 12 h starvation samples compared to standard conditions. On the other hand, the samples of reduced cell count displayed an opposing behaviour over time. Here the prolonged stimulation increased the divergence of the resulting Akt phosphorylation. Additional experiments with alteration of both cell count and starvation period did not reveal any positive development towards more consistent results (Fig. S2). Although the 12 h starvation samples showed promising results for the 60 min timepoint, the spread in outcomes for 30 min was still unacceptable. Furthermore, the 60 min time point was not feasible for following experiments as the signal intensity of insulin-induced Akt phosphorylation at this point was already on a decline (see Fig. 10B, Exp.1).

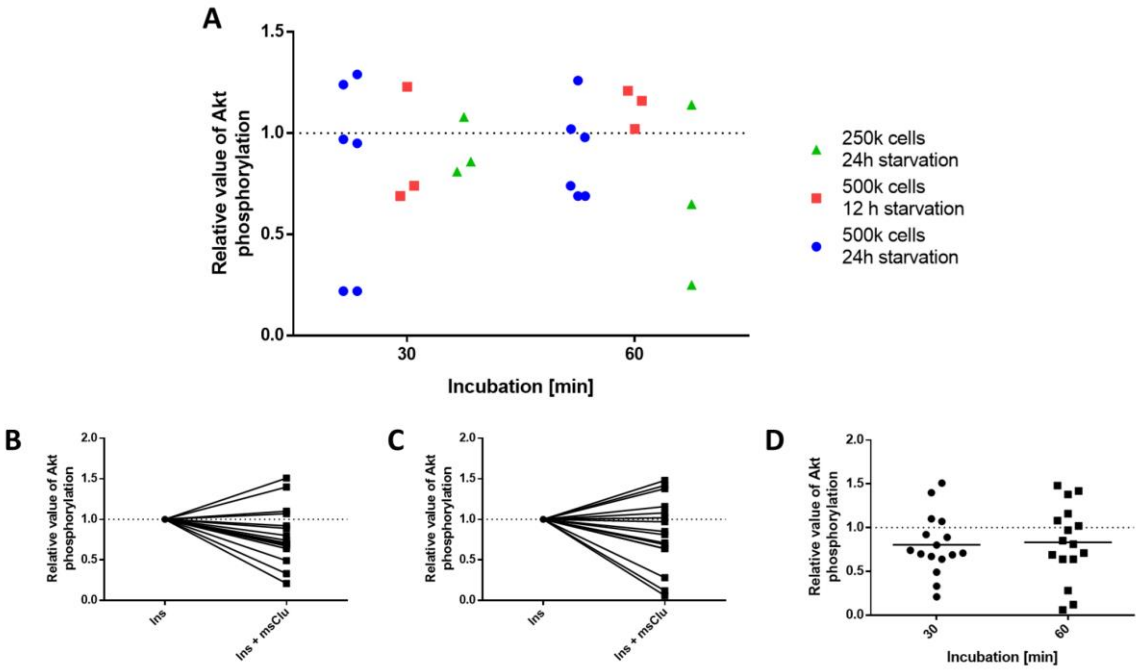

Fig. 11: Summary of the ambivalent effect of Clusterin on Akt phosphorylation and its dependency on cell density or starvation level during N2A cultivation. *N2A were again treated with 5 µg/mL msClu and 0.5 µg/mL insulin for the indicated time. Gathered whole cell lysates were analysed by Western blot to determine Akt phosphorylation levels. Collected blot data was quantified with Image Studio Lite by standardising every Akt phosphorylation signal to its corresponding total Akt protein signal. The standardised pAkt values of samples treated with msClu and insulin were normalised to their respective insulin-only pAkt value which was set to 1. (A) Cultivation conditions of N2A were altered to evaluate their influence on the Clusterin effect. Besides the two standard values for cell count (500k cells) and starvation time (24 h) two additional values (250k cells, 12 h starvation) were introduced to reduce possible cell stress effects. When one parameter of the standard values was changed, the second was kept constant. For each value three independent experiments were quantified and plotted against the respective insulin value. (B, C) Experiments performed with standard cultivation conditions (n = 16) were quantified and plotted to evaluate a potential tendency and time dependency in the gathered results. (D) Quantified pAkt values from B and C were plotted together in a scatter plot for improved visualisation.*

Conclusively, none of the changed parameters had a significant influence on the reproducibility of Clusterin-induced Akt modulation. Hence, the cell density and starvation time were not responsible for the signal ambivalence.

However, to elaborate a potential tendency towards a specific outcome, the initial experiment with standard cultivation conditions (see Fig. 10B) was executed repeatedly. The increased number of independent experiments eliminates the possibility of statistical maldistribution. The Western blot signals of both 30 and 60 min stimulation were quantified and separately displayed as relative change in Akt phosphorylation levels between samples treated with or without Clusterin (Fig. 11B and 11C). Despite the large sample size of 16 independent experiments, the two evaluations showed no obvious tendency towards lower or higher values of Akt phosphorylation. Even a comparison of both 30 and

60 min values of Clusterin stimulation in a scatter plot resulted in similar means close to the normalised insulin control (Fig. 11D).

The change of cell density and starvation period did not affect the level of Akt phosphorylation modulation by Clusterin. Furthermore, it followed no distinct pattern that could be statistically evaluated.

4.2.2.2 Cultivating N2A on low glucose medium stabilises Clusterin effects

The transmission of stimuli by signal transduction pathways is a time-dependent mechanism. While some molecules activate signalling within a few seconds others trigger a long-lasting stimulation usually with a lowered signal intensity compared to the short-term burst activation. Phosphorylation of the insulin receptor by insulin stimulation is a rather quick process triggering activation of downstream targets for an estimated 10 min (Smith & Shanley, 2013; Sedaghat, et al., 2002). For previous and future experimental approaches, the insulin level had been set to a higher than saturating concentration to guarantee consecutive activation of insulin receptors over a measurable time course. Although a constant activation of insulin receptor had been achieved as visible by elevated phosphorylation levels shown in Fig. 10A, the signal for the downstream target Akt had already been on a decline after 60 min (Fig. 10B, Exp. 1). Therefore, the next step was to determine insulin-induced Akt phosphorylation at multiple time points. The ambivalence in Akt phosphorylation by Clusterin at 30 and 60 min could be based on varying deactivation times of the phosphorylation cascade between the experiments in the monitored time course. For more precise results, earlier time points had to be compared. In the following experiments, a period of 5 to 30 min was chosen for the monitoring of Akt phosphorylation (Fig. 12A). Interestingly, only the values at 5 min and 30 min displayed comparable results, whereas the examined samples for 10 and 20 min between the two experiments showed controversial outcomes. The pronounced variation in insulin-only and insulin + Clusterin-stimulated samples within those two time points foreclosed a possible coincidence. The observed differences in signal intensity must have stemmed from altered reactions of the cells upon Clusterin addition.

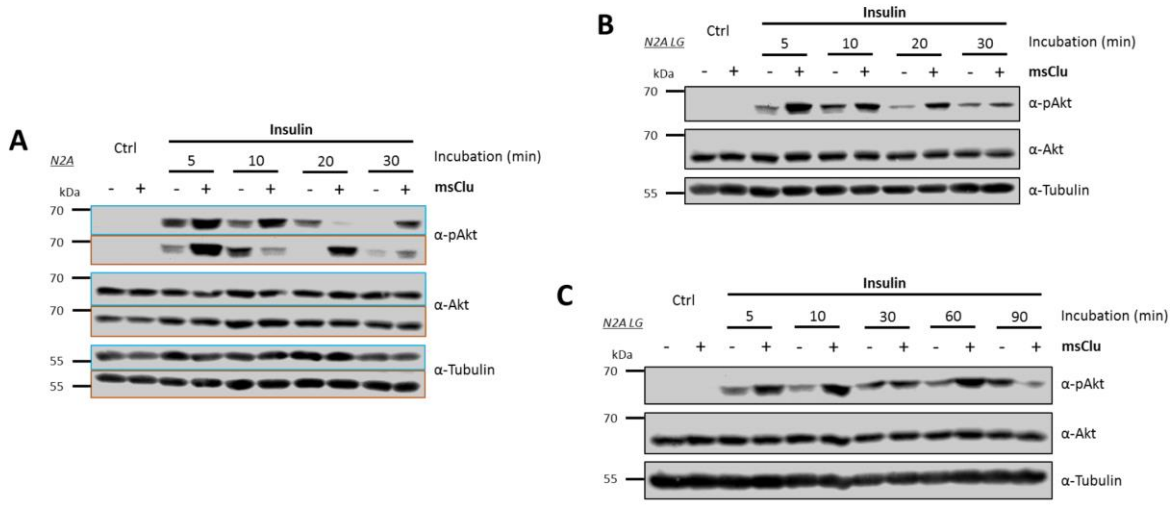

Fig. 12: Introduction of the new N2A LG cell model and its influence on the modulating effects of Clusterin during insulin treatment. *The treatment of N2A was kept constant at 5 µg/mL msCLu and 0.5 µg/mL insulin for the indicated time. Cell lysates were subject to Western blot analysis. (A) Effects of Clusterin on Akt phosphorylation were monitored in the early phase after stimulation to determine a potential time dependency. Depicted are two independent experiments (blue- and red-bordered) to visualise the bivalent experimental results. (B, C) The DMEM component of standard growth medium for N2A was replaced with DMEM containing low doses of glucose during the whole passaging and cultivation process. The phosphorylation level of Akt after stimulation was measured over the indicated period of time.*

Reconsidering the experimental setup, one particular aspect of the cell cultivation protocol drew the attention. For optimum cultivation conditions, N2A were grown in medium containing DMEM with an elevated level of glucose compared to physiological conditions. This was necessary due to the cancerous nature of N2A cells which leads to an increased demand for glucose. However, since glucose itself is an essential regulator in glucose metabolism and therefore also influences the impact of insulin stimulation, the modulation of Akt phosphorylation could be influenced as well leading to the inconsistent results. In cell culture, glucose was shown to alter the binding affinity of insulin to the insulin receptor (Traxinger & Marshall, 1990). This could be the decisive variable in the observed results of Clusterin-induced Akt alteration. To confirm this hypothesis, N2A cells were cultured and kept in medium containing low glucose DMEM (LG) from the beginning of cell seeding. With these cells, the experiment from Fig. 12A was repeated to directly compare the influence of glucose on the Akt phosphorylation levels (Fig. 12B). As a matter of fact, the usage of LG in the cultivation process of N2A inevitably led to a consistent elevation of Akt phosphorylation in the Clusterin-treated sample compared to the insulin-only sample over the full course of 30 min incubation. Additional experiments with prolonged incubation up to 90 min revealed a second boost of Akt phosphorylation by Clusterin around 60 min, before the signal intensity subsided in both insulin-only and Clusterin-treated samples

after 90 min. Reactivation of signal transduction pathways is not surprising as it was previously shown to occur in irradiated MCF-7 cells as well (Criswell, et al., 2005).

These results clearly stated that the high glucose content in the cultivation medium was the crucial factor for the ambivalent behaviour of Akt phosphorylation in Clusterin addition. The usage of LG not only allowed a consistent Clusterin-dependent Akt stimulation but also revealed a time dependency in the course of incubation. However, the results were not sufficient to clarify the effects of high or low glucose medium on the efficacy of insulin stimulation and Akt phosphorylation levels in the presence of Clusterin. Additional experiments examining the phosphorylation levels of Ins-R during stimulation over 90 min, for example, again displayed no significant alteration between insulin and insulin + Clusterin samples (Fig. S3). In both samples, the Ins-R phosphorylation levels were equally elevated.

4.2.3 Low glucose-cultured N2A display a stressed cell character

The experiments conducted with the N2A cells cultured in LG medium finally yielded constant results throughout all performed experiments. The results clearly showed a significant boost in Akt phosphorylation when cells were cotreated with insulin and Clusterin. Although no effects were visible in the phosphorylation levels of Ins-R, the N2A cell model with LG medium was a potential starting point for future experimental setups. With these setups, the role of Clusterin in signal transduction pathways and in particular insulin signalling could be further studied and the underlying mechanism could be elucidated. Nevertheless, there was another aspect in this process that had to be clarified before following experiments were conducted. Since Clusterin is a high molecular weight protein, the possibility existed that the observed effects on Akt phosphorylation were due to general protein effects. Insulin triggers the endocytosis of amino acids and the synthesis of proteins through Akt activation. Added Clusterin could be potentially endocytosed, decomposed in lysosomes and used for the elevated protein synthesis by insulin treatment. The degradation of Clusterin would release its amino acids which in turn could stimulate Akt phosphorylation and members of associated signalling pathways through yet unknown mechanisms (Dalle Pezze, et al., 2016; Tato, et al., 2011; Flati, et al., 2010). Since all previously shown control samples with Clusterin-only treatment did not show any stimulation of Akt, this suggests that stimulation with insulin (or other factors) was a prerequisite for the modulation by Clusterin, regardless of it being a specific or unspecific effect.

4.2.3.1 Low glucose leads to general protein-dependent Akt activation

The effect of Clusterin had to be reevaluated by introducing protein controls, to check for a possible overall protein effect triggering Akt phosphorylation during insulin stimulation. One of the chosen controls was bovine serum albumin (BSA) as it is one of few proteins that is ubiquitously present in the blood serum in high concentrations. This renders it a perfect control protein as Clusterin exhibits similar characteristics as BSA. As a second candidate glutathione S-transferase (GST) was used. Since this protein is typically located in the cytoplasm, the possibility of cross reactions with receptors on the cell surface is unlikely during stimulation with insulin. The first experiments that were conducted with the two control proteins were in high glucose-cultured N2A to check if they would display similar ambivalent behaviour. With both BSA and GST, there was a low but detectable increase in Akt phosphorylation compared to the insulin sample within 10 min (Fig. 13A). The increased phosphorylation levels stabilised in the 30 min sample to the level of the insulin sample. The two protein controls seemed to have an effect on Akt phosphorylation, however, the intensity was by no means comparable to the effects often seen with Clusterin. In the GST experiment the difference was nearly insignificant and the effect of both proteins only lasted for about 10 min whereas a Clusterin influence was detectable even at 60 min post-stimulation (Fig. 10B, Exp. 1). A bivalent alteration of pAkt similar to Clusterin could also be observed for BSA (data not shown).

With N2A LG cells, the observations differed only slightly (Fig. 13B). The increase in Akt phosphorylation within the first 10 min was slightly increased compared to the normal N2A cells but still didn't reach the impact level Clusterin exhibited on Akt stimulation (the absent signal in the 90 min insulin sample in the GST blot is ascribed to irregularities in the immunostaining process). A more interesting observation was the stimulation of Akt phosphorylation in the GST-only-stimulated sample. This brought up the assumption that the mechanism of protein endocytosis previously suggested for Clusterin was actually taking place in case of GST treatment (see 4.2.3). GST seemed to be taken up by the cells to be degraded to amino acids which stimulated Akt phosphorylation. This assumption was based on the fact that GST is usually located in the cytoplasm and therefore has no corresponding receptor on the cell surface.

The simultaneous treatment of N2A with insulin and BSA or GST had only minor and short-lived effects on the phosphorylation levels of Akt. Introduction of the N2A LG cell model slightly increased the positive effects of BSA and GST on Akt phosphorylation but demonstrated an unexpected stimulation of pAkt in the GST-treated control sample.

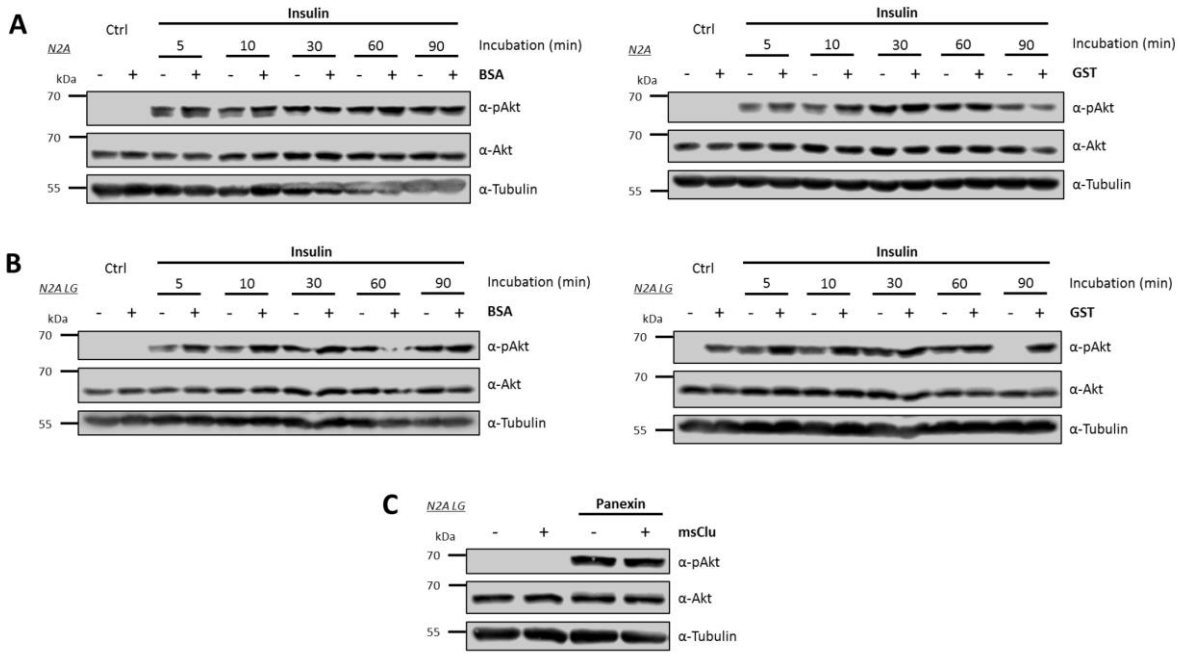

Fig. 13: Modulation of pAkt signals by addition of BSA or GST during IGF-1 stimulation of N2A and N2A LG cells. *(A, B) N2A were either cultivated in normal or low glucose growth medium, followed by serum starvation and stimulation with insulin (5 µg/mL) and either BSA or GST (both 5 µg/mL) as protein controls. (C) Stimulation of N2A with msClu (5 µg/mL) and Panexin (2%), as described in Fig. 9D, was repeated with N2A cultured in low glucose growth medium as a control and linkage to the RTK Array kit. In all depictions Akt phosphorylation was monitored over the indicated period of time and analysed by Western blot.*

Considering these results and the conditions the cells were cultivated in, the only possible reason for such a protein-based phenomenon was occurring cell stress. Since N2A are neuroblastoma cells, they possess an elevated demand for glucose. The amount of glucose in the LG medium used for cultivation was probably insufficient when cells were grown over an extended period of time and in high density. This hypothesis was backed by the results gathered when the Panexin experiment of Fig. 9D was repeated with N2A LG cells (Fig. 13C). In all LG attempts the samples with and without Clusterin were identical in their Akt phosphorylation levels whereas in normal-cultured N2A cells they showed at least a variation in most of the conducted experiments. Potentially stressed cells would react vigorously on Panexin treatment since it is a serum supplement containing vast amounts of glucose, amino acids and other vital nutrients and metabolites. Therefore, the consequences resulting from an addition of Clusterin to the cells would be masked by the intense activation of Akt by Panexin leading to the observed homogeneous results in N2A LG.

Despite the observations that both BSA and GST slightly increase Akt phosphorylation in combination with insulin in the early phase of stimulation, the results were doubtful. The stressed cell character in N2A LG cells influenced their response towards applied stimuli and especially towards potential amino

acid sources. These results also challenged the data received in the N2A LG experiments conducted with Clusterin since the observed increase in Akt activation could have also just stemmed from its protein character. However, when looking at the effect of Clusterin in normal N2A (Fig. 12A), be it positive or negative, it was obvious that the impact on Akt phosphorylation was indisputably higher than in BSA-treated samples and even more so when compared to GST treatment (Fig. 13A). This led to the conclusion that although there might have been a minor protein effect by Clusterin treatment in N2A LG, (Fig. 12B and C) the marked increase in pAkt by Clusterin treatment is mainly ascribed to a consequence of a distinct mechanism triggered by Clusterin and its interaction with insulin. Furthermore, it became clear that the N2A LG cell model did not meet the requirements for a stable and reliable cell model to study the effects of Clusterin on signal transduction pathways.

4.2.3.2 Phenotypical changes are observed in N2A cultured in low glucose medium

Further analysis of N2A cultured in LG medium was conducted to confirm the assumption that these cells experience increased cell stress during cultivation or at least show alterations to normal-cultured N2A. The first conspicuous feature of N2A LG cells was the decreased proliferation rate during cultivation. To reach full confluency in a T75 flask, these cells took about twice as long compared to normal N2A. Furthermore, during the cultivation process the medium had to be replaced several times to guarantee continuous growth whereas normal N2A could be kept in the same medium for at least seven days. The reduced amount of glucose also impaired the cells' ability to properly attach to the surface after cells were passaged or transferred to new culture vessels. To further support these findings, the cells were visually studied during the cultivation process as well. Both normal and LG N2A were cultured analogous to the conditions present during cell cultivation to insulin stimulation. Cells were transferred to a 6-well plate and grown for 24 h. Before the substitution with serum-depleted medium, pictures of both wells were taken (Fig. 14, 0 h). After another 24 h on serum-depleted medium, pictures were taken again (Fig. 14, 24 h). Although similar amounts of cells were seeded, the sample containing the N2A LG cells showed decreased density in the 0 h sample compared to high glucose-cultivated N2A. This was both due to impaired attachment and decreased growth rate. As a logical consequence, the cell density in the serum-depleted sample was also decreased. The most striking observation, however, was the morphological malformations observed in N2A LG cells (Fig. 6, black arrows). These malformations seemed to be either swollen or fused cells that completely lost the morphological characteristics of typical N2A cells. The occurrence of such cells was even more

elevated in the serum-depleted wells whereas in serum-depleted normal N2A they rarely manifested. Increased density or cell stress could have been possible reasons for this phenomenon. Additionally, the overall morphology revealed impaired axon formation in N2A LG.

Taken together, the cultivation of N2A in LG medium had a severe impact on the morphological and metabolic integrity of these cells. These observations strengthened the hypothesis of increased cell stress in N2A LG cells, rendering them unusable for future signal transduction experiments.

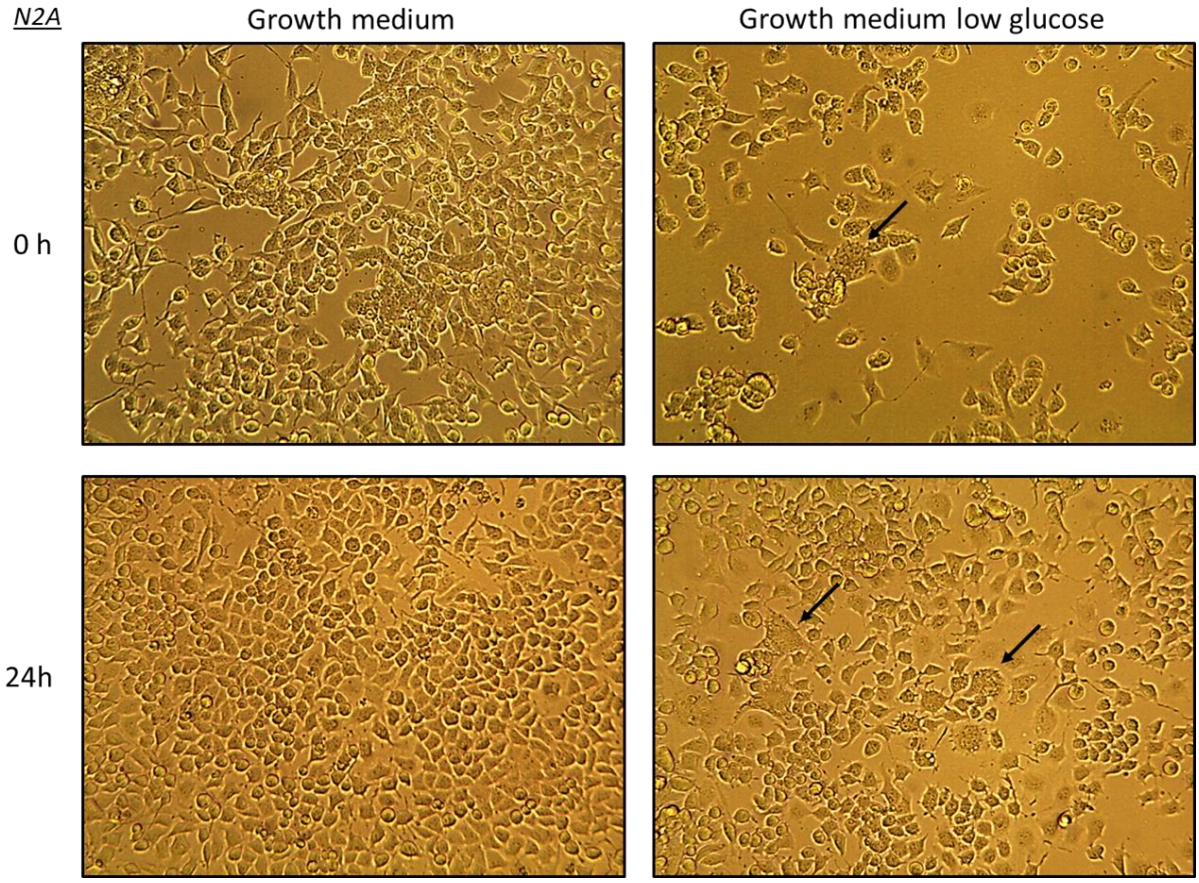

Fig. 14: Visual examination of growth rate and morphology of N2A cells cultivated in regular or LG medium. *As usual, 500K N2A cells per well on a 6-well plate were cultivated in either standard or low glucose growth medium. After 24 h, pictures of the cells were taken (0 h) and growth medium was substituted with respective serum-depleted medium. Cells were kept in the incubator for another 24 h before a second picture was taken (24 h). At this point the cells are usually treated for subsequent experiments, like Western blot. Black arrows highlight significant morphological features.*

4.3 Characterisation of the IGF-1-Clusterin-interplay in the modulation of signal transduction pathways

All efforts to establish a cellular model to examine the possible influence of Clusterin on the insulin signalling mechanism in a neuronal environment failed. Although preliminary data revealed promising results for the modulation of Akt phosphorylation, none of them yielded consistent results. While the signals of Clusterin stimulaton in normal N2A cells were intense, yet inconsistent, the cultivation of N2A cells in low glucose medium showed stabilised Clusterin effects but caused elevated stress levels which influenced the examination of signalling pathways. Thus, neither one of the two tested cell models met the requirements needed for a characterisation of Clusterin involvement in signal transduction pathways.

One possibility to bypass these problems was to aVol.on the idea to establish a cell model related to Alzheimer's disease. However, preliminary experiments with other cell lines such as HEK-293, EA.hy926 or Hep G2 showed similar inconsistent outcomes for the stimulation with insulin and Clusterin (data not shown). This further backed the assumption that the high glucose content was responsible for the alterations in the respective experiments. A solution could have been a cell line that could easily be cultivated on LG medium without triggering stress events, however, such cell line was not available. An alternative to keep the cellular model with N2A cells and to stay close to the subject of Alzheimer's disease was the substitution of insulin with IGF-1, a close molecular relative. IGF-1 is able to stimulate the insulin receptor as well as heterodimers of insulin and IGF-1 receptor. With this solution, the results from the RTK kit and also the following data about Akt phosphorylation could still be used as a basis for discussion. Furthermore, recent studies had revealed a correlation of brain IGF-1 levels to the risk for Alzheimer's disease (Westwood, et al., 2014) and comparisons to observed insulin effects (Gasparini & Xu, 2003). IGF-1 is classified as a growth factor which has only minor effects on glucose metabolism granting it the advantage to be less influenced by glucose levels compared to insulin.

4.3.1 IGF-1 qualifies as a novel Clusterin ligand with a glucose-independent Akt stimulation

The IGF-1 growth factor is closely related to insulin and is therefore able to activate both IGF-1 and insulin receptors. In the results of the RTK Array kit (Fig. 9B), however, it did not play any role since Panexin was devoid of growth factors. Thus, the effects of IGF-1 and Clusterin on the IGF-1 receptor

phosphorylation had to be examined separately. As with insulin in Fig. 12C, the effects of simultaneous stimulation of N2A cells with IGF-1 and Clusterin was monitored over an extended period of time. The samples were analysed in a Western blot by staining for pIGF-1 receptor signals with a specific antibody (Fig. 15A, left panel). As already expected the staining also showed an increase in the receptor phosphorylation levels after IGF-1 stimulation but no significant changes between the samples stimulated with or without Clusterin. The observations were similar to the results gained from the experiments with insulin stimulation. Since the experiments with the RTK Array kit did not include IGF-1 stimulation, there was no basis to assume a possible modulation of pIGF-1 receptor levels by Clusterin addition. Besides the previously mentioned hypothesis that the specific antibodies do not cover the essential receptor phosphorylation sites addressed by Clusterin, it had to be considered that Clusterin simply did not influence the phosphorylation of IGF-1 receptor directly.

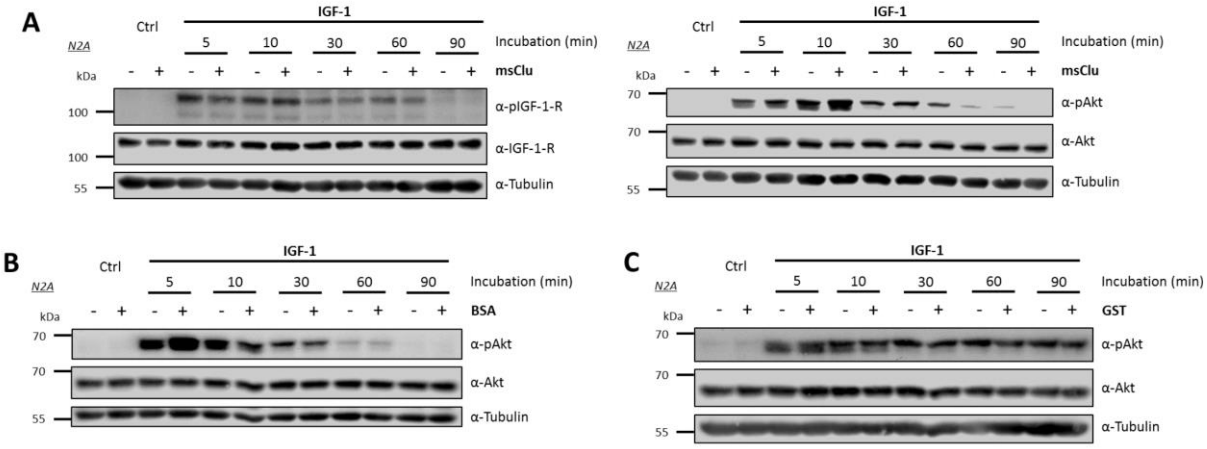

Fig. 15: IGF-1, a glucose-independent insulin relative, is used as substitute for insulin to examine the effects of Clusterin on signal transduction pathways. *After cultivation on serum depleted medium for 24 h N2A cells were stimulated with 50 ng/mL IGF-1 and with or without 5 µg/mL of either msClu (A), BSA (B) or GST (C) for the indicated time. Harvested whole cell lysates were used in Western blot analysis.*

The crucial part of the IGF-1 stimulation, however, was the phosphorylation of Akt in the presence of Clusterin. The samples from the above experiment were again stained with pAkt antibodies (Fig. 15A, right panel). Although the signals were not as prominent as with insulin, the Western blots clearly showed a definite increase of Akt phosphorylation levels in the samples treated with Clusterin. This elevation was detectable over approximately 30 min post-stimulation which matched the results seen with insulin (Fig. 12A and B). At 60 min post-stimulation both the IGF-1 and IGF-1 + Clusterin signal were on a decline. The advanced reduction of pAkt in the 60 min Clusterin sample compared to the respective IGF-1-treated sample could be caused by slightly delayed pAkt deactivation or an increased negative feedback based on the elevated Akt phosphorylation after Clusterin addition.

To verify IGF-1 as a new stimulant of Akt phosphorylation, the effects of BSA and GST as protein controls were be analysed as well. A stimulation with GST caused no significant change in the Akt phosphorylation signals compared to IGF-1-only treatment over the complete monitored time span (Fig. 15C). These results were an evidence for an actual specific effect of the Clusterin molecule on the alteration of Akt phosphorylation. The treatment of BSA yielded similar results to GST, however, showed an increase in Akt phosphorylation in the 5 min sample which immediately subsided after 10 min (Fig. 15B). This behaviour was already observed by another research group in association with insulin (Coffey, et al., 2015). They revealed a connection between Akt stimulation and albumin endocytosis triggered by insulin treatment. The endocytosed albumin in turn further amplified Akt phosphorylation. Furthermore, they could prove an involvement of LRP2 in the process of albumin endocytosis. This receptor from the LDL-receptor family is also a well-described interaction partner of Clusterin, rendering it a potential target for the elucidation of the mechanistic background associated with the observed Clusterin effects on Akt phosphorylation.

4.3.2 The LRP2 receptor is not involved in observed Clusterin effects

Several studies addressed the scavenging ability of Clusterin in combination with LRP2 binding (see 1.1.3.2). Furthermore, this interaction of Clusterin and LRP2 was also studied for possible mechanisms in signal transduction which involved the scaffolding proteins Dab-1/2 (Oleinikov, et al., 2000; Gotthardt, et al., 2000). These insights suggest a potential involvement of LRP2 in the stimulation of IGF-1 signalling pathways by Clusterin. To study the effect of LRP2 in the process of IGF-1 stimulation, the LDL receptor-specific chaperone RAP was used to mask the binding sites of LRP2 for all known ligands leading to subsequent endocytosis events. If Clusterin acted via activated endocytosis of LRP2 the substitution with RAP would yield analogous results. The experimental realisation of this theory actually did show an elevated Akt phosphorylation in the RAP-treated sample (Fig. 16A). However, the temporal activation pattern closer resembled the one observed in the BSA-stimulated blots (Fig. 15B) despite the slightly longer duration of up to 10 min. The drop at 30 min in the RAP-treated sample could not be accredited to improper staining as this result occurred in several experiments executed repeatedly. Since the results for RAP-treatment prompted further questions, it was suspected whether N2A cells actually express LRP2. Subsequent PCR analysis of isolated N2A cDNA with primers specifically targeting LRP2 revealed a complete absence of LRP2 mRNA in the transcriptome of N2A (Fig. 16B). In addition to LRP2, two other members of the LDL-receptor family, namely ApoER2 and

LRP1, were also analysed, as RAP is able to bind all LDL-receptor family members at least to some extent. PCR-analysis for those two receptors yielded a positive result (Fig. 16B).

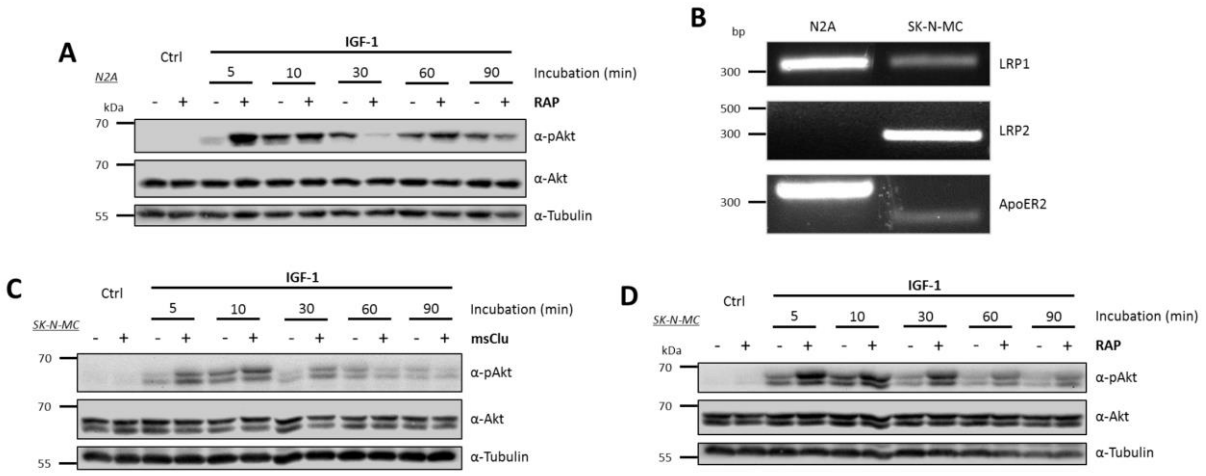

Fig. 16: The role of the bona-fide Clusterin receptor LRP2 in Clusterin-dependent elevation of Akt phosphorylation as examined in N2A and SK-N-MC cells after blockage of LRP2 with RAP. *(A) N2A were treated and subsequently analysed as described in Fig. 15 except for the substitution of msClu with the LDL-receptor chaperone RAP (5 µg/mL). (B) Total mRNA gathered from both N2A and the human neuroblastoma cell line SK-N-MC was reversely transcribed. Resulting cDNA was scanned for appearance of LRP1, LRP2 and ApoER2 transcripts with target-specific primers in a PCR. (C, D) SK-N-MC were subjected to treatment with IGF-1 (50 ng/mL) and either msClu or RAP (both 5 µg/mL) for the indicated period of time, followed by analysis of cell extracts with Western blot.*

The negative result for LRP2 screening in N2A entailed a search for an alternative cell line to further investigate a role of LRP2 in Clusterin-mediated Akt phosphorylation. A neuroblastoma cell line from humans, called SK-N-MC, emerged as a possible candidate since it possessed comparable attributes like N2A. The immediate PCR-screening of this cell line showed the desired results of a positive LRP2 Vol. (Fig. 16B). Furthermore, SK-N-MC also possessed ApoER2 and LRP1 mRNA transcripts. Before the RAP treatment was tested on the new cell line, its response to combined Clusterin and IGF-1 treatment had to be examined with the typical experimental setup. Interestingly, the Akt phosphorylation was also elevated in the Clusterin-treated samples (Fig. 16C) and also showed a similar temporal pattern as the experiment executed in N2A (Fig. 15A, right panel). The subsequent addition of RAP to IGF-1-stimulated SK-N-MC cells also caused a prominent elevation of Akt phosphorylation with a peak at 5 min that continuously dropped over the following 90 min (Fig. 16D). To determine whether the effects of Clusterin and RAP on Akt phosphorylation both occur via the activation of PI3K, an upstream molecule in the Akt signalling pathway (see 1.2.3.2), cells were pretreated with the specific PI3K inhibitor LY294002 before stimulation. The inhibition of PI3K in the RAP-treated experiments showed a clear inhibition of Akt phosphorylation in all stages of the experiment (Fig. S4). In contrast, the Clusterin-treated experiment displayed variations in the 5 min samples. While application of the

inhibitor abrogated any IGF-1-induced Akt activation, the presence of Clusterin retained a positive phosphorylation signal to some extent.

The RAP experiment in N2A cells yielded results similar to its counterpart with IGF-1. The two observed stimulation patterns of Akt phosphorylation for either Clusterin or RAP application, however, differed in their temporal course of activation but were consistent across both tested cell lines. This suggested that either Clusterin had a lower affinity to LDL-receptors causing a delay in activation or, as the PI3K inhibitor experiment would suggest, the mechanisms for RAP and Clusterin stimuation were independent from each other. The PCR screening together with the consistent Western blot results of pAkt elevation in both cell lines proved that LRP2 is not involved in the Clusterin-induced processes, but did not exclude a possible role of other members of the LDL-receptor family.

4.3.3 Human Clusterin exerts similar effects as murine Clusterin on IGF-1 stimulation

In the following experiments, it was of interest to determine whether the effect of murine Clusterin (msClu), as seen in the previous experiments, was also true for the human variant of Clusterin (hsClu). Since murine Clusterin was able to trigger Akt effects in the human cell line SK-N-MC, the opposite with human Clusterin in N2A cells were tested as well. This approach should also establish a connection to the results gathered in the RTK Array kit, which were gained with hsClu (Fig. 9A and B). Before the purified recombinant human Clusterin was tested in cellular-based experiments, the structural differences to the murine variant were intensively studied.

4.3.3.1 Comparison of structural features between human and murine Clusterin

The two sequences for msClu (NP_038520.2) and canonical variant 1 hsClu (NP_001822.3, also see 1.1.1.2) were aligned with the EMBOSS Needle tool. Comparison of both sequences revealed a 76.4% identity (solid lines) between both amino acid sequences (Fig. 17). The similarity, which lies at 87.5%, considered variations in some amino acids that display equal physico-chemical properties (dotted lines). Both sequences contained the typical RXXR cleavage site (red) for furin-like proprotein convertases (see 1.1.2). Additionally, the alignment showed the high homology in the cysteine cluster (yellow) which is responsible for the intramolecular disulphide bonding. Variations between both sequences could be seen in the distribution of N-glycosylation sites (green). While five sites shared the

same positioning within the amino acid sequence, the human Clusterin had its sixth glycosylation site located on the α-chain close to the N-terminus. In contrast, the murine Clusterin contained only two glycosylation sites on the α-chain but an additional one on the β-chain located closely to the C-terminal side of the cysteine cluster. A fourth structural characteristic that was highlighted were the predicted amphipatic α-helices in human Clusterin. Since many studies had failed to reveal the structure of Clusterin with typical biochemical methods (see 1.1.2), the secondary folding state could only be predicted *in silico* (Tsuruta, et al., 1990; Jones & Jomary, 2002). Relevant data for the prediction in msClu were not available. However, further *in silico* studies were performed for rat Clusterin which shares high identity with murine Clusterin. These studies also revealed a high homology in amino acid sequence and localisation of the amphipatic α-helices between human and rat Clusterin. Based on these facts it was assumed that murine and human Clusterin share the same homologies in amphipatic α-helix distribution.

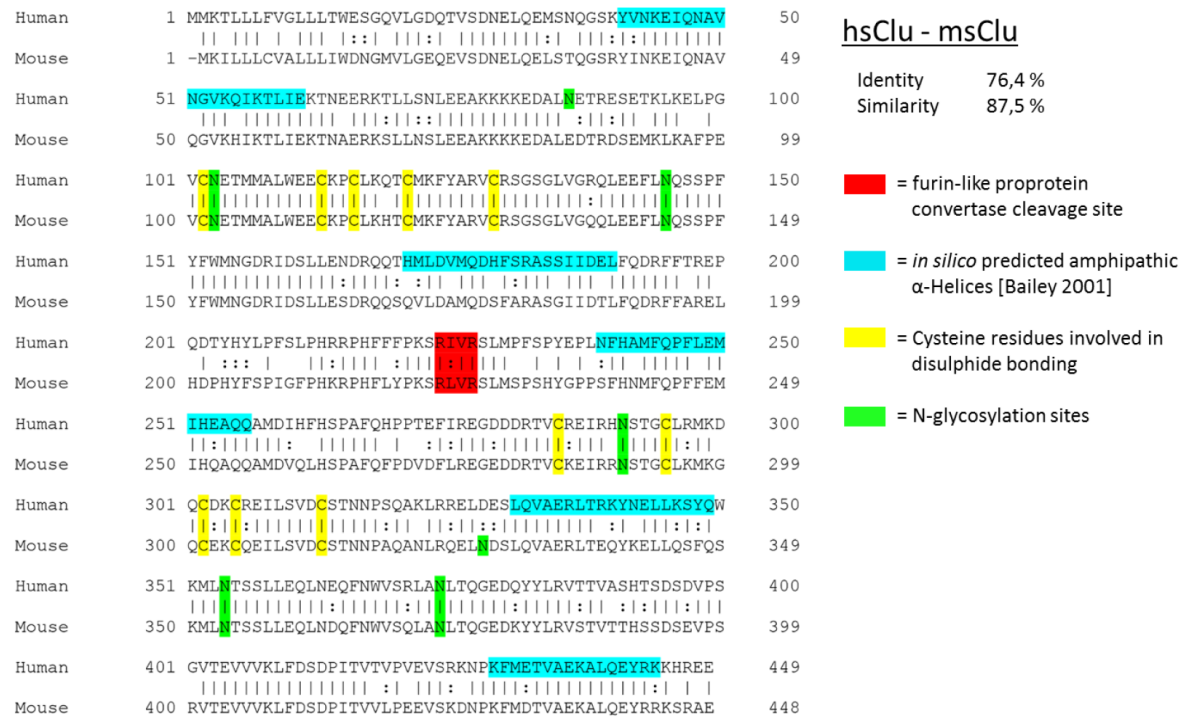

Fig. 17: Amino acid sequence alignment of hsClu and msClu with highlighted crucial structural domains. *The two amino acid sequences of hsClu (NP_001822.3) and msClu (NP_038520.2) were aligned with the online tool EMBOSS Needle and graphically modified to visualise essential structural features and the homology between both variants.*

4.3.3.2 Human Clusterin enhances IGF-1-induced Akt phosphorylation in both human and murine cell lines

With this information in hand the next step was to elucidate the effect of hsClu on pAkt activation in N2A and SK-N-MC cell lines. First, N2A cells were incubated with IGF-1 and hsClu for the usual 90 min. The Western blot analysis showed again an increase in pAkt signals in the Clusterin-treated samples (Fig. 18A). However, the signal intensity of the elevated pAkt signal was far less prominent when compared to msClu. Moreover, the increase in phosphorylation quickly subsided after 10 min whereas with msClu it lasted for about 30 min. Similar experiments with SK-N-MC yielded comparable results showing reduced activation and duration of Akt phosphorylation levels compared to msClu stimulation (Fig. 18B). Taken together, the observations made with hsClu present a positive effect of Clusterin on the Akt phosphorylation but with a reduced intensity compared to msClu. Although, both Clusterin variants share high homology, the efficacy in modulation of signal transduction varied.

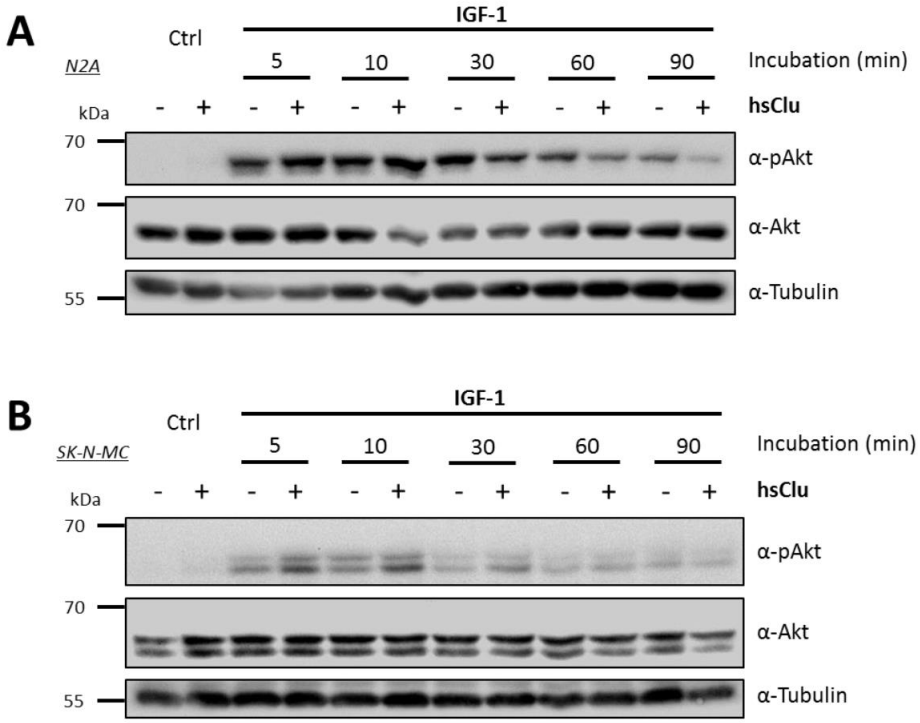

Fig. 18: Examination of human Clusterin for its ability to exhibit modulating effects on pAkt. *Cultivated and serum-starved N2A (A) or SK-N-MC (B) cells were treated with IGF-1 (50 ng/mL) and with or without hsClu (5 µg/mL) for indicated times. Whole cell lysates were examined in a Western blot approach.*

4.3.4 Functional properties of Clusterin are concentration dependent and administration form independent

Studies by Jo et al. postulated an inhibitory effect of cancer cell-derived Clusterin on the IGF-1-induced Akt phosphorylation. In their experimental setup HeLa-conditioned medium was used as a combined Clusterin and IGF-1 source to stimulate both serum-deprived HeLa and HEK-293 cells. Their findings contrast strongly with the observations made in this work where a clear induction of pAkt by Clusterin was observed. Furthermore, Jo and co-workers used conditioned medium gathered from transiently Clusterin-transfected HEK-293T cells, preincubated it with 2 ng IGF-1 and applied it on NB4 cells. Again, their observation was a reduction of Akt phosphorylation in the presence of Clusterin despite the non-cancerous origin of HEK-293 cells. In my work, a slightly modified approach was checked for its reproducibility in N2A cells. The conditioned medium collected from HEK-293 stably transfected with Clusterin (HEK-msClu-CM) or vector control (HEK-CM) was mixed with 50 ng IGF-1 (standard concentration in previous experiments) and added to N2A cells. Interestingly, the results disproved the published data of Jo et al. in N2A cells and confirmed previously gathered facts about msClu elevating Akt phosphorylation (Fig. 19A). Both HEK-CM and HEK-msClu-CM increased pAkt activation slightly compared to the IGF-1 control. To clarify the rather weak stimulation of pAkt by the conditioned medium in relation to stimulation with isolated recombinant Clusterin, the conditioned medium was further analysed. The essential parameter was the concentration of Clusterin in the conditioned medium which was determined by TCA precipitation of 500 µL medium and subsequent analysis with Western blot. The precipitated fractions of two independent medium preparations showed similar Clusterin contents in the HEK-msClu-CM samples (Fig. 19B). Both HEK-CM precipitations showed Clusterin concentrations below the detection limit. To quantify Clusterin concentrations in the CM, purified msClu was also loaded in ascending concentrations. This standard revealed that the levels of Clusterin applied with the HEK-msClu-CM were far below the standard concentration of 5 µg used in previous experiments. This explained the low increase in pAkt activation upon HEK-msClu-CM application.

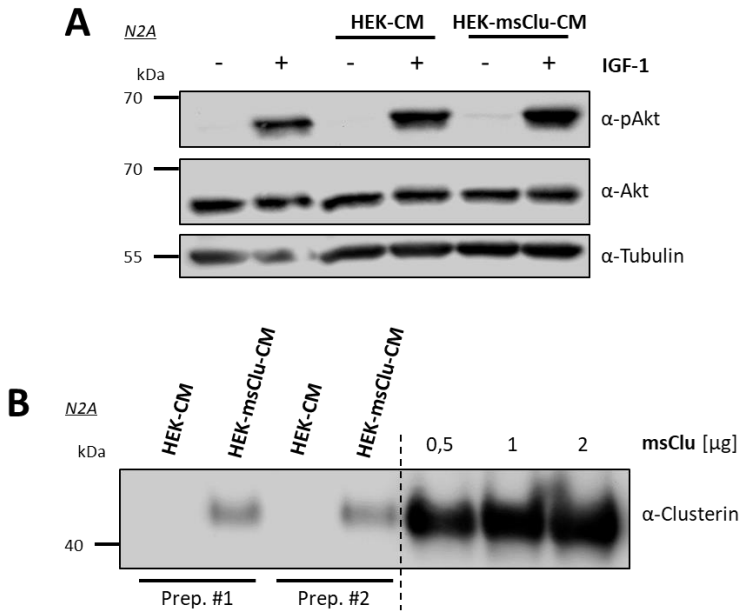

Fig. 19: Analysis of Clusterin-conditioned medium from transfected HEK-293 for its Clusterin concentration and its ability to alter Akt phosphorylation. *Normal HEK-293 (HEK) and HEK-293 stably transfected with murine Clusterin (HEK-msClu) were cultivated in T75 flasks until full confluency. Growth medium was substituted with starvation medium for 48 h. Supernatant was collected and separated from cellular debris (CM). (A) After 24h serum starvation N2A cells were treated with 50 ng/mL IGF-1 and 500 µL/mL of either HEK (HEK-CM) or HEK-msClu conditioned medium (HEK-msClu-CM) for 10 min. (B, left side) 500 µL conditioned medium of both normal HEK (-) and stably transfected HEK (+) was TCA-precipitated. Precipitated protein was resuspended and fully loaded on a SDS-PAGE to determine Clusterin content. Two independent conditioned medium preparations (Prep) were tested. (B, right side) As a concentration scale, different amounts of purified recombinant msClu were loaded as well (B, left side). All mentioned samples were harvested and whole cell lysates/CMs were analysed in Western blot.*

In the introductory section, a negative role of intracellular Clusterin forms on antiapoptotic mechanisms was illustrated. As an approach to evaluate a possible role of occurring intracellular Clusterin variants in the transient transfection conditions used by Jo et al., N2A cells were transiently transfected with the msClu vector. The Clu gene was under control of a constitutively active CMV-promotor. The high load of newly synthesised proteins could lead to formation of intracellular Clusterin forms (for mechanisms see 1.1.1.4). After 24 h of serum deprivation the cells were stimulated with IGF-1 and subsequently analysed by Western blot. Similar to the results in the analysed HEK-CM, the supernatants of transiently transfected N2A displayed no detectable Clusterin signals and correspondingly no elevation in Akt phosphorylation despite the presence of Clusterin in the cell lysates (data not shown). Neither high levels nor any possible effect of intracellular Clusterin forms was detectable in N2A. Therefore, an undiscovered influence of intracellular Clusterin in the experiments executed by Jo et al. was foreclosed.

All collected data showed that in the used experimental setup the application form of applied Clusterin was irrelevant for the influence on Akt phosphorylation but not the concentration of Clusterin which

in turn was essential for the intensity of the pAkt activation. These results further strengthen the contradiction between this work and the publication by Jo and co-workers.

4.4 Investigation of additional signalling pathways for an influential effect of Clusterin

The modulation of signal transduction pathways by Clusterin was verified in combination with insulin and IGF-1. However, the initial screening with the RTK Array kit did not take growth factors into account as Panexin was devoid of any growth factors. With this large group of signalling molecules still being unstudied it raised the question whether Clusterin is also able to alter the effects of these signalling molecules. Furthermore, it was of interest whether other signalling branches are affected by Clusterin as well.

4.4.1 Clusterin exhibits no effect on EGF stimulation

The previously mentioned studies by Jo et al. also evaluated possible effects of Clusterin on EGF-mediated Akt phosphorylation. Their experiments showed no significant elevation of Akt or ERK phosphorylation in the presence of Clusterin-conditioned HEK-293 supernatant. Since the experiments with N2A cells already revealed opposing results for the IGF-1-mediated Akt phosphorylation, the influence of Clusterin on EGF stimulation in N2A was also studied. The application of EGF on N2A cells did not trigger any Akt phosphorylation events (Fig. 20A). Published data confirmed the assumption that N2A cells do not express endogenous EGFR. This explains the absent Akt activation by EGF. However, staining for ERK phosphorylation yielded a positive result and displayed a time-dependent activation upon EGF application (Fig. 20A). Nevertheless, Clusterin addition had no modulating effect on the ERK phosphorylation level. The control experiment executed with BSA showed a slight increase at 5 min post-stimulation (Fig. 20B) which was similar to the observations in IGF-1-mediated Akt phosphorylation (Fig. 15B) that was attributed to the endocytosis events accompanied by BSA treatment (see 4.3.1). In case of EGF, studies demonstrated increased albumin secretion upon EGF stimulation (de Juan, et al., 1992) as well as ERK phosphorylation directly triggered by albumin-mediated EGFR activation (Reich, et al., 2005).

Despite the general notion that N2A cells do not express (sufficient amounts of) EGFR, the results demonstrated a distinct activation of ERK phosphorylation upon EGF stimulation. Furthermore, the

EGF experiments of Jo and co-workers could be confirmed in N2A cells, at least in case of absent Clusterin effects on ERK phosphorylation.

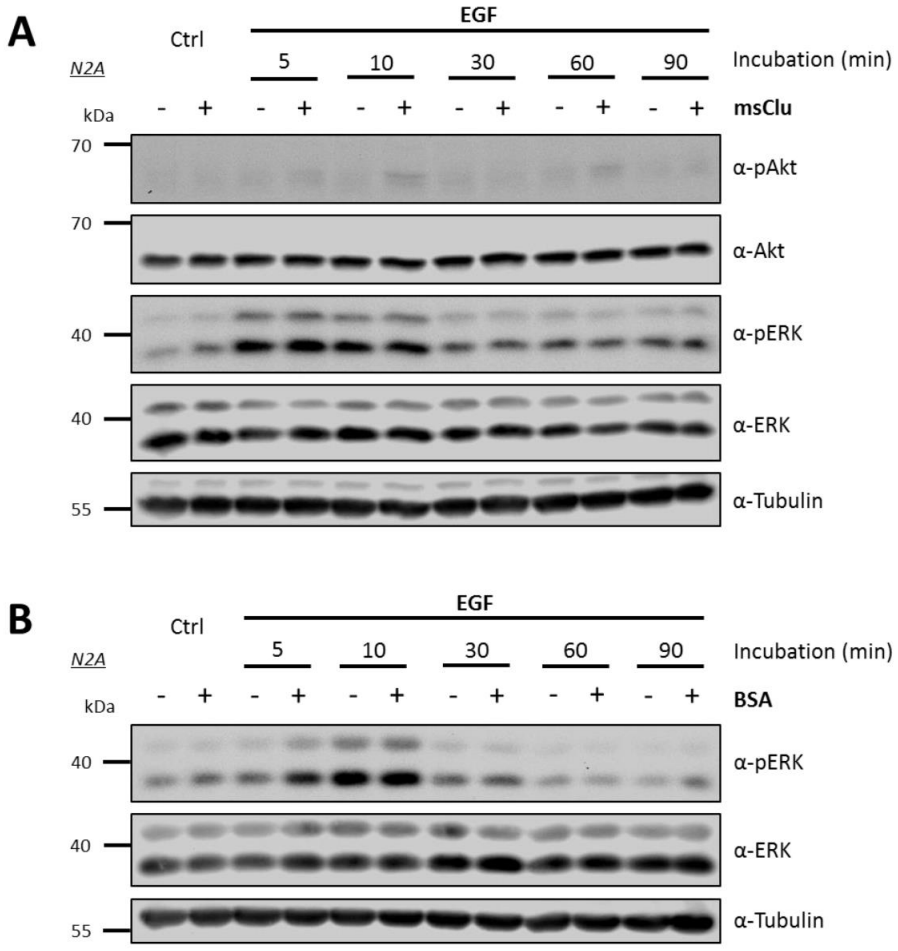

Fig. 20: Examination of the ability of both Clusterin and BSA to modulate the EGF-triggered signalling pathway. *N2A cells were stimulated as described in Fig. 15 with IGF-1 being substituted with EGF (50 ng/mL) and cells being treated with either msCLu (A) or BSA (B) (both 5 µg/mL). Besides the usual analysis of the whole cell lysates for Akt by Western blot, ERK phosphorylation was included in the screening.*

4.4.2 Investigation of Clusterin effects on HGF in Hep G2 is obstructed by high cellular stress levels

An essential growth factor that had to be examined as well was HGF. The screening for potential Clusterin receptors with the RTK Array kit revealed a potential modulation of HGF-R by Clusterin (Fig. 9B). To further examine these preliminary results, cells had to be stimulated with HGF and Clusterin. N2A cells, however, were not suitable for this approach because they do not express HGF-R. PCR analysis of the previously used human neuroblastoma cell line SK-N-MC also showed a negative

result for HGF-R (Fig. 21 A). As a consequence, a new cell line had to be used which expressed appropriate amounts of HGF-R. An obvious choice was the hepatocellular carcinoma-derived Hep G2 cell line that displayed a positive PCR screening result for HGF-R (Fig. 21A). After determining the optimal experimental conditions for Hep G2, the cells were treated with HGF and msClu over the standard time period. Interestingly, the combined treatment of HGF and Clusterin displayed an increased activation of Akt phosphorylation such as observed with IGF-1 (Fig. 21B). This activation was gradually ascending over the whole duration of the experiment. The ERK phosphorylation level which was screened in parallel was also affected proportionally. Repetition of the experiment with the protein control BSA markedly increased Akt and ERK phosphorylation in a comparable manner (Fig. 21C). Together with the observation that the experimental control samples without HGF stimulation in both experiments displayed increased ERK and especially Akt phosphorylation levels, these findings demonstrated a considerable resemblance to the insulin effects seen in N2A LG cells. As a consequence, it was assumed that the Hep G2 cells, similar to the N2A LG cells, experienced cellular stress during the preparation and stimulation process. Since there was no possibility to distinguish between actual Clusterin effects and general protein effects based on the stressed cell status, further ambitions to elucidate a potential role of Clusterin on HGF stimulation in Hep G2 were aVol.oned.

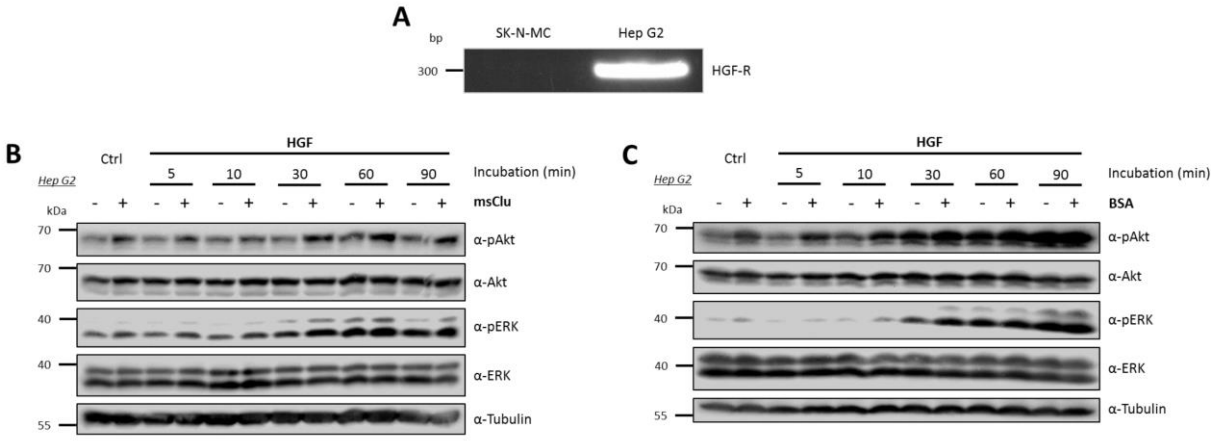

Fig. 21: Investigation of Clusterin and BSA effects on HGF-induced signal transduction activation in Hep G2 cells. *(A) cDNA of both SK-N-MC and Hep G2 were analysed for HGF-R transcripts with the help of PCR and target specific primers. (B, C) Cultivated Hep G2 were serum-starved for 2 h before stimulation with 50 ng/mL HGF in the presence or absence of either 5 µg/mL msClu or BSA. Whole cell lysates were both screened for Akt and ERK phosphorylation in a Western blot.*

4.4.3 Re-examination of previous experiments towards ERK modulation reveals small side effects

In preceding experiments light was shed on the possible involvement of ERK phosphorylation in Clusterin-mediated signal transduction modulation (see 4.4.1). Although neither of the approaches yielded any positive or applicable results, it could not be excluded that Clusterin might influence ERK in other experimental setups. Especially in relation to the contradictory work of Jo et al. it was of utmost interest to assess the extent of potential Clusterin-mediated modulations on various signal transduction molecules. All previously addressed experimental combinations of cell lines, stimulants and Clusterin variants were re-evaluated for their effect in ERK phosphorylation levels. Despite the large number of studied samples and observed alterations in pAkt levels, only two experiments revealed interesting data whereas the rest showed no significant or noteworthy outcomes. The first considerable observation was made in insulin-treated N2A LG cells. The samples in the first 10 min after stimulation showed an increase in ERK phosphorylation in the presence of msClu (Fig. 22A). It could be assumed that this is caused by the already elicited cellular stress level of N2A LG, however, parallel examination of the GST control experiment demonstrated no variation in the pERK signal (Fig. 22B).

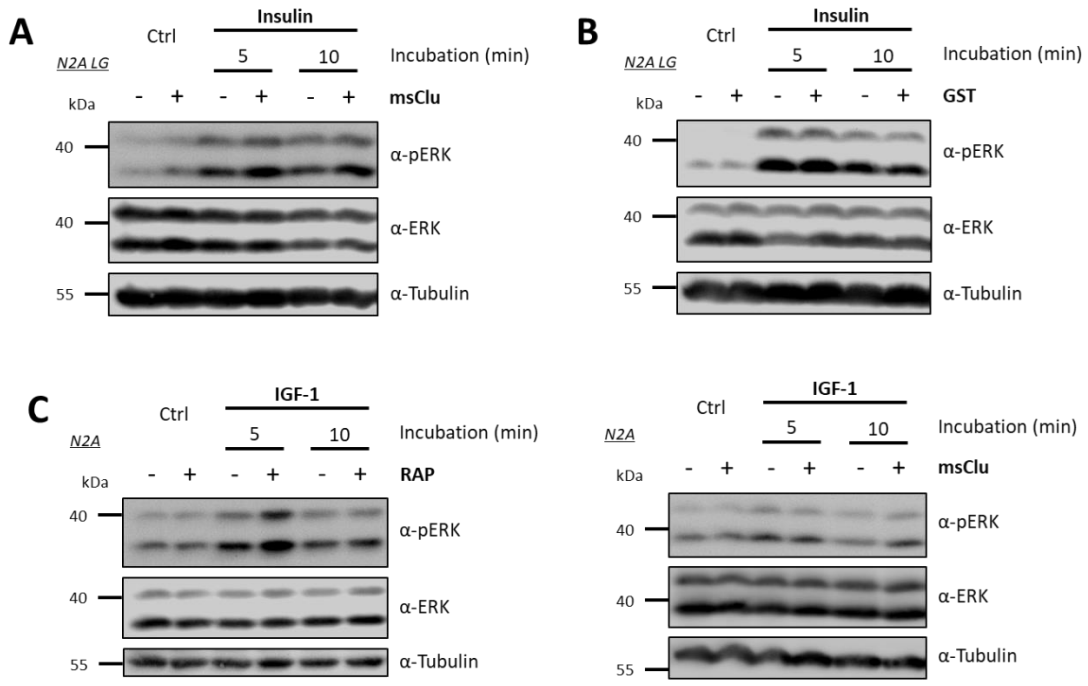

Fig. 22: Demonstration of additional effects of Clusterin on ERK phosphorylation after stimulation with insulin/IGF-1 in both N2A and N2A LG. *Depicted Western blots are reanalysed whole cell lysates from previous experiments to determine ERK phosphorylation levels. Lysates from N2A cultivated in low glucose medium and treated with insulin plus either msClu (A, see also Fig. 12C) or GST (B, see also Fig. 13B) were reused as well as standard N2A lysates stimulated with IGF-1 and RAP (C, left panel) or msClu (C, right panel) respectively (C, see also Fig. 16A). For better depiction purposes, Western blot results were cropped to values with significant alterations.*

The second interesting outcome for pERK signalling was seen in the re-examination of the afore mentioned RAP influence on the phosphorylation of Akt in IGF-1-treated N2A cells as demonstrated in Fig. 16A. The pERK signals in this experiment exhibited increased levels in the presence of RAP after 5 min (Fig. 22C, left panel) which in turn could not be detected in corresponding Clusterin experiments (Fig 22C, right panel). This result supported the notion that the observed RAP-mediated elevation of Akt phosphorylation was based on a mechanism irrelevant for the Clusterin effect.

4.5 Consequences of the IGF-1/Clusterin Interplay and its potential function in a physiological context

The effects of Clusterin on the stimulation of Akt phosphorylation were extensively studied in both human and murine cell lines. There were no doubts about the fact that Clusterin modulates IGF-1-induced signal transduction activation and evidences existed that similar effects are true for insulin stimulation. The questions that arose from these findings were what impact pAkt modulation by Clusterin could have on downstream mechanisms and the physiological relevance of the observed Clusterin effect. To answer these questions, treated cells had to be examined for phenotypical changes to narrow down the possibilities of potential mechanistical alterations. Subsequently, the mechanism of the Clusterin effect had to be further elucidated which would help to allocate its target location to possible cell types or tissues in a complex living organism and thus, establish connections to various pathologies.

4.5.1 Akt phosphorylation enhancement by Clusterin and IGF-1 is reflected in MTS studies

The Akt molecule is a central player and an upstream molecule in many signalling cascades. A variety of receptors are linked to Akt and its activation of downstream targets. Based on the large network of possible downstream targets, Akt phosphorylation can trigger a variety of different cellular responses involving cell survival and proliferation. Due to the plethora of interacting partners it was not feasible to establish approaches examining the influence of Clusterin-induced Akt phosphorylation on the activation of downstream targets or the modulation of gene targets. A more practical strategy was the examination of phenotypical changes following activation of Akt. One essential parameter in this context was the overall cell viability which is a characteristic variable for the activity of cellular

metabolic turnover and an indicator for potential proliferation events. An efficient and easy to execute procedure to evaluate the cell viability is the application of a MTS assay. With this method, the cell viability can be directly measured in the culture vessel. The added MTS compound reacts with NADH and NADPH molecules, which are generated by metabolically active cells, forming a colorimetric compound that can be analysed photometrically. The intensity of colour formation is directly proportional to the number of cells in the measured vessel.

4.5.1.1 Clusterin treatment leads to increased cell viability

The MTS assay was used to elucidate the effect of IGF-1-mediated Akt phosphorylation and its elevation by addition of Clusterin. Simultaneously, the long-term effect of this modulation was examined. Equal amounts of N2A cells were plated and stimulated accordingly for a period of 6 h.

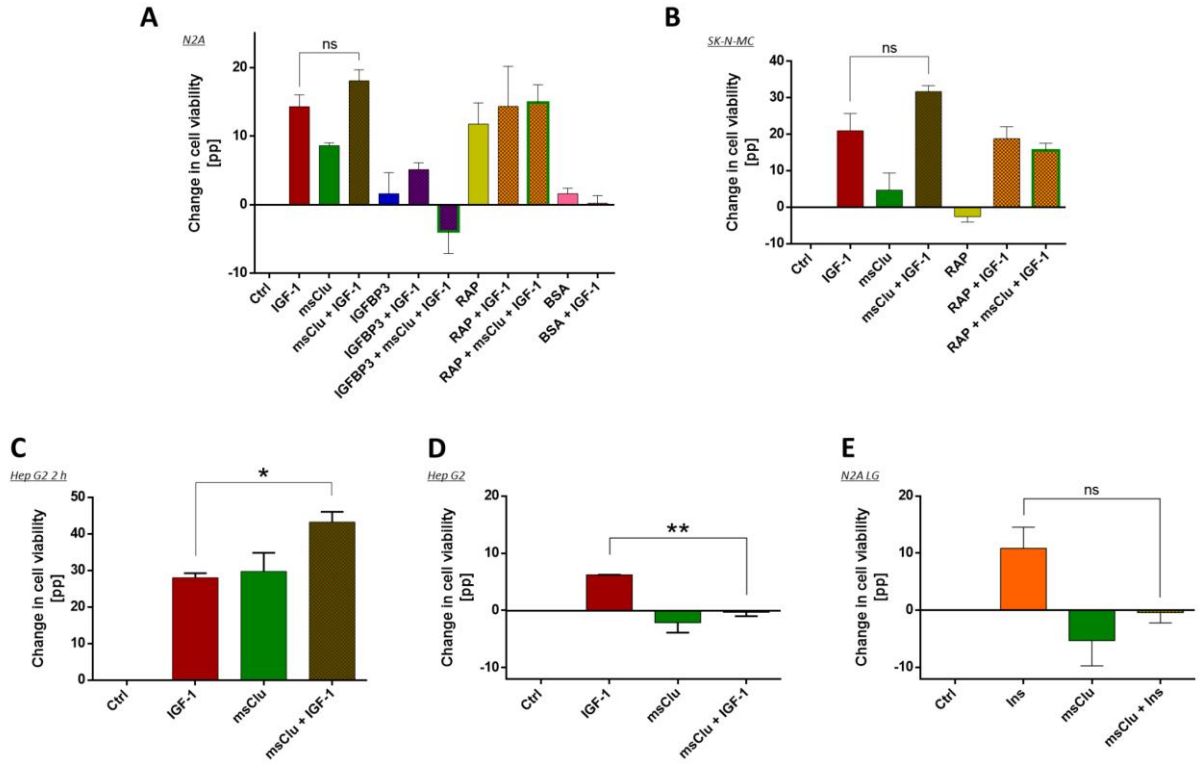

Fig. 23: Influence of IGF-1 cotreatment with Clusterin, RAP, BSA and IGFBP3 on the cell viability of N2A, SK-N-MC and Hep G2 cells. *Results gathered from the MTS experiments with N2A (A), SK-N-MC (B), Hep G2 serum deprived for 2 h (C) or 24 h (D) prior to stimulation and N2A cultured on low glucose medium (E) were subtracted from the control sample (Ctrl). The differences in percentage points compared to the control sample were plotted together. Cells were stimulated with the indicated substances in concentrations of 50 ng/mL for IGF-1, 5 µg/mL for msClu, BSA and RAP as well as 1.25 µg/mL for IGFBP3. Data is shown as ± SEM gathered from three independent experiments with triplicates for each sample. The determining change in cell viability between IGF-1-treated and IGF-1 + msClu-treated samples was statistically analysed by a two-tailed one-way ANOVA followed by Tukey's test (ns = not significant, * = P < 0.05, ** = P < 0.01).*

Although the Akt elevation by Clusterin was only detectable for approximately 30 min, the cells had to be cultivated over an extended time for the development of phenotypical changes. A control plate was directly measured at the point of stimulation to determine the basal cell activity in the MTS assay. This value was later on subtracted from the actual measurement. The initial experimental situation was similar to the experiments executed for Western blot analysis. The N2A cells were treated with IGF-1 together with various combinations of msClu, RAP and BSA as control. Additionally, the molecule IGFBP3 was added to the spectrum of potential modulators. As described in 1.2.1.2, this molecule is the major interacting partner of IGF-1 in the blood, binding approximately 80% of the total IGF-1.

The analysed data of the MTS assay delivered astonishing results. The previously observed pAkt elevation in the presence of Clusterin was reflected in the MTS assay by also elevated levels of cell viability compared to the IGF-1-only sample (Fig. 23A). The fact that the variation in both data sets was not statistically ascertainable did not alleviate the obvious difference in cell viability between the IGF-1 and IGF-1 + Clusterin samples. Furthermore, this alteration was also detectable in SK-N-MC cells despite the fact that statistical analysis also failed to evaluate differences (Fig. 23B).

Surprisingly, the IGF-1 + BSA sample, showing slight alterations of pAkt in Western blot analyses, yielded no significant change in cell viability (Fig. 23A). In fact, it abrogated the positive effect of IGF-1. This further proved the hypothesis that the effects of Clusterin and BSA are based on different mechanisms.

In case of RAP, the sample together with IGF-1 showed no distinct alteration compared to the IGF-1-only sample in both N2A (Fig. 23A) and SK-N-MC (Fig. 23B). The further addition of msClu to the IGF-1 + RAP sample had no influence on the level of cell viability in neither cell line. This suggests a possible involvement of members of the LDL-receptor family in the displayed Clusterin effect which could be blocked by RAP. A surprising part of the MTS assay was the elevated cell viability level in the samples solely treated with msClu or RAP (Fig. 23A). Both data sets showed markedly increased cell viability whereas BSA alone had no impact. The two molecules msClu and RAP seem to have alternative routes to stimulate cell viability which can only be speculated about. The observations in SK-N-MC cells, however, rendered this suggestion ambiguous since neither msClu nor RAP significantly altered the level of cell viability (Fig. 23B).

The last investigated modulator IGFBP3 showed the expected results that IGFBP3 alone did not alter cell viability but diminished the positive effect when applied with IGF-1 (Fig. 23A). More surprisingly was the effect of Clusterin on the cell viability when combined with IGF-1 and IGFBP3. In contrast to the analogous sample with RAP, Clusterin noticeably reduced cell viability in combination with IGFBP3.

This result was by no means in accordance with the previously described observations made in the MTS assay and therefore defies any explanation.

The MTS assay verified the Clusterin effect on cell viability in both N2A and SK-N-MC cells and broadened the perspective to its influence on phenotypical changes. Mechanistically spoken, the RAP results directed the attention closer to a possible involvement of LDL-receptor family members in the Clusterin-mediated effects. In combination with IGFBP3, Clusterin revealed its suppressive role on IGF-1-induced cell viability.

4.5.1.2 High stress levels in Hep G2 and low glucose-cultured N2A are confirmed by MTS analysis

Additional MTS assays were performed with Hep G2 and N2A LG to determine the consequence of the observed Clusterin-induced Akt activation in these cell lines. For comparison, Hep G2 cells were stimulated as N2A with IGF-1 and msClu to evaluate the change in cell viability in a comparable context. The Hep G2 cells displayed markedly elevated cell viability levels in the sample treated with both IGF-1 and msClu which clearly exceeded those of IGF-1-only treated samples (Fig. 23C). Surprisingly, the data set of Clusterin-only treatment showed similar levels of cell viability as the IGF-1 samples. In neither N2A nor SK-N-MC cells the effect of Clusterin alone was as high as in Hep G2 which could have already been an indicator for the previously mentioned stress levels of Hep G2. This assumption was further reinforced by the results gathered from Hep G2 that were exposed to enhanced stress by extended serum deprivation for 24 h. Besides the fact that IGF-1 stimulation had only limited effects on cell viability compared to less stressed Hep G2, effects of both msClu and IGF-1 + msClu treatment were entirely abrogated (Fig. 23C). Comparable results were also observed in N2A LG cells treated with insulin and/or msClu (Fig. 23E).

These results confirmed the suggested occurrence of elevated stress levels in Hep G2 and N2A LG. Furthermore, they shed light on the role of Clusterin during cellular stress. Despite the increased pAkt activation by Clusterin seen in Western blot analysis, its effects on cell viability in the long run exhibited a proapoptotic character.

4.5.2 Clusterin is not able to sustain IGF-1 effects in the presence of IGFBP3

After the cellular response of Clusterin-induced pAkt elevation was addressed, a question that was still pending was its role in a physiological context. The most likely location for an encounter between IGF-1 and Clusterin is the blood stream. In this scenario, however, IGF-1 is already mostly bound to IGFBP3. To analyse the behaviour of IGF-1 in the presence of IGFBP3, N2A cells were simultaneously treated with both compounds. The addition of IGFBP3 caused an attenuation of IGF-1-induced Akt phosphorylation over the whole period of 30 min (Fig. 24A). A subsequent experiment was conducted to elucidate the possibility of Clusterin to increase the availability of IGFBP3-bound IGF-1 and to recover its stimulating effect on pAkt. To cover three possible theories, IGF-1 was preincubated with msClu, IGFBP3 or both for 10 min. Pretreatment with IGFBP3 should evaluate a possible protective role of Clusterin against IGFBP3 binding to IGF-1, whereas Clusterin preincubation should clarify a possible Clusterin ability to liberate IGF-1 from IGFBP3. The parallel preincubation was used to determine the affinity of both molecules to IGF-1. Interestingly, all three conditions led to the sole result of complete inhibition of Akt phosphorylation (Fig. 24B). This implicated that IGFBP3 exhibits an exceptional high affinity to IGF-1 which masks all effects on pAkt by IGF-1 and Clusterin. Furthermore, it challenged the assumption of a potential IGF-1-Clusterin-interaction which was also postulated by Jo et al., as Clusterin was not able to protect IGF-1 from binding to IGFBP3.

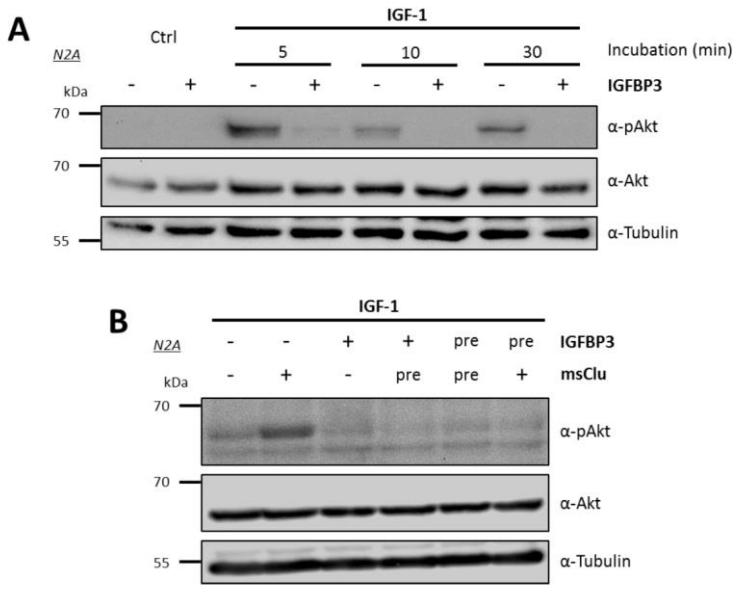

Fig. 24: Demonstration of negative effects of IGFBP3 on IGF-1-induced Akt phosphorylation and the suppression of the synergistic effects of Clusterin. *(A) N2A cells were treated with 50 ng/mL IGF-1 and with (+) or without (-) 1,25 µg/mL IGFBP3 after 24 h of serum deprivation for the indicated time. (B) Serum depleted N2A were preincubated with either 5 µg/mL msClu, 1,25 µg/mL IGFBP3 or both as indicated (pre) for 10 min. Subsequently, cells were stimulated with 50 ng/mL IGF-1 and with (+) or without (-) either 5 µg/mL msClu or 1.25 µg/mL IGFBP3. All harvested whole cell lysates were analysed in a Western blot.*

4.5.3 Enhancing abilities of Clusterin seem to be based on active interactions with IGF-1

The preincubation experiments with Clusterin and IGFBP3 did not distinguish between just a difference in IGF-1 affinity or the fact that Clusterin does not bind IGF-1. The postulated interaction of Clusterin with IGF-1 by Jo and co-workers was based on the reduction of detectable IGF-1 when incubated with Clusterin-conditioned medium. To further evaluate this statement and clarify the observations made in the experiments with IGFBP3, an ELISA approach was elaborated to measure possible interactions. For this ELISA strategy, purified samples of both IGF-1 and Clusterin were used to exclude possible side effects and specify obtained results. IGF-1 was coated on ELISA 96-well plates overnight and incubated with Clusterin the following day. Positive binding of Clusterin to IGF-1 was measured by targeting the His-tag of Clusterin. The signals were detected by a colorimetric reaction driven by alkaline phosphatase activity.

4.5.3.1 Clusterin is able to bind IGF-1 and to a lesser extent other growth hormones

In a first experiment the ability of Clusterin and IGFBP3 to bind IGF-1 was screened. As control molecules BSA and RAP which were also His-tagged were applied onto coated IGF-1. The gathered data for Clusterin treatment revealed a definite binding of Clusterin to coated IGF-1 (Fig. 25A). This confirmed the observations of IGF-1 binding by Jo and co-workers. As expected, the IGFBP3 binding affinity to coated IGF-1 was about three times as high as the values for msClu (Fig. 25A). Interestingly, the control samples with BSA and RAP did not show any interaction with IGF-1. This was again in accordance with the assumption that observed modulations of pAkt signals by those two molecules follow a different mechanism compared to Clusterin since they did not interact with IGF-1 directly.

Despite the poorly verified data situation regarding Clusterin effects with other growth factors, the three previously utilised stimulants HGF, EGF and insulin were also screened for possible Clusterin interaction. The ELISA measurements revealed that Clusterin exhibited markedly reduced affinity to all three molecules compared to IGF-1 binding (Fig. 25B). Although the results only displayed relative values, meaning that binding to insulin for example could still be sufficient for possible Clusterin effects, it yet pushed IGF-1 in the spotlight for further investigation.

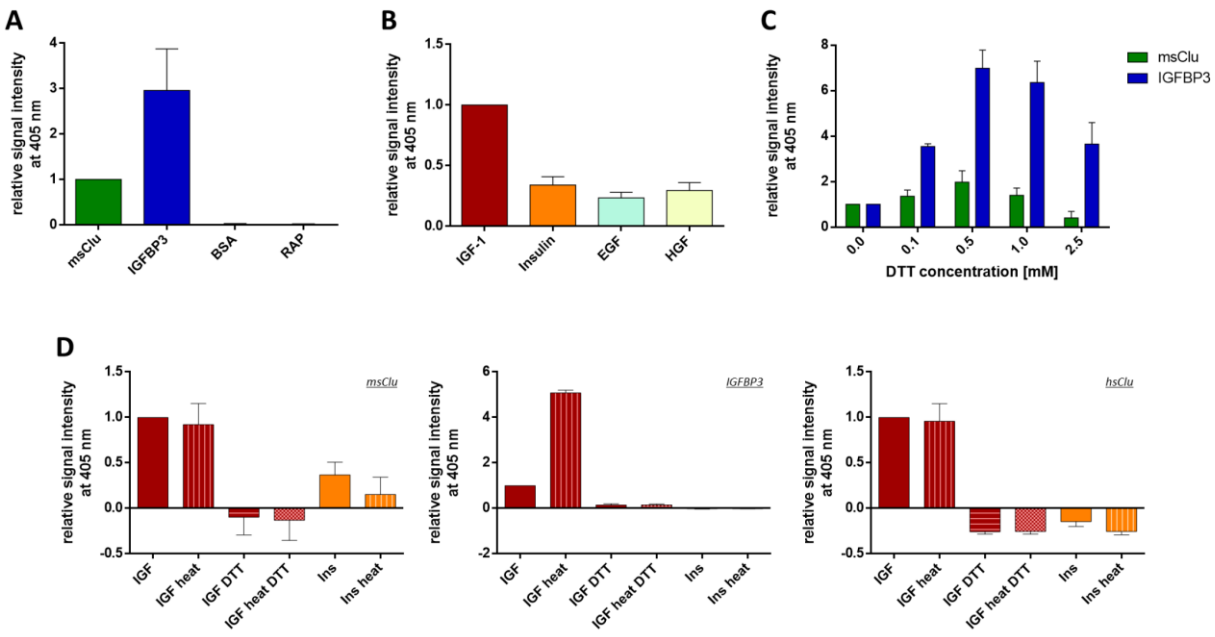

Fig. 25: ELISA-based analysis of the ability of Clusterin and IGFBP3 to bind IGF-1 and other growth factors in their native and denatured state. *(A) For the detection of Clusterin binding capabilities, 100 ng/well IGF-1 were coated overnight on an ELISA 96-well plate. For the detection stoichiometrically equal amounts of msClu (1 µg/well), IGFBP3 (0,5 µg/well), BSA (1 µg/well) and RAP (0,6 µg/well) were added to the coated wells and the amount of bound protein was measured by immunodetection of their respective His-tags. (B) Binding ability of msClu (1 µg/well) was also measured for coated insulin, EGF and HGF (100 ng/well each). (C) Influence of various DTT concentrations on the binding capabilities of both msClu (1 µg/well) and IGFBP3 (0,5 µg/well) to coated IGF-1 (100 ng/well) was determined. DTT was added to the msClu or IGFBP3 stock directly prior to application on the ELISA plate. (D) Before coating of IGF-1 or insulin (both 1 ng/µL), some samples were pretreated with heat (60 °C) and/or DTT (20 mM; resulting in a final concentration of 0.5 mM during coating process) in a volume of 25 µL coating buffer for 3 h. Control samples without heat treatment were kept at 4 °C during the incubation time. Samples were diluted with coating buffer to a final volume of 1 mL. After coating, binding of msClu, hsClu (both 1 µg/well) and IGFBP3 (0,5 µg/well) was measured as usual. All sample sets were measured in duplicates and were normalised to their respective control which was set to 1 (first column in each graph). Final data is shown as ±SEM of at least three independent experiments.*

One of these following investigations was to determine the susceptibility of IGF-1-Clusterin-interaction to reducing conditions provoked by DTT. As a reference, the experiment was also executed with IGFBP3. The gathered data revealed surprising results for both molecules. Despite increasing concentrations of DTT during the incubation of Clusterin/IGFBP3, both molecules exhibited an ascending IGF-1 binding capability peaking at 0,5 mM DTT (Fig. 25C). Only during higher concentrations of DTT the ability to bind IGF-1 started to decrease for both molecules. IGFBP3 displayed an astonishing sevenfold increase in IGF-1 binding at DTT concentrations of 0,5 mM. A reason for this observation could have been structural changes in IGF-1 upon low DTT concentration which made it more accessible for the binding of both IGFBP3 and Clusterin. It was unlikely that an alteration in structure of IGFBP3 and msClu was the reason since both molecules show similar behaviour during DTT treatment but share no distinct structural features.

4.5.3.2 Physicochemical alterations of IGF-1 influence the binding affinity of both Clusterin and IGFBP3

Clusterin with its chaperone and scavenging ability can bind damaged or denatured proteins and cell debris. A hypothesis that arose from those abilities was that Clusterin could be a substitute for IGFBP3 when IGF-1 is denatured to maintain its transport and ability to trigger signal transduction pathways. To test this hypothesis, IGF-1 and also insulin were subjected to extensive heating over a period of 3 h. Literature mentions that IGF-1 is heat-stable up to temperatures of 80 °C, therefore IGF-1 was also stressed with 20 mM DTT alone or in combination with heat. Binding of msClu, IGFBP3 and hsClu to differently treated IGF-1 and insulin was again measured by ELISA. Interestingly, all three tested compounds displayed diminished binding capabilities to both DTT-treated IGF-1 samples and the heat-treated insulin (Fig. 25D). A surprising observation was the difference in binding of native insulin between msClu and hsClu as hsClu did not exhibit any detectable binding to insulin. As stated in the literature, heat treatment alone was insufficient to alter IGF-1 structure to such an extent that binding was attenuated, or in this case the chaperone activity of Clusterin was activated. In case of IGFBP3, heat treatment actually increased its affinity to IGF-1 fivefold. By scrutinising the literature, it emerged that IGFBP3 acts as chaperone for IGF-1 under stress conditions which could explain the increased affinity, despite the heat stability of IGF-1. The treatment with DTT, however, did not activate the chaperone activity of either IGFBP3 or Clusterin. It is of note that the amount of DTT did not interfere with the binding since the incubation volume for the treatment of IGF-1 was chosen so that the final concentration of DTT during the coating process was at the optimal concentration of 0,5 mM (see Fig. 25C). Besides this fact, the wells were washed several times before Clusterin and IGFBP3 were actually added to the coated IGF-1. Nevertheless, it could not be excluded that 0,5 mM DTT could interfere with the coating of IGF-1, however, studies with ovalbumin and calreticulin demonstrated no change in binding when DTT was present during coating (Svaerke & Houen, 1998).

4.5.3.3 Combined heat and DTT treatment of IGF-1 leads to structural alterations and decreased activity

To further understand the behaviour of Clusterin and IGFBP3 towards denatured and reduced IGF-1, the impact of DTT and heat treatment on the structural changes of IGF-1 were studied intensively. IGF-1 was heat- and DTT-treated as previously mentioned and subsequently analysed by HPLC. The crucial section in all four chromatograms containing the specific IGF-1 peaks were combined in one

graph to visualise the changes caused by different treatment conditions (Fig. 26A). The peaks clearly demonstrate that DTT and heat alone did not alter the hydrophobic level of IGF-1. The combination of both heat and DTT, however, drastically increased hydrophobicity of IGF-1 which led to a delay in retention time. Analogous experiments with insulin displayed partial separation of α- and β-chain (peak 2 and 3) after treatment with DTT and full separation when heated additionally (Fig. 26C). Separation of the two insulin chains was accompanied by a shift in retention time and appearance of two separate peaks for each chain. Denaturing events could not be visualised by HPLC due to the necessary TFA in the mobile phase buffers which also denatured the control sample.

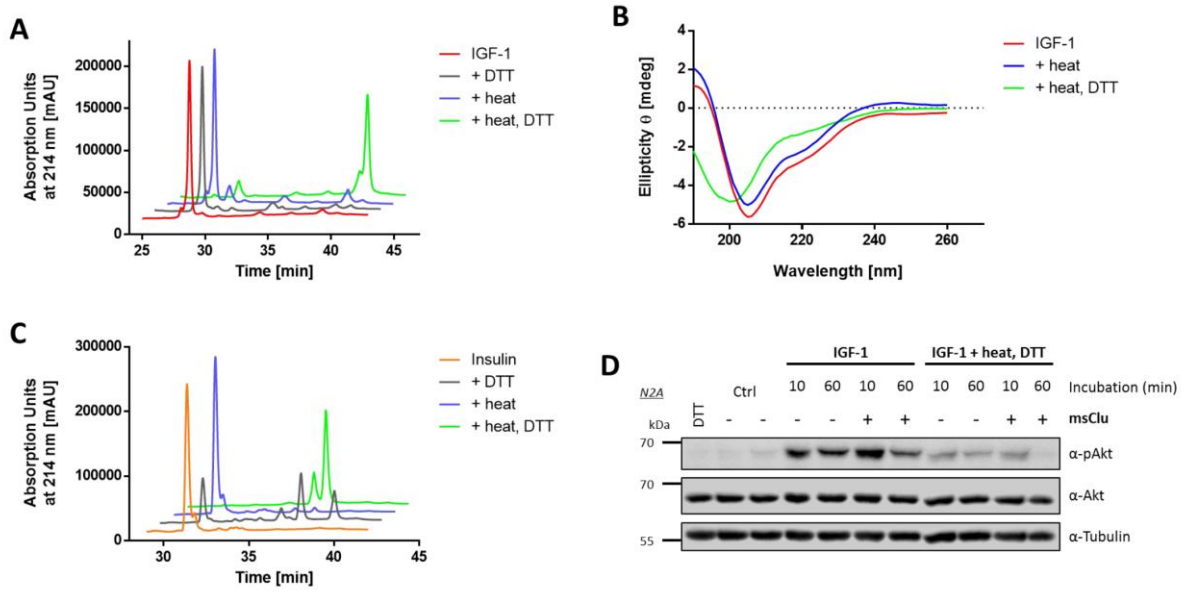

Fig. 26: Biochemical analysis of the physical structure and biological behaviour of IGF-1 in denaturing conditions. *IGF-1 and insulin were pretreated with either heat (60 °C) and/or DTT (20 mM) for 3 h. Samples not treated with heat were kept at 4 °C for the period of incubation. (A, C) RP-HPLC analysis of 100 µL IGF-1/insulin (50 µg/mL) with or without mentioned pretreatments. Chromatograms were confined to relevant retention time spans and stacked along an invisible z-axis to visualise changes caused by the pretreatments. Data sets are representatives of at least three independent experiments. (B) Changes in secondary structure were monitored by CD-spectroscopy analysis of IGF-1 (50 µg/mL) and indicated pretreatments. Resulting spectra were fitted according to the description in 3.22 and one data set for each sample was chosen as a representative of two independent experiments. (D) Pretreated and native IGF-1 (10 µg/mL) were used to stimulate (50 ng/mL IGF-1 on cells) N2A in the presence or absence of msClu (5 µg/mL) for the indicated time. As a control, cells were treated with DTT only (first column; final concentration in medium was 0,1 mM, which is in relation to the concentration added with pretreated IGF-1). Harvested whole cell lysates were analysed by Western blot.*

To precisely analyse structural changes in treated IGF-1, the samples were analysed by CD-spectroscopy (Fig. 26B). The sole treatment with heat caused a rearrangement in α-helices and β-sheets distribution of IGF-1 (Table S1) which seemed to have no influence on the binding to Clusterin (Fig. 25D). In case of simultaneous heat and DTT treatment, the structural composition of IGF-1 severely changed in the α-helical proportion verifying the results seen in HPLC (Fig. 26A) and ELISA (Fig. 25D). As a concluding experiment the DTT and heat-treated IGF-1 was compared to native IGF-1

for its ability to stimulate Akt phosphorylation and the effect of Clusterin on this treatment in a Western blot (Fig. 26D). Interestingly, the denatured IGF-1 was not able to trigger Akt phosphorylation in N2A cells as compared to native IGF-1. Furthermore, Clusterin was not able to modulate the Akt stimulation when denatured IGF-1 was used. This was in agreement with the impaired binding of Clusterin to denatured IGF-1. However, these results were not sufficient to fully elucidate the active binding of IGF-1 by Clusterin independently from its chaperone activity. The Western blot experiment should have been repeated with DTT-only-treated IGF-1 to exclude possible disturbances of Clusterin binding by DTT and to verify the results seen with heat and DTT-treated IGF-1.

4.6 The necessity of structural key features in the Clusterin molecule

Structural alterations of IGF-1 were shown to abrogate its ability to stimulate Akt phosphorylation and attenuate binding to Clusterin. It was however not known whether the binding of Clusterin to IGF-1 is merely an unspecific binding based on the chaperone/scavenger activity of Clusterin or mediated by specific structural features. To approach this issue, Clusterin had to be structurally analysed. This was executed by introduction of site-directed mutations and subsequent analysis of alterations in binding capabilities compared to native Clusterin.

4.6.1 Introduction of mutations in structural key features of Clusterin alter its physicochemical behaviour

Target locations for the introduction of mutations were two essential key elements in the structural composition of the Clusterin molecule. The first element was the amphipatic α-helix located close to the C-terminus of the Clusterin α-chain. It was shown to be involved in binding of soluble Aβ and human IgG (see 1.1.2). The formation of the α-helix was disturbed by introduction of two proline via substitution of two amino acids within the helix. These proline act as so-called helix breaker because the nitrogen atom in their peptide group cannot form intermolecular hydrogen bridge bonds that are necessary for secondary structure formation. The mutations were introduced by *in vitro*-mutagenesis with a specific primer containing codons for three prolines. As a target, the human Clusterin sequence was chosen, since an additional human Clusterin mutant was already present in the laboratory that was also planned to be used. By this way the results would be more comparable. Sequence analysis of plasmids containing the newly generated mutated Clusterin gene revealed that all screened plasmids

incorporated only two of the three designated prolines (Fig. 27A). The present mutations were Q177P and H179P (Fig. 27C) and the generated Clusterin mutant was named hsClu-Pro.

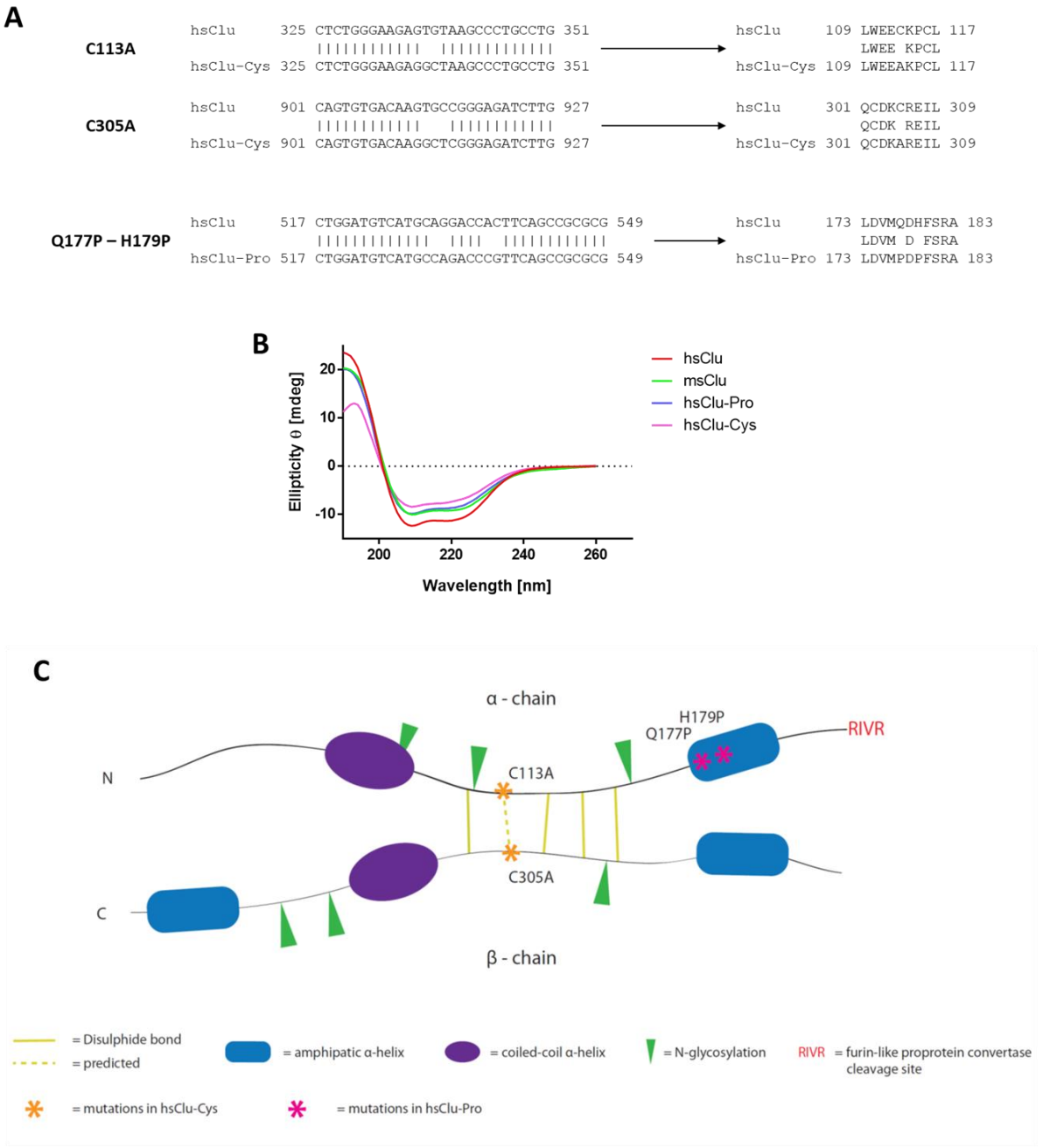

Fig. 27: Site-directed introduction of cysteine and proline mutations and their influence on the structural arrangement of Clusterin. *Specific cysteine and proline mutations generated by in vitro-mutagenesis were introduced into the hsClu nucleic acid sequence. (A) Mutated Clusterin sequences were analysed and aligned (NBCI nBlast) with hsClu (NP_001822.3) and changes in the amino acid sequence (translated with SerialCloner) of the expressed proteins were predicted (NCBI pBlast). HsClu-Cys contains mutations of the two cysteines C113 and C305, which were substituted by alanine. For the proline mutant hsClu-Pro the second amphipathic α-helix was targeted by substituting a glutamine at position 177 and a histidine at 179 with a proline. Sequence alignments were confined to relevant sequence sections. For full nucleic acid sequence alignment refer to Fig. S11. (B) Isolated recombinant Clusterin variants (100 µg/mL each) were analysed by CD-spectroscopy as described in 3.22. Data shows representative spectra of two independent experiments. (C) Graphical depiction of introduced cysteine (orange asterisks) and proline (pink asterisks) mutations in hsClu and their localisation in structural domains.*

The second *in vitro*-mutagenesis targeted the cysteine cluster domain of both chains. This area was assumed to be part in the binding of LRP2 and other LDL-receptor family members (see 1.1.2). The crucial amino acids in this domain are the cysteine residues which form intramolecular disulphide bonds. The goal with the mutagenesis was to completely eliminate one of those bonds. The best target of all five disulphide bonds was the one formed between cysteine residue 2 and 9 or C113 and C305 respectively (Fig. 27C). This bond was the only one that had not been conclusively verified in previous studies. The occurrence of structural changes in the mutant compared to wildtype Clusterin assessed by following experiments would not only shed light on the structural relevance of the cysteine cluster but also indirectly prove the existence of this disulphide bond. Sequence analysis of the vector containing the cysteine mutants proved the successful substitution of both cysteines with alanines (Fig. 27A). Alanine was chosen as a substitute because it contains a hydrophobic residue with a minor sterical extent. Since the cysteine cluster domain is located at the core of the Clusterin molecule, a small hydrophobic amino acid was the ideal choice. The newly generated mutant was called hsClu-Cys.

As with msClu (Fig. S5) and hsClu, both mutants were also purified from the supernatant of stably transfected HEK-293 by Ni-affinity FPLC (Fig. S6, S7). First altering effects by mutated Clusterin were already suspected during purification steps. The yield of both mutants, especially the hsClu-Pro mutant, was markedly decreased in comparison to wildtype hsClu, although expression level screenings of the isolated clones yielded outstanding amounts of secreted Clusterin (Fig. S9). A possible disturbance of the secretory pathway (see 1.1.1.4) by structural alterations could not be excluded.

4.6.1.1 Mutations cause changes in the distribution of secondary structure elements

As a first experiment the mutants were surveyed via CD-spectroscopy to analyse variations in secondary structure distribution. The mutants were compared to the results gained from analysing msClu and hsClu. The spectra clearly demonstrated a shift in the curve shape of both mutants in comparison to the wildtype hsClu (Fig. 27B). Interestingly, the spectrum of msClu also differs from hsClu but is similar to the one gained from hsClu-Pro. Transformation of the spectra into numerical results revealed a decrease in α-helical content in all Clusterin variants compared to hsClu (Table 4). The numbers for msClu and hsClu-Pro resembled the observations made in the spectra with similar distribution of secondary structures, although hsClu-Pro showed a high discrepancy in both β-turns and unordered regions. Of all measured Clusterin variants the hsClu-Cys mutant displayed the highest variation in α-helix ratio with a reduction of almost 20 percentage points. This observation was quite

surprising since the mutated disulphide bond is thought to connect the two Clusterin chains and does not form any intrachain conjunctions which could potentially stabilise α-helical structures. Furthermore, the mutated cysteine residues are flanked by additional cysteines that form disulphide bonds which lie in close proximity. This means that the directly affected area covered by this single mutated disulphide bond is very short. Hence, potential changes within the proximity of the mutation would not solely be able to cause the observed tremendous reduction of the α-helical proportion in hsClu-Cys. As a conclusion, the disulphide bond deletion must have global effects on the overall structural conformation of Clusterin.

Table 4: Secondary structure distribution analysed by CD-spectroscopy and subsequent analysis with CDSSTR.

	Distribution in [%]			
	α-Helices	β-Sheets	Turns	Unordered
Clusterin human	53,5 ± 1,3	11,1 ± 4,4	10,4 ± 4,6	25,7 ± 8,0
Clusterin mouse	45,9 ± 1,8	11,5 ± 6,5	14,9 ± 4,6	26,6 ± 4,4
Clusterin Pro-Mutant	44,9 ± 1,7	17,2 ± 7,3	17,6 ± 11,1	20,4 ± 14,7
Clusterin Cys-Mutant	35,1 ± 1,3	14,6 ± 4,6	18,4 ± 4,2	31,4 ± 6,9

4.6.1.2 Deletion of the Cys 2-9 disulphide bond destabilises the Clusterin molecule

The examination of overall molecular changes was continued with HPLC. Besides hsClu, msClu and hsClu-Cys another in the laboratory already available Clusterin variant, called hsClu-RIVQ, was used as a control mutant with intact chaperone activity. This mutant comprises a point mutation in the furin-like proprotein convertase recognition site RXXR which causes an ablation of the cleavage without having an influence on the secondary structure formation (see 1.1.2, 80).

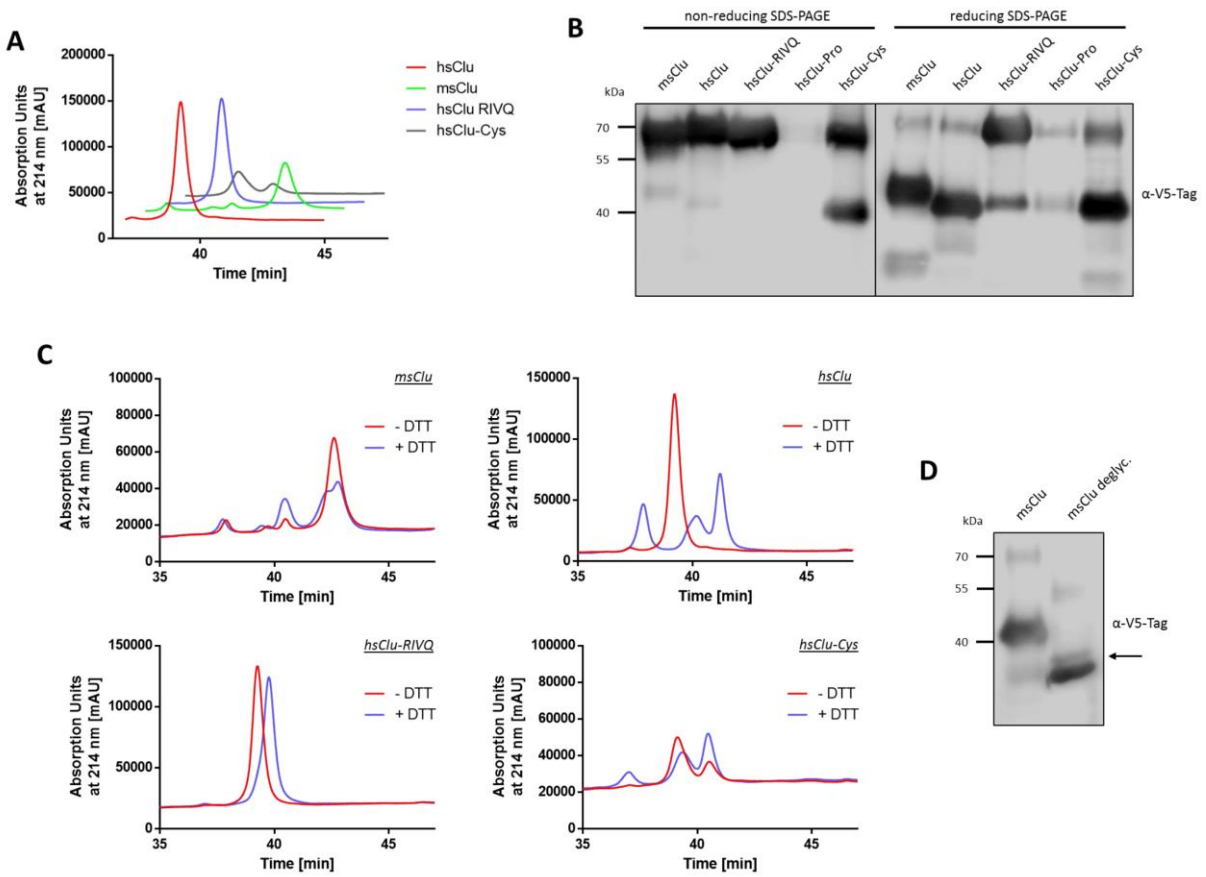

Fig. 28: Biochemical analysis of the molecular stability of Clusterin and its mutant variants in a reducing environment. *(A) Analysis of purified recombinant Clusterin mutants (125 µg/mL) by RP-HPLC. Depicted segment shows the relevant retention time span for Clusterin detection. Sample sets are stacked along an invisible z-axis for comparison. (B) Different Clusterin variants (5 µg) were mixed with SDS-loading buffer with (reducing) or without (non-reducing) DTT and loaded onto a SDS-PAGE. Samples were visualised by V5-tag staining in a Western blot. (C) RP-HPLC analysis from A was repeated with or without the addition of DTT (20 mM). Samples were quickly incubated with DTT for 10 min at rt before application. Data sets were depicted as overlay to visualise changes in the chromatograms. Graphs are representatives of at least three independent experiments. (D) Western blot analysis of msClu treated with PNGase F (deglyc.). Black arrow indicates residual partially deglycosylated Clusterin.*

The hsClu-Pro mutant was not included in the HPLC experiment since the yield of this Clusterin variant was so low that its usage in experiments was limited. The resulting HPLC chromatograms of the analysed Clusterin variants displayed an increased hydrophobic character of msClu compared to hsClu (Fig. 28A). However, the striking result was the appearance of two distinct peaks in the hsClu-Cys sample. It was assumed that either impurities caused the appearance of a second peak or that obviously the two Clusterin chains in the sample were separated. To evaluate this observation the experiment was repeated but with the addition of DTT-pretreated Clusterin samples. If the assumption with separated chains was true, the addition of DTT would change the chromatograms of hsClu towards the results seen for hsClu-Cys. Surprisingly, this was exactly the case in the observed HPLC chromatograms (Fig. 28C). In both hsClu and hsClu-Cys the (residual) main peak was reduced by DTT pretreatment and the appearance/elevation of two separated peaks could be seen. The msClu samples demonstrated similar results, whereas the hsClu-RIVQ mutant was not affected by DTT treatment since

this variant was not cleaved into two chains. The addition of DTT was accompanied by a slight shift of the peaks due to alterations of the separation column caused by DTT.

The addition of DTT to the HPLC analysis confirmed the assumption that hsClu-Cys exhibits decreased molecular stability. This observation could be verified by using Western blot analysis (Fig. 28B). The purified Clusterin samples were loaded in equal amounts on two independent SDS-PAGEs, one with reducing and one with non-reducing conditions. The non-reducing SDS-PAGE clearly revealed a partial separation of the hsClu-Cys, whereas other Clusterin variants only occurred as a single molecule. In the reducing SDS-PAGE the chains of msClu, hsClu and hsClu-Cys separated while the RIVQ mutant was not affected by reducing conditions. The appearance of a weak signal in the hsClu-RIVQ lane could stem from diffusion processes caused by overload. Two further remarkable observations were the discrepancy between the molecular weight of msClu and hsClu chains which was caused by altered distribution of the N-glycosylation sites between the subunits in both molecules (see Fig. 17). A second observation was the absence of a signal in the hsClu-Pro lane. It was speculated that the structural redistribution caused by the mutation could lead to a masking of the V5-tag.

Both HPLC and Western blot analyses demonstrated a molecular instability of the hsClu-Cys mutant. With the structural changes induced by mutations in key domains of Clusterin further elucidated, it was then necessary to examine the impacts on functionality.

4.6.2 The Clusterin chaperone activity is dependent on its disulphide bonds in both a reducing and non-reducing environment

The best described function of Clusterin in literature is its ability to keep misfolded proteins in solution. Therefore, the determination of functional limitations would best be done by monitoring the chaperone activity of all Clusterin mutants. To increase the spectrum of possible effects caused by structural alterations a new control was added. This control consisted of msClu/hsClu treated with PNGase F to eliminate the N-linked glycosylations. To verify the digestion, the treated and non-treated msClu samples were loaded on a SDS-PAGE. The following Western blot analysis showed positive removal of glycosylation (Fig. 28D), however, a weak band (black arrow) also appeared which was caused by only partially deglycosylated msClu. Similar results were gained from hsClu digestion (data not shown). Full deglycosylation, as shown in a previous study (Rohne, et al., 2014), was only achievable by addition of DTT during the digestion process. Since the samples had to be used in following DTT-sensitive experiments, further deglycosylation was relinquished.

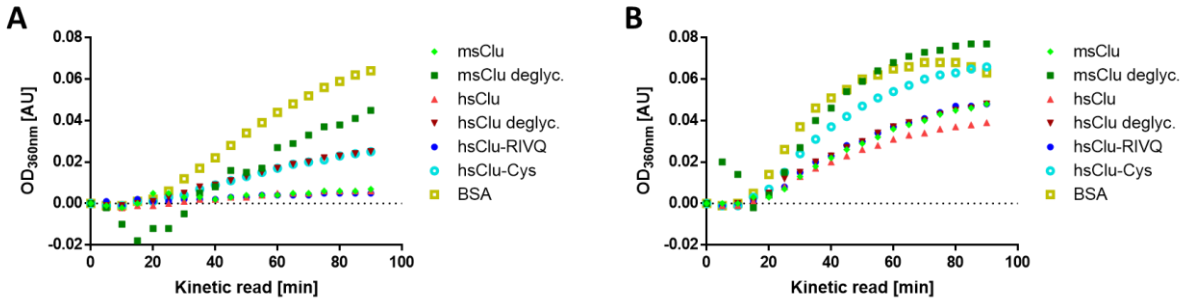

Fig. 29: Comparison of the chaperone activity of different Clusterin variants in non-reducing and reducing environments. *Chaperone activity of different Clusterin variants was measured by a chaperone assay. Samples were pretreated at 37 °C with (B) or without (A) DTT (20 mM) for 12 h before the samples were prepared for measurement. During the chaperone assay the turbidity at 360 nm under constant 50 °C was measured over a period of 150 min. Several Clusterin variants and BSA as a control were incubated with the client catalase. Increased heat precipitation of catalase was proportional to elevated turbidity and inversely proportional to the activity of added chaperones to keep it soluble. Data sets were cut at 90 min where the limit of turbidity measurement was reached. For optimised visualisation of the data sets only every other data point was plotted. Depicted graphs are representatives of four independent experiments.*

For the chaperone assay all Clusterin samples were mixed with catalase in a specific precipitation buffer. Catalase served as a client for Clusterin during the heat denaturation. Increased catalase precipitation was accompanied by opacification of the reaction solution which was measured at 360 nm. Clusterin should prevent the precipitation of catalase by keeping it in solution with its chaperone activity. For the variants msClu, hsClu and hsClu-RIVQ this behaviour was observed in the chaperone assay, while the negative chaperone control BSA displayed a robust increase in opacity development (Fig. 29A). As expected and postulated (Rohne, et al., 2014), deglycosylated hsClu demonstrated limited chaperone activity visible by an increase in solution turbidity. The same was true for deglycosylated msClu which displayed a further increase in turbidity. Interestingly, hsClu-Cys also showed impaired chaperone activity similar to the level of deglycosylated hsClu. The experiment was repeated with the addition of DTT to the reaction solution to analyse the effects of chaperone activity in a reducing environment. The addition of DTT led to drastic changes in the chaperone activity of used Clusterin variants (Fig. 29B). An increase in turbidity after DTT treatment was expected in every Clusterin variant since this was also demonstrated by Rohne and co-workers (Rohne, et al., 2014). However, two striking changes were the highly elevated values for both hsClu-Cys and deglycosylated msClu which actually showed no chaperone activity similar to the BSA negative control. These observations suggested that msClu is more dependent on glycosylation to exhibit chaperone activity compared to hsClu. Furthermore, if the mutations in hsClu-Cys had only affected the disulphide bonding then it would have been expected that DTT treatment in the chaperone assay would have yielded similar activity for both hsClu and hsClu-Cys as disulphide bonds were eliminated by DTT. As a consequence, the mutation of a single disulphide bond in the hsClu-Cys mutant must have had extensive influence on the structural composition of Clusterin to cause these major impairments in chaperone activity.

4.6.3 Both hsClu-Cys and hsClu-Pro display severe impairments in the binding of IGF-1

The insightful observations about structural and functional alterations of Clusterin mutants were finally transferred back to the initial question about the mechanism involved in Clusterin binding to IGF-1. In a previous experiment it was shown that hsClu could also bind IGF-1 (Fig. 25D). To analyse the extent of IGF-1 binding, hsClu was compared to IGFBP3. The line-up of both samples revealed a markedly increased binding ability of hsClu compared to IGFBP3 (Fig. 30A). Additionally, the deglycosylated hsClu which displayed decreased chaperone activity was also included. Surprisingly, the deglycosylation also impaired the binding to IGF-1 which stands in close correlation to the observations in the chaperone assay. In a next step, the different Clusterin mutants and their IGF-1 binding capabilities were compared to hsClu and msClu (Fig. 30B).

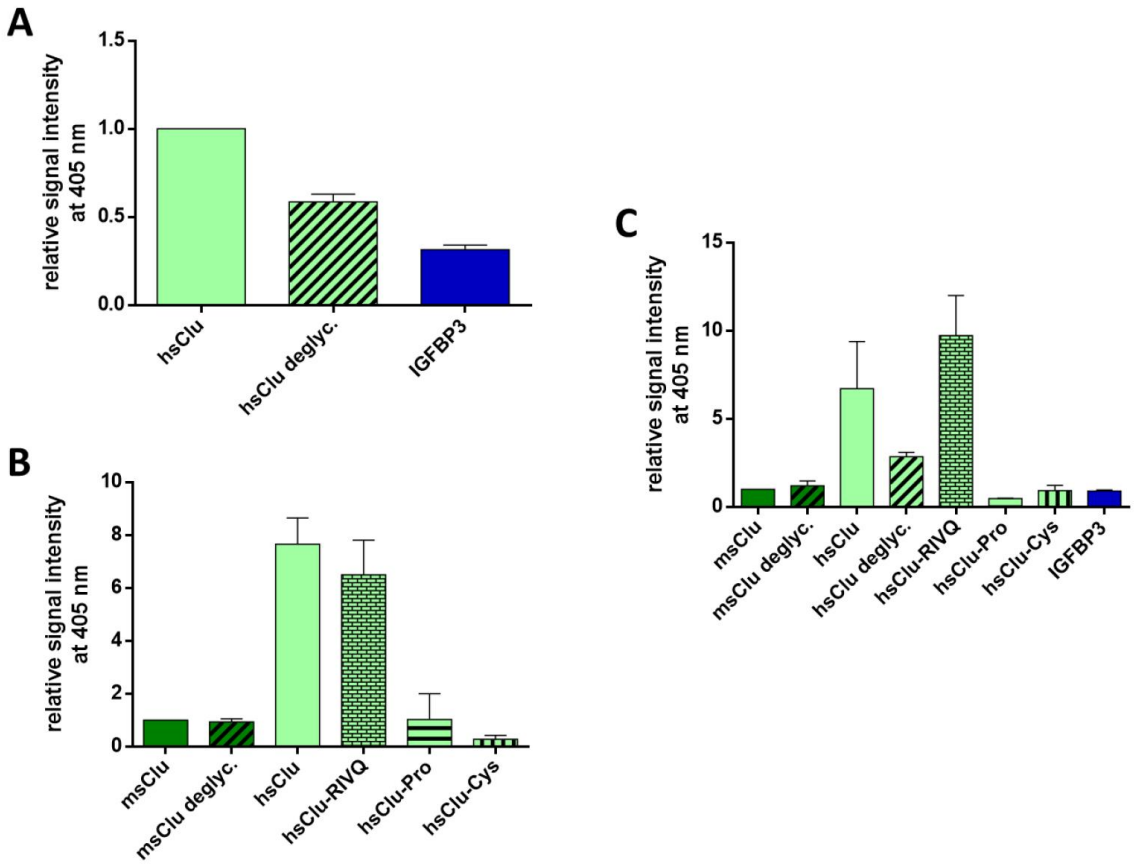

Fig. 30: Analysis of IGF-1 binding abilities of different Clusterin variants and comparison of their unspecific binding character. *(A) ELISA analysis of Clusterin binding to coated IGF-1 (100 ng/well) as in Fig. 25 was repeated with hsClu, hsClu deglyc. (1 µg/well each) and IGFBP3 (0,5 µg/well). (B) IGF-1 binding of both msClu and hsClu were compared to msClu deglyc. and Clusterin mutants (all with 1 µg/well). (C) The uncoated control samples of previously mentioned ELISA experiments, which are subtracted from the sample data during the evaluation and standardisation, were gathered and analysed. Observed signals are a result of unspecific binding affinity of Clusterin variants to the plate surface or powdered milk contents, which are used for blocking. All mentioned data sets are normalised to a standard sample (first column in each panel) which is set to 1 and are displayed as ±SEM of at least three independent experiments.*

The first interesting observation was the eightfold increase of IGF-1 binding in the hsClu sample compared to msClu. This verified the results for the comparison of both Clusterin variants to IGFBP3 (Fig. 25A, Fig. 30A). As expected, the hsClu-RIVQ mutant displayed no significant change in IGF-1 binding similar to the behaviour in the chaperone assay. This excluded the posttranslational cleavage from the list of potential structural features necessary for IGF-1 binding. Contrary results to hsClu deglycosylation were gained from the analysis of deglycosylated msClu as it did not display any change in IGF-1 binding to the wildtype msClu.

The most striking results, however, were the values for the two mutants hsClu-Cys and hsClu-Pro which yielded an exceptional loss of IGF-1 binding capability. The structural alterations caused by the introduction of mutations proved that distinct key domains in the Clusterin molecule were essential for the binding of IGF-1. However, the levels of IGF-1 binding in both mutants were not fully abrogated. In case of hsClu-Pro, the values reached those of msClu which correlated to the analogous results from the structural analysis (Fig. 27B, Table 4). Similar correlations could be seen for hsClu-Cys with its altered structural distribution and reduced IGF-1 binding compared to msClu (Fig. 30B). These differences suggested that the disulphide bonds and their potential global modifications in the molecule are crucial for both chaperone activity and IGF-1 interaction of Clusterin. Therefore, a distinct conclusion whether chaperone activity was the mechanism needed for IGF-1 binding could not be fully drawn with the present data.

A final phenomenon that was yet to be elucidated was the marked difference in IGF-1 binding between msClu and hsClu. Despite the slight differences in secondary structure distribution and the allocation of N-glycosylations in the molecules they do share high amino acid similarity and comparable activity in the chaperone assay. Yet the binding to IGF-1 greatly differed between both Clusterin variants. To shed light on this circumstance, the IGF-1 binding assay data was again studied. Surprisingly, the blank values in the IGF-1 ELISA assays, which are subtracted from the actual samples, revealed some interesting facts. Those samples are treated similarly to the actual samples but are not coated with IGF-1. The only targets for Clusterin present in those wells are the blocking solution components that cover the well surface. The blanks of all executed ELISA tests were collected, normalised and displayed in a graph (Fig. 30C). This graph showed elevated values for hsClu, deglycosylated hsClu as well as hsClu-RIVQ which corresponded to unspecific binding events of those Clusterin variants to molecules present in the blocking solution. Although these values were subtracted from the raw data before normalisation, the distribution pattern somewhat resembled the final results for IGF-1 binding (Fig. 30B). This line-up demonstrated an increased unspecific binding character of hsClu compared to msClu which could affect the final values and lead to the observed eightfold increase. The unspecific binding character of hsClu might have partly stemmed from the variations in glycosylation pattern

since deglycosylation drastically reduced the binding to molecules in the blocking solution but also reduced binding to IGF-1.

5 Discussion

Previous discoveries described in the Introductory part as well as the observations and results gathered in the course of this project shed light on the significance of Clusterin in maintaining physiological processes. The relevance of Clusterin in cellular signalling pathways was addressed with specifically designed experiments illustrated in this work. In the following section, the acquired knowledge and insights as to the role of Clusterin and its functionality will be seized and commented on. Furthermore, the gained data will be set into a scientific context by connecting and comparing it with published data. During these concluding remarks, the relevance of this work for future projects will be assessed and the necessity of subsequent experiments for the scientific apprehension of the mechanisms involving Clusterin and signal transduction will be outlined.

5.1 Modulation of insulin stimulation by Clusterin yields inconclusive results

In several previous studies Clusterin was shown to be involved in the insulin metabolism. The Clusterin gene is under control of a variety of different regulatory elements (see 1.1.1.1). One element that is present upstream of the Clu promotor is a so-called E-Box-like element (Oh, et al., 2015). This element was found to be activated by SREBP-1c which in turn is activated by insulin stimulation. Other studies also revealed an increased Clusterin expression during porcine and rat pancreas development (Schweiger, et al., 2007; Min, et al., 1998) as well as in the regeneration process of pancreatic β-cells (Kaya-Dagistanli & Ozturk, 2013; Kim, et al., 2001). All three observations demonstrated a connection between Clusterin expression and the formation of insulin-secreting tissue. Additional correlations in further studies were an increased insulin resistance under Clusterin deficiency (Kwon, et al., 2014; Hoofnagle, et al., 2010) which is a key feature for Diabetes type 2 (see 1.2.1.1). SNPs in the Clusterin gene were found to be associated with Diabetes type 2 development (Daimon, et al., 2011). The occurrence of Diabetes type 2 is a crucial risk factor for the emergence of Alzheimer's disease (see 1.1.3.1). Besides the known ability of Clusterin binding to aggregated Aβ, this fact closely links the Clusterin molecule to the pathogenesis of AD. The idea to study the influence of Clusterin on the insulin-mediated signal transduction pathway arose from the combination of the published data described above and the preliminary experiments executed in this work as well as the often-suggested ability of Clusterin to influence signalling pathways. By using the N2A neuronal cell model, the gathered results were closer related to the AD pathology.

5.1.1 Revelation of insulin receptor as potential Clusterin target

The screening for potential receptor targets of Clusterin with the RTK Array kit highlighted InsR as a receptor regulated by Clusterin treatment. These initial experiments were executed in HEK-293 cells, since they express most of the screened RTKs and yield a highly concentrated whole cell lysate from a small-scale experiment which was needed for the RTK Array kit. As a consequence of the results from the RTK Array kit, the subsequent goal was to examine the physiological role of Clusterin together with insulin in the onset of AD. Therefore, the murine neuroblastoma cell line N2A was chosen as a cell model for the examination of this role. However, the decrease in InsR phosphorylation levels was not reproducible in subsequent analyses of N2A cells treated with insulin. In these experiments, a specific antibody targeting the tyrosine residue of InsR at position 1185 (according to manufacturer, Antibody targets pTyr-1146 after numbering system in (Ullrich, et al., 1986), which is equal to 1185) was used. Together with two additional Tyr residues at 1189 and 1190, these phosphorylation sites are the first targets after receptor stimulation and are essential for the activation of its kinase activity. As a consequence, the designed experiments only screened for the initial activation of the InsR, which turned out to be unaffected by Clusterin addition. The used RTK Array kit on the other hand had a different approach. In a first step the InsR molecules were captured by polyclonal antibodies targeting an epitope outside of potential phosphorylation sites. These captured molecules were then stained with an unspecific antibody targeting the overall phosphorylation of tyrosine residues. The fact that the cytosolic domain of the InsR contains 13 prominent tyrosine residues with a potential phosphorylation (Fig. 31) of which four are essential for the binding of adaptor molecules reveals the complexity of the InsR phosphorylation pattern (Hanke & Mann, 2009). Therefore, a reduction of the overall InsR tyrosine phosphorylation level as present with Clusterin treatment in the RTK kit does not inevitably implicate an impairment of InsR stimulation. It could also originate from phosphorylation events being focused on a specific Tyr residue which trigger a unique signalling response while phosphorylation of unnecessary tyrosines is blocked. A comparable mechanism for selective IRS phosphorylation was already observed for leptin-modulated insulin signalling in hepatoma cells (Szanto & Kahn, 2000). Since InsR activation in the RTK kit was achieved by treatment with the serum supplement Panexin which contains insulin, it is very likely that cross-activation of the InsR by other components of Panexin could lead to increased phosphorylation levels. The addition of Clusterin in turn could block this cross-activation explaining the drop in detected pTyr levels. Evidences that are indicative for this hypothesis are the ability of Clusterin to unspecifically bind a plethora of different molecules which could inhibit potential InsR cross-activation and the fact that the InsR regulation is highly sensitive even to simple dietary changes (Youngren, 2007). However, by substituting Panexin with insulin, any cross-activations mediated by other components were eliminated. Nevertheless, the

question that was still pending was whether Clusterin itself causes changes in the phosphorylation pattern of InsR. Despite the phosphorylation screening with the approach of 2D-gel electrophoresis showing no significant changes when Clusterin was present during insulin treatment, this question cannot be answered conclusively. As already mentioned in 4.1, the possibility exists that potential changes in the InsR phosphorylation were masked by dominant spots or were below the detection limit of the Western blot approach. One way to overcome these problems would have been the utilisation of a phos-tag SDS-polyacrylamide gel after isoelectric focussing. With this method, it is possible to clearly separate molecules with different amounts of phosphorylation as well as molecules with similar levels but different sites of phosphorylation. In conclusion, the question whether Clusterin influences the InsR activation by altering its phosphorylation state cannot be elucidated with the gathered data. Evidences suggest that Clusterin is able to modulate InsR phosphorylation, however, the experimental setup does not clarify whether the observed Clusterin effect results from direct modulation of the InsR or from an indirect interaction with potential stimulants. A definite conclusion can be drawn for the initial InsR phosphorylation events as it was repeatedly shown that Clusterin had no influence on insulin-mediated stimulation of tyrosine residue 1185.

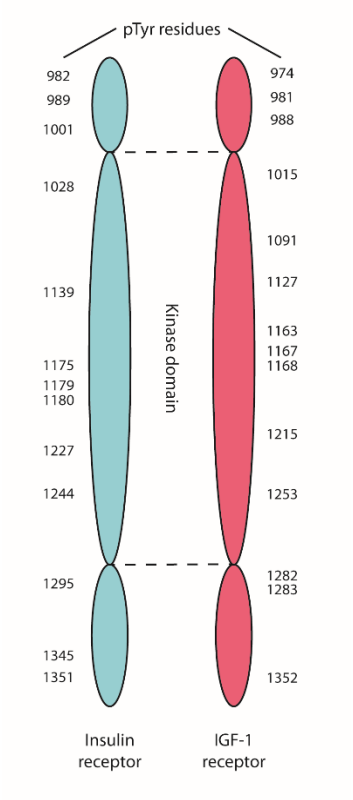

Fig. 31: Schematic depiction of the cytoplasmic domain of insulin- and IGF-1 receptor with highlighted pTyr residues. *The middle part of the cytoplasmic domain is the so-called kinase domain which is responsible for the autophosphorylation of the receptor. The numbers on each side of the drawings represent the various Tyr residue positions in the amino acid sequence of both receptors. Redrawn from (Hanke & Mann, 2009).*

5.1.2 Akt acts as a downstream target of Clusterin treatment during insulin stimulation

Despite the fact that Clusterin displayed no change in initial insulin-mediated InsR phosphorylation, subsequent experiments with the downstream target Akt revealed robust alterations in phosphorylation by Clusterin treatment. Past studies already described modulating effects of Clusterin on the phosphorylation level of Akt in various physiological conditions mainly associated with cellular stress (Jun, et al., 2011; Xiu, et al., 2013; Jo, et al., 2008). Similar to the afore mentioned studies, the results in this work demonstrated no effect on pAkt by Clusterin itself, but in combination with a stimulant a modulation by Clusterin was observable. However, the observed effects during insulin stimulation varied drastically between subsequent repetitions of the experiments, making it impossible to verify any observation or to determine a signal tendency. Since different outcomes for pAkt-dependent Clusterin effects were already postulated (see above) in cellular models experiencing high stress, it was assumed that the divergent results in the executed experiments with insulin stem from a potentially increased stress level of the monitored cells. Therefore, the typical parameters causing cell stress like cell density and starvation duration were altered which, however, had no effect on the ambivalent results. A trigger for the divergent results caused by Clusterin during insulin treatment could not be found under the experimental conditions prior to insulin stimulation. Nevertheless, Clusterin exhibited remarkable effects on the insulin-mediated pAkt level, despite the bivalent results. This renders Clusterin and insulin as a valuable couple for future experiments to elucidate their potential involvement in the occurrence of Diabetes type 2 and subsequently as risk factor for AD.

5.1.3 Low glucose medium in insulin-mediated experiments stabilises Clusterin effects but triggers cellular stress responses

The repetition of insulin-stimulating experiments in low glucose medium was based on the knowledge that glucose is a crucial regulating factor for insulin metabolism. Hence, it also influences the signal transduction pathway triggered by insulin and modulated by Clusterin. The regulating effect of glucose was already observed in a previous study where absence or presence of glucose altered the outcome of insulin-mediated leptin secretion and mRNA upregulation (Tsubai, et al., 2016). In this work, the low levels of glucose during cell cultivation stabilised the effects of Clusterin co-stimulation showing a markedly increased pAkt level compared to sole insulin treatment. This observation confirmed the previous suggestion that the high glucose concentration before and during the stimulation of N2A cells

influenced the pAkt signals, triggered by insulin and Clusterin application. In contrast to high glucose medium, which contained 4.5 mg glucose per 1 g medium (assuming growth medium has a density of 1 g/mL)(or 25 mmol/L), the low glucose medium only had a glucose concentration of 1 mg/g (or 5.6 mmol/L). By comparing these values with literature values in wet weight of brain tissue (approximately 810 µg/g, (Criego, et al., 2005)) or CSF (2.5 – 4.4 mmol/L, (Roos, 2005; Eisenhut, et al., 2003)), it clearly shows that low glucose medium closer resembles the physiological state present in the brain. Since the cell model with N2A should imitate a basic neuronal *in-vitro* brain model, the results for insulin and Clusterin stimulation in LG medium could be an initiation point for the discovery of a potential mechanism involved in AD pathology. The development of AD was linked to occurring Diabetes type 2 which is, among other symptoms, distinguished by increased insulin resistance. Besides the already observed protective function of Clusterin in AD in relation to elimination of misfolded Aβ (see 1.1.3.1), it might also be able to overcome or delay insulin resistance by the observed increased activation of pAkt during insulin exposure. Similar to observations with mutated InsR (Krook, et al., 1996) or the formation of insulin resistance by diacylglycerol (Samuel, et al., 2010), Clusterin could bypass the canonical activation of the InsR via a different mechanism to facilitate proper insulin stimulation. A second potential risk factor of AD is leptin resistance (Bonda, et al., 2014). Leptin is known for its ability to inhibit appetite and regulate lipid metabolism and plays a complex role in neuronal integrity. Expression of Leptin mRNA and secretion of the mature protein is stimulated by insulin via the transcription factor SREBP-1c (Tsubai, et al., 2016) (Fig. 32). Increased levels of leptin were shown to be favourable for AD protection (Folch, et al., 2012; Lieb, et al., 2009). Paradoxically, obesity, which is actually a risk factor for Diabetes type 2 and therefore AD, causes high basal levels of leptin (Considine, et al., 1996). Intensified studies solved this controversy as they revealed the previously mentioned risk factor leptin resistance. This physiological condition leads to diminished leptin signalling (Arch, 2005) and subsequently to translocation of leptin to reactive astrocytes (Maioli, et al., 2015) where it was shown to inhibit insulin signalling (Sartorius, et al., 2012) (Fig. 32). High levels of leptin in the periphery during obesity increase insulin resistance (Hennige, et al., 2006) which in turn increases leptin secretion, eventually resulting in a vicious circle. Clusterin, which is also stimulated by insulin and SREBP-1c activation (see 5.1), forms a complex with leptin (Bajari, et al., 2003) and facilitates its endocytosis via LRP2-Leptin receptor-interaction (Gil, et al., 2013) into hypothalamic cells causing potentiation of the leptin effect on phosphorylation levels of STAT3 (Byun, et al., 2014) (Fig. 32). Additionally, serum leptin-Clusterin-complexes are also endocytosed by interaction with ApoER2 and VLDLR, however, with unknown effect (Bajari, et al., 2003). Assumptions that can be drawn from these studies are that the mechanism of elevated leptin signalling through complexation with Clusterin could be similar for insulin and that Clusterin might also act as a mediator to overcome

leptin resistance. Additionally, these mechanisms can be intertwined with the suggestion that Clusterin might exhibit protective function in the face of ongoing leptin resistance by preventing the translocation of leptin to astrocytes via LDL-receptor family-mediated endocytosis and through its observed boost of insulin signalling.

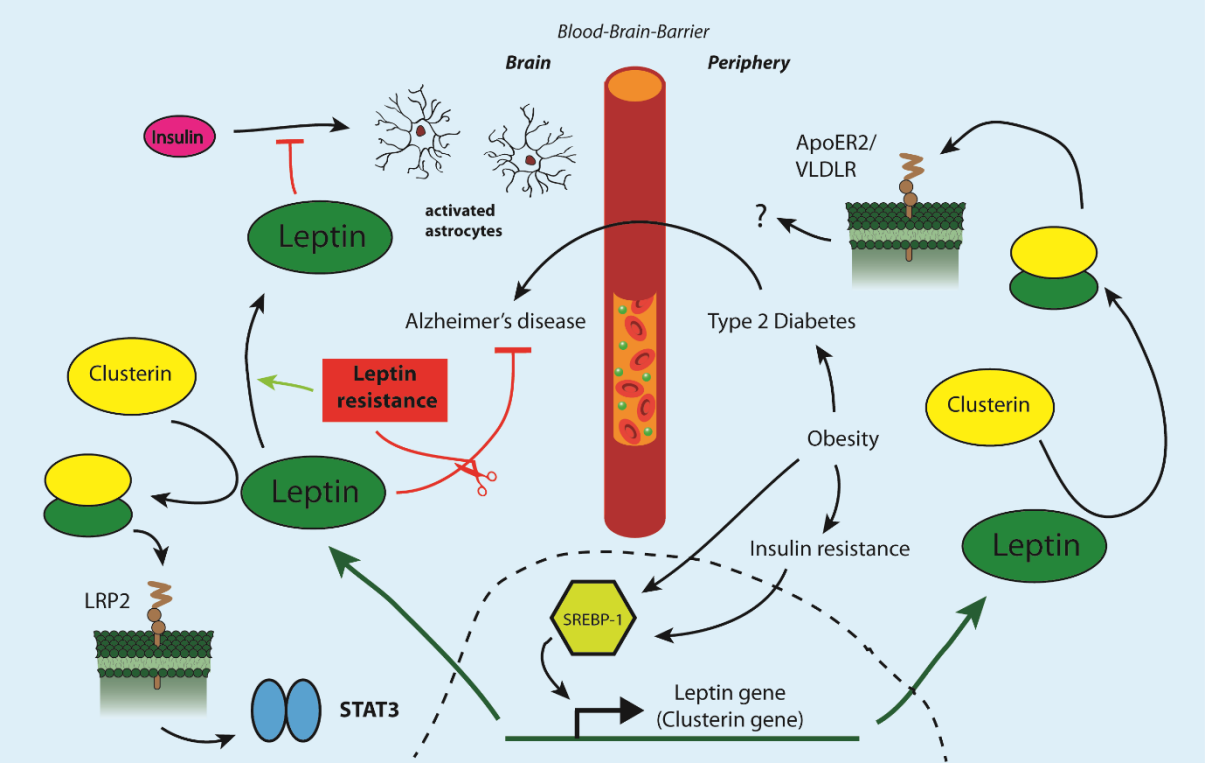

Fig. 32: Overview of some aspects of Leptin signalling and the involvement of Clusterin. *The expression of Leptin is triggered by obesity and insulin resistance. Although it is known that obesity is a risk factor for AD, the elevated levels of Leptin inhibit the onset of the AD pathology. The crucial consequence of obesity, however, is the formation of a Leptin resistance that disrupts the protective mechanism of Leptin (red scissors) and leads to reallocation of Leptin (green arrow) to activated astrocytes where it blocks insulin signalling. In the process of increased Leptin expression, Clusterin plays a crucial by forming a complex with Leptin that can bind to LDL receptor family members in both the brain and the periphery.* ***For information about references see respective paragraphs.***

Nevertheless, all observations stem from in experiments conducted with N2A and subsequent suggestions about potential mechanisms and functions were challenged by the results gathered from protein control Western blots. These results displayed elevated pAkt levels upon insulin exposure in combination with BSA or GST comparable to Clusterin but with less intensity. Additionally, GST-only treatment in cells grown in LG medium triggered pAkt which was in contrast to normal cultured cells. As for BSA, it was already known that it is able to trigger Akt phosphorylation (Coffey, et al., 2015). In case of GST no such effects were found in literature. Resupplying starved cells with FBS increased pAkt levels and similar observations were made with Panexin yielding markedly increased Akt

phosphorylation which even masked the previously observed ambivalent effects after insulin co-treatment under regular medium. Taken together, these results suggested an increased stress level in N2A cells cultivated with LG medium. This assumption was further backed by distinct morphological alterations and an impaired growth rate of LG N2A as well as a negative effect of Clusterin on their cell viability. Alterations in morphology during low glucose administration were already obseeved in other cell types (Foster, et al., 2015), however, cell viability was not affected. One reason might have been a different demand of glucose between various cell lines. N2A are neuroblastoma-derived cells and cancer cells are known for their increased glucose turnover.

Since treatment of N2A with insulin and Clusterin yielded disputable results for both cultivation methods, a consequence to closer elaborate the suggested mechanism of Clusterin in brain physiology and AD pathology would be the usage of a cell line with a reduced glucose demand. This would enable usage of LG medium and could lead to consistent and unambiguous data.

5.2 Clusterin promotes positive effects of IGF-1 stimulation

The inconclusive results for the stimulation of N2A cells with insulin and Clusterin enforced the search for a different studying model that is closely related. By exchanging insulin with IGF-1 a highly similar substitute could be tested for potential modulation by Clusterin. Since IGF-1 is less influenced by glucose, the N2A cells could still be used to retain the *in-vitro* brain model. A previous publication already examined the influence of Clusterin on IGF-1-mediated signal transduction pathways in HeLa, HEK-293 and NB4 cells (Jo, et al., 2008). In this study, a simultaneous source of Clusterin and IGF-1 HeLa conditioned medium had been harvested and reapplied to fresh cells which had led to activation of pAkt. A 65 °C heating step of CM prior to application had further boosted Akt phosphorylation levels. The conclusion drawn from this data was that Clusterin binds IGF-1 and blocks its ability to activate Akt. However, this binding can be reversed by heat which leads to formation of high molecular weight complexes and degradation of Clusterin thereby releasing the heat-stable IGF-1. Based on these data, Clusterin was described as a negative regulator of IGF-1 signalling. These observations are in stark contrast with the results gathered in this work.

5.2.1 The activation of Akt is the major link in the Clusterin-associated signalling pathway

Using IGF-1 we could demonstrate comparable pAkt stimulation in the presence of Clusterin as seen upon insulin treatment. Corresponding experiments aiming at the screening of the IGF-1-R phosphorylation showed no significant differences. This backs the assumption of an involvement of different phosphorylation sites being linked to the Clusterin effects (see 4.3.1). Since IGF-1 is also able to stimulate InsR and the phosphorylation patterns observed for IGF-1-R and InsR are similar, it may be reasonable to assume that the insulin-stimulated experimental results are relevant. Experiments executed with the PI3K-specific inhibitor LY293004 revealed the involvement of the upstream signalling molecule PI3K in activating pAkt. IGF-1 was also shown to stimulate ERK phosphorylation but Clusterin failed to significantly modulate the signal. Only in the early phase of N2A LG stimulation, Clusterin addition caused an elevated pERK signal which was ascribed to the cellular stress levels and the potential cytoprotective feature of Clusterin (Kim, et al., 2009; Kim, et al., 2010). Studies demonstrated that IGF-1 can also stimulate STAT3 activation (Zong, et al., 2000). However, the stimulation of N2A cells with IGF-1 demonstrated no significant levels of phosphorylated STAT3 (data not shown), although positive stimulation with IGF-1 could be shown in primary neuronal cells (Yadav, et al., 2005) and with IL-6 in N2A (Zorina, et al., 2010). Therefore, a possible modulation of the JAK/STAT pathway by Clusterin was excluded. With two of three crucial IGF-1-R downstream signalling molecules eliminated and the gathered evidence about Clusterin modulating effects, it was very likely that Clusterin acts via Akt phosphorylation mediated by PI3K. Nevertheless, it cannot be excluded that side pathways are also involved in this process but it is certain that the data for IGF-1 are in accordance with observations on insulin and this is in marked contrast to the study by Jo and co-workers (see 5.2). On the other hand, a second study suggested similar positive effects of Clusterin on pAkt, however, their strategy was a siRNA knockdown of endogenous Clusterin (Ma & Bai, 2012). The problem in this approach was the fact that the cell model was constantly exposed to high levels of endogenous Clusterin and that basal pAkt levels were already elevated. As a consequence of the Clusterin knockdown, Akt phosphorylation levels in untreated cells were decreased which relativised subsequent experiments with IGF-1 and Clu-siRNA where an equivalent drop in pAkt was observed.

5.2.2 Akt phosphorylation depends on the concentration of secreted Clu

In the study by Jo et al. the core statement is that cancer cell-derived Clusterin is responsible for the downregulation of pAkt (Jo, et al., 2008). In additional experiments they also reported similar effects

for Clusterin-conditioned medium derived from transiently transfected HEK-293T cells. The source of Clusterin in this work were stably transfected HEK-293 cells. The conditioned medium was harvested and purified to gain highly pure recombinant Clusterin which was used for the stimulation experiments. This purified Clusterin mediated an increase in pAkt levels during IGF-1 stimulation. The two approaches differed in two parameters, namely transfection status and Clusterin application form. In case of transfection, a transient approach could cause changes in the translation and secretion machinery. Several previous studies focused their work on the characterisation of intracellular Clusterin forms and their effect on cellular processes. The occurrence of these intracellular forms was ascribed to several different mechanisms involving both transcription and translation of Clusterin (see 1.1.1.2 & 1.1.1.3). One crucial factor was ER stress caused by an increased protein load which could be triggered by transient transfection of Clu-encoding vectors with constitutive promotors. By transiently transfecting N2A cells with the msClu-containing vector and subsequent stimulation with IGF-1, this circumstance was studied but resulted in no visible modulation of pAkt levels. This excluded the involvement of intracellular Clusterin forms which was in accordance with a previous study that revealed the low levels of mentioned Clusterin forms (Prochnow, et al., 2013). Additionally, the conducted transient transfections demonstrated only low concentrations of Clusterin in the culturing medium and whole cell lysate yielding no sign for occurring ER stress. The low concentration of Clusterin, however, was taken as an indicator for the examination of the second crucial difference - the Clusterin application form - between this work and the studies by Jo and co-workers. The conditioned medium from stably transfected HEK-293 cells was compared to that of wild type HEK-293, which express only marginal levels of endogenous Clusterin. Both media only had slight but definite boosting effects on the pAkt levels which was referred to the low levels of Clusterin in the conditioned media that were several magnitudes lower than the concentration used for recombinant Clusterin stimulation. In the publication by Jo et al. the concentration of Clusterin in the used medium was not determined, neither was the amount of conditioned medium used during experiments clear.

In conclusion, the differences seen in pAkt phosphorylation between the gathered data and literature cannot be ascribed to different sources or application forms of Clusterin but to the used concentration. A difference between the concentrations of endogenous levels and overexpression of Clusterin on pAkt stimulation was already demonstrated in hepatocarcinoma cells (Xiu, et al., 2013).

5.2.3 Clusterin effects on IGF-1 stimulation are conserved among mouse and human

Additional evidence for the irrelevance of the Clusterin source was shown in the experiments conducted with human Clusterin which demonstrated similar outcomes to msClu. An amino acid sequence alignment revealed a high homology and identity of both molecules, however, the α-helices, crucial for protein-protein interactions, could not be compared due to the lack of prediction data for msClu secondary structure. Despite the differences in glycosylation site distribution between human and murine Clusterin resulting in assumed differences in binding properties to IGF-1 (see 4.3.3.1), the expected modulation of pAkt stimulation was unaffected. Furthermore, the effects in N2A could be transferred to the human brain cell model SK-N-MC, a common cell line for AD-based studies (Chan, et al., 2007; Kamarehei, et al., 2014). Hence, the results establish a link back to the observations made in the initial RTK Array kit which was performed with human Clusterin in a human cell line. In addition, the reproducibility of pAkt modulation with murine Clusterin in human cell lines and vice versa underlines the specificity of the observed modulation, rendering it a potential generally valid mechanism in the IGF-1-dependent signal transduction pathway. Yet, an interesting difference between the murine and human neuronal cell stimulation could be observed in the Western blot data. While addition of IGF-1 (and Clusterin) to murine cell lines mainly stimulated one visible Akt isoform, the human cell line demonstrated activation of two. Each of the three different Akt isoforms is known to favour a specific cellular response, including glucose metabolism, cell cycle control and embryonic development (Gonzalez & McGraw, 2009; Dummler, et al., 2006). Determination of the Akt isoforms activated by IGF-1 would require specific antibodies and acrylamide gels with higher resolution. Thus, no conclusion can be drawn from the observations made in the Western blots. Nevertheless, it was obvious that msClu and hsClu exhibited different stimulation patterns on Akt isoforms when applied to SK-N-MC cells. While hsClu favoured one distinct isoform, msClu displayed a time-dependent change in Akt isoform phosphorylation. The consequences of this variation are starting points for future experiments to further characterise the mechanism underlying Clusterin-mediated pAkt modulation. The elucidation of this issue can be addressed by Akt isoform knockout analysis and subsequent monitoring of occurring changes in both Clusterin efficacy and phenotypical changes.

5.2.4 Involvement of the LDL-receptor family

The LDL-receptor family consists of seven members which are known to play pivotal roles in various developmental and metabolic processes (see 1.2.2.2). In case of insulin metabolism, it was

demonstrated that InsR interacts with LDLR causing a decreased LDL clearance which can be reversed by insulin addition (Ramakrishnan, et al., 2012). Similar interaction was shown with LRP1 and InsR resulting in beneficial effects, as it promotes insulin signalling and counteracts insulin resistance, a risk factor for AD (Liu, et al., 2015). Furthermore, LRP2 was also described as a binding partner for insulin in the renal recovery of molecules from the glomerular filtrate (Orlando, et al., 1998). In association with IGF-1-R, LRP2 was also shown to internalise IGF-1 during transport across the blood-brain-barrier (Bolós, et al., 2010). This transport ability of LRP2 promotes the clearance of Aβ from the CSF. The endocytosis of LRP2-bound Aβ is mediated by IGF-1 signalling (Fig. 33, Fig. 34) which targets and dephosphorylates Dab-2, an adapter molecule essential for the endocytic regulation (Carro, et al., 2005). Despite its regulating function, Dab-2 can also act as a scaffold molecule for the activation of signal transduction pathways (Diwakar, et al., 2008) (Fig. 5). Signalling by the LDL-receptor family was reported and intensively studied for some members (Boucher, et al., 2002; Revuelta-López, et al., 2015; Sharaf, et al., 2013), while others are still poorly investigated (May, et al., 2005). The members of the LDL-receptor family are known to interact with Clusterin, with LRP2 being the best described binding partner (see 1.2.2.2). The linkage between LRP2 and IGF-1 metabolism suggested an involvement of LRP2 in the Clusterin-mediated modulation of pAkt levels during IGF-1 stimulation (Fig. 33). The mechanism of a potential increase in LRP2 endocytosis rate in the presence of Clusterin was mimicked by the application of the chaperone RAP. Among all described ligands, this molecule displays the highest affinity to the LDL-receptors (Herz & Strickland, 2001; Korenberg, et al., 1994) which is an essential feature in the maturation of the receptors (see 1.2.2.2). Based on the hypothesis of an LRP2 involvement, RAP should exhibit similar effects as Clusterin provided that LRP2 is an essential component in the observed results. Addition of RAP to IGF-1-stimulated N2A and SK-N-MC cells indeed increased the levels of pAkt but subsequent transcriptome screenings of both cell lines eliminated LRP2 as a potential candidate for the Clusterin effect since N2A cells are devoid of LRP2. An earlier study already demonstrated that Clusterin can stimulate Akt phosphorylation independently of the LRP2 involvement (Jun, et al., 2011). RAP, however, is also able to bind to other members of the LDL-receptor family like ApoER2 and VLDLR which are well described receptors for Clusterin interaction (Leeb, et al., 2014). Despite the observation that the phosphorylation patterns in the Western blot with IGF-1 differ between Clusterin and RAP addition, the evidences point towards an involvement of LDL-receptors.

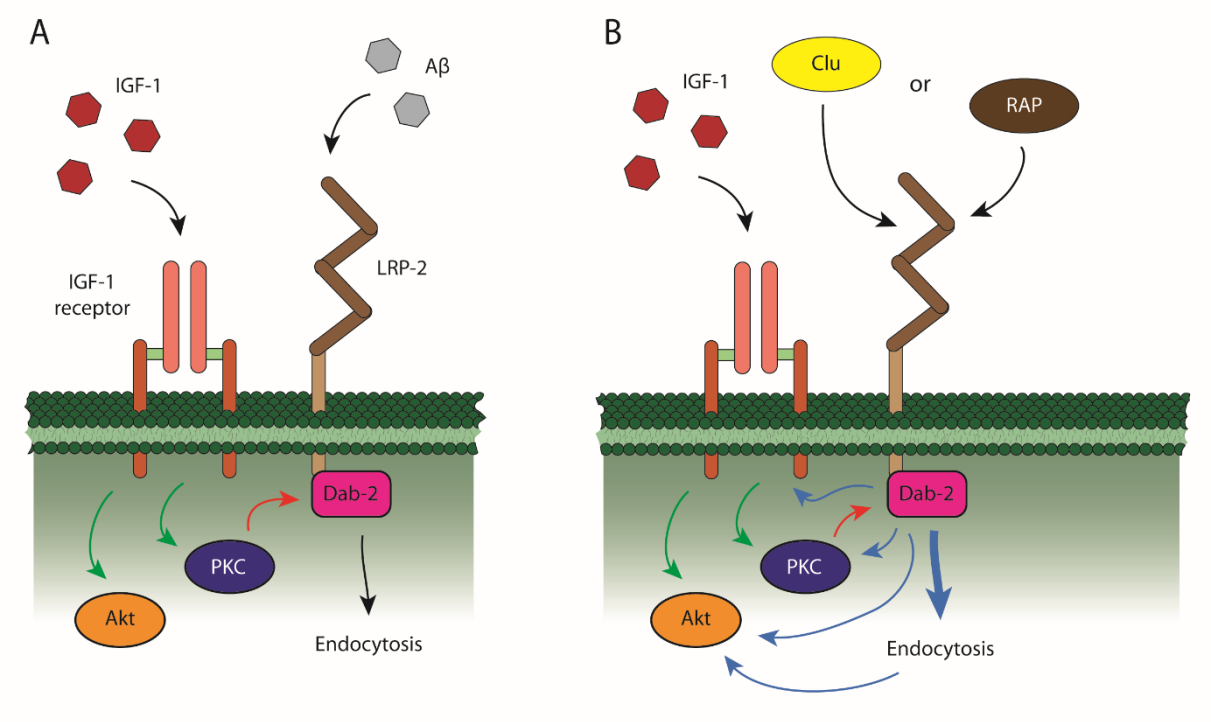

Fig. 33: Schematic depiction of the hypothetical involvement of LRP2 in Clusterin-mediated Akt phosphorylation. *(A) Depiction of Aß clearance via LRP2 and the enhancing effects of IGF-1 stimulation. IGF-1 treatment triggers phosphorylation (green arrows) of Akt and PKC which in turn dephosphorylates (red arrow) Dab-2, leading to endocytosis. (B) Hypothetical effects (blue arrows) of the addition of either Clusterin (Clu) or RAP on IGF-1 receptor and down-stream targets. The question behind this hypothesis is whether the Clusterin-mediated Akt modulation is dependent on LRP2 and whether it can be reproduced with RAP.*

Clusterin was shown to form a complex with leptin that interacts with ApoER2 and VLDLR (see 5.1.3). Since both used cell lines were tested positive for ApoER2, this observation could be a potential basis for a mechanism involving Clusterin and IGF-1. Additional clues for this hypothesis were provided by a RAP preincubation experiment with SK-N-MC cells that showed a decrease in pAkt levels when cells were treated simultaneously with RAP and Clusterin upon 10 min of IGF-1 stimulation (Fig. S10). These results could be even confirmed after 60 min of incubation, when the signals for Clusterin and IGF-1 stimulation already equalised in the absence of RAP. Surprisingly, RAP preincubation abrogated the positive effect of Clusterin addition on pAkt levels after 10 min of incubation. This observation could be caused by blockage and subsequent endocytosis of LDL-receptors after RAP preincubation, rendering them unavailable for a potential Clusterin-induced mechanism. The MTS analysis in both cell lines was in accordance with the described preincubation experiments as was the sample treated with RAP, Clusterin and IGF-1 did not exceed the viability levels seen for RAP and IGF-1 (no synergistic effect) or IGF-1 only. To evaluate the occurrence of potential endocytic events, N2A cells treated with IGF-1 and Clusterin were checked for internalised Clusterin molecules in whole cell lysates by Western blot. This approach, however, did not yield any results possibly due to the low amounts of endocytosed

Clusterin which were below the detection limit (data not shown). A more sensitive approach would have been a fluorescent staining of Clusterin and subsequent fluorescence microscopy.

Nevertheless, all the gathered data from both literature and executed experiments point towards an involvement of the LDL-receptor family in the observed pAkt modulation by Clusterin. However, to fully elucidate the role of receptors such as ApoER2 and VLDLR, further strategies to investigate this matter have to be elaborated.

5.2.5 Physiological relevance of observed Clusterin effects on Akt phosphorylation during IGF-1 stimulation

The growth factor IGF-1 is a crucial factor in the development and maturation of neuronal cells (O'Kusky & Ye, 2012). Its stimulation of Akt phosphorylation via the IGF-1-receptor is the key mechanism for triggering of cellular growth and various other responses (see 1.2.1.2). As described in 5.2.4, the activation of the IGF-1 receptor is also essential for the clearance of Aβ. In an MTS assay the consequence of elevated pAkt levels upon IGF-1 and Clusterin stimulation on the cell viability was elaborated. Addition of Clusterin resulted in a marked increase in cell viability compared to the IGF-1-only sample, whereas the protein control BSA actually abrogated the positive effect of IGF-1 addition. During these assays, the IGF-1 concentration used was below the average plasma IGF-1 concentration (Duron, et al., 2012; Hertze, et al., 2014; Watanabe, et al., 2005). In conclusion, the Clusterin stimulation had a positive effect on cell growth and metabolism, which could well occur *in vivo*, as demonstrated by elevated Clusterin mRNA in living neurons after neuronal degeneration (Strocchi, et al., 1999).

Furthermore, Clusterin was shown to scavenge necrotic debris (Bartl, et al., 2001) and to inhibit amyloid formation (Hatters, et al., 2002). This feature is crucial for the development of AD. Although the mechanisms of amyloid formation by Aβ and phosphorylated Tau are still not fully elucidated, it is known that Clusterin plays a pivotal role in the clearance of Aβ (see 1.1.3.1) and is interfering with Aβ aggregation ((Narayan, et al., 2011; Beeg, et al., 2016), also see 1.1.3.1). A correlation between increased Aβ deposits and elevated Clusterin levels was demonstrated which also pointed towards the critical factor of the Aβ-Clusterin-ratio ((Miners, et al., 2017), also see 1.1.3.1).

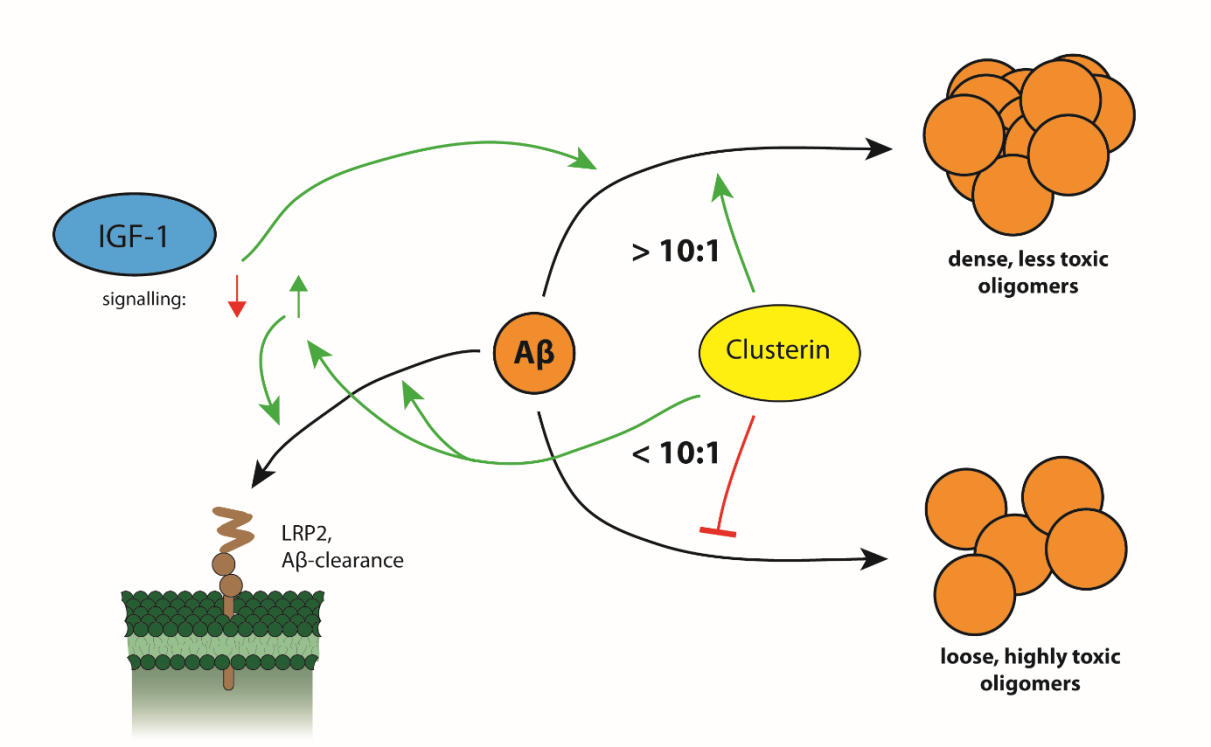

Fig. 34: Role of Clusterin and IGF-1 in the clearance of Aß. *The effect of Clusterin on the formation of Aß plaques is dependent on the ratio between Clusterin and monomeric Aß. During a low load of Aß molecules, Clusterin inhibits plaque formation and causes clearance of Aß via LRP2. This clearance is further supported by elevated IGF-1 signalling. When the Aß load exceeds a certain level, Clusterin facilitates oligomerisation of Aß molecules to a dense and less toxic aggregate. Low levels of IGF-1 signalling favour the formation of these aggregates. For information about references see respective paragraphs.*

Besides Clusterin, the IGF-1 signalling pathway showed a protective function against Aβ neurotoxicity as well (Doré, et al., 1997). Additionally, IGF-1 regulates Tau phosphorylation, a second trigger for AD development, by inhibiting formation of fibrils (Cheng, et al., 2005; Hong & Lee, 1997). These mechanisms suggested IGF-1 to be a crucial risk factor in the developmental processes of late-onset AD. This suggestion could be demonstrated by a potential formation of an IGF-1 resistance. The resistance was associated inter alia with decreased Akt phosphorylation and increased APP mRNA levels (Steen, et al., 2005) and was accompanied by insulin resistance which shares similar signalling molecules (Talbot, et al., 2012). A crucial component in the development of IGF-1 resistance is the IGF-1 receptor. The results and opinions on the role of IGF-1-R in the development of AD, however, are highly divergent. While some studies revealed an involvement of IGF-1-R in cytoprotective events in the face of Aβ stress (Niikura, et al., 2001) or a development of AD-like neuropathology after receptor blockage (Carro, et al., 2006), others stated a decreased neurotoxicity of Aβ in the absence of IGF-1-R (O'Neill, et al., 2012) and formation of less toxic condensed Aβ aggregates resulting from reduced IGF signalling (Cohen, et al., 2009) (Fig. 34). Since addition of Clusterin to IGF-1-stimulated cells did not alter the phosphorylation level of pIGF-1-R, the suggestion arose that Clusterin might be

able to circumvent the IGF-1-R in the process of pAkt stimulation leading to either positive or negative effects in AD development. Furthermore, the elevation of pAkt could result in neuroprotection in the early phase of AD by boosting the effects of IGF-1 on Aβ clearance and neuronal growth. This would correlate with the increased levels of Clusterin mRNA observed during neuronal loss (Strocchi, et al., 1999). The increasing load of Aβ in the extracellular space in ongoing AD eventually leads to oligomerisation which is blocked by Clusterin to maintain active clearance (Fig. 34). However, when a specific ratio of Aβ and Clusterin is reached, it was demonstrated that Clusterin actually enhanced aggregation (see 1.1.3.1). This could be a second line of defence as densely aggregated Aβ is less toxic compared to somewhat soluble oligomers. Aβ aggregation led to a delay in AD progression which was shown in IGF-1-R-depleted model organisms (O'Neill, et al., 2012; Cohen, et al., 2009). The occupation of Clusterin with increasing amounts of Aβ could withdraw it from the co-stimulating events with IGF-1. This would decrease the activation of the IGF-1 signalling pathway as seen in IGF-1-R depletion and subsequently leading to an additional signal for Aβ aggregate formation. Despite the inability to clear high molecular aggregates from the brain, the aggregation mediated by Clusterin could be a last line of defence during AD, that potentially decreases severity and increases the lifespan of the individuum during an otherwise early lethal pathology.

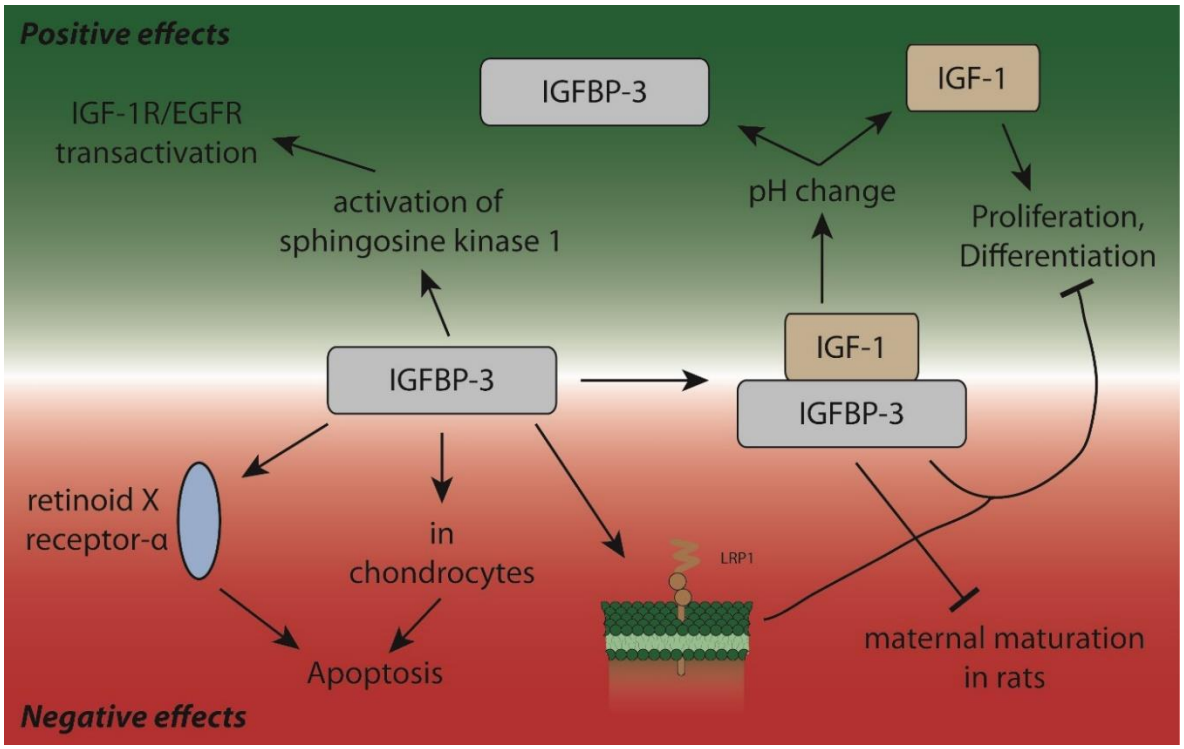

Fig. 35: Positive and negative effects of IGFBP3 and its binding to IGF-1. *IGFBP3 alone can positively influence the activation of IGF-1-/EGF-receptor but can also activate apoptosis and inhibit proliferation under certain circumstances. When bound to IGF-1, it inhibits the positive effects of IGF-1 in differentiation and maturation processes. This complex of IGF-1 and IGFBP3 can be disbanded by a change in pH.* ***For information about references see respective paragraphs.***

A crucial factor in the IGF-1 metabolism are the IGF-binding proteins (IGFBP), especially IGFBP3. Serum IGF-1 is mainly bound to IGFBP3 (see 1.2.1.2) which regulates its prosurvival and growth stimulus (Fig. 35). Targeted proteolytic shedding of the IGFBP3-IGF-1 complex releases bound IGF-1, rendering it biologically active. The presence of IGFBP3 in the serum is an essential regulator for many physiological processes such as the regulation of maternal maturation in rat infants (Lékó, et al., 2017) (Fig. 35). Most effects are directed towards antiproliferative mechanisms mainly based on its ability to bind IGF-1. Its regulation shows high complexity involving other growth factor signal transduction such as the EGF-mediated pathway (Takaoka, et al., 2006). In contrast, studies also demonstrated IGF-1-independent mechanisms of IGFBP3-induced apoptosis (Longobardi, et al., 2003) and a potential involvement of the endocytic receptor LRP1 in the transmission of such effects (Huang, et al., 2003). Additional target receptors of IGFBP3 are even found in the nucleus, i. e. the retinoid X receptor-α (Liu, et al., 2000) (Fig. 35), which in turn requires active endocytosis of IGFBP3. Structural changes of IGFBP3 mediated by changes in the pH environment were associated with promoting effects of IGFBP3 on IGF-1 function (Conover, et al., 1996). In combination with an activation of sphingosine kinase 1, IGFBP3 displayed synergistic activation on IGF-1-R and EGF-R (Martin, et al., 2009). The antiproliferative effect of IGFBP3 was visible in the executed MTS assay where addition of IGFBP3 nearly fully abrogated the proliferative effect of IGF-1. Western blot studies confirmed the absence of pAkt stimulation by IGF-1 addition in the presence of IGFBP3. The hypothesis of Clusterin competing with IGFBP3 for the binding of IGF-1 to increase IGF-1 bioavailability, was disproven by the fact that Clusterin was not able to protect IGF-1 from binding to IGFBP3. Nonetheless, Clusterin could play an essential role in the IGF-1/IGFBP3 regulatory system in the brain since IGFBP3 levels in the CSF are considerably lower (approximately 9,4 ng/mL, (Bunn, et al., 2005)) than in the serum (approximately 2 – 4 µg/mL, (Hu, et al., 2016)). As a comparison, blocking of low physiological IGF-1 signalling (50 ng/mL) in the Western blot analysis was achieved with 1,25 µg/mL IGFBP3. In the face of AD, IGFBP3 was shown to contribute to Aβ neurotoxicity and tau phosphorylation, opposing the prosurvival effects of IGF-1 (Watanabe, et al., 2015). However, it was also demonstrated that IGFBP3 can have neuroprotective effects during Aβ exposure (Sung, et al., 2014) possibly regulated by the binding of the prosurvival factor humanin (Ikonen, et al., 2003). Humanin did not interfere with the binding of IGF-1 nor were any ternary complexes detectable. Clusterin could be the crucial factor for enabling the binding of IGFBP3 to humanin by depriving IGFBP3 from IGF-1 based on the elevated utilisation in signal transduction mediated by Clusterin. This would introduce two separate pathways directed towards neuronal protection.

Two additional observations from the MTS assay were quite surprising but rather complicated to interpret. One of these observations was the negative effect of Clusterin addition to the sample

stimulated with IGFBP3 and IGF-1 which demonstrated occurring cell death. A reason for this phenomenon could be an ongoing endocytosis of IGFBP3 mediated by Clusterin which would trigger intracellular binding of IGFBP3 to corresponding receptors causing apoptosis as described above. The second observation was the increased levels of cell viability in the Clusterin and RAP-only stimulated samples. Surprisingly, the viability elevation was less prominent in SK-N-MC cells for Clusterin and even absent for RAP. Possibly, the N2A cells could utilise random proteins to boost cell proliferation, however, similar a behaviour was not observed in the BSA-only sample. Thus, the explanation for the observed effects remains unclear.

Taken together, it could be shown that Clusterin had a marked impact on the cell viability during IGF-1 stimulation which could be an advantage in the prevention of AD or its progression. Nevertheless, this hypothesis involves highly complicated regulation processes, such as regulation of IGF-1 signalling, Aβ metabolism as well as IGFBP3 involvement, which have to be further elucidated by subsequent studying approaches. As a result, this work provides promising starting points for the revelation of the role of Clusterin in AD and the underlying mechanism.

5.3 Other growth factors specify the spectrum efficacy of Clusterin

The previous experiments have shown that Clusterin is able to modulate signal transduction of both insulin and IGF-1. Furthermore, the RTK Array kit has shown that HGF-R is also a potential target for Clusterin. These observations raised the question whether further growth factors are influenced in the presence of Clusterin. The screening for different molecules not only increases the potential spectrum of interaction partners but also strengthens the observations made for insulin and IGF-1 and increases their significance in case of negative results. As new target molecules, the already suspected HGF was chosen in addition to EGF, a crucial growth factor in nearly every human tissue.

5.3.1 Combined application of EGF and Clusterin displays no effects

The EGF signalling via EGFR is known to stimulate a variety of different pathways similar to IGF-1. Two central signalling molecules are the already mentioned Akt and ERK which are both addressed by EGF stimulation (Galbaugh, et al., 2006; Gao, et al., 2005). EGF-mediated cell responses are also seen in various brain areas and neuronal cell types with effects usually involving neuronal proliferation and integrity (Mazzoni & Kenigsberg, 1992). An involvement of EGF in the development of AD is only poorly studied to this point. It was demonstrated that EGF is able to inhibit ApoE4 and Aβ-mediated cell death

(Thomas, et al., 2016) but might also cause progression of AD in later stages through its stimulating effect on protein synthesis leading to increased secretion of Aβ (Refolo, et al., 1989). However, this increase in Aβ secretion was accompanied by elevated Clusterin gene expression triggered by EGF as well (Gutacker, et al., 1999). Despite the limited knowledge concerning the involvement of EGF in AD, it still qualified as a potential target for Clusterin. A study examining the effect of Clusterin on astrocytes revealed an EGFR-dependent signalling pathway stimulating ERK phosphorylation via the sole interaction with Clusterin (Shim, et al., 2009). This aspect of Clusterin signalling was further addressed by Jo et al. who demonstrated no significant change in either EGF-induced Akt or ERK phosphorylation in the presence of Clusterin (Jo, et al., 2008). In case of ERK phosphorylation, similar results were gathered in this work, however, the more interesting observation was the complete absence of Akt phosphorylation. First speculations about an absence of EGFR in N2A were eliminated by literature which revealed a definite presence of EGFR in N2A (Llorens, et al., 2013). Furthermore, these studies also displayed a clear positive activation of pAkt stimulated by EGF addition (Gómez-Villafuertes, et al., 2015). An insufficient concentration of EGF for stimulation experiments could be excluded from the list of potential causes as the working concentration was several fold higher (50 ng/mL) compared to physiological (approximately 0,5 ng/mL in serum, (Futamura, et al., 2002)) or functional (1-10 ng/mL, (Simpson, et al., 1982)) concentrations. Based on these facts, it was assumed that EGF is not involved in Clusterin-associated modulation of signalling pathways.

5.3.2 HGF-induced Akt phosphorylation is elevated by Clusterin in a cell model experiencing increased stress levels

The initial screening for interaction partners of Clusterin with the RTK Array kit revealed a modulative effect of Clusterin on the phosphorylation of HGF-R similar to the observation with Ins-R. HGF-R, also called c-Met, regulates cell motility and proliferation which are stimulated by binding of the corresponding ligand HGF to the receptor (Organ & Tsao, 2011). In the experimental setup of the RTK Array kit, the only added stimulator was the artificial serum supplement Panexin containing insulin but devoid of any growth factors. It was, however, possible to stimulate the HGF-R with this serum supplement. Furthermore, the used cell line HEK-293 is known to show no endogenous levels of HGF (Dua, et al., 2011) which excludes any autocrine mechanisms. At this point, the reason for the HGF-R phosphorylation stimulation in the RTK Array kit assay could not be elucidated. Nevertheless, the effect of Clusterin on the phosphorylation level of HGF-R was unambiguous. HGF-R was shown to be involved in AD, since studies revealed a decrease of HGF-R mRNA levels in AD brains (Hamasaki, et al., 2014). On the contrary, the levels of HGF in the brain were elevated in AD patients (Fenton, et al., 1998) which

was ascribed to prosurvival activities during the development of AD (Sharma, 2010). To combine both the observations from the RTK Array kit and the study, results regarding the involvement of HGF-R in AD, the previously used brain cell models (N2A, SK-N-MC) were planned to be stimulated with HGF and checked for Akt phosphorylation. However, neither N2A (data not shown) nor SK-N-MC displayed any mRNA levels of HGF-R which rendered them useless for the planned experiments. Since preliminary experiments with HGF-stimulated HEK-293 yielded no evaluable results (data not shown), the hepatocellular carcinoma cell line Hep G2 was used instead. The stimulation of Hep G2 with HGF and Clusterin demonstrated similar modulations of Akt phosphorylation compared to IGF-1 although the signal peak was delayed temporally. Despite the convincing positive modulation by Clusterin the control samples of the performed Western blots strongly resembled those of the insulin-stimulated N2A LG cells. This observation raised the assumption that the Hep G2 cells were also stressed during HGF stimulation. Subsequent MTS analysis confirmed this hypothesis, as Hep G2 cells already showed elevated cell viability levels when only Clusterin was added. The demonstrated effect markedly reversed to a decrease in cell viability when the stress levels were increased prior to stimulation by prolonged cultivation on serum-free medium.

Both MTS and Western blot results demonstrated a prevalent stressed state in Hep G2 cells. Despite the Clusterin-induced upregulation of pAkt even in the absence of HGF, the data tend to a positive regulation of Akt phosphorylation by Clusterin during HGF stimulation. These results could be confirmed via a cell line that expresses HGF-R and that is able to maintain normal cell conditions during a period of serum starvation.

5.4 Uncovering the Clusterin-IGF-1-interplay

Clusterin is a molecule known to bind a plethora of different proteins. Studies have shown that it is able to bind both native ligands and denatured proteins (Harris & Fahrenholz, 2006). Depending on the interaction partner, different structural domains in the Clusterin molecule are responsible for the binding (see 1.1.2). The fact that binding of stressed proteins and LRP2 is mediated by two independent domains raised the suggestion that Clusterin acts as a scavenger protein (Lakins, et al., 2002). This suggestion was confirmed later on (Wyatt, et al., 2011). Jo et al. already demonstrated an actual interaction of Clusterin with IGF-1. This interaction was confirmed in this work although the observed outcome based on Akt phosphorylation differed vastly. In comparison to other growth factors, IGF-1 showed a markedly elevated binding affinity to Clusterin. By comparing the ability of Clusterin to bind to coated IGF-1 with that of IGFBP3, RAP and BSA, it became clear that IGFBP3 is the major interaction partner of IGF-1. Still, Clusterin demonstrated a moderate affinity whereas RAP and BSA did not bind

to IGF-1. Therefore, the underlying mechanism of Clusterin-mediated Akt phosphorylation and elevated cell viability supposedly differs from the events triggered by RAP or BSA in both Western blot and MTS studies.

The question that arose from the observed interaction of Clusterin and IGF-1 was whether there is a distinct binding site for IGF-1 in the Clusterin molecule or whether its chaperone activity is merely responsible for the binding of IGF-1. To investigate these implications, IGF-1 was treated with denaturing conditions to detect changes in binding affinity. Furthermore, Clusterin mutants were generated and monitored for alterations as to their ability to bind IGF-1.

5.4.1 Structural alterations of IGF-1 impair binding by Clusterin

The interaction of Clusterin with IGF-1 could be proven by ELISA assays. To elucidate the binding capabilities of Clusterin to denatured IGF-1, the growth hormone was heat-treated prior to the binding studies. The results did not show any significant changes in binding affinity of Clusterin to heat-treated IGF-1. This was in accordance with literature as IGF-1 exhibits a strong resistance to elevated heat even up to approximately 80 °C (Clark, et al., 2014; Mireuta, et al., 2014). In case of IGFBP3, the heat treatment of IGF-1 markedly increased its binding affinity by fivefold. Previous studies already mentioned a possible chaperone activity of IGFBPs assisting in the proper formation of the native IGF-1 molecule (Hober, et al., 1994). The pre-treatment of IGF-1 with heat could lead to small conformational changes triggering the potential chaperone activity of IGFBP3 or making the molecule more accessible for binding of IGFBP3. However, when IGF-1 is pre-treated with either DTT alone or in combination with heat, IGFBP3 as well as Clusterin are not able to establish a solid binding to IGF-1. In this setup, the reduction of IGF-1 with the reducing agent DTT was already sufficient for full binding inhibition. A potential direct interference of DTT with this interaction was excluded, since the DTT concentration during the ELISA binding incubation step was similar to the DTT concentration that showed the highest binding efficacy for both IGFBP3 and Clusterin in the preliminary DTT serial dilution. HPLC analyses of the differently treated IGF-1 entities revealed that only combined treatment with DTT and heat had a serious impact on the hydrophobicity of the molecule. This treatment led to a scrambled variant of IGF-1 which only occurs during strong denaturing conditions paired with reducing agents (Chang, et al., 1999). DTT alone was insufficient to disturb the overall integrity of IGF-1, so was heat treatment which is in accordance with the heat resistance stated in literature. By looking at the results gathered from CD-spectroscopy, the HPLC data was defined more precisely in terms of structural alterations. While heat treatment alone already caused a redistribution in the α-helix and β-sheet ratio, the application of DTT and heat together further changed the distribution of secondary structure elements

of IGF-1. Due to the large amounts of IGF-1 needed for the CD-spectroscopy measurements, the DTT-only sample could not be implemented.

Previous studies proved the existence of a second IGF-1 isoform that forms in the presence of low DTT concentrations (Hober, et al., 1992). This isoform is characterised by mismatched disulphide bond distribution but shows similar CD-spectroscopy chromatograms (Miller, et al., 1993). Although the HPLC chromatograms show no sign of this IGF-1 isoform, probably due to a poor peak resolution and the constant high concentration of DTT in the corresponding DTT sample, it is assumed that this isoform is responsible for the abrogated binding affinity of Clusterin to DTT-treated IGF-1. During the washing steps in the ELISA assay the DTT is removed which enables IGF-1 to re-establish the disulphide bonds possibly causing the mismatch formation of the isoform. A subsequent study also presented that the mismatched IGF-1 isoform has impaired binding affinity to the IGF-1-R compared to native IGF-1 (Narhi, et al., 1993). In this work, it could be shown that DTT and heat-treated IGF-1 is not able to trigger Akt phosphorylation and that addition of Clusterin does not rescue IGF-1 stimulation.

Despite the fact that Clusterin exhibits chaperone activity it is not able to bind mismatched or denatured IGF-1. Furthermore, it does not sustain its enhancing effect on Akt phosphorylation in the presence of denatured IGF-1. These facts raised the assumption that Clusterin contains a distinct binding site for IGF-1 that only recognises native IGF-1 but does not involve its chaperone activity. The presence of mismatched IGF-1 in the ELISA assays was further backed by the observation that IGFBP3 binding was also abrogated which is in accordance with literature (Heding, et al., 1996).

5.4.2 Site-directed mutations influence the folding state of Clusterin

Recent studies about Clusterin often address the occurrence of polymorphisms in the Clusterin gene in association with different pathologies such as Alzheimer's disease. Some of these polymorphisms are found in structural elements that are known for their highly conserved nature or their involvement in Clusterin activities (Woody & Zhao, 2016). To determine the necessity of structural key features in the Clusterin molecule for the binding of IGF-1, two domains known for their binding ability (see 1.2) were mutated. One mutation targeted the highly conserved disulphide cluster with a double mutation of the 2-9 disulphide linkage. The second mutation, a so-called helix breaker, was introduced into the amphipatic α-helix located at the C-terminus of the α-subunit. The essential character of these α-helical domains was suggested by a study in which a proline substitution in one of the α-helices was assumed to be involved in the recurrence of haemolytic-uremic syndrome (Ståhl, et al., 2009). The approach to mutate an α-helix within the Clusterin molecule was previously targeted in a work by

Stewart (Stewart, 2007). Her approach to introduce a proline substitution in the α-helix located at the C-terminus of the α-subunit failed at the isolation of the secreted Clusterin mutant. In this work, the helix was targeted with two consecutive proline substitutions. Despite the promising expression levels in preliminary experiments, the proline mutant as well as the cysteine mutant were only poorly secreted in a large-scale purification process compared to the wild type protein. These observations were first indications for an alteration in the secretory pathway of both Clusterin mutants. The fact that mutations influence the proper secretion of Clusterin was already previously shown (Bettens, et al., 2015). The CD-spectroscopy revealed the impact of the introduced mutations on the secondary structure distribution. The distribution for the wild type Clusterin was close to the values in literature (Rohne, et al., 2014), however, the proline mutant displayed a decrease in the α-helical content comparable to murine Clusterin. Since there is no prediction data concerning secondary structures in murine Clusterin, an evaluation of a possible structural similarity between murine Clusterin and the proline mutant cannot be conducted. Since murine Clusterin also shows altered hydrophobicity in the HPLC analysis is was obvious to analyse the proline mutant as well. However, this approach failed due to the poor yield of isolated proline-mutated Clusterin and the high concentrations needed for HPLC analysis. The mutation of the cysteine residues not only showed a marked decrease in the α-helical content in CD-spectroscopy but also yielded evidence for the actual existence of this disulphide bond. The 2-9 disulphide bond was not only chosen for its involvement in binding activities but also because of its not fully proven state (see 1.2). The HPLC analysis revealed that substitution of the two cysteine residues led to an alteration in the retention time and the appearance of a second peak. This peak pattern was also observable by treatment of wild type Clusterin with DTT. These results suggested a destabilising effect of the introduced cysteine mutations on the stability of the Clusterin chain linkage which in turn would be an indirect evidence for the existence of this disulphide bond. Further analysis by Western blot backed this assumption as hsClu-Cys already showed partial disintegration of the two Clusterin chains in a non-reducing environment. In case of hsClu-Pro, the Western blot analysis only demonstrated weak signals although similar amounts of protein were loaded. The introduction of the helix breaker could possibly lead to a different folding of the protein which could mask the V5-tag targeted by the staining antibody.

The introduction of two different mutations in crucial domains of the Clusterin molecule caused changes in the secondary structure distribution compared to the wild type protein. Although the substitution of the two cysteine residues only aimed for the removal of the disulphide bond, the impact on the secondary structure distribution suggested a more complex involvement in the folding process of Clusterin. Nevertheless, the cysteine mutation yielded evidence for the actual existence of the 2-9 disulphide bond.

5.4.3 Characterisation of the domains in the Clusterin molecule that are essential for its chaperone activity and IGF-1 binding

The experiments with two Clusterin mutants had shown that small changes in structurally crucial domains of the molecule can lead to serious changes in its native folding state and integrity. Further characterisation of these changes was conducted by monitoring their impact on chaperone activity, the major function of Clusterin ((Humphreys, et al., 1999), see 1.1). As an additional control sample for the chaperone assay, the hsClu-RIVQ mutant was introduced which lacks proteolytical cleavage of the two chains but maintains its chaperone activity in a non-reducing environment. Furthermore, it was shown that glycosylation is essential for the chaperone activity (Rohne, et al., 2014). Therefore, both msClu and hsClu were treated with PNGase F. The treatment of msClu and hsClu (data not shown) only resulted in a partial deglycosylation which was already demonstrated earlier (Rohne, et al., 2014). However, the described approach to reach full deglycosylation could not be applied as it involves treatment with DTT which would interfere with subsequent analyses. Due to the low yields of hsClu-Pro, once again only the cysteine mutant was included in chaperone assays. Taken together, the chaperone assay was executed with msClu, hsClu, their corresponding deglycosylated variants, the three mentioned mutants and BSA as a negative control. Of these molecules only the deglycosylated variants and the hsClu-Cys mutant showed unexpected results. The previously observed structural change in the cysteine mutant is also reflected in an impaired chaperone activity. In case of the deglycosylated hsClu, literature states that the impact of deglycosylation and especially partial deglycosylation in a non-reducing environment is only marginal (Rohne, et al., 2014). However, the results showed a marked impairment of chaperone activity which is inexplicable with the present data. A similar situation applies for deglycosylated msClu that exhibited an even more pronounced loss of chaperone activity. Murine Clusterin is only poorly studied but based on the known facts it was suggested that the difference in N-glycosylation site distribution across the molecule compared to hsClu (see 4.3.3.1) has an influence on the efficacy of the PNGase F treatment. Since the experimental conditions only result in partial deglycosylation, the extent of this partial removal could vary between murine and human Clusterin, causing differences in chaperone activity. This could be based on the different secondary structure of both molecules which was assessed by CD-spectroscopy and HPLC analysis. The addition of DTT in the chaperone assay further decreased chaperone activity of hsClu-Cys and abrogated the activity of deglycosylated msClu. An increased susceptibility of msClu to DTT was also seen in the wild type msClu whereas the hsClu wild type maintained most of its chaperone activity. However, it was expected that hsClu would be more resistant to DTT as it was described in literature (Rohne, et al., 2014). In contrast, the influence of DTT on hsClu-RIVQ as well as on deglycosylated hsClu could be confirmed.

The chaperone assay has shown that the already published negative influence of deglycosylation on chaperone activity of Clusterin also applies to msClu but with a stronger impact. The addition of DTT increased the severity of this impairment to full abrogation of chaperone activity. Similar results were also observed for hsClu-Cys. With the assumption that mutation of the cysteine residues would only affect disulphide bond formation, it was suggested that addition of DTT would equilibrate the chaperone activity of both hsClu-Cys and wild type hsClu. However, the addition of DTT nearly obstructed the chaperone activity of hsClu-Cys. Together with the observed change in structural distribution of hsClu-Cys, these results confirm that mutation of the cysteine residues has far-reaching consequences on the structural integrity and activity of the Clusterin molecule.

Since the chaperone assays revealed striking differences in the activity of different Clusterin variants and mutants, it was essential to examine their ability to bind IGF-1. Preliminary experiments with hsClu revealed a strong affinity to IGF-1 which even exceeded that of IGFBP3. In accordance with the chaperone assay, deglycosylation impaired this affinity. In contrast to hsClu, the deglycosylation of msClu had no significant impact on the binding of IGF-1. This further strengthened the assumption of a chaperone activity-independent binding of IGF-1 by msClu. Additionally, these results suggest that glycosylation of msClu, at least in part, is dispensable for IGF-1 binding. The proline and cysteine Clusterin mutants both demonstrated a marked impairment in IGF-1 binding capability. The proline mutant exhibited similar levels of IGF-1 binding as msClu which again raises the speculations of similar structural formation as seen in CD-spectroscopy. The cysteine mutant, however, displayed similar results to the chaperone assay with a highly impaired binding of IGF-1. In contrast, the hsClu-RIVQ mutant, as expected, was close to the wild type activity. To evaluate these binding events, the blank values of the ELISA assays which demonstrate the unspecific binding of the Clusterin variants to the blocking solution were analysed. The values revealed elevated unspecific binding events for hsClu and hsClu-RIVQ. The deglycosylation of hsClu reduced this unspecific binding by approximately half which is in accordance with the actual reduction for IGF-1 binding (see Fig. 30A). The cysteine and proline mutants as well as both msClu variants only showed weak unspecific binding. Assuming that the binding of Clusterin to IGF-1 is based on a specific interaction of both molecules, the elevated unspecific binding character of hsClu might be responsible for the increased values in IGF-1 binding compared to msClu. Since msClu and the other hsClu mutants lack this unspecific binding character, it is assumed that the binding affinity of Clusterin to IGF-1 is altered in the hsClu mutants as well as in msClu compared to hsClu. As a consequence, the structural differences introduced by mutations in essential domains of Clusterin deteriorate the unspecific binding character of the molecule which also influence its chaperone activity.

The question still pending is what causes the low binding specificity of hsClu compared to msClu. Based on the only known crucial structural difference, namely the N-glycosylation site distribution, a possible hypothesis is postulated. It is known that msClu lacks the N-glycosylation site at Asn86, which is in close proximity to the molten globule-like domain that is assumed to be involved in chaperone activity (Bailey, et al., 2001; Lakins, et al., 2002). This lack could be essential as for the difference in unspecific binding as well as chaperone activity. One evidence for this assumption could be the decrease in unspecific binding when hsClu is deglycosylated. A previous study demonstrated that PNGase F treatment under a non-reducing environment mainly deglycosylates the α-chain which contains the Asn86 site (Rohne, et al., 2014). A second study revealed that the β-chain is responsible for cellular lipid accumulation (Matukumalli, et al., 2017). In msClu this chain contains an additional N-glycosylation site located closely to the disulphide bond cluster. This cluster is known to be involved in several binding processes (see 1.1.2). The additional glycosylation could increase the specificity of this domain to distinct ligands which could contribute to the differences in IGF-1 binding compared to hsClu. Since the hsClu-Cys mutant had impaired chaperone and IGF-1 binding activity, it is assumed that the cysteine cluster is actually involved in IGF-1 binding and essential for chaperone activity. The lack of Asn86 and the increased importance of the cysteine cluster in both msClu and deglycosylated msClu could be a reason for the susceptibility to DTT treatment in the chaperone assay and the variation in chaperone activity.

The IGF-1 binding assays clearly demonstrated the unspecific binding character of hsClu that most likely provides the chaperone activity. Introduction of mutations in the cysteine cluster or the amphipathic α-helix located at the α-chain C-terminus abrogated this unspecific binding ability. This suggests an involvement of both domains in unspecific binding events or at least structural changes that influence other essential domains. Due to the lack of Asn86 glycosylation, it was suggested that msClu is more dependent on structural integrity and glycosylation to maintain chaperone activity. Furthermore, it was assumed that the additional N-glycosylation site on the β-chain grants the molecule a higher specificity to distinct ligands such as IGF-1.

6 Summary

In recent years the ability of Clusterin to modulate signal transduction pathways has been a highly disputed subject among research groups. Several signalling pathways were shown to be influenced in the presence of Clusterin. However, the link between extracellular Clusterin and intracellular signalling molecules was only poorly addressed. The initial goal of this work was to answer this question by revealing new interacting receptors with a special focus on members of the RTK family which are involved in crucial cellular responses. An initial screening for potential receptor targets revealed the insulin receptor as being modulated by Clusterin in the presence of a serum stimulus. Subsequent studies, however, could not verify this observation which was ascribed to the poor detection in the face of the insulin receptor's highly complex phosphorylation pattern during activation. Yet, the ability of Clusterin to modulate insulin signalling was observable at the down-stream target Akt, a molecule central for various signalling pathways. Despite the Alzheimer's disease cell model we had chosen did not generate consistent results, the data gained from these experiments provide a promising starting point for future investigations of the involvement of Clusterin in insulin signalling.

To further pursue the role of Clusterin in signal transduction, the insulin-related growth factor IGF-1 was considered another interesting candidate. Preliminary experiments demonstrated an increased activation of Akt phosphorylation when cells were co-treated with Clusterin and IGF-1, although the corresponding receptor IGF-1 receptor was not modulated. The obvious idea of an involvement of the Clusterin receptor LRP2 was disproven but did not exclude other members of the LDL receptor family such as ApoER2 and VLDLR. Both receptors had already been shown to be targets of Clusterin which can trigger a reelin-dependent signalling pathway. The enhancement of Akt phosphorylation by Clusterin was traced further down-stream to the direct changes in cellular responses. The monitoring of cell viability and metabolism also demonstrated a sound increase in the presence of Clusterin. All these results demonstrated a definite modulation of IGF-1 signalling by Clusterin and pointed towards a molecular interaction of both proteins.

This hypothesis was addressed by binding assays involving Clusterin and IGF-1. Although Clusterin possesses the ability to bind a plethora of (denatured) molecules, the experiments revealed a specific binding of native but not denatured IGF-1. By introducing variants of Clusterin carrying mutations in either an amphipatic α-helix (hsClu-Pro) or in the 2-9 disulphide bond (hsClu-Cys), the binding to IGF-1 was further characterised. These mutants not only revealed the importance of both structural elements for the correct folding and stability of Clusterin as well as an indirect evidence for the existence of the 2-9 disulphide bond, but they also demonstrated alleviated chaperone activity.

Concomitant, the binding affinity to IGF-1 was markedly reduced, although the results did not fully elucidate an involvement of Clusterin's chaperone activity in the binding process of IGF-1.

The presented data shed light on the role of Clusterin in the modulation of crucial signalling pathways involving insulin and IGF-1 stimulation. Furthermore, the role of these pathways in the development and progression of Alzheimer's disease emphasises the importance of Clusterin as a potential key factor. New revelations unveiled in this work regarding the structural domains of Clusterin and their necessity for Clu functionality and stability are the basis to further elucidate the physiological role of Clusterin

7 References

Ammar, H. & Closset, J. L., 2008. Clusterin activates survival through the phosphatidylinositol 3-kinase/Akt pathway.. *The Journal of biological chemistry,* may, 283(19), pp. 12851-12861.

Andersen, C. L. et al., 2007. Clusterin expression in normal mucosa and colorectal cancer. *Molecular \& Cellular Proteomics,* Vol. 6, pp. 1039-1048.

Arch, J. R. S., 2005. Central regulation of energy balance: inputs, outputs and leptin resistance.. *The Proceedings of the Nutrition Society,* feb, 64(1), pp. 39-46.

Artavanis-Tsakonas, S., Rand, M. D. & Lake, R. J., 1999. Notch signaling: cell fate control and signal integration in development.. *Science (New York, N.Y.),* apr, 284(5415), pp. 770-776.

Asea, A. A. A. & Brown, I. R., 2008. *Heat shock proteins and the brain: implications for neurodegenerative diseases and neuroprotection.* s.l.:Springer Science & Business Media.

Atlas-White, M., Murphy, B. F. & Baker, H. W., 2000. Localisation of clusterin in normal human sperm by immunogold electron microscopy.. *Pathology,* nov, 32(4), pp. 258-261.

Avruch, J. et al., 2001. Ras activation of the Raf kinase: tyrosine kinase recruitment of the MAP kinase cascade.. *Recent progress in hormone research,* Vol. 56, pp. 127-155.

Bailey, R. W. et al., 2001. Clusterin, a binding protein with a molten globule-like region.. *Biochemistry,* oct, 40(39), pp. 11828-11840.

Bajari, T. M., Strasser, V., Nimpf, J. & Schneider, W. J., 2003. A model for modulation of leptin activity by association with clusterin.. *FASEB journal : official publication of the Federation of American Societies for Experimental Biology,* aug, 17(11), pp. 1505-1507.

Baldridge, R. D. & Rapoport, T. A., 2016. Autoubiquitination of the Hrd1 ligase triggers protein retrotranslocation in ERAD. *Cell,* Vol. 166, pp. 394-407.

Barnes, H., Larsen, B., Tyers, M. & van Der Geer, P., 2001. Tyrosine-phosphorylated low density lipoprotein receptor-related protein 1 (Lrp1) associates with the adaptor protein SHC in SRC-transformed cells.. *The Journal of biological chemistry,* jun, 276(22), pp. 19119-19125.

Barry, O. P. et al., 2001. Constitutive ERK1/2 activation in esophagogastric rib bone marrow micrometastatic cells is MEK-independent.. *The Journal of biological chemistry,* may, 276(18), pp. 15537-15546.

Bartl, M. M. et al., 2001. Multiple receptors mediate apoJ-dependent clearance of cellular debris into nonprofessional phagocytes.. *Experimental cell research,* nov, 271(1), pp. 130-141.

Bauskar, A. et al., 2015. Clusterin seals the ocular surface barrier in mouse dry eye. *PloS one,* Vol. 10, p. e0138958.

Beeg, M. et al., 2016. Clusterin Binds to Aβ1-42 Oligomers with High Affinity and Interferes with Peptide Aggregation by Inhibiting Primary and Secondary Nucleation.. *The Journal of biological chemistry,* mar, 291(13), pp. 6958-6966.

Beglova, N. & Blacklow, S. C., 2005. The LDL receptor: how acid pulls the trigger.. *Trends in biochemical sciences,* jun, 30(6), pp. 309-317.

Bell, R. D. et al., 2007. Transport pathways for clearance of human Alzheimerś amyloid β-peptide and apolipoproteins E and J in the mouse central nervous system. *Journal of Cerebral Blood Flow \& Metabolism,* Vol. 27, pp. 909-918.

Bertrand, P. et al., 1995. Association of apolipoprotein E genotype with brain levels of apolipoprotein E and apolipoprotein J (clusterin) in Alzheimer disease.. *Brain research. Molecular brain research,* oct, 33(1), pp. 174-178.

Bettens, K. et al., 2015. Reduced secreted clusterin as a mechanism for Alzheimer-associated CLU mutations. *Molecular neurodegeneration,* Vol. 10, p. 30.

Beyreuther, K. & Masters, C. L., 1991. Amyloid precursor protein (APP) and beta A4 amyloid in the etiology of Alzheimerś disease: precursor-product relationships in the derangement of neuronal function.. *Brain pathology (Zurich, Switzerland),* jul, 1(4), pp. 241-251.

Bhardwaj, G. et al., 2001. Sonic hedgehog induces the proliferation of primitive human hematopoietic cells via BMP regulation.. *Nature immunology,* feb, 2(2), pp. 172-180.

Biroccio, A. et al., 2005. Antisense clusterin oligodeoxynucleotides increase the response of HER-2 gene amplified breast cancer cells to Trastuzumab.. *Journal of cellular physiology,* aug, 204(2), pp. 463-469.

Blaschuk, O., Burdzy, K. & Fritz, I. B., 1983. Purification and characterization of a cell-aggregating factor (clusterin), the major glycoprotein in ram rete testis fluid.. *Journal of Biological Chemistry,* Vol. 258, pp. 7714-7720.

Blaschuk, O., Burdzy, K. & FRITZ, T. B., 1982. *ISOLATION OF A GLYCOPROTEIN (CLUSTERIN) FROM RAM RETE TESTIS FLUID WHICH AGGREGATES A VARIETY OF CELL-TYPES.* s.l., s.n., pp. A3--A3.

Bolós, M., Fernandez, S. & Torres-Aleman, I., 2010. Oral administration of a GSK3 inhibitor increases brain insulin-like growth factor I levels. *Journal of Biological Chemistry,* Vol. 285, pp. 17693-17700.

Bonda, D. J. et al., 2014. Dysregulation of leptin signaling in Alzheimer disease: evidence for neuronal leptin resistance.. *Journal of neurochemistry,* jan, 128(1), pp. 162-172.

Boucher, P. et al., 2002. Platelet-derived growth factor mediates tyrosine phosphorylation of the cytoplasmic domain of the low density lipoprotein receptor-related protein in caveolae. *Journal of Biological Chemistry,* Vol. 277, pp. 15507-15513.

Brown, S. D. et al., 1998. Isolation and characterization of LRP6, a novel member of the low density lipoprotein receptor gene family.. *Biochemical and biophysical research communications,* jul, 248(3), pp. 879-888.

Bu, G., Geuze, H. J., Strous, G. J. & Schwartz, A. L., 1995. 39 kDa receptor-associated protein is an ER resident protein and molecular chaperone for LDL receptor-related protein.. *The EMBO journal,* may, 14(10), pp. 2269-2280.

Bunn, R. C., King, W. D., Winkler, M. K. & Fowlkes, J. L., 2005. Early developmental changes in IGF-I, IGF-II, IGF binding protein-1, and IGF binding protein-3 concentration in the cerebrospinal fluid of children.. *Pediatric research,* jul, 58(1), pp. 89-93.

Burkey, B. F., Harmony, J. A. & others, 1991. Intracellular processing of apolipoprotein J precursor to the mature heterodimer.. *Journal of lipid research,* Vol. 32, pp. 1039-1048.

Busciglio, J., Gabuzda, D. H., Matsudaira, P. & Yankner, B. A., 1993. Generation of beta-amyloid in the secretory pathway in neuronal and nonneuronal cells.. *Proceedings of the National Academy of Sciences of the United States of America,* mar, 90(5), pp. 2092-2096.

Byun, K. et al., 2014. Clusterin/ApoJ enhances central leptin signaling through Lrp2-mediated endocytosis.. *EMBO reports,* jul, 15(7), pp. 801-808.

Caccamo, A. E. et al., 2006. Nuclear clusterin accumulation during heat shock response: Implications for cell survival and thermo-tolerance induction in immortalized and prostate cancer cells. *Journal of cellular physiology,* Vol. 207, pp. 208-219.

Cao, C. et al., 2005. Clusterin as a therapeutic target for radiation sensitization in a lung cancer model. *International Journal of Radiation Oncology* Biology* Physics,* Vol. 63, pp. 1228-1236.

Carro, E. et al., 2005. Choroid plexus megalin is involved in neuroprotection by serum insulin-like growth factor I. *Journal of Neuroscience,* Vol. 25, pp. 10884-10893.

Carro, E. et al., 2006. Blockade of the insulin-like growth factor I receptor in the choroid plexus originates Alzheimerś-like neuropathology in rodents: new cues into the human disease?. *Neurobiology of aging,* nov, 27(11), pp. 1618-1631.

Cerniglia, G. J. et al., 2015. The PI3K/Akt Pathway Regulates Oxygen Metabolism via Pyruvate Dehydrogenase (PDH)-E1α Phosphorylation.. *Molecular cancer therapeutics,* aug, 14(8), pp. 1928-1938.

Chan, A. S. L. et al., 2007. Dopaminergic and adrenergic toxicities on SK-N-MC human neuroblastoma cells are mediated through G protein signaling and oxidative stress.. *Apoptosis : an international journal on programmed cell death,* jan, 12(1), pp. 167-179.

Chang, J. Y., Märki, W. & Lai, P. H., 1999. Analysis of the extent of unfolding of denatured insulin-like growth factor.. *Protein science : a publication of the Protein Society,* jul, 8(7), pp. 1463-1468.

Chanson, P. & Salenave, S., 2008. Acromegaly.. *Orphanet journal of rare diseases,* jun, Vol. 3, p. 17.

Cheng, C. M. et al., 2005. Tau is hyperphosphorylated in the insulin-like growth factor-I null brain.. *Endocrinology,* dec, 146(12), pp. 5086-5091.

Cheng, C. Y. et al., 1988. Rat clusterin isolated from primary Sertoli cell-enriched culture medium is sulfated glycoprotein-2 (SGP-2). *Biochemical and biophysical research communications,* Vol. 155, pp. 398-404.

Chen, W. J., Goldstein, J. L. & Brown, M. S., 1990. NPXY, a sequence often found in cytoplasmic tails, is required for coated pit-mediated internalization of the low density lipoprotein receptor.. *The Journal of biological chemistry,* feb, 265(6), pp. 3116-3123.

Chi, K. N., Zoubeidi, A. & Gleave, M. E., 2008. Custirsen (OGX-011): a second-generation antisense inhibitor of clusterin for the treatment of cancer.. *Expert opinion on investigational drugs,* dec, 17(12), pp. 1955-1962.

Choi, I., Kim, J., Park, J.-Y. & Kang, S.-W., 2013. Cotransin induces accumulation of a cytotoxic clusterin variant that cotranslationally rerouted to the cytosol. *Experimental cell research,* Vol. 319, pp. 1073-1082.

Choi-Miura, N. H. et al., 1992a. SP-40,40 is a constituent of Alzheimerś amyloid.. *Acta neuropathologica,* 83(3), pp. 260-264.

Choi-Miura, N. H. et al., 1992b. Identification of the disulfide bonds in human plasma protein SP-40, 40 (apolipoprotein-J). *The Journal of Biochemistry,* Vol. 112, pp. 557-561.

Christ, A., Herzog, K. & Willnow, T. E., 2016. LRP2, an auxiliary receptor that controls sonic hedgehog signaling in development and disease. *Developmental Dynamics,* Vol. 245, pp. 569-579.

Christensen, E. I. & Birn, H., 2002. Megalin and cubilin: multifunctional endocytic receptors.. *Nature reviews. Molecular cell biology,* apr, 3(4), pp. 256-266.

Clark, A., Milbrandt, T. A., Hilt, J. Z. & Puleo, D. A., 2014. Retention of insulin-like growth factor I bioactivity during the fabrication of sintered polymeric scaffolds.. *Biomedical materials (Bristol, England),* apr, 9(2), p. 025015.

Coffey, S., Costacou, T., Orchard, T. & Erkan, E., 2015. Akt Links Insulin Signaling to Albumin Endocytosis in Proximal Tubule Epithelial Cells.. *PloS one,* 10(10), p. e0140417.

Cohen, E. et al., 2009. Reduced IGF-1 signaling delays age-associated proteotoxicity in mice.. *Cell,* dec, 139(6), pp. 1157-1169.

Cole, G. M. & Ard, M. D., 2000. Influence of lipoproteins on microglial degradation of Alzheimerś amyloid beta-protein.. *Microscopy research and technique,* aug, 50(4), pp. 316-324.

Collard, M. W. & Griswold, M. D., 1987. Biosynthesis and molecular cloning of sulfated glycoprotein 2 secreted by rat Sertoli cells. *Biochemistry,* Vol. 26, pp. 3297-3303.

Compton, L. A. & Johnson, W. C., 1986. Analysis of protein circular dichroism spectra for secondary structure using a simple matrix multiplication. *Analytical biochemistry,* Vol. 155, pp. 155-167.

Conover, C. A., Clarkson, J. T. & Bale, L. K., 1996. Factors regulating insulin-like growth factor-binding protein-3 binding, processing, and potentiation of insulin-like growth factor action.. *Endocrinology,* jun, 137(6), pp. 2286-2292.

Considine, R. V. et al., 1996. Serum immunoreactive-leptin concentrations in normal-weight and obese humans.. *The New England journal of medicine,* feb, 334(5), pp. 292-295.

Cornell, T. T. et al., 2014. Signal Transduction Pathways in Critical Illness and Injury. *Pediatric Critical Care Medicine,* jan.

Criego, A. B. et al., 2005. Brain glucose concentrations in healthy humans subjected to recurrent hypoglycemia. *Journal of neuroscience research,* Vol. 82, pp. 525-530.

Criswell, T. et al., 2005. Delayed activation of insulin-like growth factor-1 receptor/Src/MAPK/Egr-1 signaling regulates clusterin expression, a pro-survival factor.. *The Journal of biological chemistry,* apr, 280(14), pp. 14212-14221.

Culouscou, J. M. & Shoyab, M., 1991. Purification of a colon cancer cell growth inhibitor and its identification as an insulin-like growth factor binding protein.. *Cancer research,* jun, 51(11), pp. 2813-2819.

Daimon, M. et al., 2011. Association of the clusterin gene polymorphisms with type 2 diabetes mellitus.. *Metabolism: clinical and experimental,* jun, 60(6), pp. 815-822.

Dalle Pezze, P. et al., 2016. A systems study reveals concurrent activation of AMPK and mTOR by amino acids.. *Nature communications,* nov, Vol. 7, p. 13254.

Daniel, P. et al., 2014. Selective CREB-dependent cyclin expression mediated by the PI3K and MAPK pathways supports glioma cell proliferation.. *Oncogenesis,* jun, Vol. 3, p. e108.

de Juan, C., Benito, M. & Fabregat, I., 1992. Regulation of albumin expression in fetal rat hepatocytes cultured under proliferative conditions: role of epidermal growth factor and hormones.. *Journal of cellular physiology,* jul, 152(1), pp. 95-101.

de la Monte and Suzanne, M. & Wands, J. R., 2005. Review of insulin and insulin-like growth factor expression, signaling, and malfunction in the central nervous system: relevance to Alzheimerś disease.. *Journal of Alzheimer's disease : JAD,* feb, 7(1), pp. 45-61.

de Silva and H, V. et al., 1990. Purification and characterization of apolipoprotein J.. *The Journal of biological chemistry,* aug, 265(24), pp. 14292-14297.

de Silva, H. V. et al., 1990. Apolipoprotein J: structure and tissue distribution. *Biochemistry,* Vol. 29, pp. 5380-5389.

de Silva, H. V. et al., 1990. A 70-kDa apolipoprotein designated ApoJ is a marker for subclasses of human plasma high density lipoproteins.. *Journal of Biological Chemistry,* Vol. 265, pp. 13240-13247.

DeMattos, R. B. et al., 2002. Clusterin promotes amyloid plaque formation and is critical for neuritic toxicity in a mouse model of Alzheimerś disease. *Proceedings of the National Academy of Sciences,* Vol. 99, pp. 10843-10848.

Diaz-Mendoza, M. J. et al., 2014. Reelin/DAB-1 signaling in the embryonic limb regulates the chondrogenic differentiation of digit mesodermal progenitors.. *Journal of cellular physiology,* oct, 229(10), pp. 1397-1404.

Dietzsch, E. et al., 1992. Regional localization of the gene for clusterin (SP-40, 40; gene symbol CLI) to human chromosome 8p12→ p21. *Cytogenetic and Genome Research,* Vol. 61, pp. 178-179.

Diwakar, R. et al., 2008. Role played by disabled-2 in albumin induced MAP Kinase signalling. *Biochemical and biophysical research communications,* Vol. 366, pp. 675-680.

Doré, S., Kar, S. & Quirion, R., 1997. Insulin-like growth factor I protects and rescues hippocampal neurons against beta-amyloid- and human amylin-induced toxicity.. *Proceedings of the National Academy of Sciences of the United States of America,* apr, 94(9), pp. 4772-4777.

Dua, R., Zhang, J., Parry, G. & Penuel, E., 2011. Detection of hepatocyte growth factor (HGF) ligand-c-MET receptor activation in formalin-fixed paraffin embedded specimens by a novel proximity assay.. *PloS one,* jan, 6(1), p. e15932.

Duckert, P., Brunak, S. & Blom, N., 2004. Prediction of proprotein convertase cleavage sites.. *Protein engineering, design \& selection : PEDS,* jan, 17(1), pp. 107-112.

Duguid, J. R., Bohmont, C. W., Liu, N. G. & Tourtellotte, W. W., 1989. Changes in brain gene expression shared by scrapie and Alzheimer disease. *Proceedings of the National Academy of Sciences,* Vol. 86, pp. 7260-7264.

Dukic, L. et al., 2016. The role of human kallikrein 6, clusterin and adiponectin as potential blood biomarkers of dementia.. *Clinical biochemistry,* feb, 49(3), pp. 213-218.

Dummler, B. et al., 2006. Life with a single isoform of Akt: mice lacking Akt2 and Akt3 are viable but display impaired glucose homeostasis and growth deficiencies. *Molecular and cellular biology,* Vol. 26, pp. 8042-8051.

Dunker, A. K. et al., 2001. Intrinsically disordered protein.. *Journal of molecular graphics \& modelling,* 19(1), pp. 26-59.

Duron, E. et al., 2012. Insulin-like growth factor-I and insulin-like growth factor binding protein-3 in Alzheimerś disease.. *The Journal of clinical endocrinology and metabolism,* dec, 97(12), pp. 4673-4681.

Eisenhut, M., Meehan, T. & Batchelor, L., 2003. Cerebrospinal fluid glucose levels and sensorineural hearing loss in bacterial meningitis.. *Infection,* aug, 31(4), pp. 247-250.

Emonard, H. & Marbaix, E., 2015. Low-density lipoprotein receptor-related protein in metalloproteinase-mediated pathologies: recent insights. *Met. Med,* p. 9.

Fenton, H. et al., 1998. Hepatocyte growth factor (HGF/SF) in Alzheimerś disease.. *Brain research,* jan, 779(1-2), pp. 262-270.

Ferretti, M. T. et al., 2012. Intracellular Aβ-oligomers and early inflammation in a model of Alzheimerś disease. *Neurobiology of aging,* Vol. 33, pp. 1329-1342.

Fink, T. M. et al., 1993. Human clusterin (CLI) maps to 8p21 in proximity to the lipoprotein lipase (LPL) gene. *Genomics,* Vol. 16, pp. 526-528.

Fischer-Colbrie, R. et al., 1984. Isolation and immunological characterization of a glycoprotein from adrenal chromaffin granules. *Journal of neurochemistry,* Vol. 42, pp. 1008-1016.

Flati, V. et al., 2010. Essential amino acids improve insulin activation of AKT/MTOR signaling in soleus muscle of aged rats.. *International journal of immunopathology and pharmacology,* 23(1), pp. 81-89.

Fleminger, S. et al., 2003. Head injury as a risk factor for Alzheimerś disease: the evidence 10 years on; a partial replication.. *Journal of neurology, neurosurgery, and psychiatry,* jul, 74(7), pp. 857-862.

Folch, J. et al., 2012. Neuroprotective and anti-ageing role of leptin.. *Journal of molecular endocrinology,* dec, 49(3), pp. R149--R156.

Fons, R. D., Bogert, B. A. & Hegde, R. S., 2003. Substrate-specific function of the translocon-associated protein complex during translocation across the ER membrane. *J Cell Biol,* Vol. 160, pp. 529-539.

Foster, J. W., Gouveia, R. M. & Connon, C. J., 2015. Low-glucose enhances keratocyte-characteristic phenotype from corneal stromal cells in serum-free conditions.. *Scientific reports,* jun, Vol. 5, p. 10839.

Frasca, F. et al., 1999. Insulin receptor isoform A, a newly recognized, high-affinity insulin-like growth factor II receptor in fetal and cancer cells.. *Molecular and cellular biology,* may, 19(5), pp. 3278-3288.

Fritz, I. B., Burdzy, K., Sétchell, B. & Blaschuk, O., 1983. Ram rete testis fluid contains a protein (clusterin) which influences cell-cell interactions in vitro. *Biology of reproduction,* Vol. 28, pp. 1173-1188.

Fritz, I. B. & Murphy, B., 1993. Clusterin: insights into a multifunctional protein. *Trends in Endocrinology \& Metabolism,* Vol. 4, pp. 41-45.

Fukuda, T. et al., 2016. Seminal level of clusterin in infertile men as a significant biomarker reflecting spermatogenesis.. *Andrologia,* dec, 48(10), pp. 1188-1194.

Futamura, T. et al., 2002. Abnormal expression of epidermal growth factor and its receptor in the forebrain and serum of schizophrenic patients.. *Molecular psychiatry,* 7(7), pp. 673-682.

Fuzio, P. et al., 2013. Regulation of the expression of CLU isoforms in endometrial proliferative diseases. *International journal of oncology,* Vol. 42, pp. 1929-1944.

Galbaugh, T., Cerrito, M. G., Jose, C. C. & Cutler, M. L., 2006. EGF-induced activation of Akt results in mTOR-dependent p70S6 kinase phosphorylation and inhibition of HC11 cell lactogenic differentiation.. *BMC cell biology,* sep, Vol. 7, p. 34.

Gao, J., Li, J. & Ma, L., 2005. Regulation of EGF-induced ERK/MAPK Activation and EGFR Internalization by G Protein-coupled Receptor Kinase 2. *Acta biochimica et biophysica Sinica,* Vol. 37, pp. 525-531.

Gasparini, L. & Xu, H., 2003. Potential roles of insulin and IGF-1 in Alzheimerś disease.. *Trends in neurosciences,* aug, 26(8), pp. 404-406.

Geijtenbeek, T. B. et al., 2000. DC-SIGN, a dendritic cell-specific HIV-1-binding protein that enhances trans-infection of T cells.. *Cell,* mar, 100(5), pp. 587-597.

Gelissen, I. C. et al., 1998. Apolipoprotein J (clusterin) induces cholesterol export from macrophage-foam cells: a potential anti-atherogenic function?. *The Biochemical journal,* apr, Vol. 331 (Pt 1), pp. 231-237.

Ghiso, J. et al., 1993. The cerebrospinal-fluid soluble form of Alzheimerś amyloid beta is complexed to SP-40,40 (apolipoprotein J), an inhibitor of the complement membrane-attack complex.. *The Biochemical journal,* jul, Vol. 293 (Pt 1), pp. 27-30.

Gil, S. Y. et al., 2013. Clusterin and LRP2 are critical components of the hypothalamic feeding regulatory pathway.. *Nature communications,* Vol. 4, p. 1862.

Glenner, G. G. & Wong, C. W., 1984. Alzheimerś disease: initial report of the purification and characterization of a novel cerebrovascular amyloid protein.. *Biochemical and biophysical research communications,* may, 120(3), pp. 885-890.

Goate, A. et al., 1991. Segregation of a missense mutation in the amyloid precursor protein gene with familial Alzheimerś disease.. *Nature,* feb, 349(6311), pp. 704-706.

Goedert, M., Spillantini, M. G. & Crowther, R. A., 1991. Tau proteins and neurofibrillary degeneration.. *Brain pathology (Zurich, Switzerland),* jul, 1(4), pp. 279-286.

Goetz, E. M. et al., 2011. ATM-dependent IGF-1 induction regulates secretory clusterin expression after DNA damage and in genetic instability.. *Oncogene,* sep, 30(35), pp. 3745-3754.

Gómez-Villafuertes, R., García-Huerta, P., Díaz-Hernández, J. I. & Miras-Portugal, M. T., 2015. PI3K/Akt signaling pathway triggers P2X7 receptor expression as a pro-survival factor of neuroblastoma cells under limiting growth conditions.. *Scientific reports,* dec, Vol. 5, p. 18417.

Gonzalez, E. & McGraw, T. E., 2009. The Akt kinases: isoform specificity in metabolism and cancer. *Cell cycle,* Vol. 8, pp. 2502-2508.

Gotthardt, M. et al., 2000. Interactions of the low density lipoprotein receptor gene family with cytosolic adaptor and scaffold proteins suggest diverse biological functions in cellular communication and signal transduction.. *The Journal of biological chemistry,* aug, 275(33), pp. 25616-25624.

Guler, H. P., Zapf, J. & Froesch, E. R., 1987. Short-term metabolic effects of recombinant human insulin-like growth factor I in healthy adults.. *The New England journal of medicine,* jul, 317(3), pp. 137-140.

Gupta, V. B. et al., 2016. Plasma apolipoprotein J as a potential biomarker for Alzheimerś disease: Australian Imaging, Biomarkers and Lifestyle study of aging.. *Alzheimer's \& dementia (Amsterdam, Netherlands),* Vol. 3, pp. 18-26.

Gutacker, C., Klock, G., Diel, P. & Koch-Brandt, C., 1999. Nerve growth factor and epidermal growth factor stimulate clusterin gene expression in PC12 cells.. *The Biochemical journal,* may, Vol. 339 (Pt 3), pp. 759-766.

Hamada, N. et al., 2011. Loss of clusterin limits atherosclerosis in apolipoprotein E-deficient mice via reduced expression of Egr-1 and TNF-α.. *Journal of atherosclerosis and thrombosis,* 18(3), pp. 209-216.

Hamasaki, H. et al., 2014. Down-regulation of MET in hippocampal neurons of Alzheimerś disease brains.. *Neuropathology : official journal of the Japanese Society of Neuropathology,* jun, 34(3), pp. 284-290.

Hammad, S. M. et al., 1997. Interaction of apolipoprotein J-amyloid beta-peptide complex with low density lipoprotein receptor-related protein-2/megalin. A mechanism to prevent pathological accumulation of amyloid beta-peptide.. *The Journal of biological chemistry,* jul, 272(30), pp. 18644-18649.

Hanke, S. & Mann, M., 2009. The phosphotyrosine interactome of the insulin receptor family and its substrates IRS-1 and IRS-2.. *Molecular \& cellular proteomics : MCP,* mar, 8(3), pp. 519-534.

Hanson, K. D., Shichiri, M., Follansbee, M. R. & Sedivy, J. M., 1994. Effects of c-myc expression on cell cycle progression.. *Molecular and cellular biology,* sep, 14(9), pp. 5748-5755.

Han, Z. et al., 2012. Presence, localization, and origin of clusterin in normal human spermatozoa.. *Journal of assisted reproduction and genetics,* aug, 29(8), pp. 751-757.

Hardy, J. & Allsop, D., 1991. Amyloid deposition as the central event in the aetiology of Alzheimerś disease.. *Trends in pharmacological sciences,* oct, 12(10), pp. 383-388.

Harris, J. R. & Fahrenholz, F., 2006. *Alzheimerś Disease: Cellular and Molecular Aspects of Amyloid beta.* s.l.:Springer Science & Business Media.

Hartmann, K. et al., 1991. Molecular cloning of gp 80, a glycoprotein complex secreted by kidney cells in vitro and in vivo. A link to the reproductive system and to the complement cascade.. *Journal of Biological Chemistry,* Vol. 266, pp. 9924-9931.

Hatters, D. M., Wilson, M. R., Easterbrook-Smith, S. B. & Howlett, G. J., 2002. Suppression of apolipoprotein C-II amyloid formation by the extracellular chaperone, clusterin.. *European journal of biochemistry,* jun, 269(11), pp. 2789-2794.

Hay, B. et al., 1987. Biogenesis and transmembrane orientation of the cellular isoform of the scrapie prion protein [published errratum appears in Mol Cell Biol 1987 May; 7 (5): 2035]. *Molecular and cellular biology,* Vol. 7, pp. 914-920.

Heding, A. et al., 1996. Biosensor measurement of the binding of insulin-like growth factors I and II and their analogues to the insulin-like growth factor-binding protein-3.. *The Journal of biological chemistry,* jun, 271(24), pp. 13948-13952.

Hendriks, L. et al., 1992. Presenile dementia and cerebral haemorrhage linked to a mutation at codon 692 of the beta-amyloid precursor protein gene.. *Nature genetics,* jun, 1(3), pp. 218-221.

Hennige, A. M. et al., 2006. Leptin down-regulates insulin action through phosphorylation of serine-318 in insulin receptor substrate 1.. *FASEB journal : official publication of the Federation of American Societies for Experimental Biology,* jun, 20(8), pp. 1206-1208.

Herault, Y., Chatelain, G., Brun, G. & Michel, D., 1992. V-src-induced-transcription of the avian clusterin gene. *Nucleic acids research,* Vol. 20, pp. 6377-6383.

Herault, Y., Chatelain, G., Brun, G. & Michel, D., 1993. The PUR element stimulates transcription and is a target for single strand-specific binding factors conserved among vertebrate classes.. *Cellular \& molecular biology research,* Vol. 39, pp. 717-725.

Hernandez, E. R. et al., 1992. Expression of the genes encoding the insulin-like growth factors and their receptors in the human ovary.. *The Journal of clinical endocrinology and metabolism,* feb, 74(2), pp. 419-425.

Hers, I., Vincent, E. E. & Tavaré, J. M., 2011. Akt signalling in health and disease.. *Cellular signalling,* oct, 23(10), pp. 1515-1527.

Hertze, J., Nägga, K., Minthon, L. & Hansson, O., 2014. Changes in cerebrospinal fluid and blood plasma levels of IGF-II and its binding proteins in Alzheimerś disease: an observational study.. *BMC neurology,* apr, Vol. 14, p. 64.

Herz, J. et al., 1991. 39-kDa protein modulates binding of ligands to low density lipoprotein receptor-related protein/alpha 2-macroglobulin receptor.. *The Journal of biological chemistry,* nov, 266(31), pp. 21232-21238.

Herz, J. & Strickland, D. K., 2001. LRP: a multifunctional scavenger and signaling receptor.. *The Journal of clinical investigation,* sep, 108(6), pp. 779-784.

Hober, S. et al., 1992. Disulfide exchange folding of insulin-like growth factor I.. *Biochemistry,* feb, 31(6), pp. 1749-1756.

Hober, S., Hansson, A., Uhlén, M. & Nilsson, B., 1994. Folding of insulin-like growth factor I is thermodynamically controlled by insulin-like growth factor binding protein.. *Biochemistry,* jun, 33(22), pp. 6758-6761.

Hochgrebe, T. T., Humphreys, D., Wilson, M. R. & Easterbrook-Smith, S. B., 1999. A reexamination of the role of clusterin as a complement regulator.. *Experimental cell research,* may, 249(1), pp. 13-21.

Hölscher, C., 2011. Diabetes as a risk factor for Alzheimerś disease: insulin signalling impairment in the brain as an alternative model of Alzheimerś disease.. *Biochemical Society transactions,* aug, 39(4), pp. 891-897.

Hong, M. & Lee, V. M., 1997. Insulin and insulin-like growth factor-1 regulate tau phosphorylation in cultured human neurons.. *The Journal of biological chemistry,* aug, 272(31), pp. 19547-19553.

Hoofnagle, A. N. et al., 2010. Low clusterin levels in high-density lipoprotein associate with insulin resistance, obesity, and dyslipoproteinemia.. *Arteriosclerosis, thrombosis, and vascular biology,* dec, 30(12), pp. 2528-2534.

Huang, S. S. et al., 2003. Cellular growth inhibition by IGFBP-3 and TGF-beta1 requires LRP-1.. *FASEB journal : official publication of the Federation of American Societies for Experimental Biology,* nov, 17(14), pp. 2068-2081.

Humphreys, D. T., Carver, J. A., Easterbrook-Smith, S. B. & Wilson, M. R., 1999. Clusterin has chaperone-like activity similar to that of small heat shock proteins.. *The Journal of biological chemistry,* mar, 274(11), pp. 6875-6881.

Hu, X., Yang, Y. & Gong, D., 2016. Circulating insulin-like growth factor 1 and insulin-like growth factor binding protein-3 level in Alzheimerś disease: a meta-analysis.. *Neurological sciences : official journal of the Italian Neurological Society and of the Italian Society of Clinical Neurophysiology,* oct, 37(10), pp. 1671-1677.

Ibrahim, N. M. et al., 1999. Reproductive tract secretions and bull spermatozoa contain different clusterin isoforms that cluster cells and inhibit complement-induced cytolysis.. *Journal of andrology,* 20(2), pp. 230-240.

Ikonen, M. et al., 2003. Interaction between the Alzheimerś survival peptide humanin and insulin-like growth factor-binding protein 3 regulates cell survival and apoptosis.. *Proceedings of the National Academy of Sciences of the United States of America,* oct, 100(22), pp. 13042-13047.

Iliff, J. J. et al., 2012. A paravascular pathway facilitates CSF flow through the brain parenchyma and the clearance of interstitial solutes, including amyloid β.. *Science translational medicine,* aug, 4(147), p. 147ra111.

Jacobsen, L. et al., 1996. Molecular characterization of a novel human hybrid-type receptor that binds the alpha2-macroglobulin receptor-associated protein.. *The Journal of biological chemistry,* dec, 271(49), pp. 31379-31383.

Jenne, D. E. & Tschopp, J., 1989. Molecular structure and functional characterization of a human complement cytolysis inhibitor found in blood and seminal plasma: identity to sulfated glycoprotein 2, a constituent of rat testis fluid. *Proceedings of the National Academy of Sciences,* Vol. 86, pp. 7123-7127.

Jenne, D. E. & Tschopp, J., 1992. Clusterin: the intriguing guises of a widely expressed glycoprotein. *Trends in biochemical sciences,* Vol. 17, pp. 154-159.

Jiang, L. et al., 2014. Constitutive activation of the ERK pathway in melanoma and skin melanocytes in Grey horses.. *BMC cancer,* nov, Vol. 14, p. 857.

Jo, H. et al., 2008. Cancer cell-derived clusterin modulates the phosphatidylinositol 3′-kinase-Akt pathway through attenuation of insulin-like growth factor 1 during serum deprivation.. *Molecular and cellular biology,* jul, 28(13), pp. 4285-4299.

Jones, J. I. & Clemmons, D. R., 1995. Insulin-like growth factors and their binding proteins: biological actions.. *Endocrine reviews,* feb, 16(1), pp. 3-34.

Jones, S. E. & Jomary, C., 2002. Clusterin. *The international journal of biochemistry \& cell biology,* Vol. 34, pp. 427-431.

Jones, S. E., Meerabux, J. M. A., Yeats, D. A. & Neal, M. J., 1992. Analysis of differentially expressed genes in retinitis pigmentosa retinas altered expression of clusterin mRNA. *FEBS letters,* Vol. 300, pp. 279-282.

Jun, H.-O.et al., 2011. Clusterin protects H9c2 cardiomyocytes from oxidative stress-induced apoptosis via Akt/GSK-3β signaling pathway.. *Experimental \& molecular medicine,* jan, 43(1), pp. 53-61.

Kamarehei, M., Yazdanparast, R. & Aghazadeh, S., 2014. Curcumin Protects SK-N-MC Cells from H2O2-Induced Cell Death by Modulation of Notch Signaling Pathway. *CellBio,* Vol. 3, p. 72.

Kang, B.-H.et al., 2014. Clusterin stimulates the chemotactic migration of macrophages through a pertussis toxin sensitive G-protein-coupled receptor and Gβγ-dependent pathways.. *Biochemical and biophysical research communications,* mar, 445(3), pp. 645-650.

Kang, S. S. et al., 2016. Identification of plexin A4 as a novel clusterin receptor links two Alzheimerś disease risk genes.. *Human molecular genetics,* aug, 25(16), pp. 3467-3475.

Kapron, J. T. et al., 1997. Identification and characterization of glycosylation sites in human serum clusterin. *Protein Science,* Vol. 6, pp. 2120-2133.

Kaya-Dagistanli, F. & Ozturk, M., 2013. The role of clusterin on pancreatic beta cell regeneration after exendin-4 treatment in neonatal streptozotocin administrated rats.. *Acta histochemica,* jul, 115(6), pp. 577-586.

Kim, B. M. et al., 2001. Clusterin expression during regeneration of pancreatic islet cells in streptozotocin-induced diabetic rats.. *Diabetologia,* dec, 44(12), pp. 2192-2202.

Kim, B. M. et al., 2006. Clusterin induces differentiation of pancreatic duct cells into insulin-secreting cells.. *Diabetologia,* feb, 49(2), pp. 311-320.

Kim, D. H. et al., 1998. A new low density lipoprotein receptor related protein, LRP5, is expressed in hepatocytes and adrenal cortex, and recognizes apolipoprotein E.. *Journal of biochemistry,* dec, 124(6), pp. 1072-1076.

Kim, G. et al., 2011. SREBP-1c regulates glucose-stimulated hepatic clusterin expression. *Biochemical and biophysical research communications,* Vol. 408, pp. 720-725.

Kim, H.-J.et al., 2009. Protective role of clusterin/apolipoprotein J against neointimal hyperplasia via antiproliferative effect on vascular smooth muscle cells and cytoprotective effect on endothelial cells.. *Arteriosclerosis, thrombosis, and vascular biology,* oct, 29(10), pp. 1558-1564.

Kim, J. H. et al., 2010. Protective effect of clusterin from oxidative stress-induced apoptosis in human retinal pigment epithelial cells.. *Investigative ophthalmology \& visual science,* jan, 51(1), pp. 561-566.

Kim, N. et al., 2012b. Nuclear clusterin is associated with neuronal apoptosis in the developing rat brain upon ethanol exposure. *Alcoholism: Clinical and Experimental Research,* Vol. 36, pp. 72-82.

Kim, N. et al., 2012a. Human nuclear clusterin mediates apoptosis by interacting with Bcl-XL through C-terminal coiled coil domain. *Journal of cellular physiology,* Vol. 227, pp. 1157-1167.

Kirszbaum, L., Bozas, S. E. & Walker, I. D., 1992. SP-40, 40, a protein involved in the control of the complement pathway, possesses a unique array of disulphide bridges. *FEBS letters,* Vol. 297, pp. 70-76.

Kirszbaum, L. et al., 1989. Molecular cloning and characterization of the novel, human complement-associated protein, SP-40, 40: a link between the complement and reproductive systems.. *The EMBO journal,* Vol. 8, p. 711.

Kivipelto, M. & Solomon, A., 2006. Cholesterol as a risk factor for Alzheimerś disease - epidemiological evidence.. *Acta neurologica Scandinavica. Supplementum,* Vol. 185, pp. 50-57.

Korenberg, J. R. et al., 1994. Chromosomal localization of human genes for the LDL receptor family member glycoprotein 330 (LRP2) and its associated protein RAP (LRPAP1). *Genomics,* Vol. 22, pp. 88-93.

Kosaki, A., Pillay, T. S., Xu, L. & Webster, N. J. G., 1995. The B isoform of the insulin receptor signals more efficiently than the A isoform in HepG2 cells. *Journal of Biological Chemistry,* Vol. 270, pp. 20816-20823.

Kounnas, M. Z. et al., 1995. Identification of glycoprotein 330 as an endocytic receptor for apolipoprotein J/clusterin. *Journal of Biological Chemistry,* Vol. 270, pp. 13070-13075.

Kozak, M., 2002. Pushing the limits of the scanning mechanism for initiation of translation. *Gene,* Vol. 299, pp. 1-34.

Krook, A. et al., 1996. Functional activation of mutant human insulin receptor by monoclonal antibody.. *Lancet (London, England),* jun, 347(9015), pp. 1586-1590.

Kwon, M. J. et al., 2014. Deficiency of clusterin exacerbates high-fat diet-induced insulin resistance in male mice.. *Endocrinology,* jun, 155(6), pp. 2089-2101.

Lakins, J. N. et al., 2002. Evidence that clusterin has discrete chaperone and ligand binding sites. *Biochemistry,* Vol. 41, pp. 282-291.

Lambert, J. C. et al., 2013. Meta-analysis of 74,046 individuals identifies 11 new susceptibility loci for Alzheimerś disease.. *Nature genetics,* dec, 45(12), pp. 1452-1458.

Lambert, M. P. et al., 1998. Diffusible, nonfibrillar ligands derived from Abeta1-42 are potent central nervous system neurotoxins.. *Proceedings of the National Academy of Sciences of the United States of America,* may, 95(11), pp. 6448-6453.

Lamoureux, F. et al., 2014. Clusterin inhibition using OGX-011 synergistically enhances zoledronic acid activity in osteosarcoma.. *Oncotarget,* sep, 5(17), pp. 7805-7819.

Lane-Donovan, C. & Herz, J., 2017. ApoE, ApoE Receptors, and the Synapse in Alzheimerś Disease. *Trends in Endocrinology \& Metabolism.*

Laping, N. J. et al., 1998. The age-related increase in renal clusterin mRNA is accelerated in obese Zucker rats.. *Journal of the American Society of Nephrology,* Vol. 9, pp. 38-45.

Laron, Z., 2001. Insulin-like growth factor 1 (IGF-1): a growth hormone.. *Molecular pathology : MP,* oct, 54(5), pp. 311-316.

Laskin, J. J. et al., 2012. Phase I/II trial of custirsen (OGX-011), an inhibitor of clusterin, in combination with a gemcitabine and platinum regimen in patients with previously untreated advanced non-small cell lung cancer.. *Journal of thoracic oncology : official publication of the International Association for the Study of Lung Cancer,* mar, 7(3), pp. 579-586.

Leeb, C., Eresheim, C. & Nimpf, J., 2014. Clusterin is a ligand for apolipoprotein E receptor 2 (ApoER2) and very low density lipoprotein receptor (VLDLR) and signals via the Reelin-signaling pathway.. *The Journal of biological chemistry,* feb, 289(7), pp. 4161-4172.

Lee, S. et al., 2011. Essential role of clusterin in pancreas regeneration.. *Developmental dynamics : an official publication of the American Association of Anatomists,* mar, 240(3), pp. 605-615.

Lee, Y.-N.et al., 2012. Over-expression of human clusterin increases stress resistance and extends lifespan in Drosophila melanogaster. *Biochemical and biophysical research communications,* Vol. 420, pp. 851-856.

Lékó, A. H. et al., 2017. Insulin-like growth factor I and its binding protein-3 are regulators of lactation and maternal responsiveness.. *Scientific reports,* jun, 7(1), p. 3396.

Leskov, K. S. et al., 2011. CRM1 protein-mediated regulation of nuclear clusterin (nCLU), an ionizing radiation-stimulated, Bax-dependent pro-death factor. *Journal of Biological Chemistry,* Vol. 286, pp. 40083-40090.

Leskov, K. S. et al., 2001. *When X-ray-inducible proteins meet DNA double strand break repair.* s.l., s.n., pp. 352-372.

Leskov, K. S. et al., 2003. Synthesis and functional analyses of nuclear clusterin, a cell death protein.. *The Journal of biological chemistry,* mar, 278(13), pp. 11590-11600.

Liang, H.-C.et al., 2015. Glycosylation of Human Plasma Clusterin Yields a Novel Candidate Biomarker of Alzheimerś Disease.. *Journal of proteome research,* dec, 14(12), pp. 5063-5076.

Lieb, W. et al., 2009. Association of plasma leptin levels with incident Alzheimer disease and MRI measures of brain aging.. *JAMA,* dec, 302(23), pp. 2565-2572.

Lillioja, S. et al., 1993. Insulin resistance and insulin secretory dysfunction as precursors of non-insulin-dependent diabetes mellitus. Prospective studies of Pima Indians.. *The New England journal of medicine,* dec, 329(27), pp. 1988-1992.

Li, N., Zoubeidi, A., Beraldi, E. & Gleave, M. E., 2013. GRP78 regulates clusterin stability, retrotranslocation and mitochondrial localization under ER stress in prostate cancer.. *Oncogene,* apr, 32(15), pp. 1933-1942.

Liu, B. et al., 2000. Direct functional interactions between insulin-like growth factor-binding protein-3 and retinoid X receptor-α regulate transcriptional signaling and apoptosis. *Journal of Biological Chemistry,* Vol. 275, pp. 33607-33613.

Liu, C.-C.et al., 2015. Neuronal LRP1 regulates glucose metabolism and insulin signaling in the brain. *Journal of Neuroscience,* Vol. 35, pp. 5851-5859.

Li, Y. & Bu, G., 2005. LRP5/6 in Wnt signaling and tumorigenesis. *Future Oncology,* Vol. 1, pp. 673-681.

Llorens, F. et al., 2013. PrP(C) regulates epidermal growth factor receptor function and cell shape dynamics in Neuro2a cells.. *Journal of neurochemistry,* oct, 127(1), pp. 124-138.

Lodish, H., 2008. *Molecular Cell Biology.* s.l.:W. H. Freeman.

Longobardi, L. et al., 2003. A novel insulin-like growth factor (IGF)-independent role for IGF binding protein-3 in mesenchymal chondroprogenitor cell apoptosis.. *Endocrinology,* may, 144(5), pp. 1695-1702.

Losch, A. & Koch-Brandt, C., 1995. Dithiothreitol treatment of Madin-Darby canine kidney cells reversibly blocks export from the endoplasmic reticulum but does not affect vectorial targeting of secretory proteins. *Journal of Biological Chemistry,* Vol. 270, pp. 11543-11548.

Luo, X. et al., 2014. ATM regulates insulin-like growth factor 1-secretory clusterin (IGF-1-sCLU) expression that protects cells against senescence.. *PloS one,* 9(6), p. e99983.

Macejak, D. G. & Sarnow, P., 1991. Internal initiation of translation mediated by the 5Íeader of a cellular mRNA. *Nature,* Vol. 353, p. 90.

Maioli, S. et al., 2015. Alterations in brain leptin signalling in spite of unchanged CSF leptin levels in Alzheimerś disease.. *Aging cell,* feb, 14(1), pp. 122-129.

Manavalan, P. & Johnson, W. C., 1987. Variable selection method improves the prediction of protein secondary structure from circular dichroism spectra. *Analytical biochemistry,* Vol. 167, pp. 76-85.

Martin, J. L., Lin, M. Z., McGowan, E. M. & Baxter, R. C., 2009. Potentiation of growth factor signaling by insulin-like growth factor-binding protein-3 in breast epithelial cells requires sphingosine kinase activity.. *The Journal of biological chemistry,* sep, 284(38), pp. 25542-25552.

Massague, J., Pilch, P. F. & Czech, M. P., 1980. Electrophoretic resolution of three major insulin receptor structures with unique subunit stoichiometries.. *Proceedings of the National Academy of Sciences of the United States of America,* dec, 77(12), pp. 7137-7141.

Matsubara, E., Frangione, B. & Ghiso, J., 1995. Characterization of apolipoprotein J-Alzheimerś A beta interaction.. *The Journal of biological chemistry,* mar, 270(13), pp. 7563-7567.

Matsubara, E. et al., 1996. Apolipoprotein J and Alzheimerś amyloid beta solubility.. *The Biochemical journal,* jun, Vol. 316 (Pt 2), pp. 671-679.

Matukumalli, S. R., Tangirala, R. & Rao, C. M., 2017. Clusterin: full-length protein and one of its chains show opposing effects on cellular lipid accumulation. *Scientific reports,* Vol. 7, p. 41235.

Mawuenyega, K. G. et al., 2010. Decreased clearance of CNS beta-amyloid in Alzheimerś disease.. *Science (New York, N.Y.),* dec, 330(6012), p. 1774.

Ma, X. & Bai, Y., 2012. IGF-1 activates the P13K/AKT signaling pathway via upregulation of secretory clusterin.. *Molecular medicine reports,* dec, 6(6), pp. 1433-1437.

May, P. C. & Finch, C. E., 1992. Sulfated glycoprotein 2: new relationships of this multifunctional protein to neurodegeneration. *Trends in neurosciences,* Vol. 15, pp. 391-396.

May, P. C. et al., 1990. Dynamics of gene expression for a hippocampal glycoprotein elevated in Alzheimerś disease and in response to experimental lesions in rat.. *Neuron,* dec, 5(6), pp. 831-839.

May, P., Herz, J. & Bock, H. H., 2005. Molecular mechanisms of lipoprotein receptor signalling. *Cellular and Molecular Life Sciences CMLS,* Vol. 62, pp. 2325-2338.

Mazzoni, I. E. & Kenigsberg, R. L., 1992. Effects of epidermal growth factor in the mammalian central nervous system: its possible implications in brain pathologies and therapeutic applications. *Drug development research,* Vol. 26, pp. 111-128.

Merlotti, A. et al., 2015. Fucosylated clusterin in semen promotes the uptake of stress-damaged proteins by dendritic cells via DC-SIGN.. *Human reproduction (Oxford, England),* jul, 30(7), pp. 1545-1556.

Michel, D., Chatelain, G., North, S. & Gilbert, B., 1997. Stress-induced transcription of the clusterin/apoJ gene. *Biochemical Journal,* Vol. 328, pp. 45-50.

Miller, J. A. et al., 1993. Oxidative refolding of insulin-like growth factor 1 yields two products of similar thermodynamic stability: a bifurcating protein-folding pathway.. *Biochemistry,* may, 32(19), pp. 5203-5213.

Millis, A. J. et al., 2001. Clusterin regulates vascular smooth muscle cell nodule formation and migration.. *Journal of cellular physiology,* feb, 186(2), pp. 210-219.

Min, B. H. et al., 1998. Transient expression of clusterin (sulfated glycoprotein-2) during development of rat pancreas.. *The Journal of endocrinology,* jul, 158(1), pp. 43-52.

Miners, J. S., Clarke, P. & Love, S., 2017. Clusterin levels are increased in Alzheimerś disease and influence the regional distribution of Aβ.. *Brain pathology (Zurich, Switzerland),* may, 27(3), pp. 305-313.

Mireuta, M., Birman, E., Barmash, M. & Pollak, M., 2014. Quantification of binding of IGF-1 to BI 836845, a candidate therapeutic antibody against IGF-1 and IGF-2, and effects of this antibody on IGF-1:IGFBP-3 complexes in vitro and in male C57BL/6 mice.. *Endocrinology,* mar, 155(3), pp. 703-715.

Miyake, H., Chi, K. N. & Gleave, M. E., 2000. Antisense TRPM-2 oligodeoxynucleotides chemosensitize human androgen-independent PC-3 prostate cancer cells both in vitro and in vivo.. *Clinical cancer research : an official journal of the American Association for Cancer Research,* may, 6(5), pp. 1655-1663.

Miyata, M. et al., 2001. Apolipoprotein J/clusterin is induced in vascular smooth muscle cells after vascular injury.. *Circulation,* sep, 104(12), pp. 1407-1412.

Moestrup, S. K. & Verroust, P. J., 2001. Megalin- and cubilin-mediated endocytosis of protein-bound vitamins, lipids, and hormones in polarized epithelia.. *Annual review of nutrition,* Vol. 21, pp. 407-428.

Mogi, M., Walsh, K., Iwai, M. & Horiuchi, M., 2008. Akt-FOXO3a signaling affects human endothelial progenitor cell differentiation.. *Hypertension research : official journal of the Japanese Society of Hypertension,* jan, 31(1), pp. 153-159.

Mohan, S., Bautista, C. M., Wergedal, J. & Baylink, D. J., 1989. Isolation of an inhibitory insulin-like growth factor (IGF) binding protein from bone cell-conditioned medium: a potential local regulator of IGF action.. *Proceedings of the National Academy of Sciences of the United States of America,* nov, 86(21), pp. 8338-8342.

Mohler, J., 1988. Requirements for hedgehog, a segmental polarity gene, in patterning larval and adult cuticle of Drosophila.. *Genetics,* dec, 120(4), pp. 1061-1072.

Morales, C. R. et al., 1996. Low density lipoprotein receptor-related protein-2 expression in efferent duct and epididymal epithelia: evidence in rats for its in vivo role in endocytosis of apolipoprotein J/clusterin.. *Biology of reproduction,* sep, 55(3), pp. 676-683.

Mosthaf, L. et al., 1990. Functionally distinct insulin receptors generated by tissue-specific alternative splicing.. *The EMBO journal,* aug, 9(8), pp. 2409-2413.

Murphy, B. F., Kirszbaum, L., Walker, I. D. & dÁpice, A. J., 1988. SP-40, 40, a newly identified normal human serum protein found in the SC5b-9 complex of complement and in the immune deposits in glomerulonephritis.. *Journal of Clinical Investigation,* Vol. 81, p. 1858.

Nagai, J., Sato, K., Yumoto, R. & Takano, M., 2011. Megalin/cubilin-mediated uptake of FITC-labeled IgG by OK kidney epithelial cells.. *Drug metabolism and pharmacokinetics,* 26(5), pp. 474-485.

Nakayama, K., 1997. Furin: a mammalian subtilisin/Kex2p-like endoprotease involved in processing of a wide variety of precursor proteins.. *The Biochemical journal,* nov, Vol. 327 (Pt 3), pp. 625-635.

Narayan, P. et al., 2011. The extracellular chaperone clusterin sequesters oligomeric forms of the amyloid-β(1-40) peptide.. *Nature structural \& molecular biology,* dec, 19(1), pp. 79-83.

Narhi, L. O. et al., 1993. Role of native disulfide bonds in the structure and activity of insulin-like growth factor 1: genetic models of protein-folding intermediates.. *Biochemistry,* may, 32(19), pp. 5214-5221.

Navab, M. et al., 2005. An oral apoJ peptide renders HDL antiinflammatory in mice and monkeys and dramatically reduces atherosclerosis in apolipoprotein E-null mice.. *Arteriosclerosis, thrombosis, and vascular biology,* sep, 25(9), pp. 1932-1937.

Neely, A. N., Nelson, P. B. & Mortimore, G. E., 1974. Osmotic alterations of the lysosomal system during rat liver perfusion: reversible suppression by insulin and amino acids. *Biochimica et Biophysica Acta (BBA)-General Subjects,* Vol. 338, pp. 458-472.

Niikura, T. et al., 2001. Insulin-like growth factor I (IGF-I) protects cells from apoptosis by Alzheimerś V642I mutant amyloid precursor protein through IGF-I receptor in an IGF-binding protein-sensitive manner. *Journal of Neuroscience,* Vol. 21, pp. 1902-1910.

Nishikawa, M., Miyake, H., Gleave, M. & Fujisawa, M., 2017. Effect of Targeting Clusterin Using OGX-011 on Antitumor Activity of Temsirolimus in a Human Renal Cell Carcinoma Model. *Targeted Oncology,* feb, Vol. 12, p. 69.

Nizard, P. et al., 2007. Stress-Induced Retrotranslocation of Clusterin/ApoJ into the Cytosol. *Traffic,* Vol. 8, pp. 554-565.

Novak, S. et al., 2010. Biomarkers of in vivo fertility in sperm and seminal plasma of fertile stallions.. *Theriogenology,* oct, 74(6), pp. 956-967.

Nüsslein-Volhard, C. & Wieschaus, E., 1980. Mutations affecting segment number and polarity in Drosophila.. *Nature,* oct, 287(5785), pp. 795-801.

Nuutinen, T. et al., 2007. Amyloid-beta 1-42 induced endocytosis and clusterin/apoJ protein accumulation in cultured human astrocytes.. *Neurochemistry international,* feb, 50(3), pp. 540-547.

Nuutinen, T. et al., 2005. Induction of clusterin/apoJ expression by histone deacetylase inhibitors in neural cells. *Neurochemistry international,* Vol. 47, pp. 528-538.

Nykjaer, A. et al., 1992. Purified alpha 2-macroglobulin receptor/LDL receptor-related protein binds urokinase.plasminogen activator inhibitor type-1 complex. Evidence that the alpha 2-macroglobulin receptor mediates cellular degradation of urokinase receptor-bound complexes.. *The Journal of biological chemistry,* jul, 267(21), pp. 14543-14546.

O'Bryan, M. K. et al., 1990. Human seminal clusterin (SP-40,40). Isolation and characterization.. *The Journal of clinical investigation,* may, 85(5), pp. 1477-1486.

O'Bryan, M. K. et al., 1994. The use of anticlusterin monoclonal antibodies for the combined assesment of human sperm morphology and acrosome integrity. *Human reproduction,* Vol. 9, pp. 1490-1496.

Oda, T. et al., 1995. Clusterin (apoJ) alters the aggregation of amyloid beta-peptide (A beta 1-42) and forms slowly sedimenting A beta complexes that cause oxidative stress.. *Experimental neurology,* nov, 136(1), pp. 22-31.

Oh, G.-S.et al., 2015. The E-box-like sterol regulatory element mediates the insulin-stimulated expression of hepatic clusterin. *Biochemical and biophysical research communications,* Vol. 465, pp. 501-506.

Oh, Y. et al., 1996. Synthesis and characterization of insulin-like growth factor-binding protein (IGFBP)-7. Recombinant human mac25 protein specifically binds IGF-I and -II.. *The Journal of biological chemistry,* nov, 271(48), pp. 30322-30325.

O'Kusky, J. & Ye, P., 2012. Neurodevelopmental effects of insulin-like growth factor signaling.. *Frontiers in neuroendocrinology,* aug, 33(3), pp. 230-251.

Oleinikov, A. V., Zhao, J. & Makker, S. P., 2000. Cytosolic adaptor protein Dab2 is an intracellular ligand of endocytic receptor gp600/megalin.. *The Biochemical journal,* may, Vol. 347 Pt 3, pp. 613-621.

O'Neill, C. et al., 2012. Insulin and IGF-1 signalling: longevity, protein homoeostasis and Alzheimerś disease.. *Biochemical Society transactions,* aug, 40(4), pp. 721-727.

Organ, S. L. & Tsao, M.-S., 2011. An overview of the c-MET signaling pathway.. *Therapeutic advances in medical oncology,* nov, 3(1 Suppl), pp. S7--S19.

Orlando, R. A. et al., 1998. Megalin is an endocytic receptor for insulin.. *Journal of the American Society of Nephrology,* Vol. 9, pp. 1759-1766.

Pandini, G. et al., 2002. Insulin/insulin-like growth factor I hybrid receptors have different biological characteristics depending on the insulin receptor isoform involved.. *The Journal of biological chemistry,* oct, 277(42), pp. 39684-39695.

Pende, M. et al., 2004. S6K1(-/-)/S6K2(-/-) mice exhibit perinatal lethality and rapamycin-sensitive 5′-terminal oligopyrimidine mRNA translation and reveal a mitogen-activated protein kinase-dependent S6 kinase pathway.. *Molecular and cellular biology,* apr, 24(8), pp. 3112-3124.

Pilon, M., Schekman, R. & Römisch, K., 1997. Sec61p mediates export of a misfolded secretory protein from the endoplasmic reticulum to the cytosol for degradation. *The EMBO journal,* Vol. 16, pp. 4540-4548.

Pollak, M., 2008. Insulin, insulin-like growth factors and neoplasia.. *Best practice \& research. Clinical endocrinology \& metabolism,* aug, 22(4), pp. 625-638.

Polvikoski, T. et al., 1995. Apolipoprotein E, dementia, and cortical deposition of beta-amyloid protein.. *The New England journal of medicine,* nov, 333(19), pp. 1242-1247.

Poon, S. et al., 2000. Clusterin is an ATP-independent chaperone with very broad substrate specificity that stabilizes stressed proteins in a folding-competent state.. *Biochemistry,* dec, 39(51), pp. 15953-15960.

Poon, S. et al., 2002. Clusterin is an extracellular chaperone that specifically interacts with slowly aggregating proteins on their off-folding pathway.. *FEBS letters,* feb, 513(2-3), pp. 259-266.

Prochnow, H. et al., 2013. Non-secreted clusterin isoforms are translated in rare amounts from distinct human mRNA variants and do not affect Bax-mediated apoptosis or the NF-κB signaling pathway. *PLoS One,* Vol. 8, p. e75303.

Purrello, M. et al., 1991. The gene for SP-40, 40, human homolog of rat sulfated glycoprotein 2, rat clusterin, and rat testosterone-repressed prostate message 2, maps to chromosome 8. *Genomics,* Vol. 10, pp. 151-156.

Qian, Y. et al., 2004. PI3K induced actin filament remodeling through Akt and p70S6K1: implication of essential role in cell migration.. *American journal of physiology. Cell physiology,* jan, 286(1), pp. C153--C163.

Ramakrishnan, G. et al., 2012. The association between insulin and low-density lipoprotein receptors. *Diabetes and Vascular Disease Research,* Vol. 9, pp. 196-204.

Reddy, K. B. et al., 1996. Transforming growth factor β (TGFβ)-induced nuclear localization of apolipoprotein J/clusterin in epithelial cells. *Biochemistry,* Vol. 35, pp. 6157-6163.

Refolo, L. M. et al., 1989. Nerve and epidermal growth factors induce the release of the Alzheimer amyloid precursor from PC 12 cell cultures.. *Biochemical and biophysical research communications,* oct, 164(2), pp. 664-670.

Reich, H. et al., 2005. Albumin activates ERK via EGF receptor in human renal epithelial cells.. *Journal of the American Society of Nephrology : JASN,* may, 16(5), pp. 1266-1278.

Rensing, L., 1972. Periodic geophysical and biological signals as Zeitgeber and exogenous inducers in animal organisms.. *International journal of biometeorology,* Vol. 16 Suppl, pp. 113-125.

Revuelta-López, E. et al., 2015. Hypoxia-driven sarcoplasmic/endoplasmic reticulum calcium ATPase 2 (SERCA2) downregulation depends on low-density lipoprotein receptor-related protein 1 (LRP1)-signalling in cardiomyocytes. *Journal of molecular and cellular cardiology,* Vol. 85, pp. 25-36.

Riaz, M. A., Stammler, A., Borgers, M. & Konrad, L., 2017. Clusterin signals via ApoER2/VLDLR and induces meiosis of male germ cells.. *American journal of translational research,* 9(3), pp. 1266-1276.

Rinderknecht, E. & Humbel, R. E., 1978. The amino acid sequence of human insulin-like growth factor I and its structural homology with proinsulin.. *The Journal of biological chemistry,* apr, 253(8), pp. 2769-2776.

Rizzi, F. & Bettuzzi, S., 2009. Clusterin (CLU) and prostate cancer.. *Advances in cancer research,* Vol. 105, pp. 1-19.

Rohne, P. et al., 2014. The chaperone activity of clusterin is dependent on glycosylation and redox environment.. *Cellular physiology and biochemistry : international journal of experimental cellular physiology, biochemistry, and pharmacology,* 34(5), pp. 1626-1639.

Roos, K., 2005. *Principles of Neurologic Infectious Diseases.* s.l.:McGraw-Hill Education.

Rosemblit, N. & Chen, C. L. C., 1994. Regulators for the rat clusterin gene: DNA methylation and cis-acting regulatory elements. *Journal of molecular endocrinology,* Vol. 13, pp. 69-76.

Rosemblit, N., Feng, Z. M. & Chen, C. L. C., 1996. Analysis of the rat clusterin gene promoter and cyclic AMP-regulated mRNA stability in testicular cells. *Journal of molecular endocrinology,* Vol. 16, pp. 287-296.

Russell, D. W., Brown, M. S. & Goldstein, J. L., 1989. Different combinations of cysteine-rich repeats mediate binding of low density lipoprotein receptor to two different proteins.. *The Journal of biological chemistry,* dec, 264(36), pp. 21682-21688.

Sabatte, J. et al., 2011. Semen clusterin is a novel DC-SIGN ligand. *The Journal of Immunology,* Vol. 187, pp. 5299-5309.

Sachdev, D., 2008. Regulation of breast cancer metastasis by IGF signaling.. *Journal of mammary gland biology and neoplasia,* dec, 13(4), pp. 431-441.

Salero, E., Giménez, C. & Zafra, F., 2003. Identification of a non-canonical E-box motif as a regulatory element in the proximal promoter region of the apolipoprotein E gene. *Biochemical Journal,* Vol. 370, pp. 979-986.

Salminen, A. et al., 2009. Inflammation in Alzheimerś disease: amyloid-beta oligomers trigger innate immunity defence via pattern recognition receptors.. *Progress in neurobiology,* feb, 87(3), pp. 181-194.

Samuel, V. T., Petersen, K. F. & Shulman, G. I., 2010. Lipid-induced insulin resistance: unravelling the mechanism.. *Lancet (London, England),* jun, 375(9733), pp. 2267-2277.

Sanger, F. & Thompson, E. O. P., 1953a. The amino-acid sequence in the glycyl chain of insulin. I. The identification of lower peptides from partial hydrolysates.. *The Biochemical journal,* feb, 53(3), pp. 353-366.

Sanger, F. & Thompson, E. O. P., 1953b. The amino-acid sequence in the glycyl chain of insulin. II. The investigation of peptides from enzymic hydrolysates.. *The Biochemical journal,* feb, 53(3), pp. 366-374.

Sanger, F. & Tuppy, H., 1951a. The amino-acid sequence in the phenylalanyl chain of insulin. I. The identification of lower peptides from partial hydrolysates.. *The Biochemical journal,* sep, 49(4), pp. 463-481.

Sanger, F. & Tuppy, H., 1951b. The amino-acid sequence in the phenylalanyl chain of insulin. II. The investigation of peptides from enzymic hydrolysates.. *The Biochemical journal,* sep, 49(4), pp. 481-490.

Santilli, G., Aronow, B. J. & Sala, A., 2003. Essential requirement of apolipoprotein J (clusterin) signaling for IkappaB expression and regulation of NF-kappaB activity.. *The Journal of biological chemistry,* oct, 278(40), pp. 38214-38219.

Sartorius, T. et al., 2012. Leptin affects insulin action in astrocytes and impairs insulin-mediated physical activity.. *Cellular physiology and biochemistry : international journal of experimental cellular physiology, biochemistry, and pharmacology,* 30(1), pp. 238-246.

Scheuner, D. et al., 1996. Secreted amyloid beta-protein similar to that in the senile plaques of Alzheimerś disease is increased in vivo by the presenilin 1 and 2 and APP mutations linked to familial Alzheimerś disease.. *Nature medicine,* aug, 2(8), pp. 864-870.

Schofield, P. N., 1992. *The insulin-like growth factors: structure and biological functions.* s.l.:Oxford University Press, USA.

Schwarz, M. et al., 2008. Potential protective role of apoprotein J (clusterin) in atherogenesis: binding to enzymatically modified low-density lipoprotein reduces fatty acid-mediated cytotoxicity.. *Thrombosis and haemostasis,* jul, 100(1), pp. 110-118.

Schweiger, M., Steffl, M. & Amselgruber, W. M., 2007. Clusterin expression in porcine endocrine cells during islet development.. *Hormone and metabolic research = Hormon- und Stoffwechselforschung = Hormones et metabolisme,* dec, 39(12), pp. 862-866.

Sedaghat, A. R., Sherman, A. & Quon, M. J., 2002. A mathematical model of metabolic insulin signaling pathways.. *American journal of physiology. Endocrinology and metabolism,* nov, 283(5), pp. E1084--E1101.

Seino, S., Seino, M., Nishi, S. & Bell, G. I., 1989. Structure of the human insulin receptor gene and characterization of its promoter.. *Proceedings of the National Academy of Sciences of the United States of America,* jan, 86(1), pp. 114-118.

Selkoe, D. J., 1991. The molecular pathology of Alzheimerś disease.. *Neuron,* apr, 6(4), pp. 487-498.

Sharaf, A. et al., 2013. ApoER2 and VLDLr are required for mediating reelin signalling pathway for normal migration and positioning of mesencephalic dopaminergic neurons. *PloS one,* Vol. 8, p. e71091.

Sharma, S., 2010. Hepatocyte growth factor in synaptic plasticity and Alzheimerś disease.. *TheScientificWorldJournal,* mar, Vol. 10, pp. 457-461.

Shibata, M. et al., 2000. Clearance of Alzheimerś amyloid-ss(1-40) peptide from brain by LDL receptor-related protein-1 at the blood-brain barrier.. *The Journal of clinical investigation,* dec, 106(12), pp. 1489-1499.

Shim, Y.-J.et al., 2009. Epidermal growth factor receptor is involved in clusterin-induced astrocyte proliferation.. *Neuroreport,* mar, 20(4), pp. 435-439.

Shoji, M. et al., 1992. Production of the Alzheimer amyloid beta protein by normal proteolytic processing.. *Science (New York, N.Y.),* oct, 258(5079), pp. 126-129.

Sillén, A. et al., 2011. Linkage to the 8p21.1 region Including the CLU gene in age at onset stratified alzheimerś disease families.. *Journal of Alzheimer's disease : JAD,* 23(1), pp. 13-20.

Simpson, D. L., Morrison, R., de Vellis, J. & Herschman, H. R., 1982. Epidermal growth factor binding and mitogenic activity on purified populations of cells from the central nervous system.. *Journal of neuroscience research,* 8(2-3), pp. 453-462.

Sivamurthy, N., Stone, D. H., Logerfo, F. W. & Quist, W. C., 2001. Apolipoprotein J inhibits the migration, adhesion, and proliferation of vascular smooth muscle cells.. *Journal of vascular surgery,* oct, 34(4), pp. 716-723.

Slaaby, R. et al., 2006. Hybrid receptors formed by insulin receptor (IR) and insulin-like growth factor I receptor (IGF-IR) have low insulin and high IGF-1 affinity irrespective of the IR splice variant.. *The Journal of biological chemistry,* sep, 281(36), pp. 25869-25874.

Smith, G. R. & Shanley, D. P., 2013. Computational modelling of the regulation of Insulin signalling by oxidative stress.. *BMC systems biology,* may, Vol. 7, p. 41.

Sol, I. S. et al., 2016. Serum clusterin level in children with atopic dermatitis.. *Allergy and asthma proceedings,* jul, 37(4), pp. 335-339.

Soos, M. A., Field, C. E. & Siddle, K., 1993. Purified hybrid insulin/insulin-like growth factor-I receptors bind insulin-like growth factor-I, but not insulin, with high affinity.. *The Biochemical journal,* mar, Vol. 290 (Pt 2), pp. 419-426.

Soos, M. A., Navé, B. T. & Siddle, K., 1993. Immunological studies of type I IGF receptors and insulin receptors: characterisation of hybrid and atypical receptor subtypes.. *Advances in experimental medicine and biology,* Vol. 343, pp. 145-157.

Soos, M. A. & Siddle, K., 1989. Immunological relationships between receptors for insulin and insulin-like growth factor I. Evidence for structural heterogeneity of insulin-like growth factor I receptors involving hybrids with insulin receptors.. *The Biochemical journal,* oct, 263(2), pp. 553-563.

Soos, M. A. et al., 1990. Receptors for insulin and insulin-like growth factor-I can form hybrid dimers. Characterisation of hybrid receptors in transfected cells.. *The Biochemical journal,* sep, 270(2), pp. 383-390.

Springer, T. A., 1998. An extracellular beta-propeller module predicted in lipoprotein and scavenger receptors, tyrosine kinases, epidermal growth factor precursor, and extracellular matrix components.. *Journal of molecular biology,* nov, 283(4), pp. 837-862.

Sreerama, N., Venyaminov, S. Y. & Woody, R. W., 2000. Estimation of protein secondary structure from circular dichroism spectra: inclusion of denatured proteins with native proteins in the analysis. *Analytical biochemistry,* Vol. 287, pp. 243-251.

Sreerama, N. & Woody, R. W., 2000. Estimation of protein secondary structure from circular dichroism spectra: comparison of CONTIN, SELCON, and CDSSTR methods with an expanded reference set. *Analytical biochemistry,* Vol. 287, pp. 252-260.

Ståhl, A.-l.et al., 2009. A novel mutation in the complement regulator clusterin in recurrent hemolytic uremic syndrome. *Molecular immunology,* Vol. 46, pp. 2236-2243.

Steen, E. et al., 2005. Impaired insulin and insulin-like growth factor expression and signaling mechanisms in Alzheimerś disease--is this type 3 diabetes?. *Journal of Alzheimer's disease : JAD,* feb, 7(1), pp. 63-80.

Stewart, E. M., 2007. *Structural and functional characterisation of the extracellular chaperone clusterin,* s.l.: s.n.

Strittmatter, W. J. et al., 1993. Apolipoprotein E: high-avidity binding to beta-amyloid and increased frequency of type 4 allele in late-onset familial Alzheimer disease.. *Proceedings of the National Academy of Sciences of the United States of America,* mar, 90(5), pp. 1977-1981.

Strocchi, P., Rauzi, F. & Cevolani, D., 1999. Neuronal loss up-regulates clusterin mRNA in living neurons and glial cells in the rat brain.. *Neuroreport,* jun, 10(8), pp. 1789-1792.

Stuart, W. D., Krol, B., Jenkins, S. H. & Harmony, J. A., 1992. Structure and stability of apolipoprotein J-containing high-density lipoproteins.. *Biochemistry,* sep, 31(36), pp. 8552-8559.

Sung, H. Y. et al., 2014. Amyloid beta-mediated epigenetic alteration of insulin-like growth factor binding protein 3 controls cell survival in Alzheimerś disease.. *PloS one,* 9(6), p. e99047.

Suuronen, T. et al., 2007. Epigenetic regulation of clusterin/apolipoprotein J expression in retinal pigment epithelial cells. *Biochemical and biophysical research communications,* Vol. 357, pp. 397-401.

Svaerke, C. & Houen, G., 1998. Chaperone properties of calreticulin.. *Acta chemica Scandinavica (Copenhagen, Denmark : 1989),* jul, 52(7), pp. 942-949.

Szanto, I. & Kahn, C. R., 2000. Selective interaction between leptin and insulin signaling pathways in a hepatic cell line. *Proceedings of the National Academy of Sciences,* Vol. 97, pp. 2355-2360.

Takahashi, K. et al., 1993. Role of the large extracellular domain of metabotropic glutamate receptors in agonist selectivity determination.. *The Journal of biological chemistry,* sep, 268(26), pp. 19341-19345.

Takaoka, M. et al., 2006. EGF-mediated regulation of IGFBP-3 determines esophageal epithelial cellular response to IGF-I.. *American journal of physiology. Gastrointestinal and liver physiology,* feb, 290(2), pp. G404--G416.

Takase, O. et al., 2008. Inhibition of NF-kappaB-dependent Bcl-xL expression by clusterin promotes albumin-induced tubular cell apoptosis.. *Kidney international,* mar, 73(5), pp. 567-577.

Talbot, K. et al., 2012. Demonstrated brain insulin resistance in Alzheimerś disease patients is associated with IGF-1 resistance, IRS-1 dysregulation, and cognitive decline.. *The Journal of clinical investigation,* apr, 122(4), pp. 1316-1338.

Tato, I., Bartrons, R., Ventura, F. & Rosa, J. L., 2011. Amino acids activate mammalian target of rapamycin complex 2 (mTORC2) via PI3K/Akt signaling.. *The Journal of biological chemistry,* feb, 286(8), pp. 6128-6142.

Thomas, R. et al., 2016. Epidermal growth factor prevents APOE4 and amyloid-beta-induced cognitive and cerebrovascular deficits in female mice.. *Acta neuropathologica communications,* oct, 4(1), p. 111.

Tousi, F. et al., 2012. Multidimensional liquid chromatography platform for profiling alterations of clusterin N-glycosylation in the plasma of patients with renal cell carcinoma.. *Journal of chromatography. A,* sep, Vol. 1256, pp. 121-128.

Traxinger, R. R. & Marshall, S., 1990. Glucose regulation of insulin receptor affinity in primary cultured adipocytes.. *The Journal of biological chemistry,* nov, 265(31), pp. 18879-18883.

Treadway, J. L., Frattali, A. L. & Pessin, J. E., 1992. Intramolecular subunit interactions between insulin and insulin-like growth factor 1 alpha beta half-receptors induced by ligand and Mn/MgATP binding.. *Biochemistry,* dec, 31(47), pp. 11801-11805.

Trommsdorff, M., Borg, J. P., Margolis, B. & Herz, J., 1998. Interaction of cytosolic adaptor proteins with neuronal apolipoprotein E receptors and the amyloid precursor protein.. *The Journal of biological chemistry,* dec, 273(50), pp. 33556-33560.

Trommsdorff, M. et al., 1999. Reeler/Disabled-like disruption of neuronal migration in knockout mice lacking the VLDL receptor and ApoE receptor 2.. *Cell,* jun, 97(6), pp. 689-701.

Truglia, J. A., Livingston, J. N. & Lockwood, D. H., 1985. Insulin resistance: receptor and post-binding defects in human obesity and non-insulin-dependent diabetes mellitus.. *The American journal of medicine,* aug, 79(2B), pp. 13-22.

Tsubai, T. et al., 2016. Insulin elevates leptin secretion and mRNA levels via cyclic AMP in 3T3-L1 adipocytes deprived of glucose. *Heliyon,* Vol. 2, p. e00194.

Tsuruta, J. K., Wong, K., Fritz, I. B. & Griswold, M. D., 1990. Structural analysis of sulphated glycoprotein 2 from amino acid sequence. Relationship to clusterin and serum protein 40, 40. *Biochemical Journal,* Vol. 268, pp. 571-578.

Ullrich, A. et al., 1985. Human insulin receptor and its relationship to the tyrosine kinase family of oncogenes.. *Nature,* 313(6005), pp. 756-761.

Ullrich, A. et al., 1986. Insulin-like growth factor I receptor primary structure: comparison with insulin receptor suggests structural determinants that define functional specificity.. *The EMBO journal,* oct, 5(10), pp. 2503-2512.

Urban, J. et al., 1987. Constitutive apical secretion of an 80-kD sulfated glycoprotein complex in the polarized epithelial Madin-Darby canine kidney cell line.. *The Journal of Cell Biology,* Vol. 105, pp. 2735-2743.

Viard, I. et al., 1999. Clusterin gene expression mediates resistance to apoptotic cell death induced by heat shock and oxidative stress. *Journal of Investigative Dermatology,* Vol. 112, pp. 290-296.

Wang, C. et al., 2015. Clusterin facilitates metastasis by EIF3I/Akt/MMP13 signaling in hepatocellular carcinoma.. *Oncotarget,* feb, 6(5), pp. 2903-2916.

Wang, Y. et al., 2012. Clusterin confers resistance to TNF-alpha-induced apoptosis in breast cancer cells through NF-kappaB activation and Bcl-2 overexpression.. *Journal of chemotherapy (Florence, Italy),* dec, 24(6), pp. 348-357.

Watanabe, K. et al., 2015. The participation of insulin-like growth factor-binding protein 3 released by astrocytes in the pathology of Alzheimerś disease.. *Molecular brain,* dec, 8(1), p. 82.

Watanabe, T. et al., 2005. Relationship between serum insulin-like growth factor-1 levels and Alzheimerś disease and vascular dementia.. *Journal of the American Geriatrics Society,* oct, 53(10), pp. 1748-1753.

Westwood, A. J. et al., 2014. Insulin-like growth factor-1 and risk of Alzheimer dementia and brain atrophy.. *Neurology,* may, 82(18), pp. 1613-1619.

Whitmore, L. & Wallace, B. A., 2004. DICHROWEB, an online server for protein secondary structure analyses from circular dichroism spectroscopic data. *Nucleic acids research,* Vol. 32, pp. W668--W673.

Whitmore, L. & Wallace, B. A., 2008. Protein secondary structure analyses from circular dichroism spectroscopy: methods and reference databases. *Biopolymers,* Vol. 89, pp. 392-400.

WHO & others, 2016. *Global report on diabetes.* s.l.:World Health Organization.

Willnow, T. E. et al., 1996a. Defective forebrain development in mice lacking gp330/megalin.. *Proceedings of the National Academy of Sciences of the United States of America,* aug, 93(16), pp. 8460-8464.

Willnow, T. E. et al., 1996b. RAP, a specialized chaperone, prevents ligand-induced ER retention and degradation of LDL receptor-related endocytic receptors.. *The EMBO journal,* jun, 15(11), pp. 2632-2639.

Willnow, T. E., Sheng, Z., Ishibashi, S. & Herz, J., 1994. Inhibition of hepatic chylomicron remnant uptake by gene transfer of a receptor antagonist.. *Science (New York, N.Y.),* jun, 264(5164), pp. 1471-1474.

Wilson, M. R. & Zoubeidi, A., 2017. Clusterin as a therapeutic target.. *Expert opinion on therapeutic targets,* feb, 21(2), pp. 201-213.

Wisniewski, T., Ghiso, J. & Frangione, B., 1991. Peptides homologous to the amyloid protein of Alzheimerś disease containing a glutamine for glutamic acid substitution have accelerated amyloid fibril formation.. *Biochemical and biophysical research communications,* sep, 179(3), pp. 1247-1254.

Won, A. J. et al., 2016. Discovery of urinary metabolomic biomarkers for early detection of acute kidney injury.. *Molecular bioSystems,* jan, 12(1), pp. 133-144.

Wong, P. et al., 1993. Genomic organization and expression of the rat TRPM-2 (clusterin) gene, a gene implicated in apoptosis.. *Journal of Biological Chemistry,* Vol. 268, pp. 5021-5031.

Wong, P. et al., 1994. Molecular characterization of human TRPM-2/clusterin, a gene associated with sperm maturation, apoptosis and neurodegeneration. *The FEBS Journal,* Vol. 221, pp. 917-925.

Woody, S. K. & Zhao, L., 2016. Clusterin (APOJ) in Alzheimer's Disease: An Old Molecule with a New Role. In: *Update on Dementia.* s.l.:InTech.

Wyatt, A. R. et al., 2011. Clusterin facilitates in vivo clearance of extracellular misfolded proteins.. *Cellular and molecular life sciences : CMLS,* dec, 68(23), pp. 3919-3931.

Xiu, P. et al., 2013. Secretory clusterin contributes to oxaliplatin resistance by activating Akt pathway in hepatocellular carcinoma.. *Cancer science,* mar, 104(3), pp. 375-382.

Xiu, P., Dong, X.-F., Li, X.-P. & Li, J., 2015. Clusterin: Review of research progress and looking ahead to direction in hepatocellular carcinoma.. *World journal of gastroenterology,* jul, 21(27), pp. 8262-8270.

Xu, M. et al., 2015. Clusterin silencing sensitizes pancreatic cancer MIA-PaCa-2 cells to gmcitabine via regulation of NF-kB/Bcl-2 signaling.. *International journal of clinical and experimental medicine,* 8(8), pp. 12476-12486.

Yadav, A., Kalita, A., Dhillon, S. & Banerjee, K., 2005. JAK/STAT3 pathway is involved in survival of neurons in response to insulin-like growth factor and negatively regulated by suppressor of cytokine signaling-3.. *The Journal of biological chemistry,* sep, 280(36), pp. 31830-31840.

Yamaguchi, Y. et al., 1993. Ligand-binding properties of the two isoforms of the human insulin receptor.. *Endocrinology,* mar, 132(3), pp. 1132-1138.

Yang, C.-R.et al., 2000. Nuclear clusterin/XIP8, an x-ray-induced Ku70-binding protein that signals cell death. *Proceedings of the National Academy of Sciences,* Vol. 97, pp. 5907-5912.

Yang, C.-R.et al., 1999. Isolation of Ku70-binding proteins (KUBs). *Nucleic acids research,* Vol. 27, pp. 2165-2174.

Yang, Y. & Yee, D., 2012. Targeting insulin and insulin-like growth factor signaling in breast cancer.. *Journal of mammary gland biology and neoplasia,* dec, 17(3-4), pp. 251-261.

Yerbury, J. J. et al., 2007. The extracellular chaperone clusterin influences amyloid formation and toxicity by interacting with prefibrillar structures.. *FASEB journal : official publication of the Federation of American Societies for Experimental Biology,* aug, 21(10), pp. 2312-2322.

Yerramilli, M., Farace, G., Quinn, J. & Yerramilli, M., 2016. Kidney Disease and the Nexus of Chronic Kidney Disease and Acute Kidney Injury: The Role of Novel Biomarkers as Early and Accurate Diagnostics.. *The Veterinary clinics of North America. Small animal practice,* nov, 46(6), pp. 961-993.

Youngren, J. F., 2007. Regulation of insulin receptor function.. *Cellular and molecular life sciences : CMLS,* apr, 64(7-8), pp. 873-891.

Yu, B. et al., 2016. Clusterin/Akt Up-Regulation Is Critical for GATA-4 Mediated Cytoprotection of Mesenchymal Stem Cells against Ischemia Injury.. *PloS one,* 11(3), p. e0151542.

Zeller, K. I. et al., 2006. Global mapping of c-Myc binding sites and target gene networks in human B cells. *Proceedings of the National Academy of Sciences,* Vol. 103, pp. 17834-17839.

Zhang, J. et al., 2016. Prognostic Role of Secretory Clusterin in Multiple Human Malignant Neoplasms: A Meta-Analysis of 26 Immunohistochemistry Studies.. *PloS one,* 11(8), p. e0161150.

Zlokovic, B. V., 1996. Cerebrovascular transport of Alzheimerś amyloidβ and apolipoproteins J and E: Possible anti-amyloidogenic role of the blood-brain barrier. *Life sciences,* Vol. 59, pp. 1483-1497.

Zlokovic, B. V. et al., 1996. Glycoprotein 330/megalin: probable role in receptor-mediated transport of apolipoprotein J alone and in a complex with Alzheimer disease amyloid beta at the blood-brain and blood-cerebrospinal fluid barriers. *Proceedings of the National Academy of Sciences,* Vol. 93, pp. 4229-4234.

Zong, C. S. et al., 2000. Mechanism of STAT3 activation by insulin-like growth factor I receptor.. *The Journal of biological chemistry,* may, 275(20), pp. 15099-15105.

Zorina, Y., Iyengar, R. & Bromberg, K. D., 2010. Cannabinoid 1 receptor and interleukin-6 receptor together induce integration of protein kinase and transcription factor signaling to trigger neurite outgrowth.. *The Journal of biological chemistry,* jan, 285(2), pp. 1358-1370.

Zoubeidi, A. et al., 2010. Clusterin facilitates COMMD1 and I-kappaB degradation to enhance NF-kappaB activity in prostate cancer cells.. *Molecular cancer research : MCR,* jan, 8(1), pp. 119-130.

8 Supplemental Data

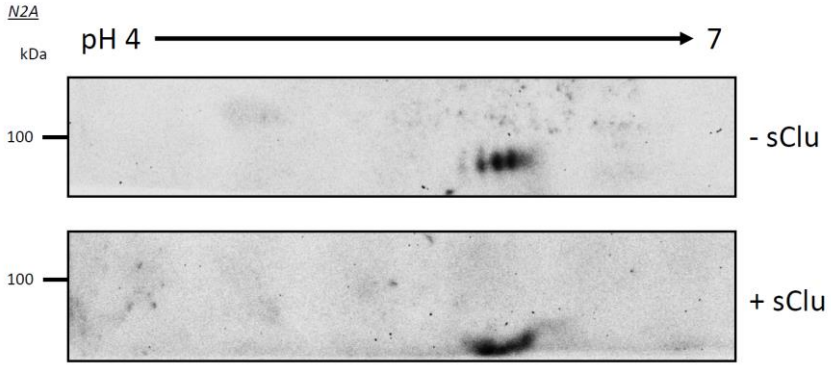

Fig. S 1: Isoelectric focusing of insulin-stimulated whole cell lysates to determine phosphorylated Ins-R entities. *250 µg of whole cell lysates harvested from N2A cells treated with 0.5 µg/mL insulin in the presence or absence of 5 µg/mL msClu for 30 min were analysed in a 2D-gel electrophoresis. The prepared samples were loaded on a gel strip with a gradient ranging from pH 4 to 7. After the second dimension SDS-PAGE procedure, the gel was analysed by Western blot with a total Ins-R primary antibody.*

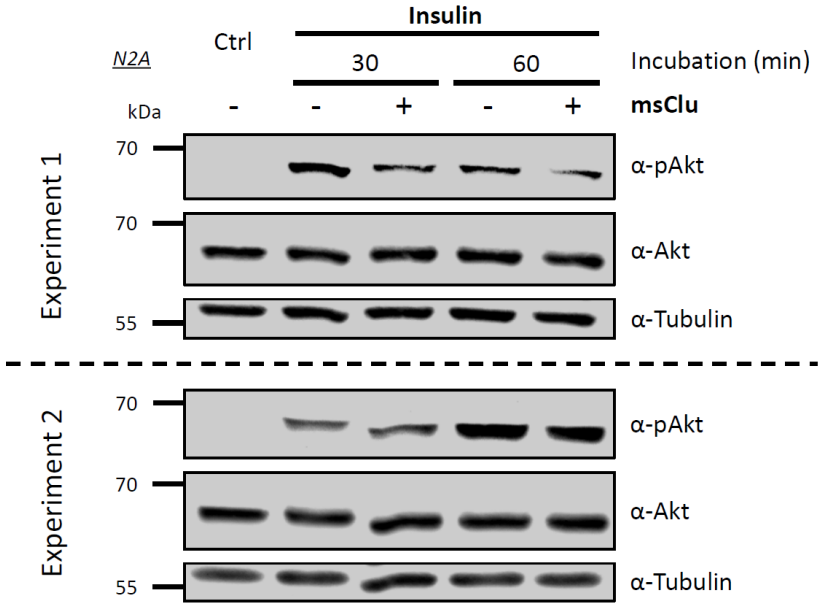

Fig. S 2: Demonstration of the inconclusive results yielded from experiments with altered cell number and starvation conditions in N2A cells. *For each sample 250k N2A cells were seeded, cultivated on LG for 24 h and subsequently serum-starved for 12 h. After treatment with 0.5 µg/mL in the presence or absence of 5 µg/mL msClu for 30 and 60 min, the cells were harvested and lysates were analysed in a Western blot. Panels show two independent experiments.*

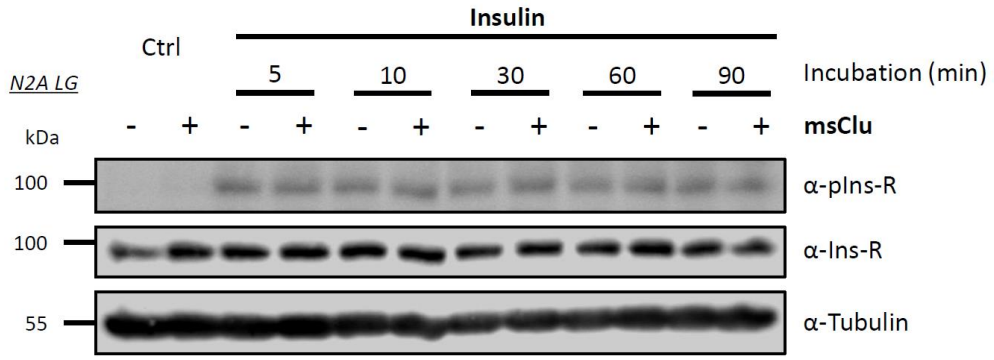

Fig. S 3: Examination of the phosphorylation activation of Ins-R by Clusterin during insulin treatment. *The Western blot analysis targeting Akt phosphorylation in N2A treated with 0.5 µg/mL insulin and 5 µg/mL msClu was repeated for the detection of Ins-R phosphorylation levels.*

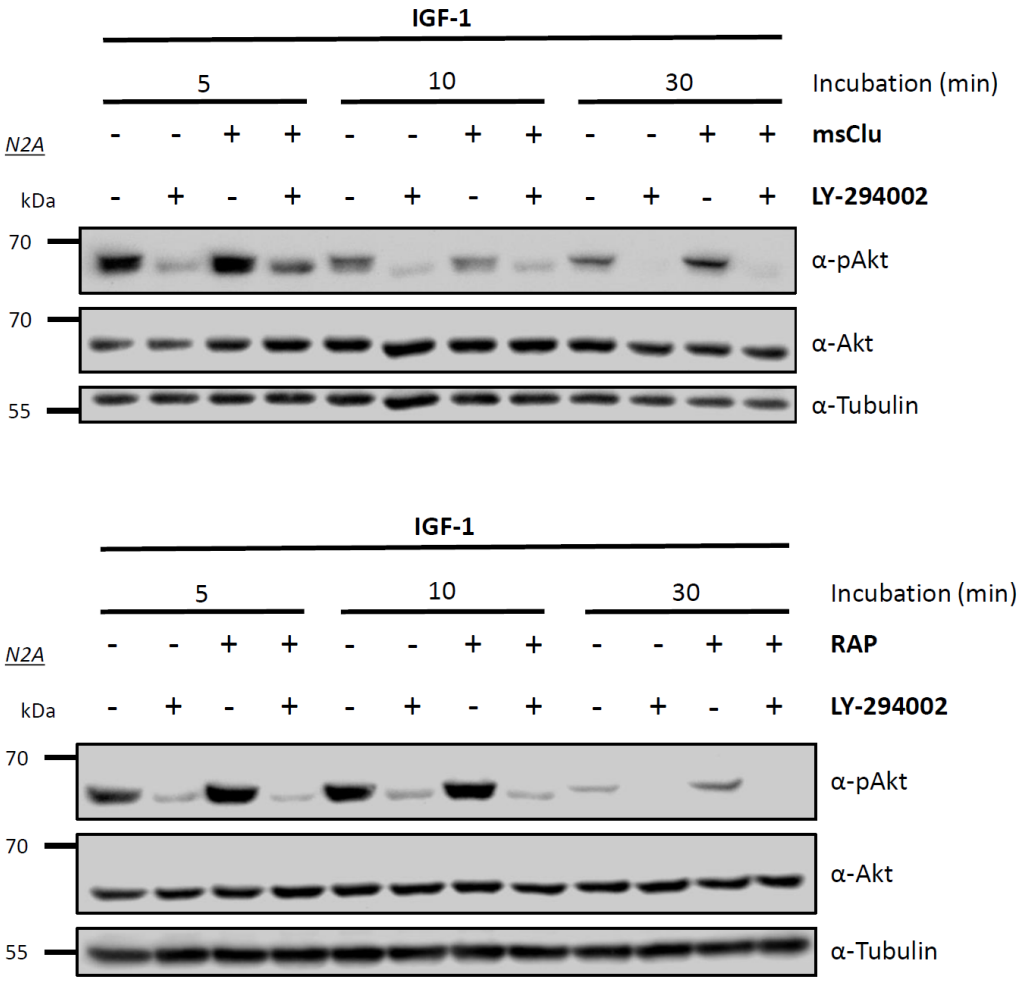

Fig. S 4: Influence of the PI3K inhibitor LY294002 on the Clusterin-/RAP-induced Akt modulation. *After 24 h of serum starvation, N2A cells were pretreated with 40 µM LY294002 for 30 min. Subsequently, the cells were treated with 50 ng/mL IGF-1 in the presence or absence of msClu (A) or RAP (B). The harvested whole cell lysates were analysed by Western blot.*

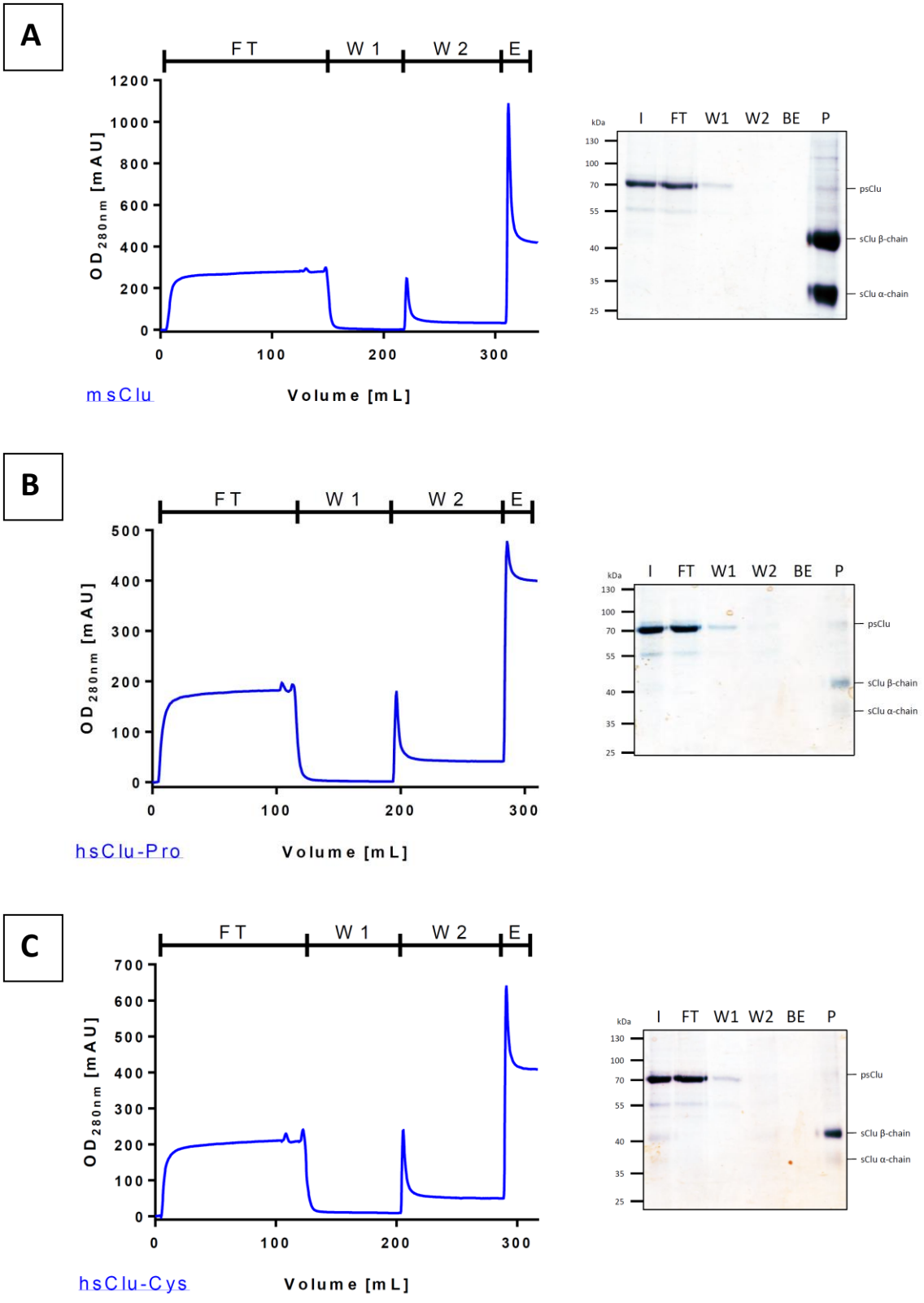

Fig. S 5: FPLC-purification data of recombinantly produced Clusterin variants in stably transfected HEK-293. *The purification of msClu (A), hsClu-Pro (B) and hsClu-Cys (C) were performed by FPLC. The documented chromatograms (left panels) show loading of the sample (FT), first (W1) and second (W2) washing steps and the final elution (E) of the bound protein of interest. For the subsequent evaluation of the purified protein, 30 µL of each fraction were analysed by SDS-PAGE and stained with Coomassie Brilliant Blue (right panels). In addition, 30 µL of the input solution (I) and flow-through after buffer exchange (BE) were loaded, as well as 5 µL of the final purified protein solution (P).*

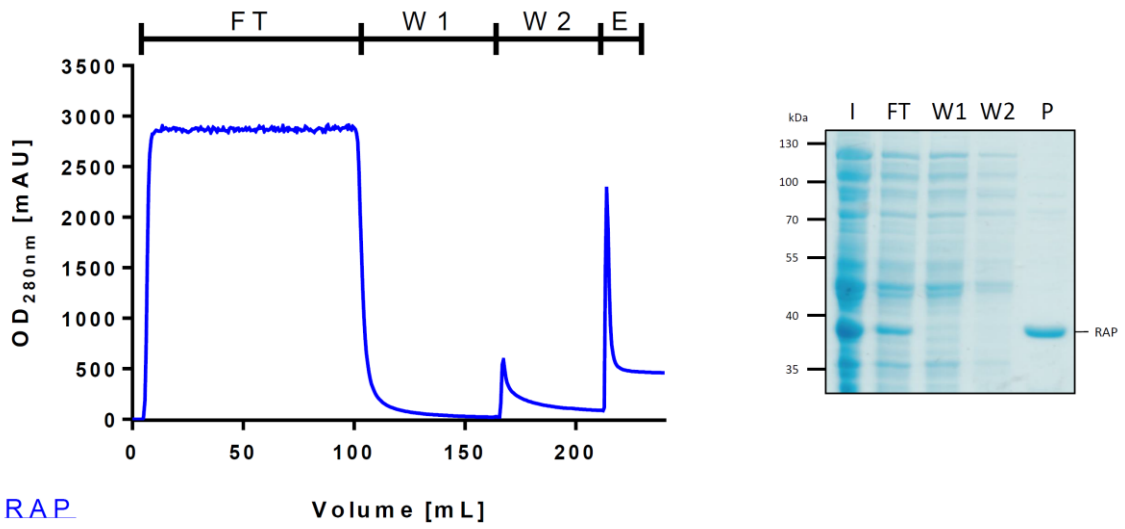

Fig. S 6: FPLC-purification of recombinant RAP from soluble bacterial cell lysate. *Documentation of the FPLC run and following evaluation by Coomassie staining was done in accordance with the conditions described in Fig. S5.*

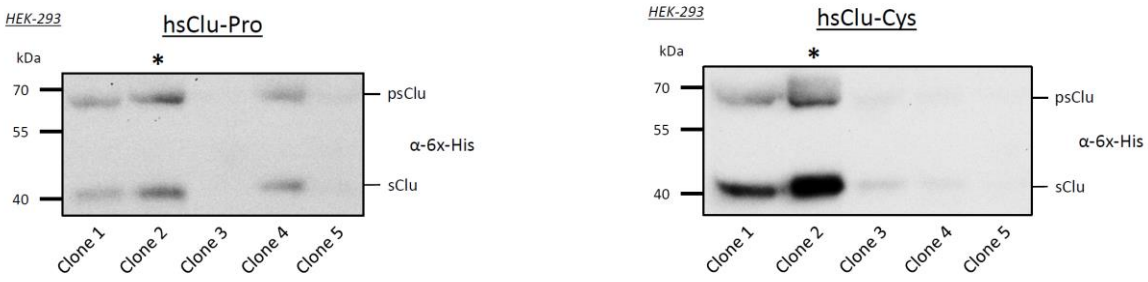

Fig. S 7: Evaluation of the expression levels of stably transfected HEK-293 with Clusterin mutant variants. *The stably transfected and selected single clones for the mutants hsClu-Pro and hsClu-Cys were seeded on 6-well plates and cultivated to full confluency. The cells were serum-starved for 24 h and the supernatant was collected for further analysis. The content of Clusterin in 30 µL supernatant was analysed by Western blot. The clone with the highest expression/secretion level (marked with asterisk) was selected for subsequent purification procedures.*

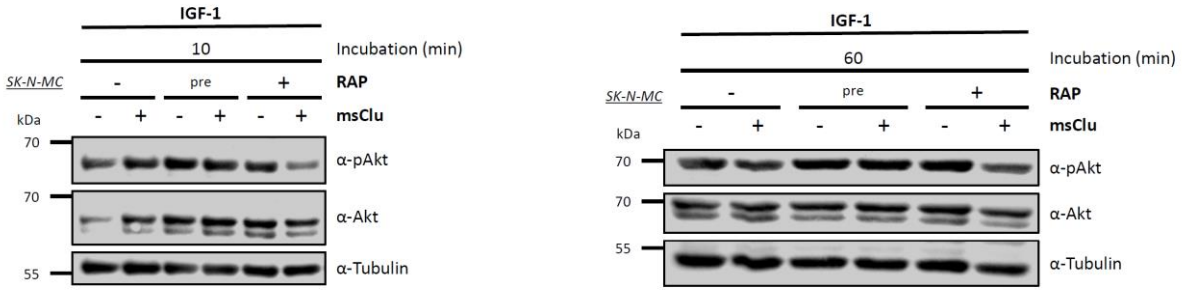

Fig. S 8: Demonstration of the influence of preincubation experiments with RAP on Clusterin-induced modulation of Akt. *Serum-starved SK-N-MC cells were partially treated with 5 µg/mL RAP for 30 min (pre) prior to stimulation with 50 ng/mL IGF-1, 5 µg/mL msClu and/or 5 µg/mL RAP as indicated for 10 (A) or 60 min (B). Harvested lysates were analysed by Western blot.*

Fig. S 9: Sequence alignments of native human Clusterin and mutated variants. *Examination of introduced mutations in the nucleic acid sequence of native human Clusterin (Query) leading to the generation of hsClu-Cys (left) and hsClu-Pro (right) (both Sbjct). Alignments were performed with the NCBI Blast tool.*

Receptor Tyrosine Kinases

	Target	Phosphorylation Site	Family
1	EGFR/ErbB1	pan-Tyr	EGFR
2	HER2/ErbB2	pan-Tyr	EGFR
3	HER3/ErbB3	pan-Tyr	EGFR
4	FGFR1	pan-Tyr	FGFR
5	FGFR3	pan-Tyr	FGFR
6	FGFR4	pan-Tyr	FGFR
7	InsR	pan-Tyr	Insulin R
8	IGF-IR	pan-Tyr	Insulin R
9	TrkA/NTRK1	pan-Tyr	NGFR
10	TrkB/NTRK2	pan-Tyr	NGFR
11	Met/HGFR	pan-Tyr	HGFR
12	Ron/MST1R	pan-Tyr	HGFR
13	Ret	pan-Tyr	Ret
14	ALK	pan-Tyr	LTK
15	PDGFR	pan-Tyr	PDGFR
16	c-Kit/SCFR	pan-Tyr	PDGFR
17	FLT3/Flk2	pan-Tyr	PDGFR
18	M-CSFR/CSF-1R	pan-Tyr	PDGFR
19	EphA1	pan-Tyr	EphR
20	EphA2	pan-Tyr	EphR
21	EphA3	pan-Tyr	EphR
22	EphB1	pan-Tyr	EphR
23	EphB3	pan-Tyr	EphR
24	EphB4	pan-Tyr	EphR
25	Tyro3/Dtk	pan-Tyr	Axl
26	Axl	pan-Tyr	Axl
27	Tie2/TEK	pan-Tyr	Tie
28	VEGFR2/KDR	pan-Tyr	VEGFR

Signaling Nodes

	Target	Phosphorylation Site	Family
29	Akt/PKB/Rac	Thr308	Akt
30	Akt/PKB/Rac	Ser473	Akt
31	p44/42 MAPK (ERK1/2)	Thr202/Tyr204	MAPK
32	S6 Ribosomal Protein	Ser235/236	RSK
33	c-Abl	pan-Tyr	Abl
34	IRS-1	pan-Tyr	IRS
35	Zap-70	pan-Tyr	Zap-70
36	Src	pan-Tyr	Src
37	Lck	pan-Tyr	Src
38	Stat1	Tyr701	Stat
39	Stat3	Tyr705	Stat

Fig. S 10: Detailed description of the PathScan® RTK Signal Antibody Array kit slides and their arrangement.

Data array type	Linear data array * 2
Horizontal axis	Wavelength [nm]
Vertical axis(1)	CD [mdeg]
Vertical axis(2)	HT [V]
Start	260 nm
End	190 nm
Data interval	1 nm
Data points	71

Measurement Information

Instrument	
Name	J-815s
Model Name	J-815
Serial No.	B045361168
Accessory	MPTC-490S
Accessory S/N	B004961326
Cell	#
Temperature	20.00 C
Control Sonsor	Holder
Monitor Sensor	Holder
Start Mode	Start immediately
Cell Length	1 mm
Photometric	
Mode	CD, HT
Measure Range	260 - 190 nm
Data pitch	1 nm
Sensitivity	Standard
D.I.T.	1 sec
Bandwidth	5.00 nm
Start Mode	Immediately
Scanning Speed	Step Scan
Baseline	
Correction	None
Shutter Control	Auto
CD Detector	PMT
PMT Voltage	Auto
Accumulations	5

Fig. S 11: In-depth information of the experimental conditions used in CD-spectrophotometry of Clusterin and IGF-1 studies.

Table S 1: Secondary structure distribution of treated and untreated IGF-1 analysed by CD-spectroscopy and subsequent evaluation with CDSSTR.

	Distribution in [%]			
	α-Helices	β-Sheets	Turns	Unordered
IGF-1	19,6 ± 1,6	14,7 ± 9,9	13,9 ± 7,5	52,2 ± 15,7
IGF-1 heat	7,7 ± 1,6	27,9 ± 14,6	17,5 ± 8,4	46,6 ± 19,3
IGF-1 heat+DTT	3,0 ± 1,9	22,5 ± 8,6	14,4 ± 8,5	58,3 ± 17,6

9 Abbreviations

The following list contains abbreviations used throughout this entire thesis. Abbreviations commonly used in scientific language and known in the field of life sciences (e. g.: RNA, DNA, Akt, ERK, etc.) are not explicitly listed.

aa	amino acid
AD	Alzheimer's disease
Amp	ampicillin
AP-1	activator protein-1
ApoE	apolipoprotein E
ApoJ	apolipoprotein J
AP	alkaline phosphatase
APP	amyloid precursor protein
APS	ammonium persulfate
AU	absorption unit
Aβ	amyloid β
Cam	chloramphenicol
CHAPS	3-[(3-cholamidopropyl)dimethylammonio]-1-propanesulfonate
CLE	Clusterin element
Clu	Clusterin
CM	conditioned medium
CSF	cerebrospinal fluid
Ctrl	control
DC	dendritic cell
DC-SIGN	dendritic cell-specific intercellular adhesion molecule-3-grabbing non-integrin
DEPC	diethyl pyrocarbonate
DMEM	Dulbecco's modified Eagle's medium
EPD	EGF-precursor homology domains
ER	endoplasmic reticulum
ERAD	ER-associated degradation
EtBr	ethidium bromide
EtOH	ethanol
FBS	fetal bovine serum
gp	glycoprotein
GRP-78	78 kDa glucose-regulated protein
HGF-R	HGF receptor
Hsc70	heat shock cognate 71 kDa protein
hsClu	human secretory Clusterin
HRP	horseradish peroxidase
HSE	heat shock element
HSF	heat shock factor
HSP	heat shock protein
IGF-1-R	IGF-1 receptor
IGFBP	IGF-binding protein
IgG	immunoglobulin G

Ins-R/IR	insulin receptor
IRES	internal ribosome entry site
LBD	ligand binding-type repeat domains
LDL	low-density lipoprotein
Lew	lysis equilibration wash
LG	low glucose medium
MDCK	Madin Darby Canine Kidney
MEM	minimal essential medium
mpH_2O	millipore H_2O
msClu	murine secretory Clusterin
MTS	3-(4,5-dimethylthiazol-2-yl)-5-(3-carboxymethoxyphenyl)-2-(4-sulfophenyl)-2H-tetrazolium
nClu	nuclear Clusterin
NF-E2	nuclear factor-erythroid 2
ORF	open reading frame
p	phospho (used for antibody description)
PBS(T)	phosphate-buffered saline solution (+Tween20)
pNPP	*para*-nitrophenylphosphate
pp	percentage point
PUR	purine-rich element
RAP/LRPAP-1	receptor-associated protein
rh	recombinant human
rt	room temperature
RTK	receptor tyrosine kinase
sClu	secretory Clusterin
SGP-2	sulfated glycoprotein-2
sHsp	small heat shock protein
SNP	single-nucleotide polymorphism
SP	serum protein
SP-1	specificity protein 1
SSCR	signal sequence coding region
TBS(T)	tris-buffered saline solution (+Tween20)
TCA	trichloroacetic acid
TEMED	tetramethylethylenediamine
TFA	trifluoroacetic acid
VLDLR	VLDL receptor
α-	anti- (prefix for antibodies)

10 Truthful attestation

Herewith, I assure that I executed this doctoral thesis, according to §13 of the exam regulations (22. August 2012), solely on my own and did not use any sources or resources other than mentioned and that terms and data taken over in wording or content are duly marked as such.

Date, Signature of the author

11 Acknowledgement

12 Curriculum vitae